INFORMATION TO USERS

This was produced from a copy of a document sent to us for microfilming. While the most advanced technological means to photograph and reproduce this document have been used, the quality is heavily dependent upon the quality of the material submitted.

The following explanation of techniques is provided to help you understand markings or notations which may appear on this reproduction.

1. The sign or "target" for pages apparently lacking from the document photographed is "Missing Page(s)". If it was possible to obtain the missing page(s) or section, they are spliced into the film along with adjacent pages. This may have necessitated cutting through an image and duplicating adjacent pages to assure you of complete continuity.

2. When an image on the film is obliterated with a round black mark it is an indication that the film inspector noticed either blurred copy because of movement during exposure, or duplicate copy. Unless we meant to delete copyrighted materials that should not have been filmed, you will find a good image of the page in the adjacent frame. If copyrighted materials were deleted you will find a target note listing the pages in the adjacent frame.

3. When a map, drawing or chart, etc., is part of the material being photographed the photographer has followed a definite method in "sectioning" the material. It is customary to begin filming at the upper left hand corner of a large sheet and to continue from left to right in equal sections with small overlaps. If necessary, sectioning is continued again—beginning below the first row and continuing on until complete.

4. For any illustrations that cannot be reproduced satisfactorily by xerography, photographic prints can be purchased at additional cost and tipped into your xerographic copy. Requests can be made to our Dissertations Customer Services Department.

5. Some pages in any document may have indistinct print. In all cases we have filmed the best available copy.

University
Microfilms
International

300 N. ZEEB RD., ANN ARBOR, MI 48106

Sarwar, Ghulam

GEOLOGY OF THE BELA OPHIOLITES IN THE WAYARO AREA, LAS BELA DISTRICT, SOUTH CENTRAL PAKISTAN

University of Cincinnati PH.D. 1981

GEOLOGY OF THE BELA OPHIOLITES IN THE WAYARO AREA, LAS BELA DISTRICT, SOUTH CENTRAL PAKISTAN

A thesis submitted to the

Division of Graduate Education and Research
of the University of Cincinnati

in partial fulfillment of the
requirements for the degree of

DOCTOR OF PHILOSOPHY

in the Department of Geology
of the College of Arts and Sciences

1981

by

GHULAM SARWAR

B.S. University of Punjab, Pakistan, 1967
M.S. University of Karachi, Pakistan, 1969
M.S. University of Cincinnati, 1977

UNIVERSITY OF CINCINNATI

December 19 81

I hereby recommend that the thesis prepared under my supervision by Ghulam Sarwar

entitled GEOLOGY OF THE BELA OPHIOLITES IN THE WAYARO AREA, LAS BELA DISTRICT, SOUTH CENTRAL PAKISTAN

be accepted as fulfilling this part of the requirements for the degree of DOCTOR OF PHILOSOPHY

Approved by:

Keith A. De Jong

Leonard D. Larsen

William F. Jenks

ABSTRACT

A fifteen-minute quadrangle (Wayaro quadrangle, 27.5 x 24.8 kilometers) covering the ophiolites and the underlying autochthonous rocks, was mapped on a scale of 1:50,000. The ophiolites were thrust upon a sedimentary melange (Kanar Melange) which was deposited in the Paleocene-Early Eocene on the Sembar Formation of Cretaceous age.

The Kanar Melange consists of assorted millimeter to kilometer size debris of the underlying sedimentary rocks (Shirinab and Sembar Formations of Mesozoic age), the overlying ophiolitic rocks, and a few exotic rock types (e.g., a conglomerate consisting of volcanic clasts, called Porali Conglomerate). The matrix of the melange is dominantly argillaceous.

The autochthonous sequence (Shirinab Formation, Sembar Formation, and Kanar Melange) is cut by a number of melanocratic alkaline ultramafic and mafic sills and dikes called the Mor Intrusives. These intrusives are of several generations, the youngest being of Late Cretaceous-Early Eocene age. Clasts of the Porali Conglomerate resemble some of the Mor Intrusives in their petrographic and chemical features, and were probably derived from some volcanics fed by these intrusives. The time of the beginning of this igneous activity is not known; however, it appears that the igneous activity ceased with the emplacement of the Bela Ophiolites which took place in the Paleocene-Early Eocene.

The Bela Ophiolites consist of a sequence of basaltic pillow-lava, interlayered sedimentary rocks (chert, limestone, argillite), and diabase-gabbro sills. Several melange horizons are also interbedded with the argillites. The melange consists mainly of serpentinite slivers (up to several hundred meters long) and serpentinite-carbonate breccias (ophicalcite). Less commonly the melange contains boulders and blocks of other rocks of the ophiolitic suite such as peridotite, gabbro, basaltic pillow lava, chert, limestone, lithic sandstone, and occasionally their metamorphic equivalents. Matrix is formed by argillites, subordinate detrital material of serpentinite and other ophiolitic rocks mentioned above. Isolated serpentinite and breccia slabs (up to 200 meters long) are also irregularly distributed throughout the ophiolite sequence. The age of the ophiolites, as indicated by the microfauna from inter-flow pelagic limestones, is Aptian-Early Maestrichtian.

Petrographically, the pillow lavas are spilitic basalts, and, less commonly, keratophyres and basaltic andesites. Chemically, they are mostly low K-tholeiites enriched in Fe, TiO_2, light rare earths (LREE), and some other trace elements. The diabase-gabbro sills are similar to the associated lava flows; however, they tend to be more enriched in alkalis, Fe, TiO_2, LREE and some other trace elements.

A comparison with modern oceanic environments indicates that the Bela Ophiolite sequence probably originated in a large fracture zone.

This is strongly suggested by the common occurrence of foliated serpentinite and breccia-bearing melange horizons in the sequence. Chemical data also indicate that the lava flows of the ophiolite sequence are similar to those erupted in anomalous tectonic settings such as aseismic ridges, oceanic islands and fracture zones; however, no further distinction can be made by chemical means alone. The fracture zone was probably located in the Neo-Tethys Ocean during the Cretaceous and was destroyed when the ophiolites were emplaced.

The regional structure of the Wayaro area is an open NNW-SSE trending syncline that was formed after the ophiolite emplacement. The western limb of the syncline is marked by a large upthrust mass of Shirinab rocks, which forms the Piaro Ridge. The autochthonous rocks are generally folded. Compared to these, the ophiolites are strikingly less folded but are far more fractured. The fractures appear to be of several generations and were partly inherited from the oceanic regime. The structure of the area is a result of multiple deformation which continues to the present day.

ACKNOWLEDGMENTS

I would like to acknowledge the advice, discussion and critical review of this and the earlier manuscripts by Dr. Kees A. DeJong. Without his whole-hearted support and encouragement this study would not have been possible. Professors Leonard H. Larsen and William F. Jenks also provided helpful criticism and suggestions during the course of this study. I also express my thanks to professors Attila I. Kilinc, Paul E. Potter, Wayne Pryor, Arvid Johnson, and other faculty members for their valuable advice and assistance on the various aspects of this study.

Thanks are expressed to Messrs. Per Erik Litz and Andrew Janiak for their help in the preparation of thin sections. Sally Sutton, Phil Berger, Önder Gokçe, and Gregory Wahlman, fellow graduate students, are sincerely thanked for their help and suggestions which considerably improved the manuscript.

I am also grateful to a number of officers and staff members of the Geological Survey of Pakistan for providing excellent logistic support, field assistance and for many discussions during the course of field work. I am particularly indebted to Messrs. Assrarullah, Abul Farah, Waheedudin Ahmed, Ali H. Kazmi, Akhtar M. Subhani, Ghazanfar Abbas, Ishaq Durrazai, Jafar Qureshi, Mohamad Siddique, Islam Khan, and Yaqub Khan.

Thanks are due to Dr. Iqbal Mohsin of the Karachi University for his hospitality and discussions. The authorities of the WAPDA office at Wayaro are thanked for allowing the use of their rest house during part of the field stay. The hospitality and friendliness of the Wayaro-Uthal tribal authorities, especially of Chief Mir M. Khan and Punnoo are also

gratefully acknowledged. Without their support the field work would not have been possible.

Professors Rolf Schroeder of the Goethe University at Frankfurt and Dietrich Herm of the Munich University are sincerely thanked for doing the microfossil identification needed for dating the Kanar Melange and the Bela Ophiolites. Trace element analysis for this study was performed by the Phoenix Memorial Laboratory of the University of Michigan at Ann Arbor using neutron activation techniques. The director of the laboratory, Mr. John Jones, arranged the necessary funding through a U.S. Department of Energy grant to his laboratory.

Special thanks are extended to Mrs. Jean Carrol and Wanda Osborne for patiently typing this and the previous manuscripts, and suggesting several linguistic and stylistic improvements.

Finally, I thank my wife Cathy for putting up with me through all times, for warmly supporting and continuously encouraging me to the successful completion of this study.

Major funding for this research was provided by the U.S. National Science Foundation Grants INT-76-22304 and EAR-76-13682 to Dr. Kees A. DeJong.

TABLE OF CONTENTS

Page

APPENDICES (continued)

LIST OF ILLUSTRATIONS

Plate

Figure — Page

LIST OF TABLES

INTRODUCTION

General Statement

The Wayaro quadrangle, named after a village in its southwestern corner, lies in the Las Bela District of south-central Pakistan (Figs. 1 and 2). It is crossed by the road between Karachi and Bela. The area is arid and sparsely populated. The nearest town is Uthal which lies about 14 kilometers to the south. From west to east, the Bela area consists of boulder-strewn alluvial plains, the Piaro Ridge, craggy hills of dark ophiolitic rocks, and the Mor Range (Fig. 2). The Wayaro quadrangle includes, from west to east, the southern half of Piaro Ridge, a central segment of the ophiolite belt, and the central part of the Mor Range (Fig. 2).

Regional Setting

Regionally the Bela area (Fig. 2) lies within the southern part of the Kirthar-Sulaiman mountain belt which also includes two other large ophiolite outcrops located near the towns of Muslimbagh and Waziristan (Fig. 1). More ophiolite occurrences are known farther to the north toward the western Himalayas. The Bela Ophiolites (DeJong and Subhani, 1979; Gansser, 1979) form a narrow belt 450 kilometers long and are bounded to the west by the Ornach-Nal-Chaman Fault System, which is at present the western active tectonic boundary of the Indo-Pakistan Subcontinent (Figs. 1 and 2; Gansser, 1966, Lawrence and Yeats, 1979; Kazmi, 1979a).

Figure 1. Map showing the ophiolite occurrences (black areas) in Pakistan, the Kirthar Sulaiman Ranges, and the Chaman-Ornach Nal (ONF) fault system.

1: Bela Ophiolite belt

2: Ras Koh Ophiolite

3: Muslimbagh Ophiolite

4: Zhob Ophiolite

5: Waziristan Ophiolite

6: Dargai Ophiolite

7: Chilas Ophiolite

8: Burzil Ophiolite

9: Dras Ophiolite

(Location of Figure 2 is also marked.)

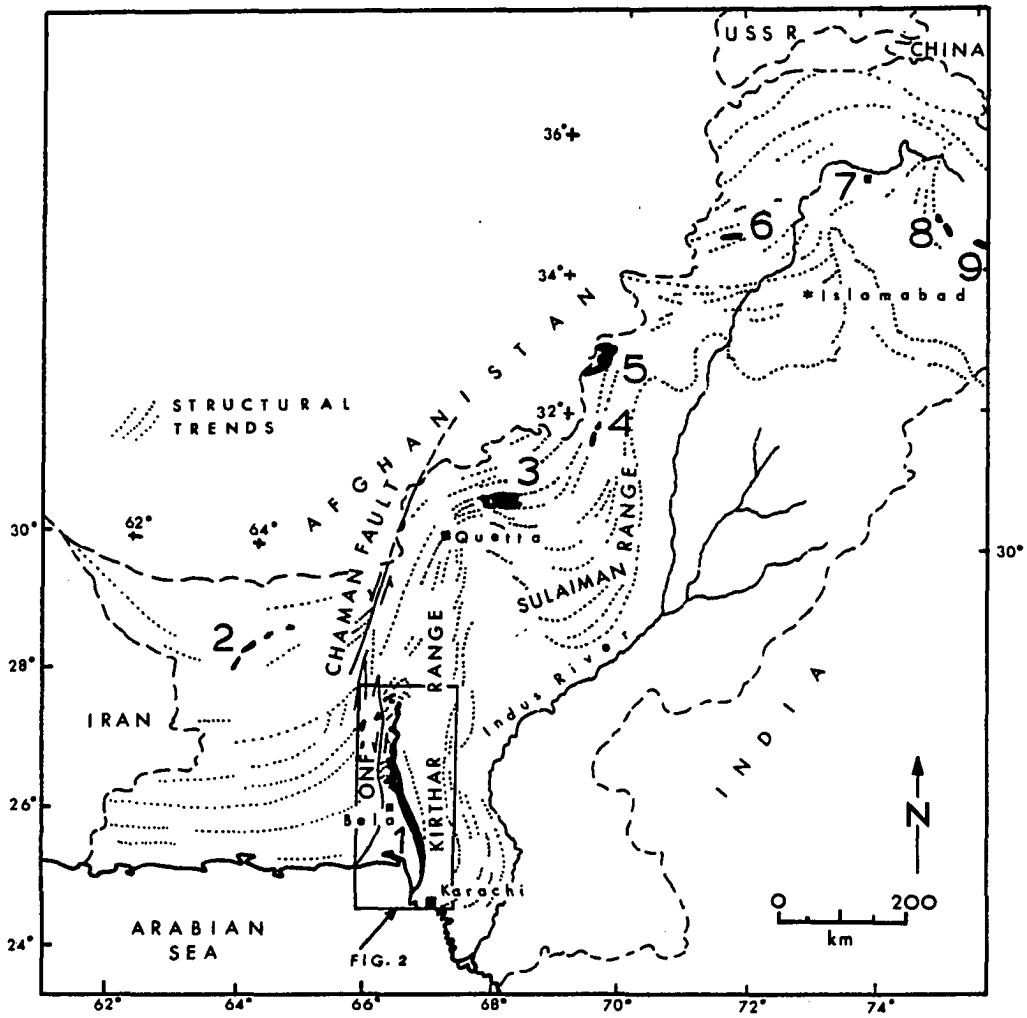

Figure 2. Schematic geologic map of the Bela Ophiolite belt. (Modified after DeJong and Subhani, 1979).

(Location shown on Figure 1).

1: Mesozoic sedimentary rocks of the Mor Range and Piaro Ridge (Shirinab and Sembar Formations)

2: Kanar Melange (Paleocene-Early Eocene?)

3: Ophiolites (Cretaceous)

4: Thar and Bad Kachu Formations (Late Cretaceous-Paleocene)

5: Gidar Dhor Group (Late Cretaceous-Early Eocene)

6: Undifferentiated Mesozoic and Tertiary sedimentary rocks.

7: Quaternary

(Location of Figures 3 and 4 is marked.)

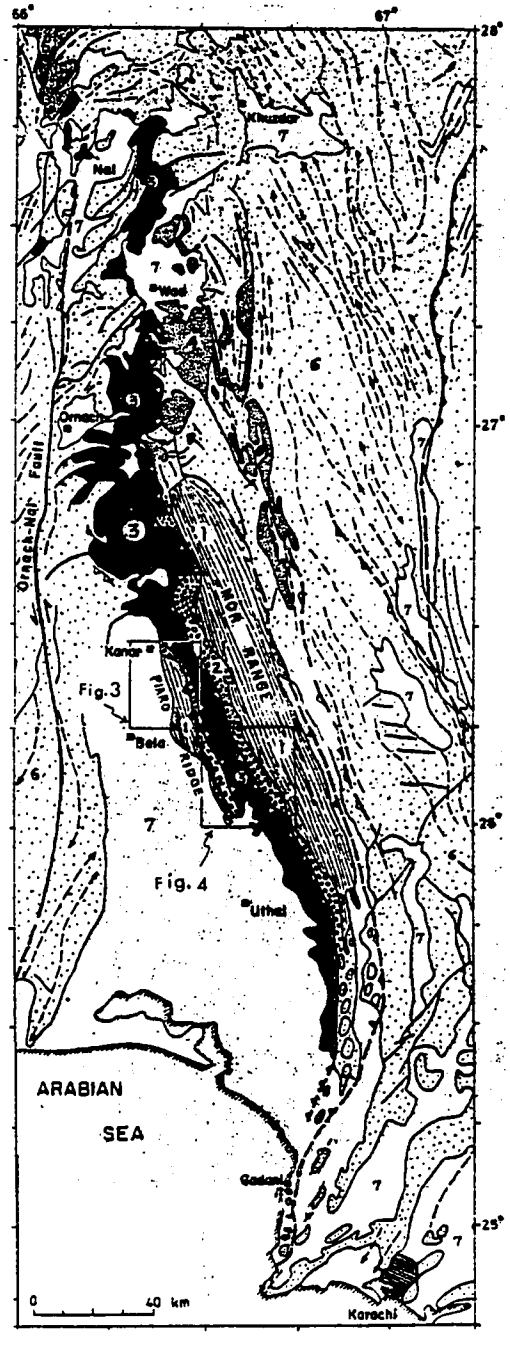

The Pakistani ophiolites are generally regarded as obducted fragments of an oceanic basin "Neo-Tethys," which was closed following the Paleocene-Early Eocene collision of the Indo-Pakistan subcontinent with the Eurasian blocks, that lay to the north and west of it (Powell, 1979). The Bela Ophiolites were emplaced during the Paleocene-Early Eocene time (Allemann, 1979) on the western margin of the Indo-Pakistan subcontinent. The ophiolites tectonically overlie a melange (Kanar Melange) that had developed on a Mesozoic carbonate and clastic sequence now exposed in the Mor Range and the Piaro Ridge (Figs. 2 and 3). Subsequently, during the Eocene, carbonates were deposited on top of the ophiolites (Allemann, 1979). The western margin was deformed in the Cenozoic as a result of convergence between the Indo-Pakistan subcontinent and the Eurasian blocks (Gansser, 1966; Powell, 1979; Sarwar and DeJong, 1979).

Previous Work

Previous knowledge of the geology of the Bela area is due to the works of Vredenburg (1909), the Hunting Survey (1960), Gansser (1979), Allemann (1979), Sarwar and DeJong (1979), and Dejong and Subhani (1979). The latter authors have published a geological map of the Kanar area which lies immediately to the northwest of the Wayaro quadrangle (Fig. 3). The Wayaro quadrangle was included in one of the reconnaissance geological maps (Bela, Sheet 11, 1:250,000, of the Hunting Survey, 1960). The present work, however, is the first detailed study of the geology of the Wayaro quadrangle.

Figure 3. Geological map of the Kanar area. (After DeJong and Subhani, 1979).

Locations of eight samples taken for this study are also shown:

Explanation:

▲ - pillow lava

● - diabase-gabbro sill

■ - fossil

o - Mor Intrusives

1 - 77-SA-4

2 - 77-SA-6

3 - 77-SA-7

4 - 77-SA-14

5 - 77-SA-17

6 - 77-SA-24

7 - 77-SA-26

8 - 77-SA-36

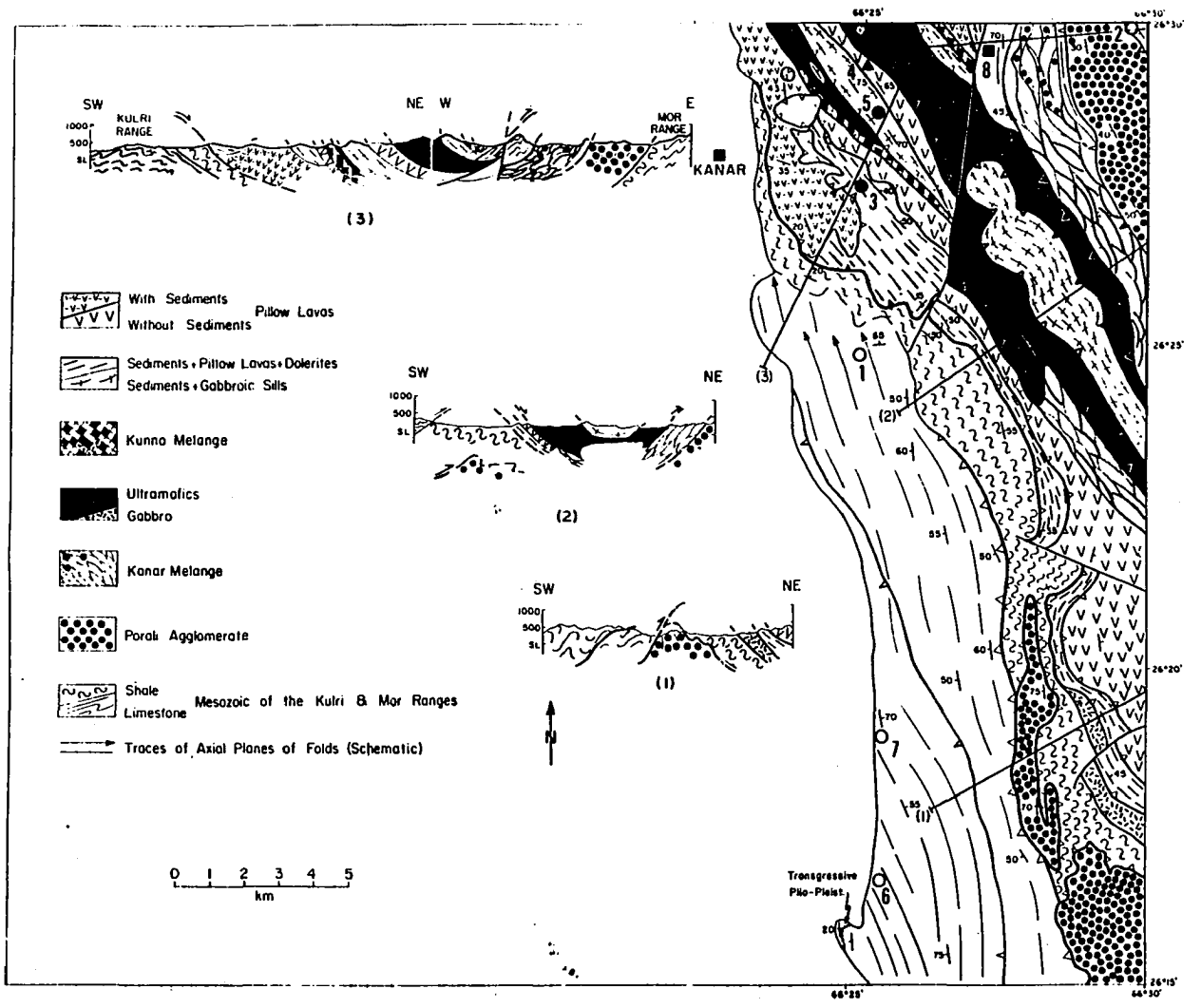

Purpose of Study and Statement of Problems

The Wayaro area offers an excellent opportunity to study the Mesozoic and Cenozoic evolution of a part of the western margin of the Indo-Pakistan subcontinent as well as the nature of the oceanic basin that once lay adjacent to it. The area is easily accessible and both the ophiolites and the underlying autochthonous sequence are well exposed. Therefore, the lithostratigraphic and structural aspects of these rocks and also their relation to each other can be satisfactorily examined. Since little was known about the area prior to my study, the purpose of my research was to examine some of the basic aspects of the geological framework. Specifically, the following questions have been posed:

(1) What are the age, lithostratigraphic and structural constitution of the Bela Ophiolites? What was their original tectonic setting? That is, do they represent obducted crust of a major oceanic basin (Atlantic Type), a marginal basin/arc (Western Pacific Type) or a fracture zone of a large ocean basin?

(2) What is the age, origin and constitution of the Kanar Melange? How does it relate to the underlying sedimentary rocks and the overlying ophiolites (Fig. 4A)?

(3) The Kanar Melange includes debris of a volcanic conglomerate (Porali Conglomerate). What was the source of this conglomerate, and where was it deposited before it was dismembered and incorporated in the Kanar Melange? Was the conglomerate derived from:

A - continental volcanic rocks? (rift type)?

B - oceanic basalts (ophiolites)?

Figure 4A. Tectonic and geographic map of the Wayaro quadrangle (location shown on Figure 2).

Black areas represent large outcrops of serpentinite or serpentinite-bearing melange. Small exposures of serpentinite-bearing rocks are marked by solid circles.

Location of Figures 5-23, and 71-73 is shown by arrow heads and number adjacent to them. In each case the arrow head points in the direction of the view shown in the corresponding figure. Location of Figures 13 and 77-79 is given by rectangles. Some large blocks in the Kanar Melange are shown by dotted lines.

Inset shows the major units identified in the area:

Allothonous

6(sh) = Shirinab Formation (Piaro Ridge)

1-5 = ophiolites (Units 1-5 are separated from one another by serpentinite-bearing melange horizons that overlie irregular unconformable surfaces)

Autochthonous

K = Kanar Melange

S = Sembar Formation

Sh = Shirinab Formation

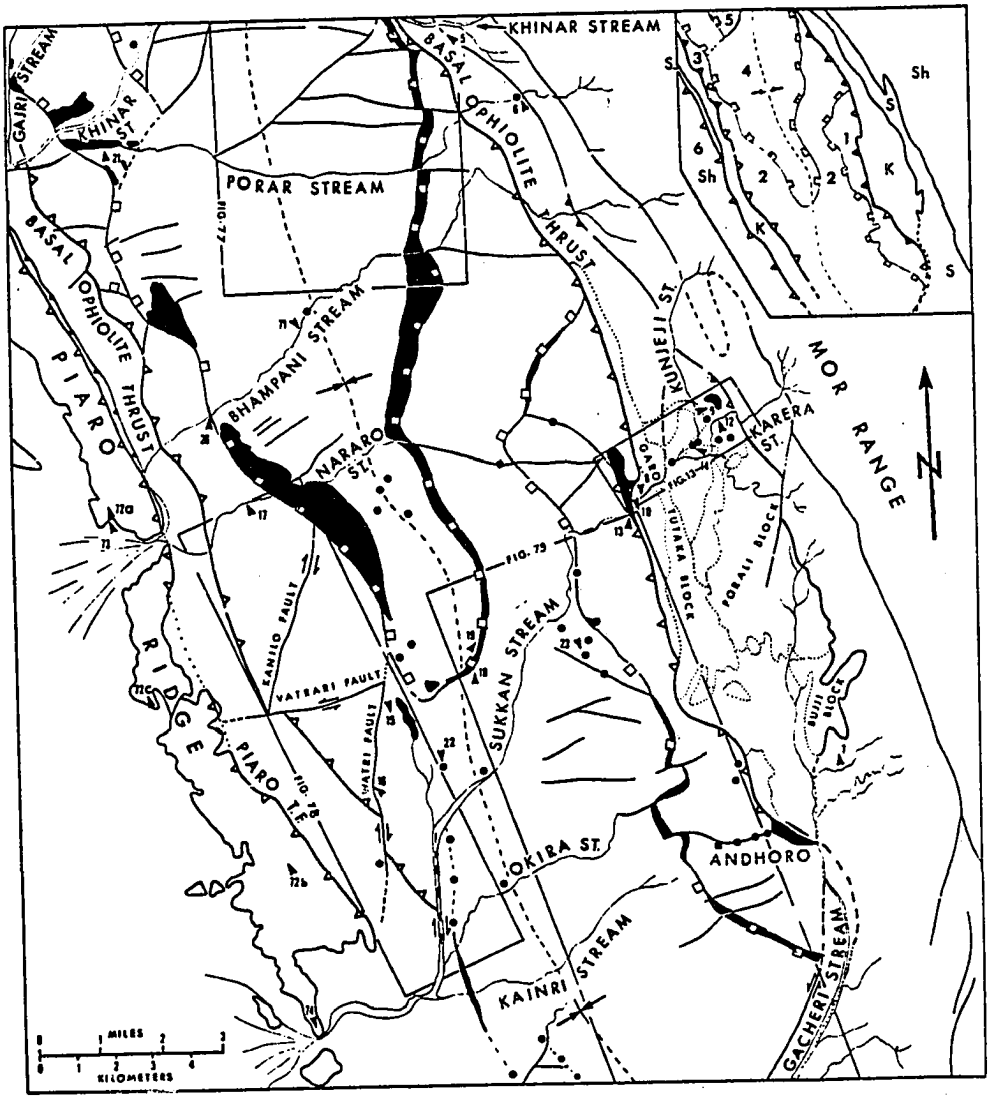

Figure 4B. Sketch map of Wayaro area showing location of samples. Geographical and geological detail is shown in Figure 4A.

Explanation:

▲ - pillow lava

● - diabase-gabbro sills

o - Mor Intrusvies (sills and dikes)

Δ - volcanic clasts from Porali conglomerate

▽ - dike in the Porali conglomerate

◇ - metamorphic and exotic rocks

□ - ophicalcite/detrital serpentinite

■ - fossiliferous rocks

9 - 78-SR-28	26 - SR-13-79	40 - SR-42-79	54 - SR-81-79
	- SR-14-79	- SR-43-79	
10 - 78-SR-29	27 - SR-15-79	41 - SR-45-79	55 - SR-82-79
11 - 78-SR-38	28 - SR-16-79	42 - SR-47A-79	56 - SR-86-79
12 - 78-SR-42	29 - SR-19-79	43 - SR-52-79	57 - SR-88-79
13 - 78-SR-46	30 - SR-20-79	44 - SR-54-79	58 - SR-89-79
14 - 78-SR-50A	31 - SR-21-79	45 - SR-56-79	59 - SR-95-79
	- SR-23-79		
15 - 78-SR-52	32 - SR-26-79	46 - SR-59-79	60 - SR-96-79
	- SR-27-79		
	- SR-28-79		
16 - 78-SR-55	33 - SR-30-79	47 - SR-60-79	61 - SR-99-79
	- SR-31-79	- SR-62-79	
17 - SR-1-79	34 - SR-32-79	48 - SR-68-79	62 - SR-101-79
	- SR-33-79		
	- SR-34-79		
18 - SR-2-79	35 - SR-35-79	49 - SR-69-79	63 - SR-104-79
19 - SR-3-79	36 - SR-36-79	50 - SR-71-79	64 - SR-105-79
20 - SR-4-79	37 - SR-37-79	51 - SR-73-79	65 - SR-106-79
21 - SR-5-79	38 - SR-38-79	52 - SR-79-79	66 - SR-108-79
- SR-9-79			
22 - SR-7-79	39 - SR-40-79	53 - SR-79-79	67 - SR-110-79
- SR-8-79		- SR-90-79	
		- SR-92-79	
23 - SR-10-79			68 - SR-111-79
24 - SR-11-79			69 - SR-112-79
25 - SR-12-79			70 - SR-114-79

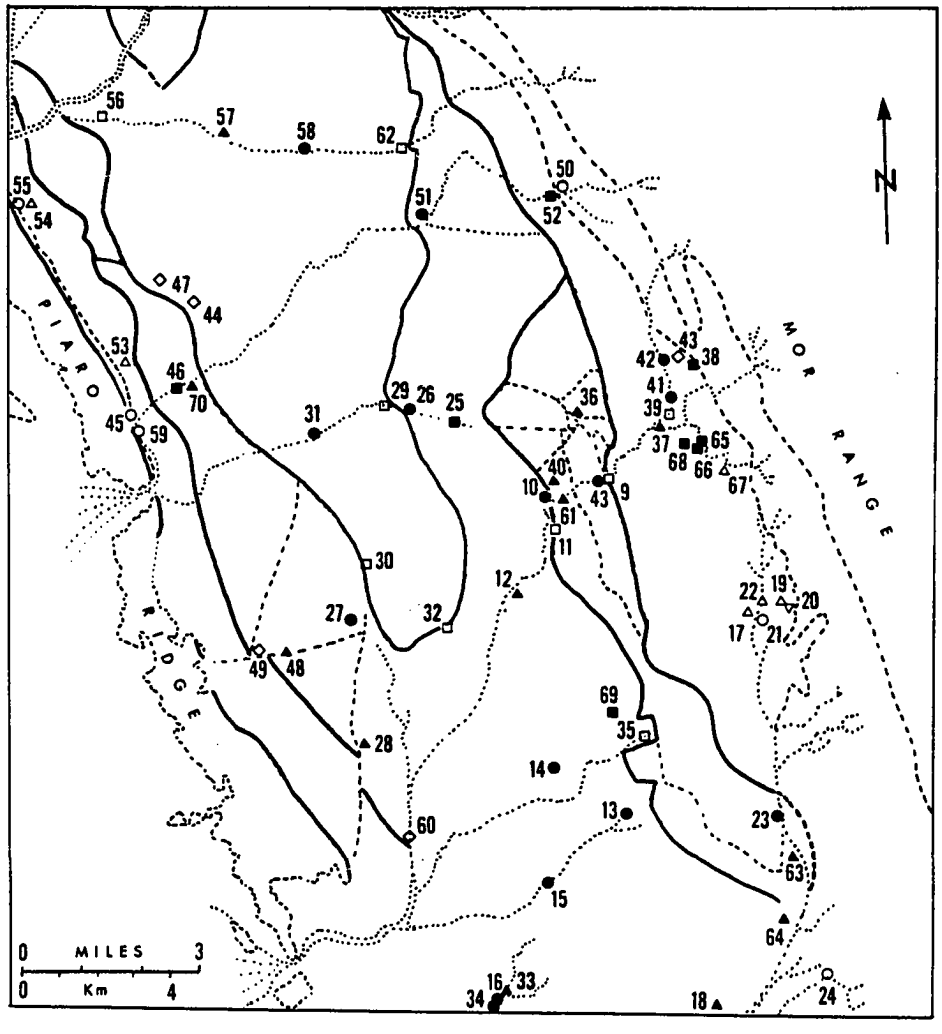

C - a subduction related island arc that might have developed on the continental margin?

(4) The autochthonous sequence (i.e., Shirinab Formation, Sembar Formation and Kanar Melange), that underlies the ophiolites, is cut by melanocratic sills and dikes called Mor Intrusives. What are the age, petrographic and chemical nature of these rocks? Is there any relation between the Mor Intrusives and the volcanic rocks of the Porali Conglomerate?

(5) What is the structure of the Wayaro quadrangle? What is the geologic relation between the Mor Range and the Piaro Ridge (Fig. 4A)?

(6) The ophiolite rocks exhibit a well developed fracture pattern visible on the aerial photographs. What is the age and origin of the fracture pattern?

Methods of Study

Fieldwork and Sampling

The Wayaro quadrangle (15 minute; area 27.5 x 24.8 kilometers) was mapped with the aid of aerial photographs (1:40,000) and the data were transferred in the field on the topographic sheet (35 J/12, scale 1:50,000). The fieldwork was carried out during the winter seasons of 1977-1978 and 1978-1979, and a total of five months were spent in the field. The Mor Range, however, could not be visited because of the tribal unrest in that area.

A small area (4 x 1.6 km) covered by the Kanar Melange was also mapped on a scale of 1:16,666. The base map for this purpose was prepared by enlarging part of the topographic sheet. This map shows the internal constitution and fabric of the Kanar Melange and also its lower and upper contacts.

Outcrop scale structural data in the Piaro Ridge were collected and subsequently plotted on the stereonets to work out the structure of this complex tectonic unit.

A total of 118 samples of rocks from the Wayaro and the adjacent Kanar area were collected for laboratory studies. In addition, 10 samples of fossiliferous clastic sedimentary rocks and pelagic limestones from the Kanar Melange and the Bela Ophiolites were collected for age determination.

Laboratory Work

Of the 128 samples, 99 were sorted out for petrographic study. Based on this, 39 fresh or relatively less altered samples were selected for the major element analysis and 20 samples were selected for trace element analyses. The number of samples selected from the different rock groups for each type of work is given in Table 1.

The locations of all samples except those of the ultramafic rocks are given in Figures 3 and 4. The ultramafic rocks are almost totally serpentinized and petrographically monotonous; for this reason, only a summary of their petrographic characters has been included (see appendix 6). The petrographic descriptions of all other rocks,

Table 1. Division of Samples from the Selected Rock Groups for Laboratory Analyses.

	Number of Samples Used for:		
	Thin Section Study	Major Element Analysis	Trace Element† Analysis
1. Mor Intrusives	12	7	4
2. Porali Conglomerate (volcanic clasts)	11	8	5
3. Bela Ophiolites:			
A. Bela volcanics (pillow basalt)	16	12	6
B. Bela Intrusives (Diabase-gabbro)	21	12	5
C. Ultramafic Rocks (serpentinite*)	12	—	—
D. Exotic*/Metamorphic Rocks*	7	—	—
E. Ophicalcite*/ Detrital serpentinite*	10	—	—
4. Fossiliferous Rocks			
Kanar Melange	6	—	—
Ophiolites	4	—	—
Total	99	39	20

† = Elements analyzed: Ba, Ca, Cr, Cs, Hf, Ni, Rb, Sc, Ta, Th, U and REE.

* = Samples came from the melange horizons found within the ophiolites.

including modes for most of the Bela volcanics and intrusives, are included in Appendices 2-5 and 7-9.

The major element analysis was done by the writer using a Perkin-Elmer atomic absorption spectrophotometer model 403 (Appendix 10A). The trace element analysis, including the rare earth elements (REE) was performed by the Phoenix Memorial Laboratory of the University of Michigan at Ann Arbor using neutron activation techniques. All major and trace element data are reported in Appendix 10B.

The petrographic and chemical analysis of the above rocks was carried out with the following aims in mind:

(1) to identify the parent magma types of the Mor Intrusives, the Porali Conglomerate volcanic clasts and the Bela mafic rocks (ophiolites).

(2) to identify a genetic relation (if any) between the Porali clasts and the Mor Intrusives, i.e., to determine whether the clasts were derived from any volcanic equivalents of the Mor Intrusives.

(3) to compare the Porali clasts with the Bela volcanics in order to find out whether the clasts were derived from the Bela Ophiolites or similar oceanic rocks.

(4) to compare, by means of chemical variation diagrams, the parent magma of the Porali Conglomerate with other known continental or oceanic rocks in order to establish the original tectonic environment of formation of its source volcanics.

(5) to compare, by means of chemical variation diagrams, the parent magma of the Bela mafic rocks (ophiolites) with other

suitable rocks from known oceanic and/or destructive continental margin settings, in order to define the original tectonic setting of the Bela Ophiolites.

Besides the above, the aerial photo scale (1:40,000) fracture pattern in three selected areas covered by the ophiolites was also analyzed with the help of rose diagrams, the results of which are presented later.

The paleontologic work was done by Professors Rolf Schroeder (Goethe University, Frankfurt) and Dietrich Herm (Munich University).

STRATIGRAPHY

The major stratigraphic units recognized in the study area are presented in Table 2 and Figure 4A.

Table 2. Major Stratigraphic and Tectonic Units Recognized in the Wayaro Area.

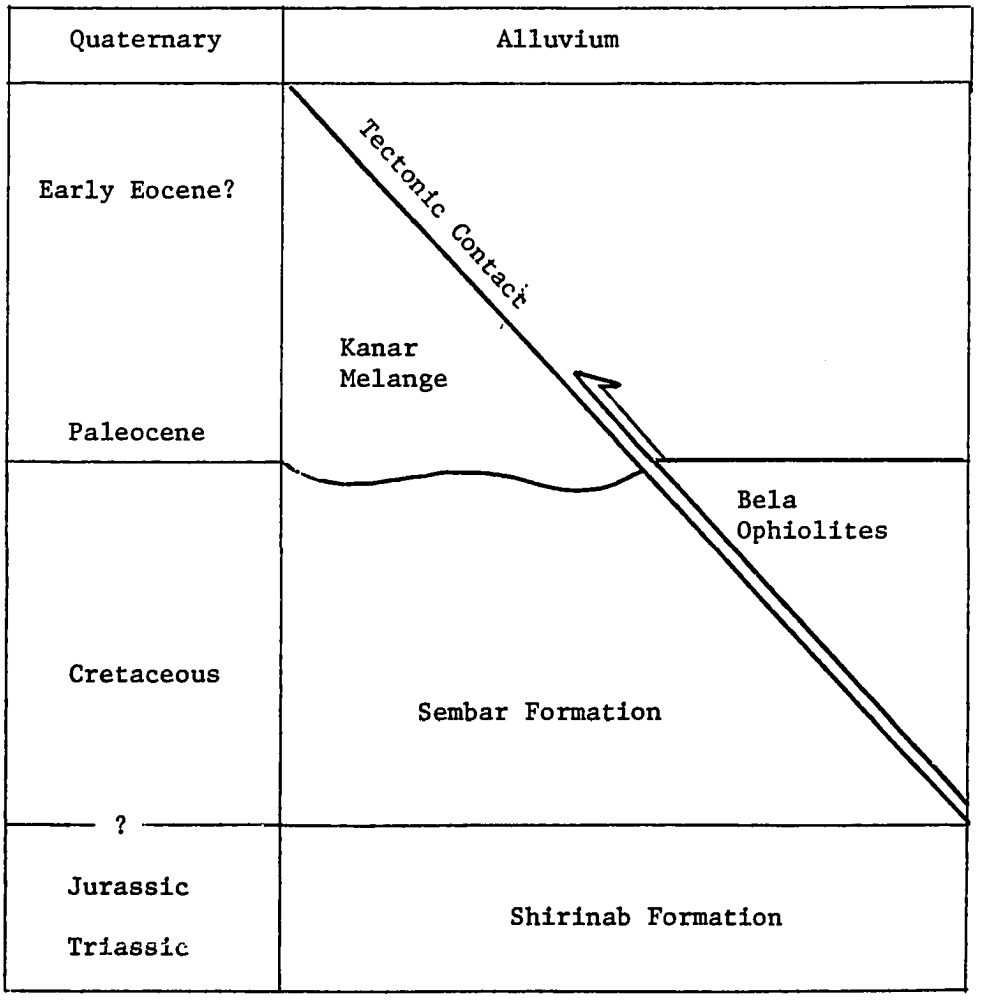

Shirinab Formation (Triassic and Jurassic)

The name Shirinab Formation is used here for a thick folded sequence of sedimentary rocks exposed in the Mor Range and Piaro Ridge (see Plate 1 and Figure 4). The Shirinab type rocks are also found in numerous isolated blocks in the Kanar Melange. These rocks were previously designated as the Windar Group (Triassic-Jurassic) by the Hunting Survey (1960). Later Shah (1977) discarded the name Windar and included the lower and upper parts of the Windar Group separately into his Wulgai Formation (Triassic) and Shirinab Formation (Jurassic). The term 'Shirinab Formation', however, was first introduced by the Hunting Survey (1960) for certain Permian-Early Jurassic sedimentary rocks in the Kalat Plateau. In the present work the formally recognized name 'Shirinab Formation' (Shah, 1977) has been used to replace the obsolete 'Windar Group' of the Hunting Survey (1960).

The Shirinab Formation consists of limestone with subordinate shale and sandstone. The limestone is dominantly micritic (mudstones and subordinate wackestones), light brownish or purplish gray to dark gray in color, resistant, ridge-forming and shows very rough weathered surfaces. It is generally thin to thick bedded (a few centimeters to 2 meters), but may locally become massive. It is also nodular in places. Broken fossil debris, consisting of crinoids, bivalves, brachiopods, gastropods, and corals, is a ubiquitous feature of the limestones and is locally abundant. The limestone may also be oolitic, pelletal or ferruginous. Many weathered surfaces are covered with irregular rusty-brown blotches. Occasionally a few beds are partially replaced by barite and calcite with or without quartz, and trace amounts of base metal sulphides.

The sandstone and shale are interbedded with limestone or occur as separate horizons. Along the western side of the Mor Range, the top part of the Shirinab Formation consists of interbedded limestone and shale which grade upward into soft olive-green shales of the Sembar Formation.

The sandstone is white to brown, fine to coarse grained, well sorted, quartzitic to orthoquartzitic, commonly ferruginous, thin to thick bedded (a few centimeters to 1-5 meters) and frequently crossbedded. Ripple marked beds are also present. The main exposures of the sandstone lie along the western slope of Piaro Ridge and in the western Mor Range, near the headwaters of the Kunjeji stream (see Fig. 4A). In the southern part of Piaro Ridge, quartzitic sandstone grades upward into gray limestones through a thick interval of crossbedded sandy or silty limestone and shale.

Melanocratic sills, and rarely dikes (Mor Intrusives) of grayish green color and one half to a few meters in thickness, are present within the Shirinab Formation.

Cretaceous-Early Eocene Rocks (Nomenclature)

Previously all Cretaceous rocks in the Bela area were included in the Bela Volcanic Group (Hunting Survey, 1960; Shah, 1977). The ultramafic and gabbroic rocks were believed to intrude the Bela Volcanic Group (Porali Intrusions, Hunting Survey, 1960).

In the present report the name Bela Volcanic Group is not used, because the rocks included in this group consist of a lower autochthonous sedimentary and an upper allochthonous ophiolitic sequence (Fig. 4A). Also, the autochthonous sequence involves Cretaceous as well as Early Tertiary rocks (see below).

The autochthonous rocks are divided into two units: the Sembar Formation and the overlying Kanar Melange. The name Sembar Formation was introduced by Williams (1959) and is commonly used to designate Lower Cretaceous sequences elsewhere in the Kirthar-Sulaiman Belt (Shah, 1977). However, in the present study the term Sembar Formation is applied to all Cretaceous strata and no attempt is made to identify three separate Cretaceous units (i.e., Sembar Formation, Goru Formation and Parh Group) as is commonly done in the Sulaiman-Kirthar Belt (e.g., Shah, 1977). The name Kanar Melange is taken from DeJong and Subhani (1979), who introduced it for an ophiolitic melange 30 kilometers north of the present study area. It was formed in Paleocene-Early Eocene time.

The overlying allothithonous sequence is named here the Bela Group. It consists of a Cretaceous ophiolitic suite commonly known as the Bela Ophiolites (DeJong and Subhani, 1979; Allemann, 1979; Gansser, 1979).

Sembar Formation (Cretaceous)

In the mapped area the Sembar Formation is exposed along the western flank of the Mor Range and along the eastern slope of Piaro Ridge. The rocks are folded and, in the western part of the area, are overthrust by the Shirinab Formation of Piaro Ridge (see Fig. 4A).

The basal part of the Sembar Formation consists of dark olive-green, soft shales with minor interbedded mudstone. The shales overlie the Shirinab Formation with a gradational (over a few meters) contact marked by sporadic small nodules (10-15 cm) of barite. Within a few tens of meters, the shales grade upward into a monotonous regular sequence of thin to medium bedded mudstones, subordinate shales and minor argillaceous

limestones. The mudstones are grayish green, brownish gray to gray, and finely laminated; they form rugged hills. The shales are soft weathering and of variegated colors such as olive green, gray, maroon or purple. Both shales and mudstones may be calcareous, carbonaceous, and occasionally silty.

Sills and, less commonly, dikes (Mor Intrusives, see p.) of aphanitic or porphyritic greenish gray basalt (?) are present in the Sembar rocks and may locally be abundant. The sills are up to 10 m thick but their average thickness is less than 5 m.

The upper contact of the Sembar Formation with the Kanar Melange has been placed where 'clean' mudstone or shale gets its first 'foreign' clasts which generally consist of Shirinab (?) or ophiolitic rocks. As shown in Figures 5 and 6, the contact appears to be a stratigraphic one. The rock-clasts are, therefore, slump masses.

Similar boulders and slabs (1-3 m long) of the Shirinab (?) limestone were observed about a kilometer south of the Bujji mountain block (Fig. 4A). Some mudstone concretions (up to 1/2 m in diameter), built around limestone boulders, were also noticed. The stratigraphic nature of the contact is obscured at places where local thrusting has occurred along it (e.g., Bhampani stream gorge).

At other places the contact between the Sembar Formation and the Kanar Melange is marked by a sudden appearance of very large blocks (up to several cubic kilometers). An example of such blocks is the Bujji mountain mass which is 3 km long and consists of folded Shirinab (?) rocks (Figs. 4A, 7). The block overlies mudstone of the Sembar Formation which is notably undeformed except near its contact with the block

Figure 5. Lower contact of the Kanar Melange (K) with the Sembar Formation (S) in the upper Khinar stream valley. The contact is marked by sudden appearance of debris of the Shirinab (?) limestone (J) in an other wise continuous section of argillites.

(Location 5, Figure 4A; sketch of photograph).

Figure 6. Lower contact of the Kanar Melange (K) with the Sembar Formation (S) in the upper Porar stream gorge. The contact is marked by sudden appearance of large blocks of pillow lava (P); blocks of gabbro, limestone (Shirinab (?) and other), and foliated serpentinite (marked by arrow) are also present above the contact. The Sembar Formation and matrix of melange consist of sheared silty or calcareous argillites; bedding is present.

(Location 6, Figure 4A; schematic field sketch).

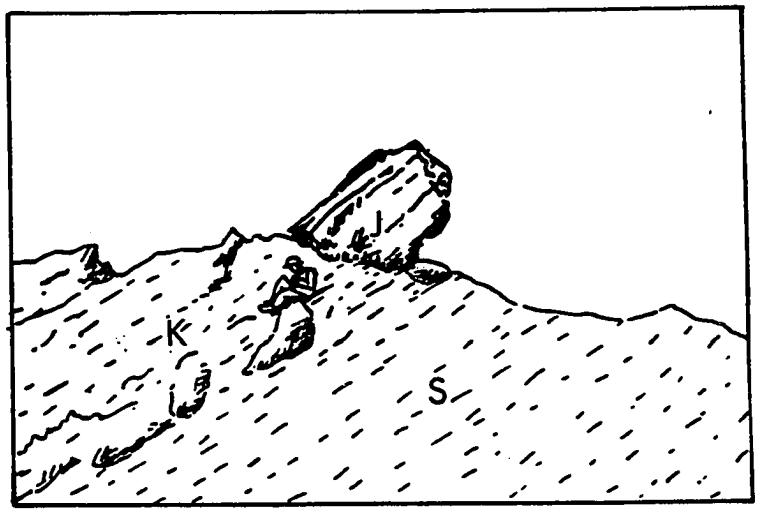

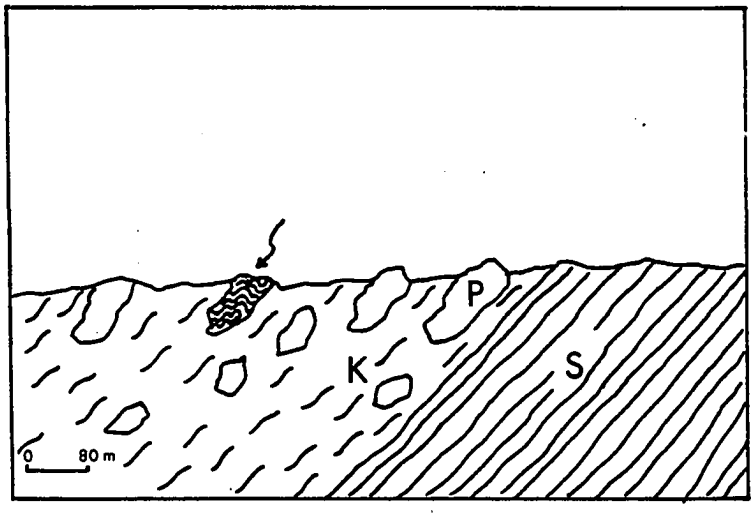

(Fig. 7). The folds are confined to the block and are discordant to its contact with the mudstone. In plan view the block is clearly an isolated mass of the Shirinab (?) rocks underlain by the Sembar Formation (Fig. 4A). These observations suggest that the Bujji mass is a large slide block. It is a part of the Kanar Melange which includes a number of other similar blocks (Fig. 4A). The presence of such large blocks in the Kanar Melange indicates that its formation might have involved removal of the upper part of the Sembar Formation. This is consistent with the observation that, in map view, the Kanar Melange clearly cuts across the strike of the Sembar Formation (Plate 1), which is sharply reduced in outcrop width north of the Bujji mass (Fig. 4A). The melange possibly occupies a channel carved in the Sembar Formation. An alternative explanation for the observed discordance would be large-scale thrusting along the base of the Kanar Melange; however, it is discarded for lack of evidence.

The age of the Sembar Formation within the Bela area is not known. It represents the lower part of the Bela Volcanic Group which was assigned a Cretaceous age (Hunting Survey, 1960). In the adjacent parts of Baluchistan it has been dated as mainly of Early Cretaceous (Neocomian) age (Shah, 1977). There is some circumstantial and paleontologic evidence that the age of the overlying Kanar Melange is Paleocene to Early Eocene. In that case, the Sembar Formation may be of Cretaceous age; however, as discussed above, its upper part appears to be missing in the study area. According to White (1981), the Sembar Formation was deposited in an outer shelf-upper slope environment.

Figure 7. View of Bujji mountain, which consists of a large isolated block of irregularly folded Shirinab (?) limestone (J), and is underlain by mudstones of the Sembar Formation (S). Arrow marks the lower contact of block. The Sembar Formation (S) dips 50 degrees to the west and is only mildly deformed as compared to the limestone block. However, along the contact it shows chaotic deformation and a few small blocks of limestone embedded in mudstone.

(Location 7, Figure 4A; sketch of photograph).

Figure 8. View of the Kanar Melange showing subangular to subrounded clasts of limestone, chert and basalt embedded in a foliated pelitic matrix. Note hammer for scale.

(Location 8, Figure 4A; sketch of photograph).

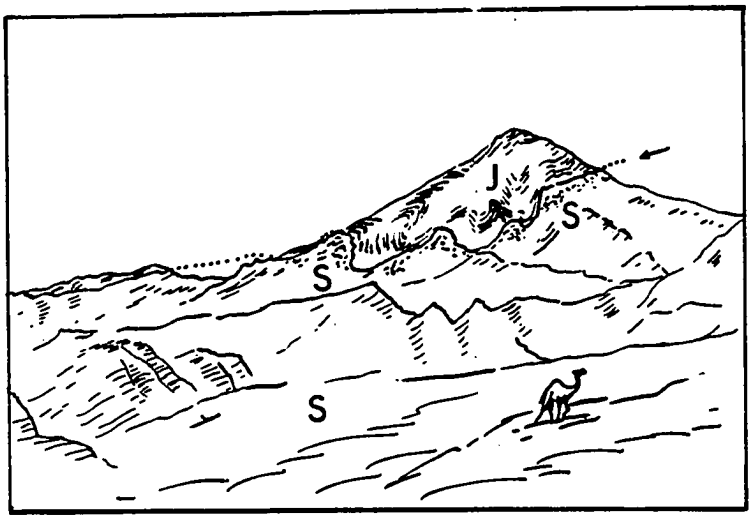

Kanar Melange (Paleocene-Early Eocene)

The term melange is used here in a descriptive sense to denote a chaotic, heterogeneous assemblage of unsorted clasts of all sizes set in a dominantly argillaceous matrix.

The Kanar Melange underlies the Bela ophiolite nappe and is exposed in two linear belts of variable width, along the western edge of the Mor Range and the eastern edge of Piaro Ridge (Fig. 4A). The eastern belt is well exposed and almost 4.5 km wide north of Bujji mountain. Southward from here, its width is sharply reduced and it is exposed as widely spaced small mounds along the southern part of the Gacheri stream (Fig. 4A). South of the mapped area, the melange reappears as a wider belt and extends more or less continuously to the Arabian Sea at Gadani (Fig. 2). North of the mapped area, this melange belt extends far beyond the Porali River.

The western melange belt is up to 2 km wide and is partly covered by alluvium except near the Sukkan stream where it is completely covered. No exposures are known farther to the south. Northward, its exposures extend a few kilometers outside the mapped area to the vicinity of Kanar (Fig. 2). The melange consists of a mixture of small pebble to huge mountain size blocks of a variety of rocks interspersed through a dominantly argillaceous matrix (Figs. 5-12). All formations shown on the map are found as clasts within the melange. It also contains a few exotic rocks. Some of the larger blocks are shown on the map but the majority of them are left in the undifferentiated melange. Figure 13 presents a detailed map view of a part of the Kanar Melange.

Matrix: The matrix of the melange consists mainly of pelitic rocks such as shales, mudstones and marls; coarse material such as lithic sandstone is less common. All matrix-forming rocks are of variegated colors, with red, maroon, gray, green, purple and brown dominant. Bedding is frequently obscured, however distinct beds are present and interlayered with chaotic horizons (Figs. 8, 10, 11).

Basaltic sills and a few dikes (Mor Intrusives), similar to those already described in the Sembar Formation, are present at places (e.g., Karera stream gorge), and indicate that at least some intrusive activity either post-dates melange formation, or was coeval with it.

Rock fragments of different kinds and sizes are irregularly distributed through the matrix (Fig. 5-13). Sorting is generally poor though occasional graded beds are present. The proportion of matrix to clasts is highly variable from place to place but is generally high. For example, along the upper part of the Gacheri stream, the melange consists of only a few blocks set in a relatively 'clean' argillaceous matrix (Fig. 4A). On the other hand, along the Kunjeji stream, blocks are chaotically jumbled against one another with thin screens of matrix filling the interblock spaces (Figs. 4A, 13). Quite often reworked matrix is found either as thin, lithic beds consisting of small (a few centimeters) tabular clasts or as pebble to large house-size blocks. The blocks are subangular to subrounded and consist of breccia of rock types that form the matrix and foreign clasts. Occasionally small, tight and disharmonic folds, confined only to a few thin beds are present. They do not affect the overlying or the underlying horizons (Fig. 11). Such folds are probably of slump origin.

Figure 9. View showing hill size blocks of some of the rock types that occur in the Kanar Melange.

P = pillow lava
J = thin bedded Shirinab (?) limestone and calcareous shale (note folding)
Sp = foliated serpentinite
S = Sembar Formation that underlies the Kanar Melange
C = partly covered argillites that form matrix of the melange

(Location 9, Figure 4A; sketch of photograph).

Figure 10. View of the Kanar Melange showing an isolated lenticular block of foliated serpentinite embedded in foliated pelitic matrix. Bedding is obscured; however, some relict beds are shown in the bottom right corner.

(Location 10, Figure 4A; sketch of photograph).

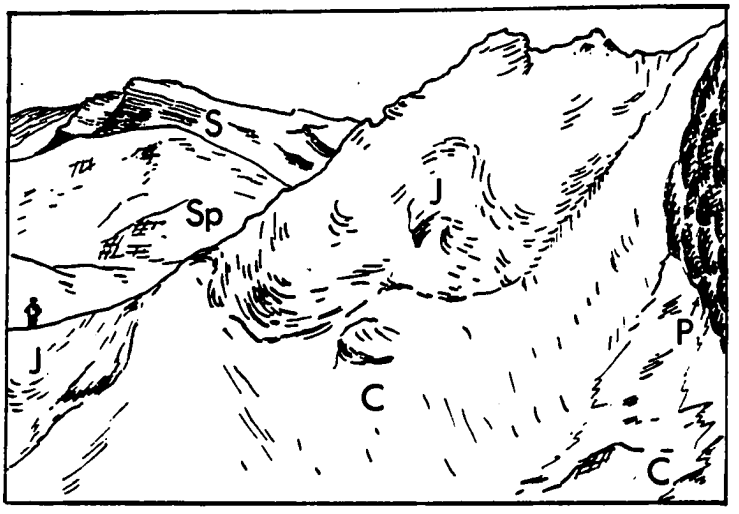

Figure 11. Slump fold in a lenticular bed of thinly laminated calcareous mudstone. Note lack of bedding in the surrounding pebbly material. Rocks above and below this (not shown) dip to the left of observer and are not folded.

(Location 11, Figure 4A; sketch of photograph).

Figure 12. Serpentinite-marl breccia. Picture shows a rectangular clast (with rounded off edges) of serpentinite embedded in a fine-grained marly matrix. White streaks and patches are veinlets of calcite.

(Location 12, Figure 4A).

Figure 13. Geological map of a part of the Kanar Melange (location shown on Figure 4A).

Blank - older alluvium; forms high terraces

A - Diabase-gabbro sills and host chert, argillite and limestone

B - Basaltic pillow lava, chert, argillite and limestone

C - Massive basalt

D - Basalt with columnar joints

E - Serpentinite-carbonate breccia (ophicalcite) and minor detrital serpentinite

F - Serpentinite

G - Pegmatitic gabbro with multiple dikes of basalt

H - Volcanic conglomerate (Porali Conglomerate)

I - Shirinab (?) rocks: Limestone, sandstone and shale

J - Chert

K - Limestone, consists of oolites and biogenic clasts

L - Matrix of melange: Dominantly pelitic rocks (with a few basaltic sills)

M - Sembar Formation (underlies melange): Mudstone and shale

● - Small exposure of serpentinite

o - Fossil locality

——— - Normal contact

---------- - Block - contact, dotted where covered

—▲—▲— - BOT - Basal Ophiolite Thrust (upper contact of melange)

⊥ - Bedding

▲ - Foliation

▲ - Pillow top

✕ - Dike

▬ - Sill

S— S⊥ - Tight complex folds (with and without dip of axial plane)

·····› - Plunging anticline

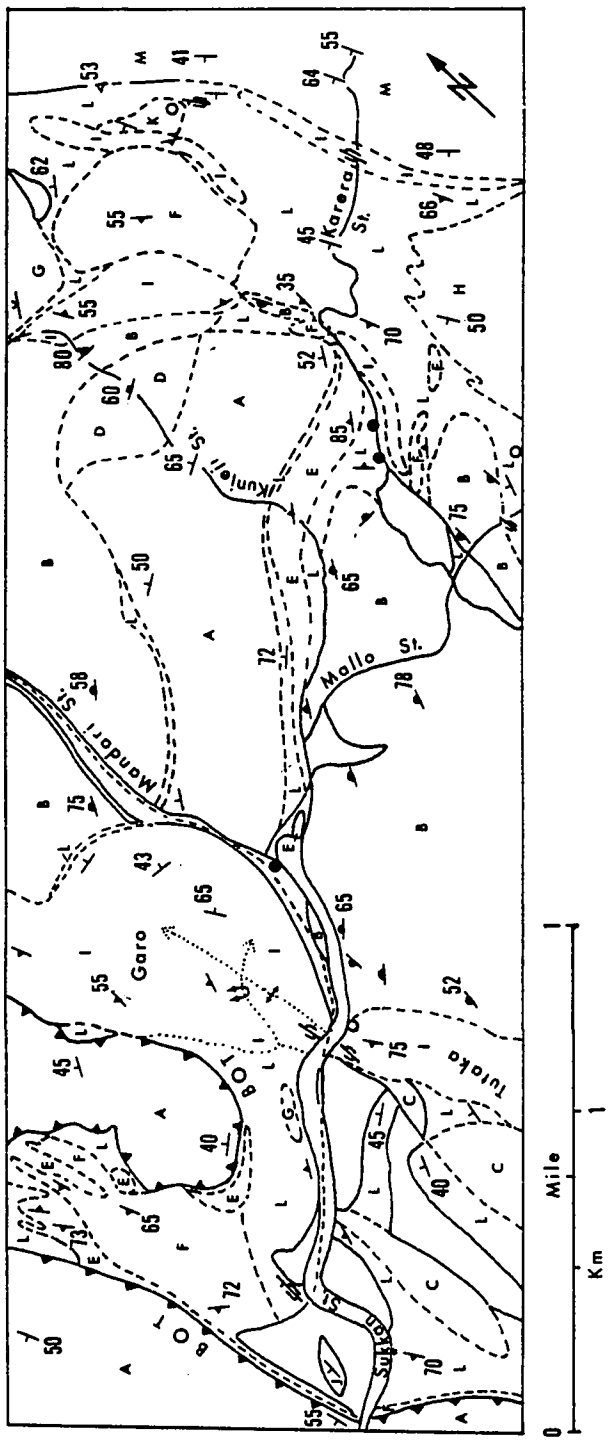

The deformation within the matrix is irregular and varies considerably. The rocks may be mildly deformed to strongly folded and foliated. The mildly deformed rocks show poorly developed bedding parallel cleavage, which in strongly deformed rocks grades into well developed foliation characterized by wavy anastomosing surfaces with a lustrous look and smooth, soapy feel (Figs. 8, 10). Foliation may destroy all traces of bedding. Tight or isoclinal folds are irregular in occurrence and not a dominant structural feature of the matrix. Fold amplitude and axial length is small (up to a few meters and few tens of meters, respectively) and plunging axial traces are common. Folds are asymmetrical with west-dipping axial planes except in the vicinity of large blocks. The attitude of large slab-shaped blocks is frequently discordant with that of the surrounding matrix. On the other hand, smaller clasts tend to be parallel with the fabric of the enclosing matrix. The foliation tightly wraps around smaller clasts (Figs. 8, 10).

Clasts: Most clasts are derived from the Shirinab Formation, the Sembar Formation and the ophiolites, but some are exotic. The Sembar type clasts are difficult to identify because they blend in with the melange matrix.

The Shirinab (?) rocks in the melange consist of limestone, with or without quartzitic sandstone and splintery interbedded shale (Fig. 13). They lithologically resemble the rocks of the Mor Range and Piaro Ridge, and some large blocks contain barite-sulphide mineralization characteristic of the Shirinab Formation. The Shirinab (?) rocks occur either as boulders, blocks, thin slivers or as mountainous slabs of several cubic

kilometers (e.g., the Bujji and the Garo-Tutaka Mountains, Figs. 7, 9, 13). In the western melange belt the Shirinab (?) rocks occur mainly as thin, linear slivers strung out along the upper contact of the melange (see Plate I). Occasional basaltic sills are present within many Shirinab (?) blocks found in both the melange belts. The sills are clearly of pre-melange age and should not be confused with those occurring in the matrix of the Kanar Melange itself.

Large Shirinab (?) blocks are generally strongly deformed (Figs. 7, 9, 13). Their rocks show close or tight folds with amplitude of up to a few tens of meters. At places the folds are disharmonic or irregular. The limestone and sandstone beds are often fractured and boudinaged along the limbs of folds, whereas the shale is pervasively sheared or foliated. Bed attitudes change frequently because of irregular refolding (e.g., Garo block, see Figs. 7-9; 13).

Some Shirinab (?) blocks consist of interlayered, finely laminated to thinly bedded, limestone and calcareous shale. They occur mainly in the eastern melange belt and form folded or foliated slivers of up to a kilometer in length (Fig. 13).

The deformation within most Shirinab (?) blocks is intense compared to that of the pelitic matrix that surrounds them. The same is true for some serpentinite blocks described below.

The ophiolitic clasts found in the Kanar Melange consist of serpentinized ultramafic rocks, serpentinite-carbonate-mud breccia (ophicalcite), sedimentary (detrital) serpentinite, diabase, gabbro, massive or pillowed basalt, chert and other associated sedimentary rocks.

The ultramafic rocks (serpentinite) occur generally as small to large (± 1 km long) lenticular masses, thin slivers and less commonly as blocks (Figs. 9, 10, 13). They are generally foliated, and mostly occur in the eastern melange belt. The rocks are mottled green in color and commonly contain 1/2 mm to 1 cm size pseudomorphs of serpentine after pyroxene with a silky luster and well preserved cleavage. The foliation is defined by wavy, closely spaced, intersecting shiny and smooth surfaces, and imparts a schistose fabric to the rock. Foliation may be irregularly folded, and is discordant with the attitude of the surrounding matrix. Locally small deformed masses of pegmatitic amphibole and pyroxenite dikes are found within a serpentinite body. Small (up to 1.5 meter thick) masses of rodingite (?) are also occasionally found as disoriented slabs immersed in serpentinite. At places serpentinite may be cut by a network of deformed carbonate and asbestos veinlets.

Serpentinite also occurs as foliated slivers interfingered with a dirty red or gray rock composed of serpentinite-carbonate-mud breccia (ophicalcite, Figs. 12, 13). However, the breccia also occurs as separate bodies. It consists of carbonate or marly matrix cementing angular to subrounded, pebbly to jeep-sized clasts mainly of serpentine (Fig. 12). Less commonly, clasts of chert, marl, altered massive or pillowed basalt, limestone and lithic sandstone are also included. The serpentinite-carbonate-mud breccia is generally foliated and apparently gives the impression of a tectonic breccia; however, some appears to be of sedimentary origin (see Appendix 7).

Blocks of detrital or sedimentary serpentinite are also present in the melange (Fig. 14). Lithologically they resemble the serpentinite-

Figure 14. Sedimentary (detrital) serpentinite that forms an isolated slab in the Kanar Melange. Note angular to well-rounded boulders of serpentinite (dark) and local gradational bedding. Dip is steep to the right of observer; top is also toward right. A few clasts of marl, chert and basalt are also present. Similar rocks also occasionally occur within ophiolites.

(Location 14, Figure 4A).

carbonate-mud breccia blocks, but can be easily distinguished from them by the presence of distinct bedding features (e.g., graded bedding and crossbedding). Such features were observed only in a few undeformed blocks though they were suspected also in several foliated serpentinite-carbonate breccias.

Gabbro, dolerite, massive and pillow basalt, and their associated sedimentary rocks occur in melange both as composite and separate slabs of up to several hundred meters dimension (Figs. 8, 9, 13). Since most of these rocks are similar to the corresponding rock types of ophiolites, they are not described here. The blocks of gabbro, basalt and their associated sedimentary rocks are not internally deformed in striking contrast to the Shirinab (?) and most serpentinite-bearing blocks of the melange.

Exotic Clasts: Among these are included those rock types that occur only in the melange. Such rocks, in order of decreasing abundance are: the Porali volcanic conglomerate, certain gabbroic and basaltic rocks, certain biogenic limestone and lithic sandstone (Fig. 13, see Plate I also). A small block of brachiopod-bearing limestone, a block of grayish white granite, and two boulders of schistose metamorphic rocks were also observed.

The Porali Conglomerate (Porali Agglomerate of DeJong and Subhani, 1979) consists of angular to well rounded clasts dominantly of dark volcanic material. Most volcanic debris consists of massive, aphanitic and/or porphyritic lava with mafic (pyroxene) phenocrysts. Vesicular or amygdaloidal varieties are less common. The volcanic clasts of the

conglomerate do not resemble the basalt of Bela Ophiolites. The former is generally gray to dark gray in color, frequently porphyritic and is generally devoid of pillow structure. The basalt of ophiolites, on the other hand, is brownish or greenish gray in color, occasionally porphyritic and commonly pillowed. The conglomerate also lacks clasts of those ultramafic rocks which are associated with the ophiolitic lavas. These differences suggest that the conglomerate was probably not derived from the ophiolites. There is, however, considerable textural and mineralogical resemblance between the basalt of the conglomerate and that of the sills and dikes (Mor Intrusives) that are found in the Shirinab Formation, Sembar Formation and the Porali Conglomerate itself.

Clasts of sedimentary rocks are less common in the Porali Conglomerate. They consist of red marl, pelagic limestone and chert; reworked conglomerate material is also present. All clasts are embedded in a calcareous/volcaniclastic matrix of sand size. The clasts may be angular to well rounded and vary in size from a small pebble to a large house, the average size being about 0.3 meter.

Bedding is generally obscured as the conglomerate is commonly poorly sorted and monotonous in lithology. However, locally it may be well bedded; grading, crossbedding and soft sediment deformational features are also present in places. Bed thickness is variable, however, beds are commonly thick (up to 3 meters). Locally, silt to pebble size material forms lenticular intercalations.

The conglomerate occurs as small boulders to several kilometer-long blocks enveloped in the matrix of the Kanar Melange. The largest block lies north of the Gacheri stream in the eastern melange belt (Fig. 4A);

it is 6 km long and reveals a 1.2 km stratigraphic thickness of the conglomerate sequence. In the western belt, isolated small hills and ridges of conglomerate form most of the melange outcrop along the eastern edge of Piaro Ridge. Shale can be seen in abrupt contact with the conglomerate at the periphery of many isolated outcrops. This suggests that the conglomerate occurs as clasts in a shaly matrix (as in the eastern melange belt) and not as a continuous horizon, as was suggested by DeJong and Subhani (1979). The Porali Conglomerate is not folded.

Exotic clasts of gabbro and basalt are also occasionally found in the Kanar Melange. Two examples are described here: Along the Kunjeji stream, a large (1.5 kilometers) block of a medium-grained to pegmatitic gabbro was observed. A number of basaltic dikes were also noted within the gabbro. The basalt varies in color (light greenish gray to gray) and texture (aphanitic to porphyritic) from dike to dike. From their mutual cross-cutting relations, three generations of dikes were identified. The dikes are up to 2 meters thick and arranged broadly subparallel to one another in strike. The proportion of dike to host rock is highly variable and both extremes are seen within the block. It is possible that this block represents the transitional zone between gabbro and a sheeted dike complex.

A unique type of massive gray basalt was observed in a large block found in the Kunjeji stream gorge. The basalt shows excellent hexagonal and rectangular columnar joints.

Fossiliferous limestone of white, red or gray color occurs in the melange as rounded boulders to small slabs of a few tens of meters length. Occasionally, it forms a large block a kilometer or more in size (see

Plate I). The white and gray limestones consist almost entirely of oolites and some foraminiferal material. The red limestone shows a mixture of small (up to a few cm) angular to subrounded carbonate clasts and fossil debris with occasional graded bedding (turbidite ?). The fossiliferous limestone was seen only in the eastern melange belt and not in the western one.

Environment of Formation and Age of the Kanar Melange: Several features of the Kanar Melange indicate that it is a tectonized sedimentary melange:

(I) The contact of the Kanar Melange and the underlying Sembar Formation is stratigraphic (Figs. 5 and 6; cf. Gucwa, 1975). The contact is irregular and well exposed along the Mor Range. Its irregularity is probably due to the formation of wide channels in the Sembar Formation at the time of melange formation (cf. Shearman, 1977). However, it is emphasized that post-depositional thrusting does occur locally along this contact (e.g., Bhampani stream gorge).

(II) The presence of bedding, graded bedding and occasional slump features in the matrix of melange (Figs. 10, 11).

(III) The rounded shapes of the pebble to boulder size clasts (Figs. 8, 11) and their disposition along certain horizons (Hsu, 1974).

(IV) The great variety of rock types (Figs. 5-14) present as clasts, including some exotics (e.g., Porali Congomerate) (cf. Hsu, 1974; Cowan, 1978).

(V) The presence of brecciated and folded blocks of mechanically resistant rocks (e.g., limestone) within the far less deformed and mechanically less strong pelitic melange matrix.

(VI) The presence of reworked melange material as lithic horizons and pebble to block size debris (cf., Cowan and Page, 1975; Smith et al., 1979).

(VII) The presence of large (up to several kilometers) blocks in the melange. These blocks consist of both ophiolitic and continental rocks (see Plate I, Figs. 4, 13) and are wrapped in the matrix that shows features (1) to (6) above. Therefore, these blocks are interpreted as slide blocks or olistoliths. Examples of slide blocks of comparable size are known also from other mountain belts (e.g., Elter and Trevisan, 1973; Rupke, 1976; Davis et al., 1979).

On the bases of above features the Kanar Melange is interpreted as a complex of olistostromes and olistoliths. It was deposited in a trough which was formed on the western margin of the Indo-Pakistan Block.

A connection between the olistostrome development and strong tectonic activity is well established (Gansser, 1974; Leonov, 1976). The fact that the Kanar Melange contains debris of both continental and oceanic rocks, and is overthrust by ophiolites, indeed suggests strong tectonic movements contemporaneous with melange formation. It appears that much of the ophiolitic debris was derived from the eastward moving and disintegrating ophiolite nappe, which finally overrode the melange. It, therefore, appears that the melange formation and the ophiolite emplacement took place simultaneously. Since the ophiolite emplacement has been dated as Paleocene-Early Eocene (Alleman, 1979), the age of the Kanar Melange is probably the same. The presence of some Aptian-Albian and Maestrichtian microfauna in the clasts of the Kanar Melange also suggests a post-Maestrichtian age for its formation (see Table 3). This

Table 3. Fossils Found in Boulders and Blocks of the Kanar Melange. (Identified by Professor Rolf Schroeder, Goethe University, Frankfurt).

Sample Number (total 6 samples)	Fossil	Age
1, 3, 4, 5, 6	Orbitoides media	Maestrichtian
1, 3, 4, 6	Siderolites calcitrapoides	
1, 3, 4, 6	Rhodophycea (Rotalgen)	
2	Orbitolina sp.	Aptian-Albian

1 - 77-SA-36 Gray pelagic limestone from a hill-size block

2 - SR-38-79 Red carbonate turbidite(?) from a block

3 - SR-76-79 Similar to 36, from a rounded boulder

4 - SR-106-79 Similar to 36, from a rounded boulder

5 - SR-108-79 Similar to 38, from a block

6 - SR-111-79 Similar to 36, from a large hill-size block

(See figures 3 and 4B for location)

notion is further supported by the lithology and internal constitution of certain other Late Cretaceous-Early Eocene rock units that occur in the northern Bela Ophiolite Belt, northern Pab Range, and their vicinity. These units are (Hunting Survey, 1960): the Thar Formation (Late Cretaceous-Paleocene), the Bad Kachu Formation (Late Cretaceous-Paleocene), the Gidar Dhor Group (Late Cretaceous-Early Eocene), and the Wad Limestone (Late Paleocene) (Fig. 2). All of these rock units are overlain by ophiolites and include debris of both ophiolitic and older continental rocks as probable olistoliths and olistostromes. The lower part of the Gidar Dhor Group has been called a "colour melange" by the Hunting Survey (1960, p. 128). Therefore, it is concluded that the Kanar Melange formed during Paleocene-Early Eocene time, and can be broadly correlated with the above rock units.

Bela Group (Cretaceous) (ophiolites)

Within the mapped area, the Bela Group is exposed in a large nappe that overlies the Kanar Melange (Fig. 4A). The group consists of an incomplete ophiolite sequence of basaltic pillow lavas (Bela Volcanics), diabase to gabbro sills (Bela Intrusives), and the associated sedimentary rocks. The latter include pelagic limestones, argillites, and cherts. Several melange horizons characterized by clasts of serpentinite, serpentinite-carbonate-mud breccia (ophicalcite) and other ophiolitic rocks, are also interbedded with the sequence.

A similar rock suite is present also elsewhere (Fig. 3) in the Bela area (Hunting Survey, 1960; DeJong and Subhani, 1979; Gansser, 1979). Subhani reports (pers. comm., 1979) that a sheeted dike complex and some

cumulate layered gabbros are present in the Wad area, some 100 kilometers north of the mapped area (Fig. 2).

Bela Volcanics: The Bela Volcanics consist mainly of spilitic pillowed basalts (Fig. 15) with pillow-breccia and massive flows occurring as minor constituents. The basalts are generally fine grained, but medium-grained and even coarse-grained varieties are locally present. Most basalts are aphanitic but porphyritic and ophitic or subophitic textures are also developed. The rocks are camel brown, reddish brown or greenish gray on weathered surfaces and greenish gray to gray on fresh ones. The average pillow size ranges from 1/2 to 1.2 meters. Locally, basalt may be vesicular or amygdaloidal. Individual flows are generally difficult to distinguish but appear to be 1.5 to 23 meters thick. The interpillow spaces are filled with dull to bright bluish green and/or red fine volcaniclastic material and cherts (Fig. 15). Pillows generally have a chilled border traversed by polygonal tensional fractures. The total thickness of flows is at least one kilometer.

The interflow sedimentary rocks consist of greenish white, red, purple or maroon porcellaneous, sublithographic limestones, marls and cherts. These are intercalated with green, maroon, purple, gray or black shales or siliceous argillites. Also associated are minor amounts of metalliferous sedimentary rocks (Mn, Fe, Cu), some tuffs and ash beds(?). The interflow sedimentary horizons are lenticular and can be as much as 100-140 meters thick. Their cumulative thickness is not known. The flows are interfingered with the sedimentary rocks.

Figure 15. Pillow lava; arrows mark the inter-pillow spaces filled with fine-grained clastic material and chert.

(Location 15, Figure 4A; sketch of photograph).

Bela Intrusives: The Bela intrusive rocks are generally thick and extensive sills that were emplaced into a sequence of pillow lavas and the associated sedimentary rocks (Fig. 16). The sills are light brownish to greenish gray weathering and greenish gray to gray in fresh; they consist of diabases and gabbros showing fine to coarse, equigranular, subophitic or ophitic textures. Individual sills vary in thickness from less than a meter to 150 meters and many thick sills can be traced for several kilometers. Mineral segregation within the bodies is either absent or only crudely developed. Most of the sills were emplaced along sedimentary horizons. Sills intruding pillow lavas without any associated sedimentary rocks were not observed. The contacts of sills are usually chilled, and are generally concordant on a large scale, though some may be discordant (Fig. 17) and wavy on a small scale. Thin shoots of dark fine-grained basalt may be present along contacts in the intruded rocks. Contact metamorphic effects are generally poor, especially in the lavas, where sills have intruded along the lava-sediment interface.

The intersill sedimentary rocks are lithologically similar to those occurring with lavas. They may vary in thickness from less than a meter to 160 meters, and frequently wedge out along strike. Formation of calc-silicates (epidote group) may be locally observed in the calcareous sedimentary rocks along the contacts with sills. The shales and mudstone are baked, silicified or hornfelsized. Generally the hornfels form only a thin (a few centimeters) border along the contact.

Melanges Within Ophiolites: These melanges occur as thin but extensive horizons associated with the sedimentary rocks that are interlayered with the lava flows and sills (Figs. 18-20). Lithologically, the melange is

Figure 16. Steeply dipping sequence of argillite, limestone (L), gabbro sills (G) and pillow lava (P) is cut by Watri fault which is shown by thick arrows in the lower part of figure. Note fault related drag in the limestone bed (L').

(Location 16, Figure 4A; sketch of photograph).

Figure 17. Part of a gabbro sill (dark) that locally cuts across limestone beds (L). Inset shows schematic cross-section of sill and the location of enlarged view.

(Location 17, Figure 4A; sketch of photograph).

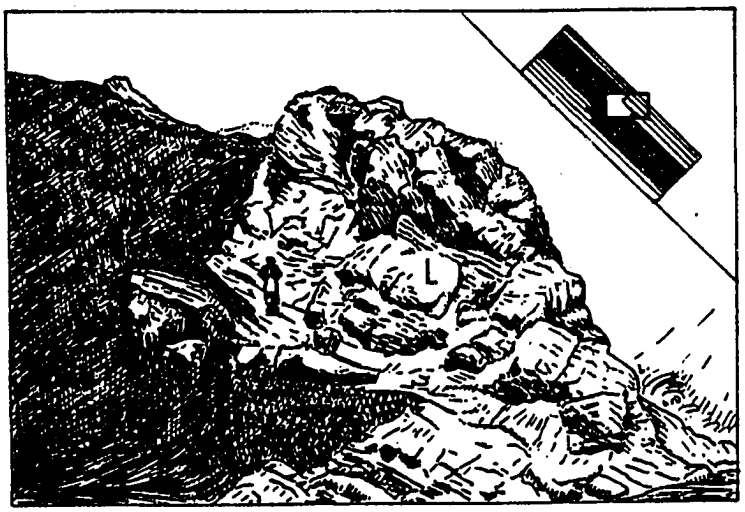

Figure 18. View of inter-ophiolite melange (M) which is underlain by pillow lava (P) and overlain by shale-mudstone beds (Sh) and topped by a gabbro sill (G). The melange consists of clasts of foliated serpentinite (S), serpentinite-carbonate-mudstone breccia (B), chert, gabbro, and basalt (not shown) embedded in an argillaceous matrix. The contact of melange and pillow lava is discordant and tectonized whereas that of the melange and overlying shale-mudstone is depositional; this is suggested by absence of deformation in the shale which fills in the upper irregular surface of both the foliated serpentinite and breccia.

(See Figure 19 also; Location 18, Figure 4A; sketch of photograph).

Figure 19. Foliated serpentinite (S) of the inter-ophiolite melange (shown in Figure 18) overlain by shale and intercalated mudstone (Sh). The shale/mudstone is essentially undisturbed and fills in the irregular surface on top of the serpentinite, strongly suggesting a depositional contact.

C = partly covered shale.

(Location 19, Figure 4A; sketch of photograph).

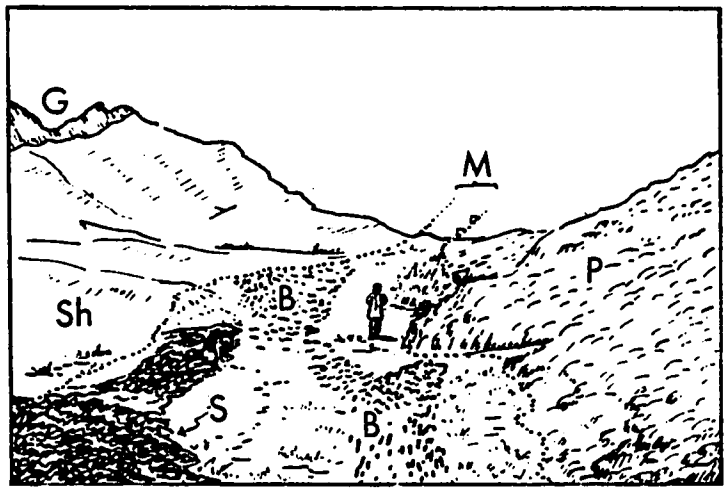

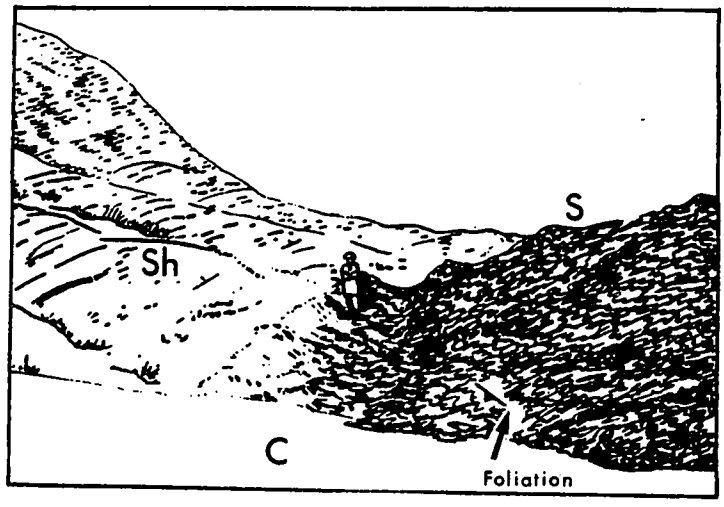

characterized dominantly by fractured, brecciated or foliated masses of highly serpentinized ultramafic rocks (serpentinite), and serpentinite-carbonate-mud breccia (ophicalcite, Figs. 18-22). Less commonly, clasts of diabase, gabbro, pegmatitic gabbro, massive or pillowed basalt, chaotic chert, lithic sandstone, limestone and marl are also found. Rarely, boulders and small blocks of serpentinized dunite, chromitite, metagabbro and amphibolite are also present (Figs. 18-22). The serpentinite-bearing clasts range in size from less than a meter to large slabs of several hundred meters length. The size of other clasts range from 1/2 meter to several tens of meters. Clasts are variable in shape but some appear to be rounded boulders. Most clasts are derived from ophiolitic rocks and are embedded in a matrix of argillaceous rocks. Clastic beds of sand to cobble-size debris of ophiolitic rocks are also locally present. At two localities well bedded sedimentary serpentinite was observed adjacent to large foliated serpentinite and breccia slivers.

The serpentinite and breccia slabs generally show irregular foliation and/or brecciation (Figs. 19, 20, 22). In contrast with these most other clasts of the melange may only be fractured and not foliated. The rocks of the matrix may be undeformed, irregularly warped, folded or chaotically mixed with the clasts along the base of the melange. The basal contacts of the melange horizons are also frequently discordant to the attitudes of the underlying rocks and cut across lithologic boundaries (see Plate I). Although the discordance can be explained by thrusting alone, it is believed that unconformable relationships, subsequently overprinted by shearing, are more likely. This follows from the fact that the upper contacts of melange horizons are generally with relatively

Figure 20. View of an inter-ophiolite melange and its basal tectonic contact (Dadi Thrust, shown by fault zone F) with pillow lava (P). Pillow lava is strongly sheared near the contact and undisturbed away from it. Melange consists of the following (foliated) rocks:

Sh = shale
S = serpentinite
B = breccia - clasts of serpentinite (up to 0.3 m), red chert, and marl set in a calcareous matrix
C = covered

S and B also occur in a similar fashion in Kanar Melange

(Location 20, Figure 4A; sketch of photograph).

Figure 21. View showing isolated outcrops of an inter-ophiolite melange surrounded by alluvium. Outcrops consist largely of serpentinite blocks; however, a few blocks of pegmatitic gabbro, massive basalt, serpentinite-mudstone breccia, and lithic sandstone are also present. View also shows two generations of alluvial terraces—a younger (T1) and an older (T2). Present-day stream channels are cut into T1 (see text for discussion). The hill in the background is Piaro Ridge.

(Location 21, Figure 4A; sketch of photograph).

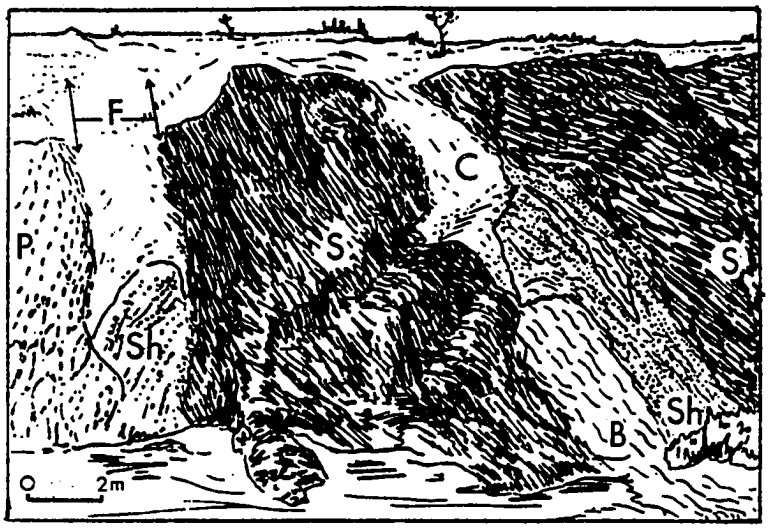

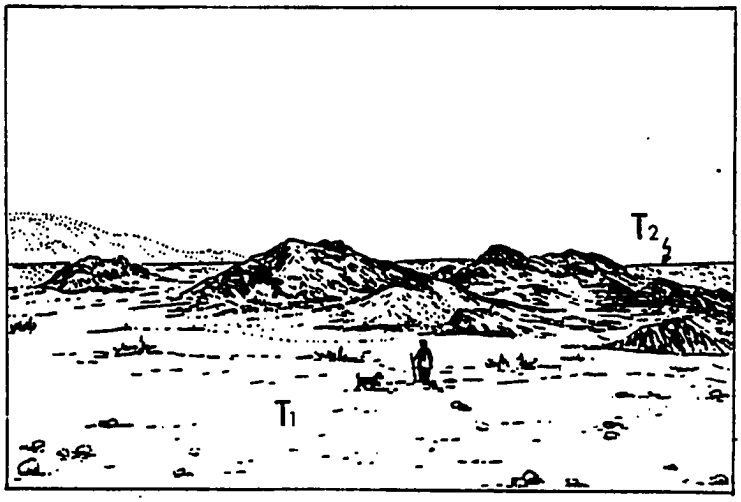

undisturbed shales and mudstones. The contrast is most striking where clearly undisturbed shales overlie foliated serpentinite and breccia slivers (Figs. 18-19) along an irregular contact. Such a relationship strongly suggests a depositional contact. Also the presence of pebble and cobble beds within the melange horizons indicates a sedimentary origin. This leads to the conclusion that the melange horizons represent ophiolitic debris that was intermittently deposited on irregular surfaces. The ophiolite sequence can be considered as a stack of rock units, separated from one another by irregular unconformable surfaces defined by the basal contacts of the melange horizons. Five rock units of this kind were recognized in the ophiolite sequence and are shown in Figure 4A (inset).

Isolated slivers of brecciated or foliated serpentinite and/or ophicalcite are also found as concordant or subconcordant masses, wrapped in relatively undisturbed argillaceous rocks, and irregularly distributed throughout the ophiolite sequence (Plate I, and Figs. 4A, 23). Clasts of other rock types such as chert, basalt, or gabbro commonly do not occur with these slivers. Most slivers are small (up to a few tens of meters long); however, large slivers are present in the northwest part of the mapped area where they are partly exposed through the alluvium (Plate I). All slivers are interpreted as slide masses.

Besides the above, foliated serpentinite, mixed with argillaceous rocks, occasionally occurs also along transverse faults. A good example of this is located along an east-west fault, east of the Andhoro copper prospect (Fig. 4A). The fault cuts an interlayered limestone/shale/gabbro sill sequence underlain by serpentinite, which appears to have

Figure 22. Breccia consisting of angular serpentinite clasts set in a matrix of finer serpentinite and carbonate material. All clasts are of serpentinite.

(Sketch of hand specimen, Location 22, Figure 4A).

Figure 23. View showing (from bottom to top) pillow lava (P), a lenticular slab (20 m thick and 140 m long) of foliated serpentinite-carbonate mudstone breccia (B), shale (S) and a gabbro sill (G). The shale and gabbro sill are members of an alternating sequence of sedimentary rocks (argillite, limestone, minor chert) and diabase-gabbro sills which form the hills in the background. Shale also occurs as screen between the pillow lava (P) and the breccia slab (B). The slab (B) lies sub-parallel to the pillow lava (P) and is depositionally overlain by the shale (S). All rocks except the breccia are essentially undeformed.

(Location 23, Figure 4A; sketch of photograph; note hut for scale).

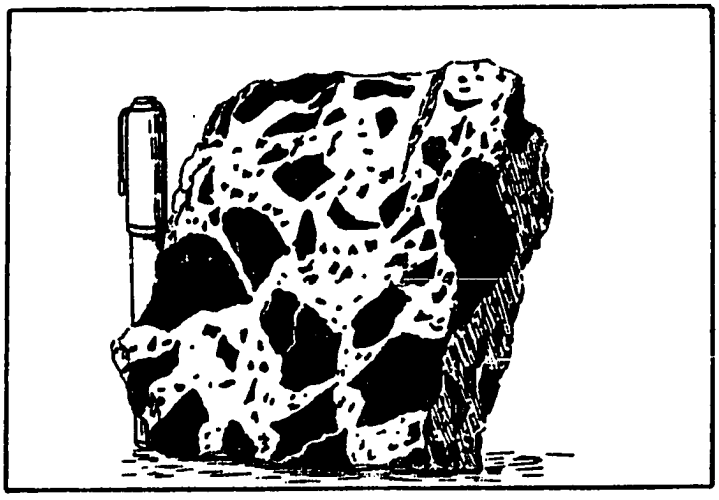

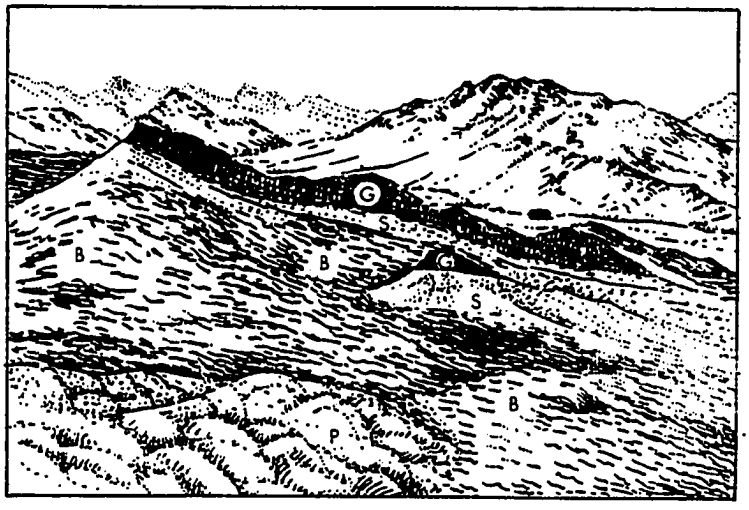

been squeezed into the fault zone. Isolated exposures of similar serpentinite are known also from a few other transverse faults (see Fig. 4A). The phenomenon can probably be explained as due to post-emplacement remobilization of serpentinite along a fault zone (Moiseyev, 1970).

Age of the Bela Ophiolites: Previously the Bela ophiolites were included in the Bela Volcanic Group of Cretaceous age (Hunting Survey, 1960; Shah, 1977) and the Porali intrusives of Late Cretaceous-Early Eocene age (Hunting Survey, 1960; Bakr and Jackson, 1964) which were believed to intrude the Bela Volcanic Group. The Hunting Survey (1960) reported the occurrence of radiolarites in the sedimentary rocks associated with the pillow lavas without making any further comments. Allemann had recognized certain "Late Cretaceous fossils" in the maroon shales associated with the gabbro sills in the adjacent Kanar area (pers. comm. to DeJong and Subhani, 1979, p. 267).

It appears from the above that the rocks now termed as the Bela Ophiolites were generally considered to be of Cretaceous age. However, there was little paleontologic information to support this notion. Table 4 represents a list of the microfauna identified in certain pelagic horizons that are interlayered with the pillow lavas. According to this work, the Bela Ophiolites are of upper lower Cretaceous-upper Cretaceous age (Aptian-Early Maestrichtian). However, this is based only on four rock samples taken from different parts of the ophiolite sequence and should be treated with caution.

Table 4. Fossils Found in Pelagic Sedimentary Rocks Interlayered with the Lava Flows of the Bela Ophiolites. (Identified by Professor Dietrich Herm, Munich University).

Sample Number* (Total 4 Samples)	Fossil	Age
SR-112-79 (light gray pelagic limestone)	Globotruncana elevata	Campian-lowermost Maestrichtian
	Globotruncana area	
	Globotruncana ventricosa	
	Globotruncana stuarti	
SR-31-79 (red marl)	Globotruncana bulloides	Turonian-Coniacian
	Globotruncana marginata	
	Globotruncana lapparenti	
	Archeoglobigerina sp.	
SR-12-79 (white sub-lithographic limestone)	Rotalipora appenninica	middle-upper Cenomanian
	Rotalipora greenhornensis	
	Rotalipora cushmani	
SR-59-79 (similar to 12)	Hedbergella sp.	Aptian-lower Albian
	Ticinella sp.	

*(see Fig. 4B for sample locations).

Quaternary

Quaternary deposits cover a large tract in the western half of the area which lies along the eastern edge of the Neogene Bela trough (Sarwar and DeJong, 1979). The material consists mainly of loose or poorly indurated coalesced fan gravels, but locally (e.g., west of Piaro Ridge), wind blown sand and silt may form patchy mounds up to a few meters thick. The sand is dumped by the prevalent western winds in the wake of a dust-storm and lies mainly along Piaro Ridge. East of Piaro Ridge almost all stream banks show high (5-20 meters) gravel terraces; sometimes two or even three of them in steps (Fig. 21). Tilted terraces occur 40 kilometers to the north at Kanar where tectonic dips of 5-25 degrees can be noticed. Within the mapped area, at several places, the level of the highest step-terrace is well above the adjacent rock outcrop (Fig. 21), indicating that in sub-recent time a much larger part of the area was buried under the gravel. The above information clearly indicates the effects of current tectonic activity in the area (see also Pennington, 1979; Kazmi, 1979; Quittmeyer et al., 1979; Lawrence and Yeats, 1979; and Sarwar and DeJong, 1979). This current uplift and deformation is largely responsible for the rejuvenated erosion and the present amount of rock exposure in the whole area.

PETROGRAPHY AND CHEMISTRY OF SELECTED ROCKS

The petrographic and chemical features of the Mor Intrusives, the Porali Conglomerate volcanic clasts, and the Bela Ophiolites are described in this section.

Mor Intrusives

Introduction

The name Mor Intrusives has been introduced here for the melanocratic sills and dikes that cut the autochthonous sedimentary sequence in the Bela area. The term "Mor" comes from the Mor Range which parallels the Bela Ophiolite Belt along its eastern side (Fig. 2), and consists largely of Shirinab Formation. It should be emphasized that melanocratic sills and dikes in the Mesozoic autochthonous sedimentary sequence are not confined only to the Bela area, but are known also from elsewhere in the Kirthar Range, e.g., in the Jurassic limestone east of the Murdar Mountain cemetery at Quetta (Fig. 1), and 50 kilometers east of there in the Cretaceous limestone near the village of Kach (Sarwar, unpublished). Gansser (1979, Figs. 7 and 28) has mentioned some mafic dikes in the Jurassic limestone below the Muslimbagh Ophiolites and also from the Bela area. White (1981) has described a diabase sill in the lower Cretaceous Goru Formation from the southern part of the Mor Range.

The Mor Intrusives have not been studied before and the following brief account is valid only for the Wayaro-Kanar area in the Las Bela District:

In the Bela area, the Mor Intrusives generally occur as sills and occasional dikes of light to dark grayish green or brown color in the Shirinab Formation, the Sembar Formation and the Kanar Melange. In hand specimen, they apparently consist of aphanitic to porphyritic mafic material with greenish gray pyroxene phenocrysts (up to 0.5 cm); however, as described later, a variety of rocks, including some ultramafic ones, is present. Thickness of sills and dikes varies from less than 0.5 m to as much as 20 m; however, most are 0.5-2 m thick. Their lateral extent is usually small (100-200 m) because of the structural complexity caused by the post-intrusion folding of the host rocks. Their contacts are commonly somewhat chilled and show slight metamorphic effects (e.g., baking) in the host shales and mudstones; even limestone host rocks are practically unaffected. A number of sills show faulted contacts with the host rocks and are folded along with the host rocks, especially along the eastern slope of Piaro Ridge.

Petrography

Eleven samples of sills and dikes were collected from the Wayaro and Kanar areas. Of these, four samples came from the Shirinab Formation, six from the Sembar Formation, and one from the Kanar Melange. Petrographic description of all samples are included in Appendix 2 and locations are shown in Figures 3 and 4. The main features of samples from the three stratigraphic units are outlined as follows:

(1) Shirinab Formation: The four samples are divided in two petrographic types.

A. without feldspar (Limburgites)

Sample 77-SA-4: Highly altered subporphyritic rock with serpentinized phenocrysts of pyroxene and olivine set in a matrix of serpentine, calcite, biotite and opaques.

Sample 77-SA-6: Glomeroporphyritic rock with phenocrysts of titanaugite and altered olivine (pseudomorphs of serpentine, calcite and chlorite) set in a matrix of altered glass, biotite, clinopyroxene, calcite and opaque minerals (Fig. 24).

The titanaugite phenocrysts in sample 77-SA-6 are very similar to those found in some clasts of the Porali Conglomerate in that they show the same anamolous blue interference color and concentric/hourglass type zoning. Based on the overall petrographic features, the above two samples can be classes as altered limburgites (Williams et al., 1954; Wilkinson, 1967; Sorensen, 1974, p. 568).

B. with feldspar and quartz (Alkali basalt)

Sample 77-SA-24: Fine-grained holocrystalline altered rock with largely carbonatized sodic plagioclase (oligoclase ?) laths, (serpentine/calcite) pseudomorphs after pyroxene and olivine, calcite, opaque minerals, accessory quartz and apatite.

Sample 77-SA-26: Porphyritic rock with sodic (oligoclase-andesine ?) plagioclase phenocrysts set in a fine-grained matrix of plagioclase, opaque minerals, chlorite and accessory quartz.

Figure 24. Altered limburgite showing a pseudomorph of calcite and serpentine after olivine with fractures lined with opaque material. Smaller phenocrysts of titanaugite are also present. Surrounding groundmass consists of opaque dust, titanaugite grains, some biotite and glass; a veinlet of chlorite and calcite is also present (parallel nicols).

(Sample No. 77-SA-6)

Figure 25. Altered porphyritic basalt showing laths of zoned plagioclase feldspar pseudomorphed by a mixture of calcite and chlorite. In the largest lath clear calcite occupies the central part. Groundmass consists of a mesostasis of tiny opaque needles, chlorite and calcite (parallel nicols).

(Sample No. SR-5-79)

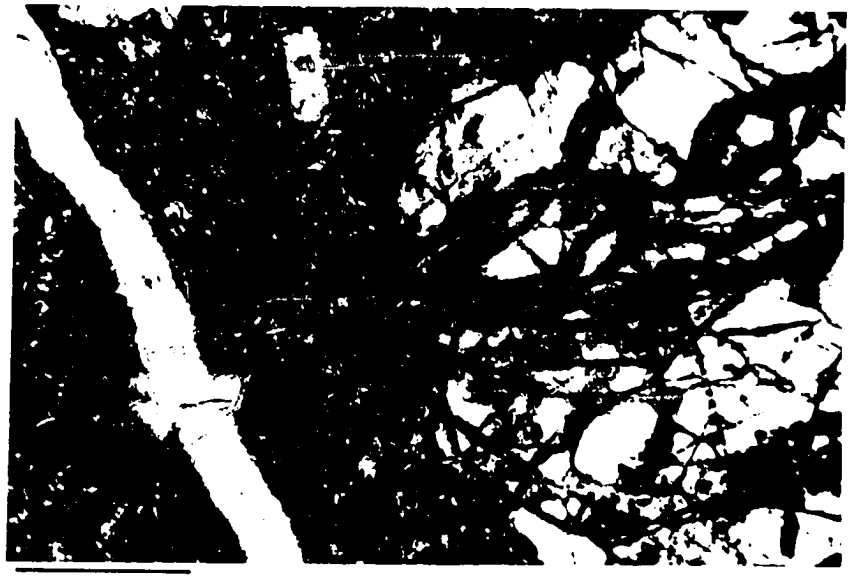

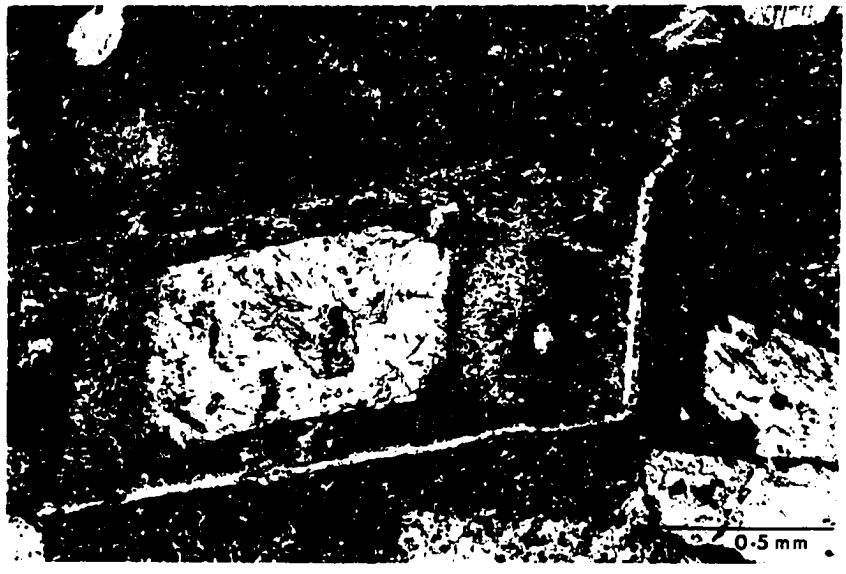

These rocks are tentatively classed as altered alkali basalts due to the presence of the sodic plagioclase (see Figure 26 also). They differ from the sills and dikes of the Sembar Formation (see below) in having oligoclase-andesine plagioclase (and accessory quartz) instead of albitic plagioclase.

(2) Sembar Formation: The sill/dike rocks of the Sembar Formation can also be grouped in two arbitrary classes.

A. highly altered basalts with secondary minerals (greenstones):

They include Samples SR-5-79, SR-11-79, SR-56-79 and SR-95-79. Except for the last one, all are porphyritic with clinopyroxene and/or plagioclase phenocrysts partly or wholly replaced by calcite and/or chlorite (Fig. 25). The groundmass consists of a variable combination of the following minerals: plagioclase microliths, chlorite, calcite, opaques (magnetite, hematite), with or without traces of brown biotite. Due to strong alteration nothing can be said about the original composition of the feldspars and pyroxenes.

B. Relatively less altered alkali basalts:

They include Samples SR-82-79 and SR-71-79. These rocks are also porphyritic. The Sample SR-82-79 consists of zoned clinopyroxene and plagioclase phenocrysts set in a matrix of acicular albitic plagioclase, chlorite, calcite, opaques and a trace of apatite. The composition of the plagioclase phenocrysts is not known.

The Sample SR-71-79 consists of albitic phenocrysts and chloritic patches (pseudomorphs after pyroxene ?) set in a matrix of plagioclase microliths, chlorite, calcite, and opaques. Though chlorite

and calcite replacement of phenocrysts and groundmass is present, it is less complete than in the altered basalts described above. However, these rocks are far more altered and texturally different from those of the Bela volcanics.

(3) Kanar Melange: The only sample (SR-9-79) from the Kanar Melange comes from a sill. The rock is porphyritic with phenocrysts of albitic plagioclase set in a matrix of glass, chlorite, calcite, opaque minerals (magnetite) and apatite. Some phenocrysts are replaced by chlorite ± calcite. The rock can be classed as porphyritic plagioclase basalt.

Chemical Affiliation: Analytical data on the major and trace element contents of the Mor Intrusives is reported in Appendix 10B.

Alkali SiO_2 Diagram: This diagram is commonly used to determine the alkaline versus tholeiitic character of igneous rocks (e.g., Moores and Vine, 1971; Carmaichael et al., 1974). Plotted on an alkali-SiO_2 diagram (Fig. 26), it can be seen that:

All of the samples fall in the field of alkali basalts with the two ultramafic samples (limburgites) showing very low SiO_2 and alkali contents. The altered basalts (greenstones) from the Sembar Formation have a higher range of SiO_2 and alkalis. The sample from the Kanar Melange (SR-9-79) shows the highest alkali content.

Na_2O:K_2O Diagram: This diagram is used to distinguish soda-rich alkaline rocks from their potash-rich equivalents (Middlemost, 1975). Plotted on a Na_2O:K_2O diagram (Fig. 27), it can be seen that one limburgite and one greenstone fall in the field of K-Series whereas all others lie in the field of Na-Series. These rocks show high Na_2O content but are low in K_2O.

Figure 26. Alkali-SiO_2 plot for the Mor Intrusives and the Porali Conglomerate rocks.

line A = from Schwarzer and Rogers (1974)

line B = Hawaii alkali basalt - tholeiite line of MacDonald and Katsura (1964).

line C = from Miyashiro (1978)

Δ = Porali Conglomerate volcanic clasts

∇ = dikes in Porali Conglomerate

o = Mor Intrusives

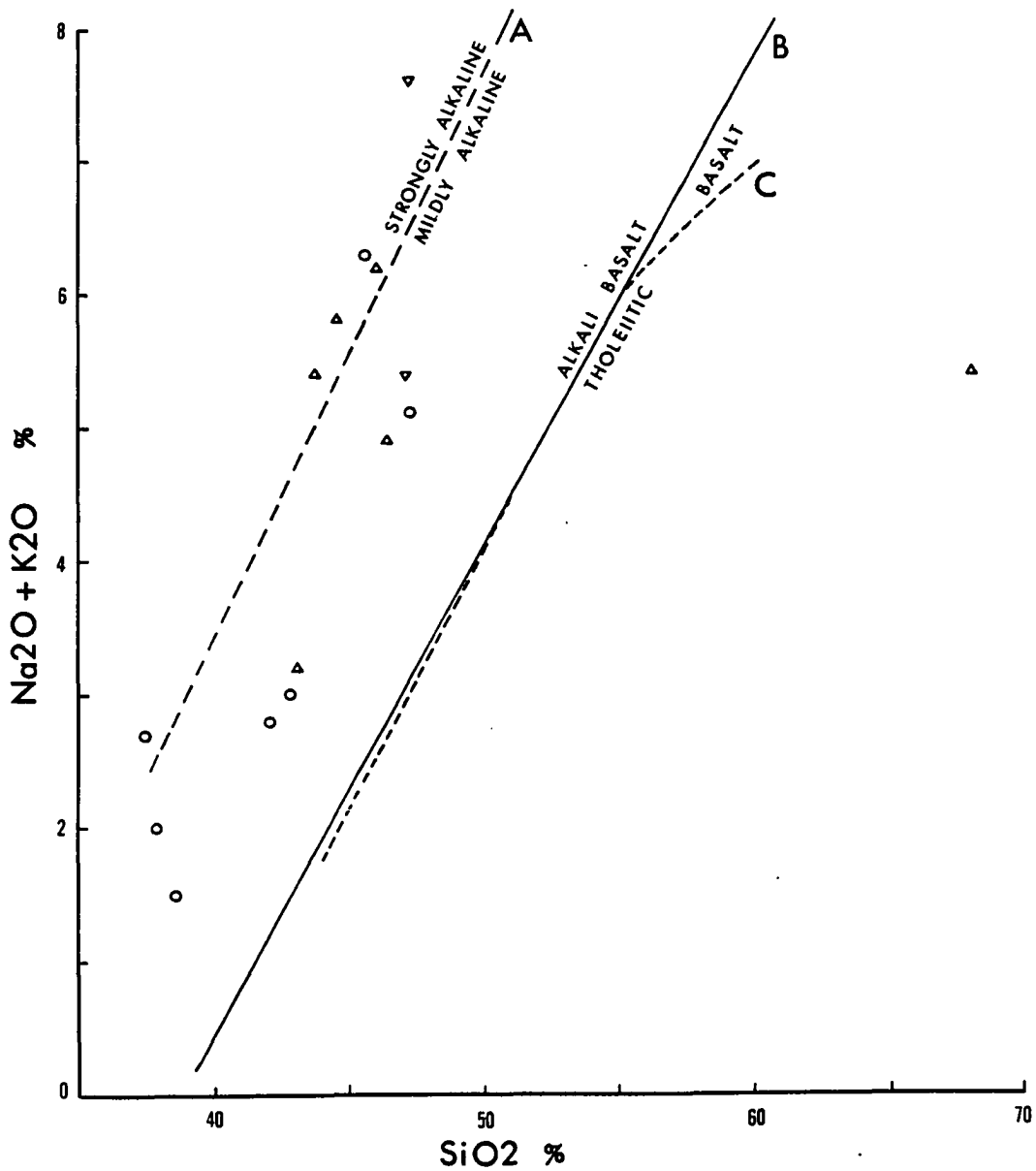

Figure 27. Na_2O versus K_2O plot for the Mor Intrusives, Porali Conglomerate volcanic clasts and two dikes that cut the conglomerate.

o = Mor Intrusvies

Δ = Porali Conglomerate

∇ = dikes that cut the Porali Conglomerate

(Diagram from Middlemost, 1975).

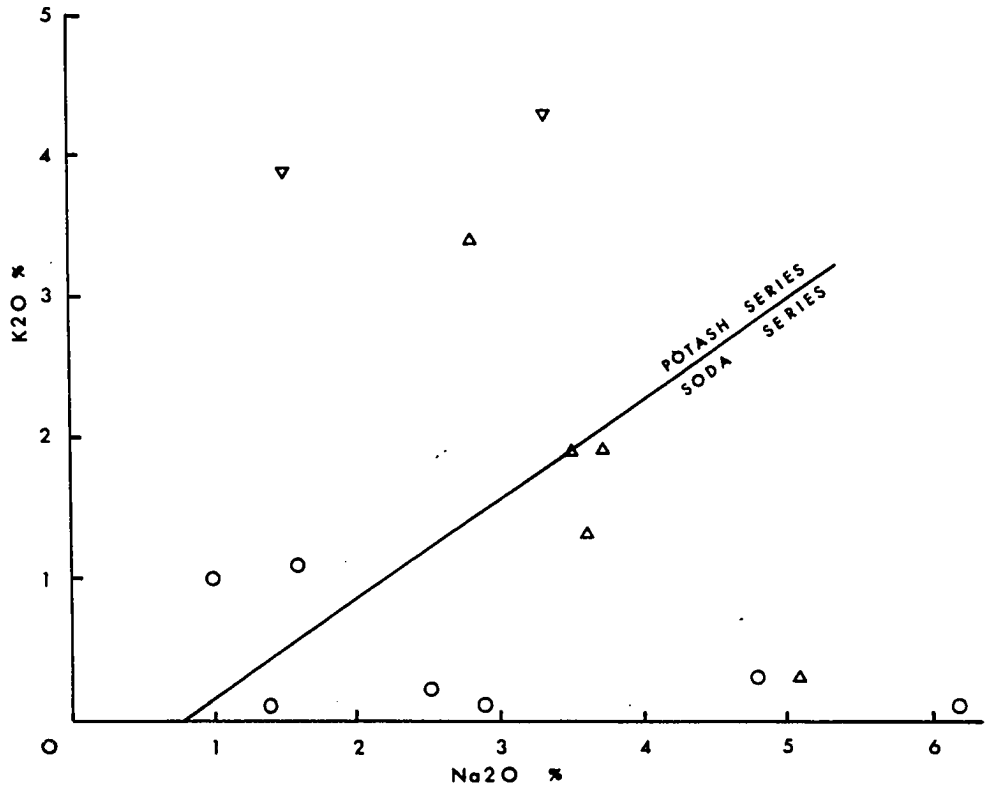

AFM Diagram: The alkaline trend of the sill and dike rocks is also manifest on an AFM diagram (Fig. 28). As shown, the limburgites are Mg-enriched and depleted in alkalis. Thus they appear to be most primitive. Other samples are alkali enriched.

Rare Earth Element (REE) Distribution: The REE data for four samples of Mor Intrusives is given in Table 5 and is plotted in Figure 29. The REE patterns are normalized by dividing each element by its average chondritic abundance (Haskin et al., 1968) and then plotted on a semi-logarithmic scale for ease of presentation.

The sills and dikes are strongly enriched in the light rare earths (LREE; i.e., La, Ce) as compared to the heavy ones (HREE; i.e., Yb, Lu). This is shown by the following ratios and Figure 29.

$$\left[\frac{La}{Sm}\right]^N = 2.75\text{-}3.8$$

$$\left[\frac{La}{Yb}\right]^N = 15.3\text{-}23.1$$

$$\left[\frac{Ce}{Yb}\right]^N = 8.4\text{-}17.31$$

Compared to the chondrites the Mor Intrusives are (125-268.94) times enriched in La and (6.9-9.38) times enriched in Lu. Except for one sample (SR-11-79), the general enrichment trend seems to be quite uniform and is devoid of any anomaly. The Sample SR-11-79 appears to be different and shows four prominent anomalies: two positive at Tb and Nd and two negative at Eu and Ce.

Figure 28. AFM plot for the Mor Intrusives and the Porali Conglomerate rocks.

o = Mor Intrusives

Δ = Porali volcanic clasts

∇ = dikes in Porali Conglomerate

Small triangle shows fractionation trends (Carmaichael et al., 1974) for three continental igneous series:

x = Skaergaard Tholeiitic Series

Y = New Zealand (East Otago) Alkaline Series

z = Moroto, East Uganda Alkaline Series

Note that both the Mor and Porali rocks apparently form an alkaline trend similar to the New Zealand/Uganda trends.

Table 5. Chondrite-normalized REE data for the analyzed rocks and certain ratios. Normalization was done by dividing the raw REE data (Appendix/OB) by the respective chondrite values from Haskin et al. (1968) listed below.

	La	Ce	Nd	Sm	Eu	Tb	Yb	Lu	LaN/YbN	LaN/SmN	CeN/YbN
Bela Volcanics											
SR-16-79	32.27	28.05	<60.23	28.85	27.69	51.77	7.59	12.64	4.25	1.2	3.7
SR-30-79	29.12	30.4	<61.97	27.88	29.3	51.87	8.62	12.79	3.38	1.04	3.52
SR-88-79	27.28	36.21	<56.94	29.4	29.44	43.55	9.29	12.7	4.01	1.27	3.9
SR-99-79	31.73	31.62	72.175	26.3	27.56	26.76	9.07	11.9	3.5	1.2	3.49
SR-104-79	33.09	28.82	<60.48	26.82	27.32	44.24	8.15	10.26	4.06	1.23	3.53
78-SR-42	26.82	21.27	<60.25	22.43	23.26	25.31	8.6	9.88	3.12	1.2	2.47
Bela Intrusives											
SR-14-79	32.3	34.7	70.48	26.43	23.52	<7.75	9.25	12.04	3.49	1.22	3.75
SR-21-79	72.7	66.05	86.12	49.92	43.54	59.61	16.57	20.39	4.39	1.45	3.99
SR-34-79	86.2	79.32	78.72	55.23	47.95	33.9	13.43	13.99	6.42	1.56	5.9
SR-45-79	37.38	37.59	<54.24	32.64	29.25	59.66	9.69	12.93	3.86	1.14	3.88
SR-73-79	49.93	46.73	65.1	35.33	34.56	37.58	12.24	14.75	4.08	1.41	3.81
Mor Intrusives											
SR-5-79	268.94	201.59	168.06	78.365	66.43	--	11.64	6.97	23.1	3.43	17.31
SR-11-79	125.59	69.05	86.21	45.7	38.75	44.83	8 19	7.95	15.33	2.75	8.43
SR-82-79	209.65	156.27	128.27	56.5	49.44	--	13.53	9.38	15.5	3.71	11.55
SR-95-79	201.94	151.7	107.62	53.16	44.24	40.69	9.49	6.95	21.28	3.8	15.99
Porali Conglomerate											
SR-1-79	333.7	249.22	198.73	76.94	69.84	41.6	17.007	8.9	19.62	4.34	14.65
SR-3-79	243.63	202.04	146.52	65.05	64.06	46.72	15.38	7.22	15.84	3.74	13.13
SR-7-79	192.74	145.54	112.23	54.31	48.06	39.74	12.33	7.3	15.63	3.55	11.8
SR-81-79	244.92	187.46	111.91	61.1	55.1	28.57	13.5	8.67	18.14	4.00	13.88
Dike in Porali Conglomerate											
SR-4-79	184.55	146.5	116.31	64.31	59.17	40.57	15.31	10.47	12.05	2.87	9.56
Chondrite	0.33	0.88	0.6	0.181	0.069	0.047	0.2	0.034			

Figure 29. REE distribution patterns for the Mor Intrusives.

Analyzed samples:

A = SR-5-79

B = SR-82-79

C = SR-95-79

D = SR-11-79

Tb content in samples A and B is below the detection limit (< 0.3/ppm and < 0.272/ppm, respectively).

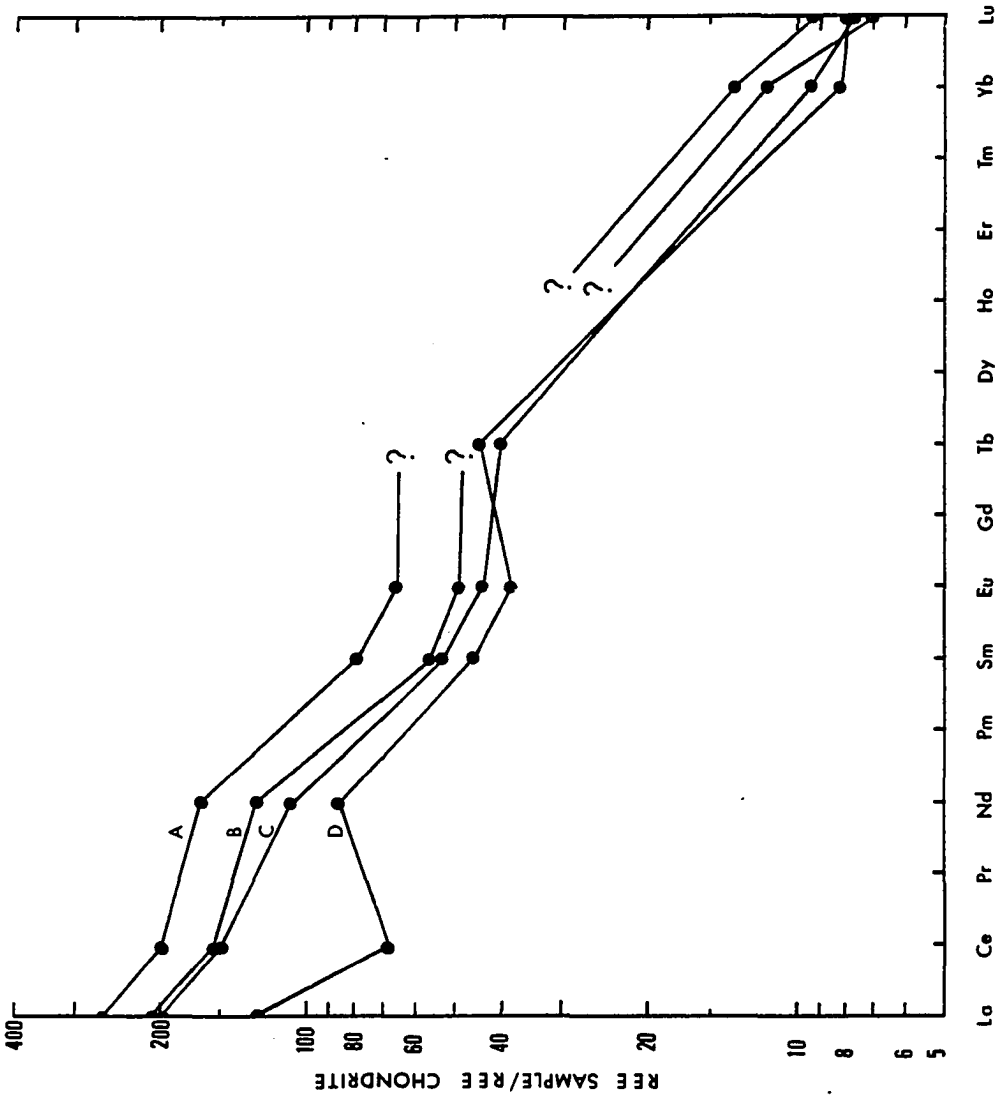

From the above observations it appears that the Mor Intrusives consist of ultramafic and mafic rocks (altered limburgites/alkali basalts). Their chemical and petrographic traits are variable but all belong to the alkaline series and are LREE enriched.

Porali Conglomerate

Problem of Its Source

As described previously the Porali Conglomerate consists mainly of volcanic clasts and occurs as boulders and blocks in the Kanar Melange, which overlies the Sembar Formation; both formations are cut by the Mor Intrusives. The Kanar Melange is overlain by the Bela Ophiolites which also include abundant basaltic rocks. Given this situation, one can assume that the source of the Porali Conglomerate was either the ophiolitic debris (oceanic source) and/or some volcanoes that once existed on the then continental margin itself (continental source); it is also possible that those volcanoes were fed by some of the Mor Intrusives.

Whatever the source of the conglomerate, the petrographic similarity between its clasts and the dikes cutting its own mass, attest to the fact that the conglomerate was initially formed within or adjacent to the area where the igneous activity took place. The monotonous volcanic character of the conglomerate, poor sorting, general lack of bedding and tremendous thickness, also indicate that its debris was rapidly laid down in thick piles not far from the source. Subsequently, the conglomerate was dismembered and incorporated in the Melange.

The petrographic and chemical features of the Porali Conglomerate are described in the following paragraphs. Later, this information will

be used to solve the problem of its source by making comparisons with the Mor Intrusives and the Bela basalts.

Petrography;

Nine samples of melanocratic volcanic clasts believed to be the most common rock type in the conglomerate, were collected. In addition, a couple of samples were taken from two different dikes that were noticed in the large conglomerate block shown in Figure 4A. Six of these samples from clasts and both from the dikes were analyzed for major elements. Of these, four clasts and one dike sample were also analyzed for trace elements. All analytical data are presented in Appendix 10B.

Clasts:

Petrographically, these rocks are brownish or greenish gray to dark gray in color and frequently exhibit porphyritic or seriate texture. The phenocrysts range in size from 1-7 mm (mostly 1.5-2.5 mm). Eight samples contain subhedral-euhedral greenish-gray titanaugite phenocrysts. In thin section, they are purplish or brownish in color and show a rather anomalous blue interference color, concentric zoning and hour-glass structure (Fig. 30). Similar titanaugite is also found in some samples from the Mor Intrusives. In one sample, phenocrysts of sodic plagioclase feldspar were also noticed beside the pyroxene (Fig. 31) and in another phenocrysts of sodic plagioclase and hornblende were noted (Fig. 32). Therefore, the titanaugite appears to be the most common phenocryst-forming mineral.

The groundmass usually consists of a variable combination of the following: glass, clinopyroxene, plagioclase, amphibole, chlorite, calcite, opaques, apatite, felspathoids (?), biotite, zeolites, and rarely

Figure 30. Augitic limburgite lava showing phenocrysts of zoned titanaugite set in a groundmass of glass, tiny platy clinopyroxene, elongated plagioclase laths and opaque minerals. Note hour-glass structure in the phenocryst (cross nicols).

(Sample No. SR-1-79)

Figure 31. Vitrophyric augitic limburgite showing a large titanaugite phenocryst and a few small plagioclase laths set in a dark glassy groundmass. Note the round amygdule which is rimmed with calcite and filled with chlorite (parallel nicols).

(Sample No. SR-90-79)

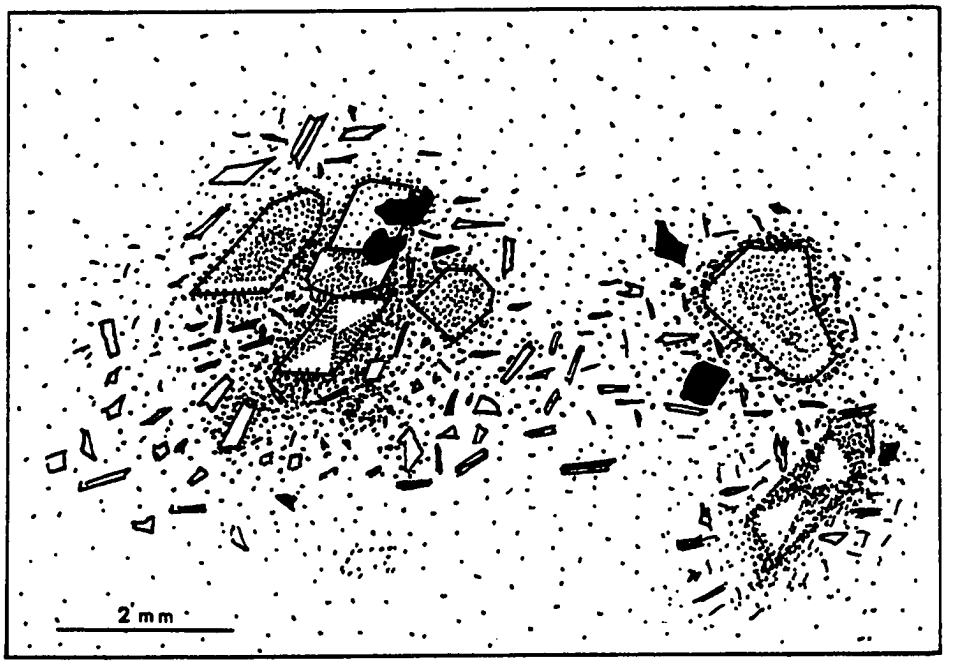

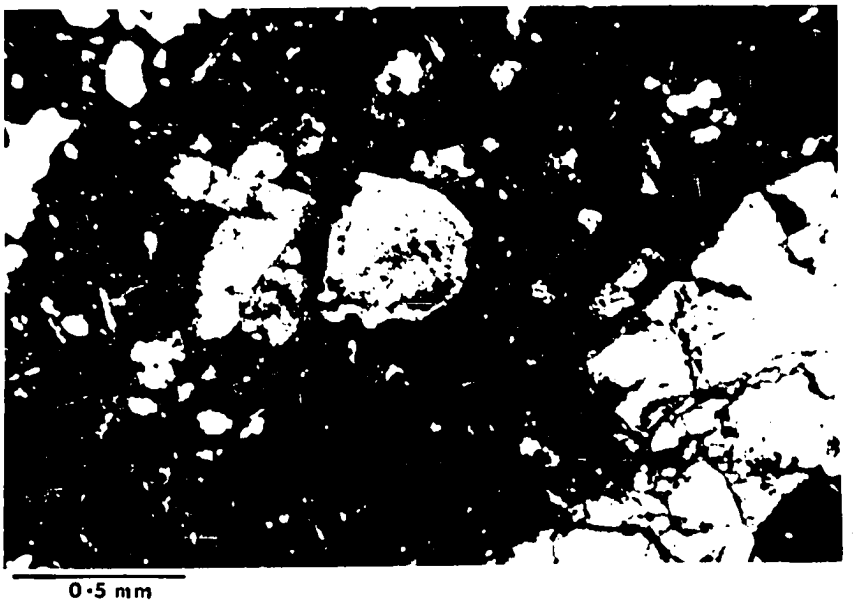

Figure 32. Intersertal basalt showing anhedral grains of hornblende and plagioclase phenocrysts set in a dark glassy groundmass (parallel nicols).

(Sample No. SR-79-79)

epidote (Figs. 30-32). However, four samples are totally devoid of feldspars. Amygdules are quite common and are filled with a variable combination of the following minerals in different samples: chlorite, calcite, zeolite, amorphous silica (rarely quartz) and sodic plagioclase; veinlets of chlorite and sodic plagioclase also occur (Figs. 31, 33).

A summary of the petrographic characteristics of the above minerals is included in Appendix 3B, and the petrography of nine samples is described in Appendix 3A.

The Porali Conglomerate involves a spectrum of variably altered porphyritic ultramafic-mafic rocks. Three kinds of rocks can be recognized on the basis of the type of phenocrysts present:

(1) Lavas with titanaugite phenocrysts alone:

	Groundmass Assemblage
A. Feldspar Free	
SR-3-79	glass plus opaque minerals; amygdules filled with calcite, chlorite, amorphous silica and zeolites
SR-8-79	clinopyroxene, glass, brown hornblende
SR-81-79	opaque minerals, chlorite, olivine (?), feldspathoid (?); amygdules and veinlets filled with calcite, chlorite and zeolite
SR-110-79	clinopyroxene, apatite, glass, opaque minerals, chlorite, calcite; amygdules and cavities filled with calcite and chlorite
B. Some feldspar present (in groundmass)	
SR-1-79	clinopyroxene, plagioclase, glass, opaque minerals, biotite, olivine (?), felspathoid (?)

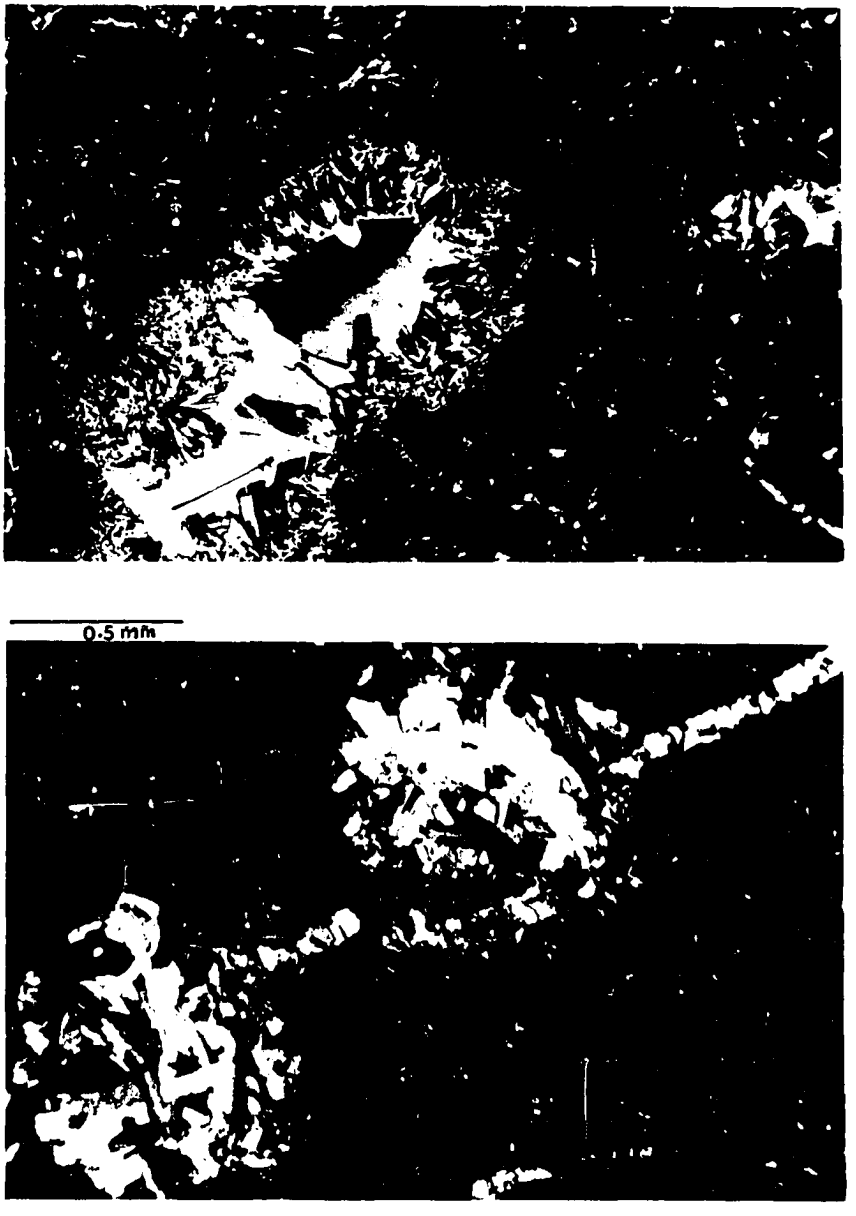

Figure 33. Amygdules in vitrophyric limburgitic lava filled with chlorite (rim) and twinned sodic plagioclase (middle): The grain at the bottom right is a titanaugite phenocryst. Groundmass consists of dark glass, tiny grains of clinopyroxene and plagioclase microliths (cross nicols).

(Sample No. SR-90-79)

SR-90A-79 clinopyroxene, glass, opaque minerals, sodic plagioclase, chlorite; amygdules and cavities filled with sodic plagioclase and chlorite

(2) Lavas with titanaugite and plagioclase phenocrysts

Groundmass Assemblage

SR-7-79 calcite, chlorite, biotite, opaque minerals (calcite partly replaces phenocrysts of sodic plagioclase, pyroxene and groundmass. Chlorite replaces pyroxene and groundmass)

SR-90B-79 glass, calcite, chlorite, plagioclase, opaque minerals; (calcite pseudomorphs plagioclase phenocrysts completely; amygdules filled with calcite, chlorite and plagioclase)

(3) Lava with sodic plagioclase phenocrysts and hornblende

SR-79-79 glass, clinopyroxene, opaque minerals; amygdules filled with chlorite, quartz, amorphous silica and zeolites

From the petrographic variability of the rocks observed even within a small sample size, it appears that the Porali Conglomerate probably involves a much greater variety of basic and ultrabasic volcanics that can be identified only through further work. The ultrabasic rocks (with titanaugite phenocrysts and little or no feldspar) can be classed as altered augitic limburgites; however, olivine, often listed as a common constituent of limburgites (Williams, et al., 1954; Carmaichael et al.,

1974) is not present as phenocrysts and only suspected in the groundmass. According to Travis (1955) olivine may or may not be present as an essential mineral. All other rocks can be put together as variably altered alkali basalts of various kinds because they contain sodic plagioclase (see Figure 26, also).

Dikes

Two melanocratic dikes were observed in the large block of the Porali Conglomerate north of the Bujji block in the eastern melange belt (Fig. 4A). The petrographic description of these dikes is included in Appendix 3B. One of them (SR-4-79) is porphyritic, clearly ultrabasic and consists of titanaugite phenocrysts set in a matrix of titanaugite, altered glass, chlorite, olivine (?), and opaques. There is no plagioclase and the pyroxene is similar to that found in the clasts forming the host conglomerate. On the whole, the dike resembles the augitic limburgites described above and is classed as such.

The second dike is fine grained, holocrystalline and consists of titanaugite (similar to that in the other dike and in the clasts of conglomerate), epidotized plagioclase laths (?), chlorite, biotite, opaques, zeolites and carbonate. It is intensely altered; however, it was probably also like other basaltic rocks described above.

Chemical Affiliation:

Alkali-SiO_2 Diagram (Fig. 26): Chemically all except one of the Porali samples plot in the field of alkali-basalts on an alkali-SiO_2 diagram. One sample (SR-80-79) has unusually high SiO_2 content (68.1%) for a mafic rock. The excess SiO_2 is probably concealed in glass because there is no free quartz in this sample (see Appendix 3B).

Na_2O:K_2O Diagram (Fig. 27): On Na_2O:K_2O plot, the Porali clasts lie mostly in the field of soda series with only one sample lying in the K-rich field. The two dikes are high in K and lie in the field of potash series.

AFM Diagram: On the AFM plot (Fig. 28) the alkaline trend of Porali samples is apparent, and is subparallel to that of the Mor Intrusives.

REE Distribution: The REE data for four samples of Porali clasts and a dike is shown in Table 5, and plotted in Figure 34.

Like the Mor Intrusives, the Porali Conglomerate samples are also strongly enriched in LREE with respect to their HREE contents as shown by the following high ratios:

$$\left[\frac{La}{Sm}\right]_N = 3.5\text{-}4.34$$

$$\left[\frac{La}{Yb}\right]_N = 15.6\text{-}19.62$$

$$\left[\frac{Ce}{Yb}\right]_N = 11.8\text{-}14.65$$

Compared to the chondrites, the Porali clasts are (192.7-333.7) times enriched in La and (7.2-8.9) times enriched in Lu. The dike sample (SR-4-79) shows an REE pattern that closely mimicks that of the clasts. However, it is less LREE-enriched as shown in Figure 34 and by the following ratios:

$$\frac{La_N}{Sm_N} = 2.87$$

$$\frac{La_N}{Yb_N} = 12.05$$

Figure 34. REE distribution pattern for the Porali Conglomerate samples and two continental basalts.

A = SR-1-79 (clast)

B = SR-3-79 (clast)

C = SR-81-79 (clast)

D = SR-7-79 (clast)

E = SR-4-79 (dike in Porali Conglomerate)

F = Range of REE patterns of Deccan basalts

G = Columbia Plateau basalt (Data for F and G from Alexander and Gibson, 1977)

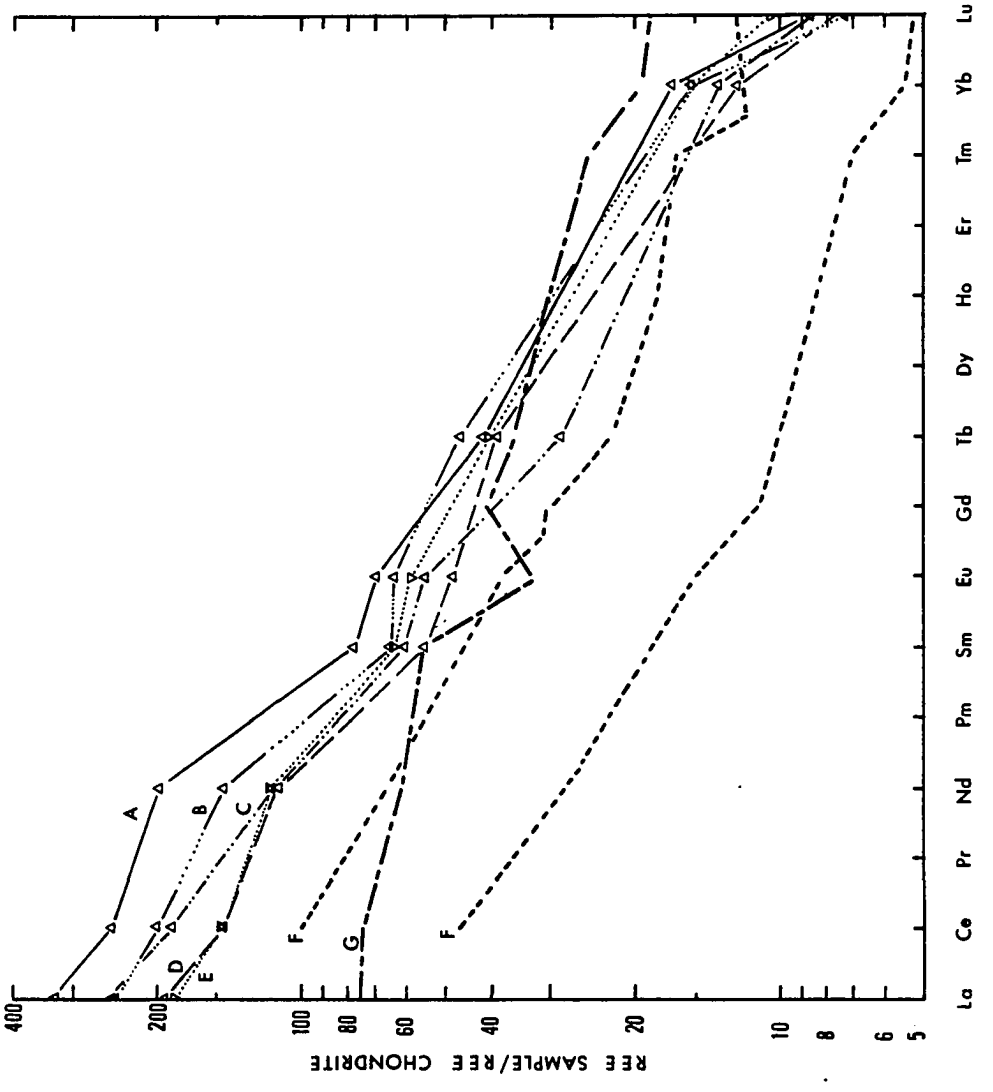

$$\frac{Ce^N}{Yb^N} = 9.56$$

The La_N ratio of the dike (184.55) is also lower than all clasts whereas its Lu_N ratio falls within their range.

The REE patterns of clasts and the dike show a consistent and uniformly enriched trend without any anomalies. The close similarity of the REE patterns between the dike and the clasts indicates that the two were derived from the same magmatic source; however, the lower (La_N) ratio for the dike suggests that is it less fractionated than the conglomerate.

Bela Group (Ophiolites)

This section describes the results of laboratory study of the common mafic and ultramafic rocks that constitute the Bela Ophiolites. Emphasis is placed on the petrography and chemistry of the mafic rocks because they are the most common rocks in the Bela Ophiolites and also because the chemistry of such rocks, especially of basalts, is generally used to solve the problem of the original tectonic setting of ophiolite rocks (e.g., Pearce and Gale, 1977). Therefore, the mafic rocks are treated first followed by a petrographic summary of some of the other interesting rocks that occur in the ophiolitic sequence; for example, the serpentinized ultramafic rocks, serpentinite-carbonate breccias, detrital serpentinite and a few exotic rocks.

Petrography of Mafic Rocks:

These rocks constitute the basaltic lava flows (Bela volcanics) and the diabasic-gabbroic sills (Bela intrusives) that intrude the lava flows

and associated rocks of the Bela Ophiolites. A total of 37 samples from these rocks were collected from the Wayaro and Kanar areas (see locations on Figs. 3-4). The samples were collected from different parts of the sequence in order to give a fair idea of the petrographic and chemical variability of these rocks. Prior to this study, a preliminary examination of the mafic rocks had indicated a rather monotonous petrographic nature of the mafic rocks; therefore, it is thought that the 37 samples (21 from sills and 16 from lava flows), are fairly representative of the petrographic range of mafic rocks. Similarly, the chemically analyzed samples of these rocks (12 sills and 12 lavas) are also considered enough to portray their general chemical features.

Lava Flows (Bela Volcanics):

The lava flows are generally aphanitic, fine grained to medium grained rocks of brownish or greenish gray to gray color. Among the textural varieties observed are: hypocrystalline-holocrystalline, equigranular-porphyritic and glomeroporphyritic, subophitic-ophitic, intersertal and trachytic types; some of these are shown in Figures 35-38.

Mineralogy of the lava flows is essentially the same as that of the associated diabase-gabbro sills, however, there are some differences. Like the diabases, both clinopyroxene and plagioclase may form phenocrysts in the porphyritic lavas. The phenocrysts are generally up to 2.5 mm, but occasionally the pyroxene phenocrysts may be up to 6 mm. Certain plagioclase phenocrysts are replaced by calcite—a feature not observed in the diabases. The subophitic-ophitic texture in the lavas is indistinguishable from its counterpart in the diabases and involves similar

Figure 35. Spilitic basalt showing poikilo-ophitic intergrowth between diopsidic pyroxene and twinned needle-like laths of sodic plagioclase feldspar (cross nicols).

(Sample No. 78-SR-42)

Figure 36. Glomeroporphyritic texture in basaltic andesite. Bunch of euhedral plagioclase phenocrysts are set in a trachytic groundmass of plagioclase microliths and dark glass (parallel nicols).

(Sample No. SR-99-79)

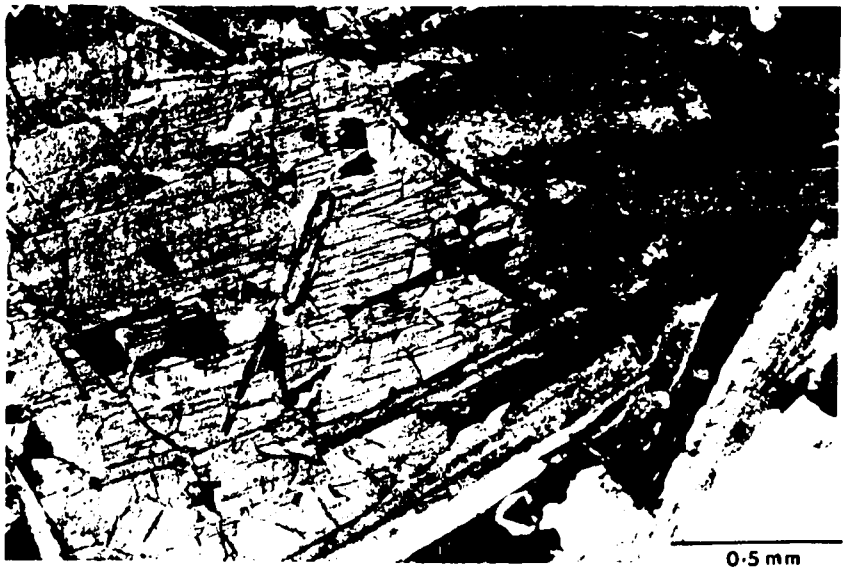

Figure 37. Spilitic basalt showing an amygdule and a few chloritized plagioclase phenocrysts set in a sub-trachytic groundmass of plagioclase microliths and glass; the amygdule is filled with chlorite (rim) and calcite (core) (parallel nicols).

(Sample No. SR-105-79)

Figure 38. A. Basalt showing a twinned clinopyroxene phenocryst and amygdules filled with chlorite; groundmass consists of opaque needles, chlorite and glass (cross nicols).

(Sample No. SR-2-79)

B. Irregularly shaped amygdules filled with banded (colloidal ?) chlorite in an altered basalt; the surrounding material consists of small equant xenomorphic clinopyroxene grains, plagioclase laths, opaque minerals, chlorite and calcite (cross nicols).

(Sample No. SR-2-79)

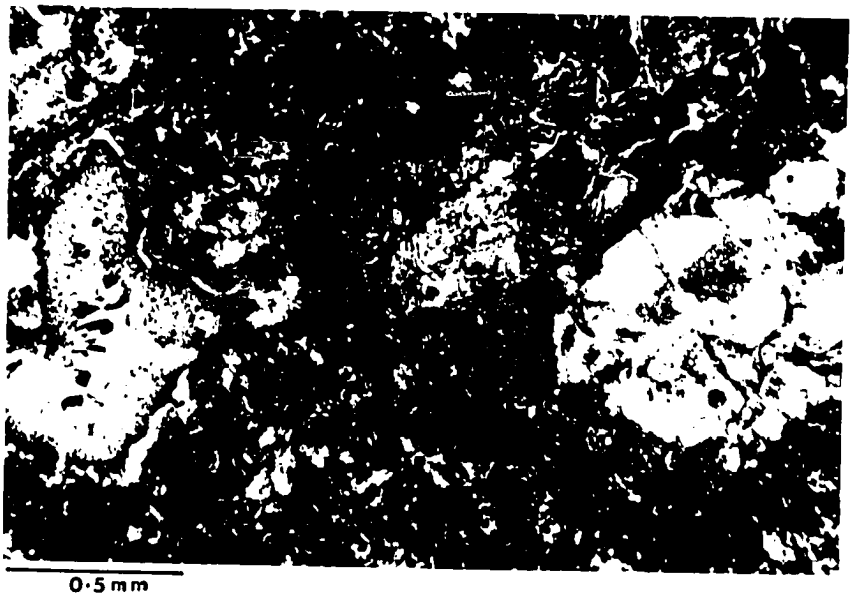

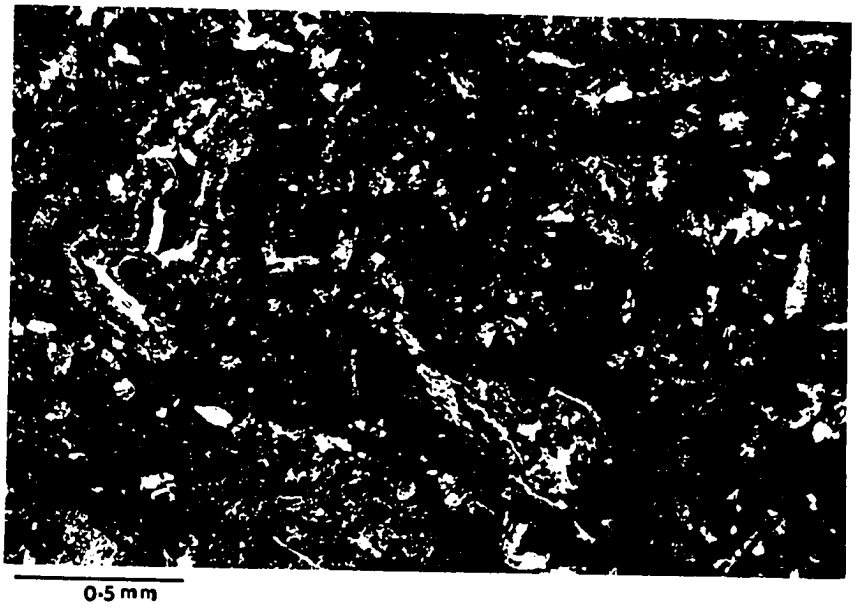

clinopyroxene and plagioclase feldspar. Some basalts are vesicular; some are amygdaloidal with cavities filled with glass, chlorite, calcite, and zeolite. The groundmass generally consists of a variable amount of glass and a variable combination of: acicular microliths of plagioclase, xenomorphic-euhedral clinopyroxene, chlorite, hornblende, opaque minerals, quartz, calcite, and zeolite. Occasionally the groundmass consists of a moss-like network of glass, acicular plagioclase and opaque minerals. The proportion of glass to other minerals is highly variable.

Petrographic description of 16 samples of basalts are included in Appendix 4B. A description of the characteristics of their mineral constituents is also included in Appendix 4A.

The lava flows are mostly spilitic basalts because of the common occurrence of sodic (albite-oligoclase) plagioclase and other minerals of the spilitic suite (see Appendix 1). Some lavas (with little or no clinopyroxene) are like keratophyres. In two cases, where the feldspar is of oligoclase-andesine composition, the lavas can be termed as basaltic andesites.

It is important to note the mineralogic similarity between the diabasic-gabbro sills and the associated lava flows. Both are olivine-free or silica-saturated rocks with sodic plagioclase and clinopyroxene commonly showing ophitic fabrics. Such coincidence suggests that both the lava flows and the sills were probably derived from the same magmatic sources and are thus genetically related.

Sills (Bela Intrusives)

These are diabasic and gabbroic rocks and vary in color from light brownish to greenish gray or gray. Texturally, they are fine to coarse

grained rock and commonly exhibit the subophitic-ophitic texture typical of diabases (Fig. 39). However, a few other textural varieties such as porphyritic, seriate, glomeroporphyritic and poikilitic are also occasionally observed (Figs. 40-42A). Even in some of these varieties the plagioclase feldspar and the clinopyroxene show a subophitic relationship.

In the ophitic varieties, elongate plagioclase laths constitute a framework with the clinopyroxene filling the interstitial spaces of variable size. Pyroxene may be partly replaced by uralitic hornblende and chlorite (Fig. 42B). The groundmass consists of a variable combination and proportion of the following minerals: plagioclase microliths, clinopyroxene, chlorite, opaque minerals including sphene, amphibole, biotite, quartz (or myrmekite), occasional epidote group minerals, apatite and zeolites. Veinlets of chlorite ± quartz and calcite are sometimes present.

In the porphyritic varieties both plagioclase and/or clinopyroxene occur as phenocrysts. The glomeroporphyritic rocks exhibit clumps of plagioclase and/or mafic minerals (clinopyroxene, opaques) set in a fine-grained mesostases of acicular plagioclase and clinopyroxene with other matrix forming minerals listed above.

The petrographic features of minerals forming the diabasic and gabbroic rocks are described in Appendix 5A, and the petrography of 21 samples is included in Appendix 5B. Olivine is only rarely seen in the Bela Intrusives (Fig. 43) and was not observed in the lava flows.

Despite the textural and mineralogical variations among samples from different locations, the diabases and gabbros are rather monotonous rocks. Most contain sodic plagioclase (albite-oligoclase) and can be

Figure 39. A. Gabbro showing ophitic texture. Large clinopyroxene (fractured, light gray) encloses small plagioclase laths (gray). Pyroxene is partly uralitized (arrow marks hornblende). Large opaque grain is skeletal magnetite or ilmenito-magnetite, and is interstitial to both pyroxene and plagioclase; note plagioclase inclusion in the opaque grain (cross nicols).

(Sample No. SR-45-79)

B. Diabase showing ophitic texture. A large clinopyroxene grain (left half) encloses a twinned lath of plagioclase and is intergrown with others (bottom right). The edges of pyroxene are replaced by a mixture of chlorite and hornblende (uralite); skeletal opaque grain is magnetite or ilmenito-magnetite.

(Sample No. 78-SR-55)

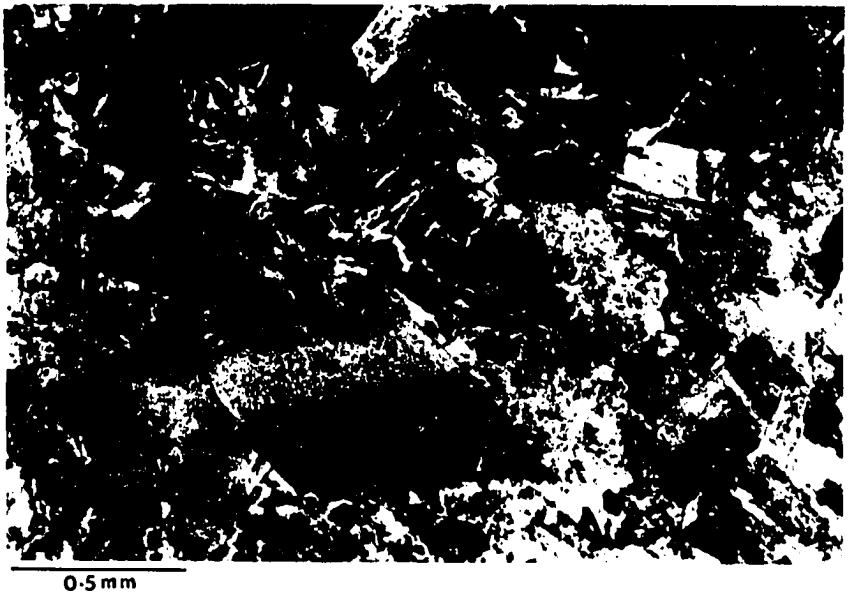

Figure 40. Poikilitic texture in diabase; a large, partly sericitized lath of plagioclase includes tiny xenomorphic grains and tongue-like plates of partly chloritized clinopyroxene. Large opaque grain along the right edge is magnetite or ilmenito-magnetite (cross nicols).

Figure 41. Intergranular texture in diabase. Small curved and twinned laths of sodic plagioclase form a network with interstitial opaque dust, a few tiny pyroxene grains, chlorite and calcite (white patchy areas) (cross nicols).

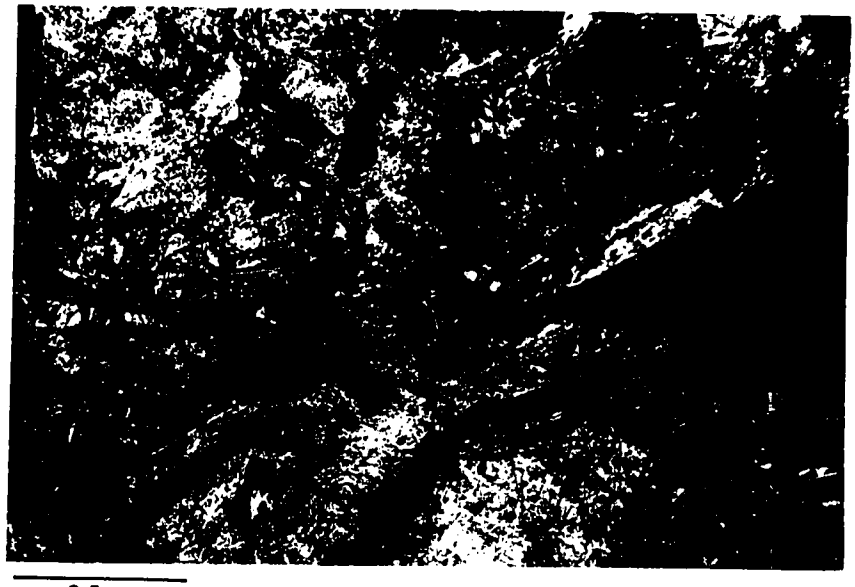

Figure 42. A. Diabase showing two generations of zoned plagioclase phenocrysts (P1 and P2). Two small clinopyroxene phenocrysts are also visible (right side); the plagioclase phenocrysts have chloritized cores. Groundmass consists of a dense mesostasis of plagioclase microliths, tiny pyroxene grains and opaque material (cross nicols).

(Sample No. 78-SR-79)

B. Hornblende replacing a large diopsidic pyroxene grain in a gabbro (parallel nicols).

P = pyroxene

H = hornblende

F = chloritized plagioclase feldspar

Figure 43. Subophitic texture in diabase showing clinopyroxene (augite ?) interstitial to elongated laths of sodic plagioclase; note the large pyroxene grain appears to have grown around olivine (densely fractured; arrow) (cross nicols).

considered to be of spilitic type. Less commonly the plagioclase is of oligoclase-andesine or andesine composition; such rocks can be termed dioritic diabases. Only one occurrence of a more differentiated rock was observed. This comes from a thin plagiogranite (or quartz-keratophyre, Appendix 5B, Fig. 44) dike that cuts through a diabase sill.

Chemical Affiliation:

General comparison with some modern basalts:

Table 6 presents the range and average of major element oxides in the lavas and sills and average composition of modern ocean ridge basalts (ORB), island arc tholeiites (IAT), marginal basin basalts (MBB) and the tholeiites from the Gibbs fracture zone (GFZ) of the Atlantic Ocean.

Compared to compositions of basaltic rocks from modern tectonic environments of which the Bela Ophiolite may possibly be considered a Cretaceous analogue (e.g., oceanic ridge, marginal basin, oceanic transform fault or island arc), the average composition of the Bela volcanics shows (Table 6):

1. lower SiO_2 than IAT and higher than others
2. lower Al_2O_3 than all types, however approaching GFZ
3. lower Fe_2O_3 than all types; however close to GFZ
4. lower MgO than all
5. lower CaO than all; however closest to GFZ
6. lower Na_2O than MBB (Mariana) and higher than others
7. lower K_2O than IAT and MBB (Mariana) and higher than others, however approaching GFZ
8. higher MnO than all
9. higher TiO_2 than all

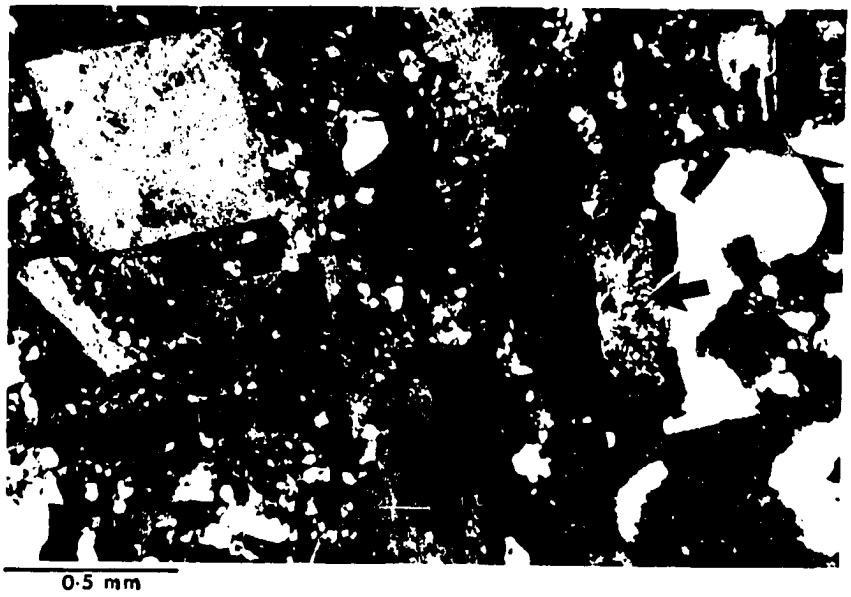

Figure 44. Plagiogranite showing laths of twinned sodic plagioclase, interstitial quartz (clear) and chlorite. Note also vermicular intergrowth (arrow) which involves all the three minerals (cross nicols).

(Sample No. SR-5-79)

Table 6. Chemical comparison of the mafic rocks from the Bela Ophiolites with modern basalts from oceanic ridge (ORB), fracture zone (GFZ), island arc (IAT) and marginal basin (MBB) environments. NE = ninety east aseismic ridge, Indian Ocean; MIOR = Mid-Indian Ocean ridge. * = Data from Ashley et al. (1979); # = Data from Hekinian and Aumento (1973); Δ = Data from Subbarao et al. (1977). Numbers preceded by sign "<" represent lower detection limits. All trace element data is in ppm.

	Bela Volcanics		Bela Intrusives				MBB*	MBB*	Gibbs F.Z.#		
	Range	Average	Range	Average	ORB*	IAT*	(Mariana)	(Lau)	(Atlantic)	NE Δ	MIOR Δ
SiO_2%	44.5 - 52.8	50.09	41.8 - 53.4	48.75	49.62	51.57	49.61	48.8	47.45		
Al_2O_3%	10.8 - 15.7	14.07	12.1 - 15.9	14.26	16.13	15.9	16.58	16.4	14.73		
Fe_2O_3%	10.2 - 13.5	12.26	8.4 - 15.5	13.48	10.69	10.56	9.53	9.67	12.05		
MgO%	5.6 - 7.5	5.31	5.3 - 7.5	6.16	7.78	6.73	6.81	8.6	7.29		
CaO%	7.5 - 15.7	10.06	7.3 - 10.1	8.53	11.34	11.74	11.38	12.6	10.54		
Na_2O%	2.1 - 3.6	3.0	2.7 - 5.0	3.34	2.75	2.41	3.23	2.4	2.42		
K_2O%	0.1 - 0.6	0.3	0.2 - 1.3	0.64	0.2	0.44	0.42	0.18	0.29		
MnO%	0.15- 0.8	0.25	0.17- 0.32	0.25	0.17	0.17	0.14	0.2	0.18		
TiO_2%	1.8 - 2.7	2.15	1.1 - 3.4	2.41	1.44	0.8	1.49	1.2	1.91		
Ba	<130.7 -225.9		<108.7 -352.9							6 -780	17
Co	42.7 - 53.07		43.8 - 50.87							25 - 78	35
Cr	81.3 -142.27		8.8 -432.22							5 -890	360
Cs	<0.49		<0.4 - 1.57							0.16- 0.79	0.128
Hf	2.7 - 3.28		2.37- 6.28								
Ni	70.9 - 98.24		< 61 -149.7							5 -520	109
Rb	<35.0		<36							19.5 - 48.7	2.54
Sc	35.23- 42.07		30.9 - 46.6							15 - 55	49
Ta	0.53- 0.98		0.4 - 1.2							-	-
Th	<0.5 - 0.94		0.9 - 2.85							-	-
U	<0.65		<0.68							0.1 -185	0.51

From the above it appears that the major chemical aspects of the Bela volcanics are broadly similar to those of the oceanic basalts from various tectonic settings. More meaningful comparisons are drawn in the various variation diagrams as follows:

Lava Flows (Bela Volcanics):

Alkali-SiO_2 Diagram: On an alkali:SiO_2 plot, 10 our of 12 Bela basalts fall in the tholeiite field whereas the remaining two lie in the alkali basalt field (Fig. 45).

K_2O-SiO_2 Diagram: Figure 46 is a K_2O:SiO_2 plot intended to distinguish low K basalts from other subalkali basalts (Middlemost, 1975). Plotted on this diagram (Fig. 46), all 12 samples fall in the field of subalkaline (tholeiite) basalts. Further, 10 our of 12 samples have $K_2O = 0.4\%$ and thus resemble the low K abyssal tholeiites (Miyashiro, 1975).

SiO_2:Fe/Mg Diagram: On an SiO_2:Fe/Mg plot (Fig. 47) which distinguishes between calc-alkaline and tholeiitic basalts (Miyashiro, 1973), all Bela basalt samples fall well within the field of tholeiites. Five samples fall only in the island arc field; five others fall in both island arc and mid-oceanic ridge fields and two samples outside both of these fields. According to Miyashiro (1975), the abyssal tholeiitic basalts have an FeO/MgO range of (0.7-2.1) which includes the FeO/MgO range of Bela volcanics (1.9-2).

Fe:Fe/Mg Diagram: That the Bela volcanics are tholeiitic and not of calc-alkaline affinity, can also be seen on a Fe:Fe/Mg plot (Fig. 48), where all samples plot in the tholeiitic field. The variation trend for

Figure 45. Alkali-SiO_2 plot for the Bela volcanics and intrusives and their comparison with certain other suitable rocks.

Line A = from Shwarzer (1974)

Line B = Hawaii alkali basalt-Tholeiite line of Macdonald and Katsura (1964)

Line C = from Miyashiro (1978)

▲ = pillow lava

● = diabase-gabbro sills

\+ = average ocean floor tholeiitic basalt (Cann, 1971, Hyndman, 1972)

◌ = range of 6 samples of fresh Carlsberg ridge basalt, Indian Ocean (Cann, 1969)

■ = average Carlsberg Ridge spilite (Cann, 1969)

▽ = average spilite (Moores and Vine, 1971)

□ = spilite basalt from the Semail ophiolite (Glennie et al., 1974)

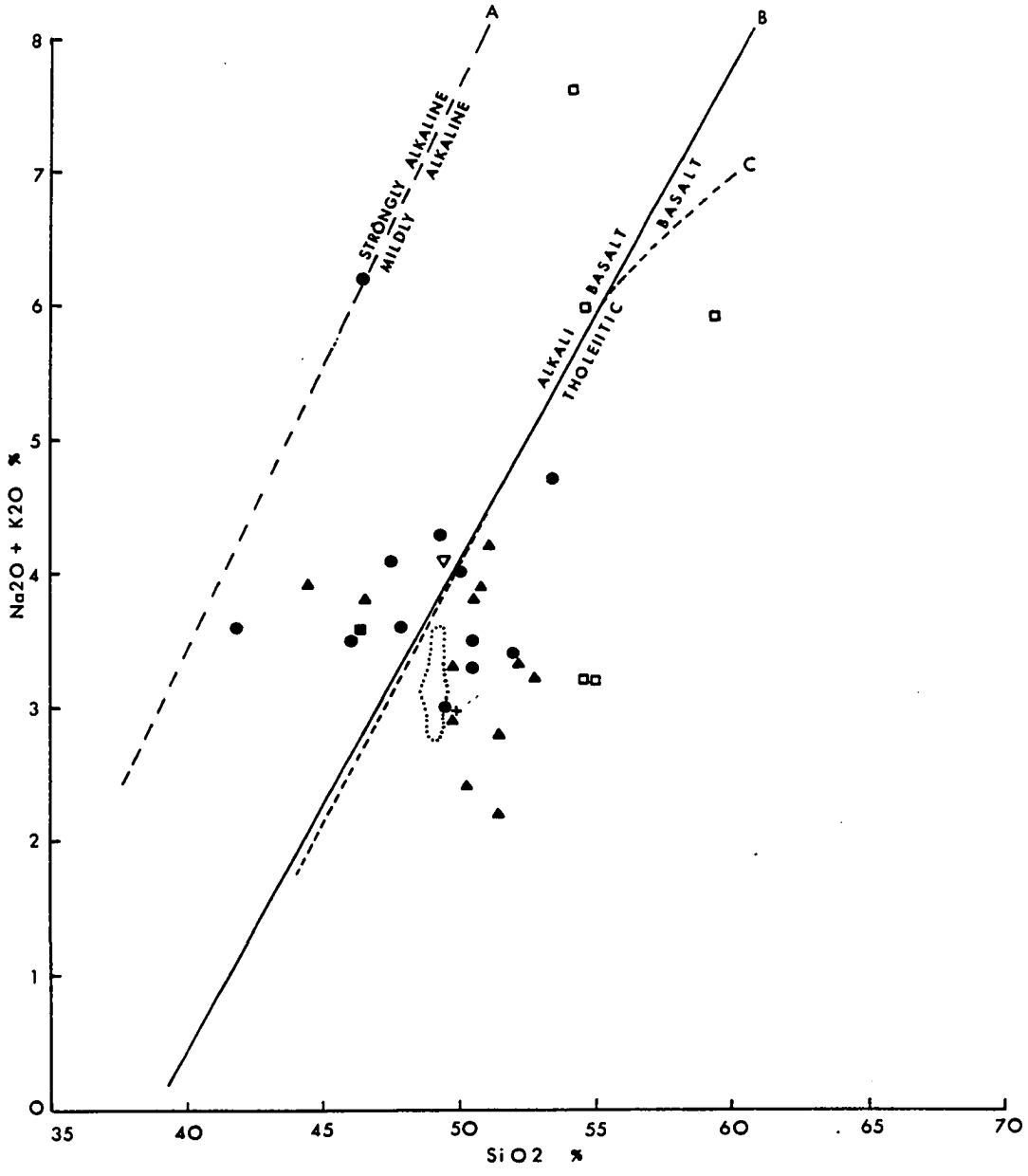

Figure 46. SiO_2-K_2O plot for the Bela volcanics and intrusives. Note that the majority of basalts are low-K tholeiites.

▲ = pillow lavas

● = diabase-gabbro sills

(Diagram from Middlemost, 1975).

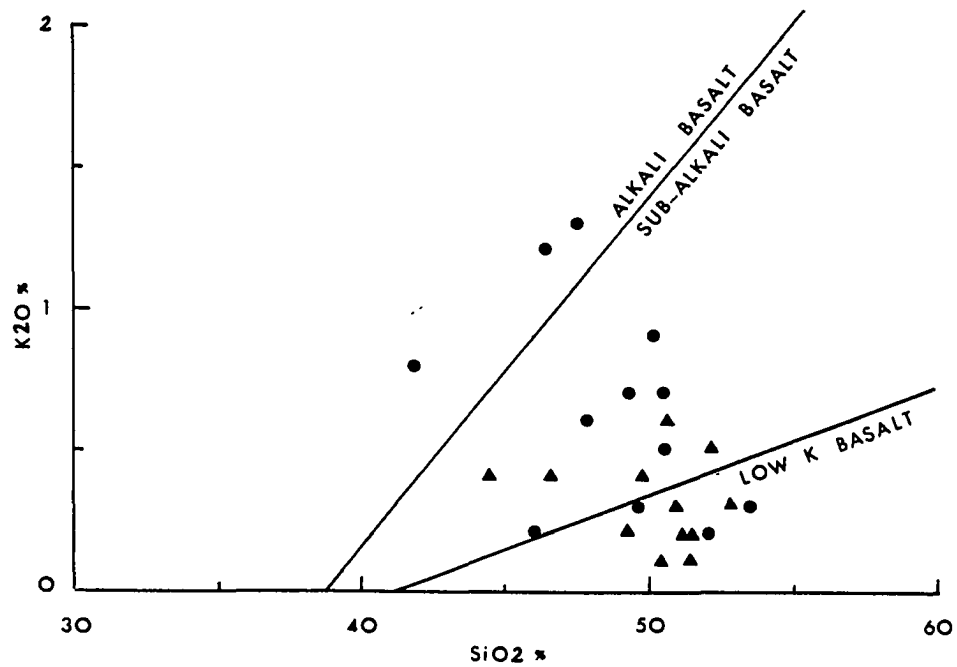

MORB (abyssal tholeiite, Saunders et al., 1979) is also plotted in this diagram. Note that the Bela basalts tend to lie along the MORB trend. As Fe/Mg ratio increases, there is a decrease in Mg and an absolute increase in Fe. Also on the SiO_2:Fe/Mg plot (Fig. 47), there is only a limited variation in SiO_2 throughout Fe/Mg (or FeO/MgO) range, indicating that the fractionation trends for Bela basalts are tholeiitic and not calc-alkaline (Kuno, 1959; Miyashiro, 1973; Saunders et al., 1979). Tholeiitic series shows enrichment in FeO (total) with a maximum during fractional crystallization, whereas the calc-alkaline series shows decrease (Miyashiro, 1975). Thus in tholeiitic rocks FeO (total) increases with the increase in FeO/MgO ratio (Miyashiro, 1975). This is apparent for Bela volcanics on the Fe:Fe/Mg plot which is not significantly different from a FeO:FeO/MgO plot.

The TiO_2 content of Bela volcanics averages 2.15% (range 1.8-2.5 except for one, which is 2.7). Thus for the Bela volcanics, $SiO_2 \approx 50\%$, $K_2O \approx 0.3\%$, FeO*/MgO < 2 and $TiO_2 \approx 2.15\%$. These characters are comparable to those of abyssal tholeiites as reported by Miyashiro (1975).

TiO_2:FeO*/MgO Diagram: The Bela basalts are plotted on a TiO_2: FeO*/MgO diagram (Fig. 49) which also shows the field of modern ocean floor basalts as suggested by Coish and Church (1979). According to them the modern ocean floor basalts have $TiO_2 \leq 2$ and FeO*/MgO ≤ 1.8. If these values are accepted then the Bela basalts are more enriched in TiO_2 and FeO with respect to the modern ocean floor basalts.

The Al_2O_3 content of the Bela basalts (average 14.07; range 10.8-15.7) is well below that of the high Al_2O_3 basalts (Al_2O_3 > 17%; Carmaichael et al., 1974).

Figure 47. SiO_2-Fe*/Mg plot for the Bela volcanics and intrusives. The line separating the fields of calc-alkaline (CA) and tholeiitic basalts is from Miyashiro (1973). The fields of island arc tholeiites (IAT) and the Mid-Oceanic Ridge basalts (MORB) are from Saunders et al. (1979).

▲ = pillow lava

● = diabase-gabbro sills

* = total iron

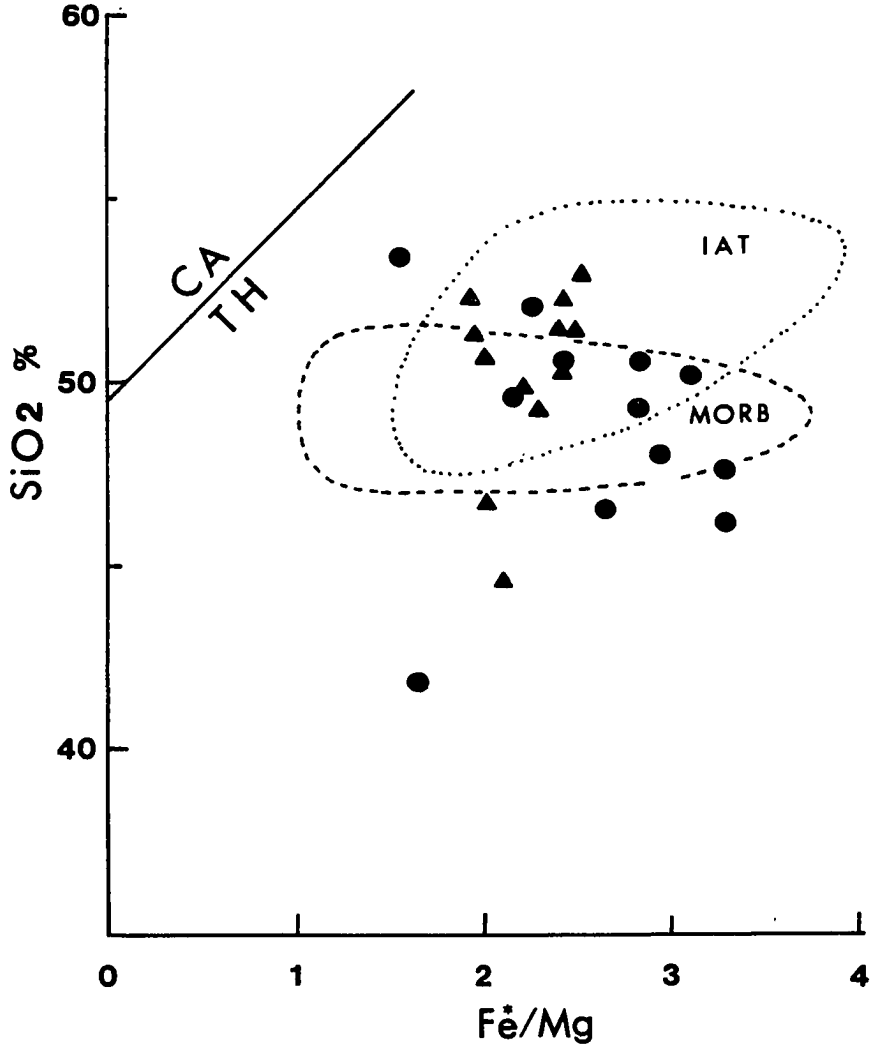

Figure 48. Fe*-Fe*/Mg plot for the Bela volcanics and intrusives. The dashed line shows Mid-Ocean Ridge basalt (MORB) differentiation trend (Saunders et al., 1979). The tholeiitic (Th) and calc-alkaline (CA) fields are from Miyashiro (1973).

▲ = pillow lavas

● = diabase-gabbro sills

* = total iron

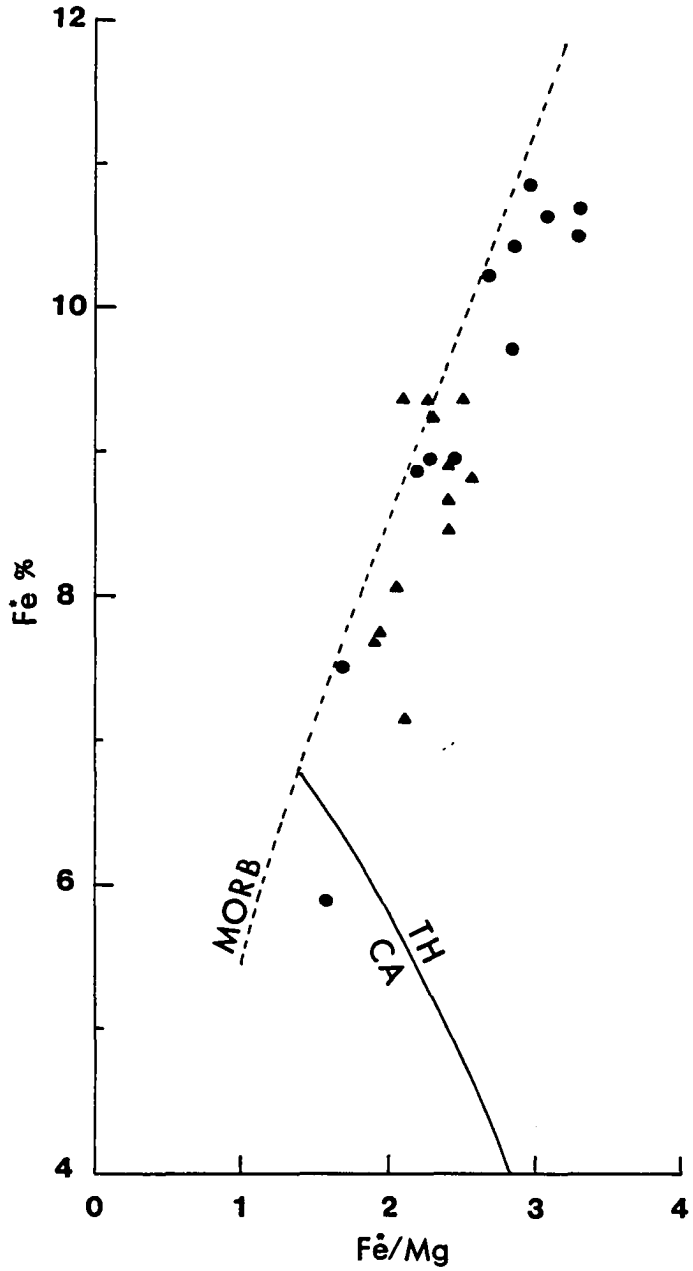

AFM Diagram: Figure 50 shows an AFM plot for the Bela basalts. It also shows variation trends for basalts from the Azores, Iceland and fields occupied by basalts from the Atlantic rift valley (ridge), Atlantic fracture zones (transform faults) and aseismic ridges (Hekinian and Thompson, 1976). As shown the Bela basalts fall in the field of the Atlantic fracture zone basalts which are overlapped by the fields of both the aseismic ridge and the Atlantic rift basalts. However, two interesting observations suggest that the Bela basalts are perhaps more like the fracture zone basalts than any other types:

1. Like the fracture zone basalts, the Bela basalts are more Fe-enriched (higher FeO*/MgO) than the Atlantic rift basalts.
2. The distinct alkali enrichment trend shown by the Azores, Iceland and aseismic ridge basalts is not shown by both the fracture zone basalts and the Bela volcanics.

Another interesting observation is that the Atlantic fracture zone basalts have a higher TiO_2 range (1.5-3%) than the Atlantic rift basalt (TiO_2 < 1.8%). For Bela basalts TiO_2 = 2.15 average (range 1.0-2.7). Thus in this respect also the Bela basalts resemble the Atlantic fracture zone basalts.

The Atlantic fracture zone basalts also show a wider range of K_2O (0.10-1%) than the rift basalts (K_2O < 0.7) (Hekinian and Thompson, 1976, p. 152). The Bela basalts show a lower range of K_2O (0.1-0.6%) than the fracture zone basalts.

Some data for the fresh tholeiitic and spilitic basalts from the Indian Ocean (Cann, 1969) and for the Semail ophiolite spilitic basalts

Figure 49. TiO_2-FeO*/MgO plot of Bela volcanics and intrusives.

▲ = basaltic pillow lava

● = diabase-gabbro sills

* = total iron

The field of modern ocean floor basalts is from Coish and Church (1979).

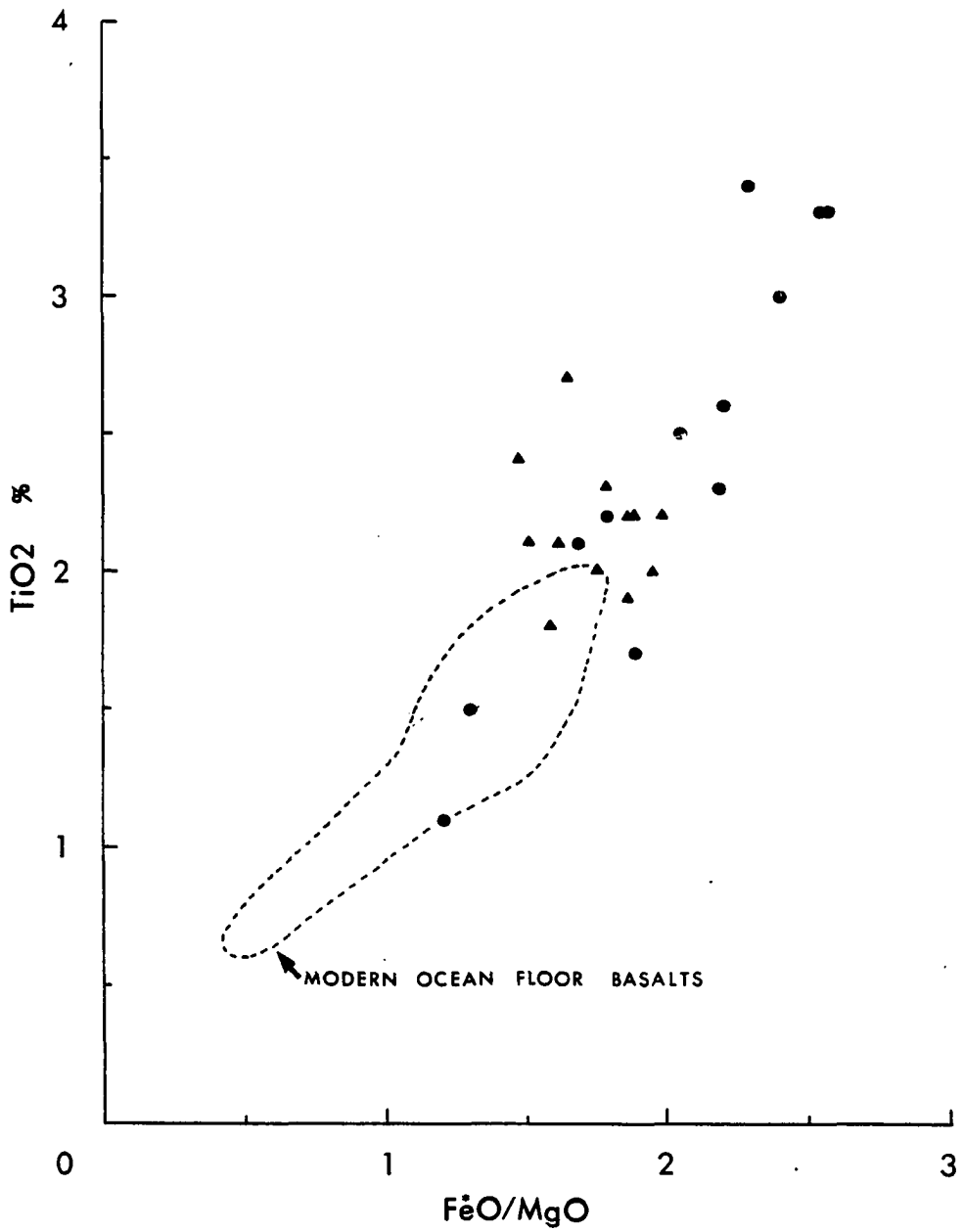

Figure 50. AFM* plot of the Bela volcanics/intrusives, certain other comparable mafic rocks from different modern oceanic tectonic environments, and Oman ophiolites. Fields of volcanic rocks from the Atlantic rift valley, Atlantic fracture zones, aseismic ridges, and differentiation trends of volcanic rocks from Iceland and Azores are from Hekinian and Thompson (1976).

▲ = Bela basalts

● = Bela diabases and gabbros

◇ = gabbroic rocks from the Kane and Romanche fracture zones (from Hekinian and Thompson, 1976)

▽ = average of 6 Carlsberg Ridge fresh tholeiites (from Cann, 1969)

x = 6 Carlsberg Ridge spilitic basalts

+ = 5 samples from spilitic basalts, Semail ophiolite, Oman (Glennie et al., 1974)

* = $N_2O + K_2O$ - FeO (total iron) - MgO plot

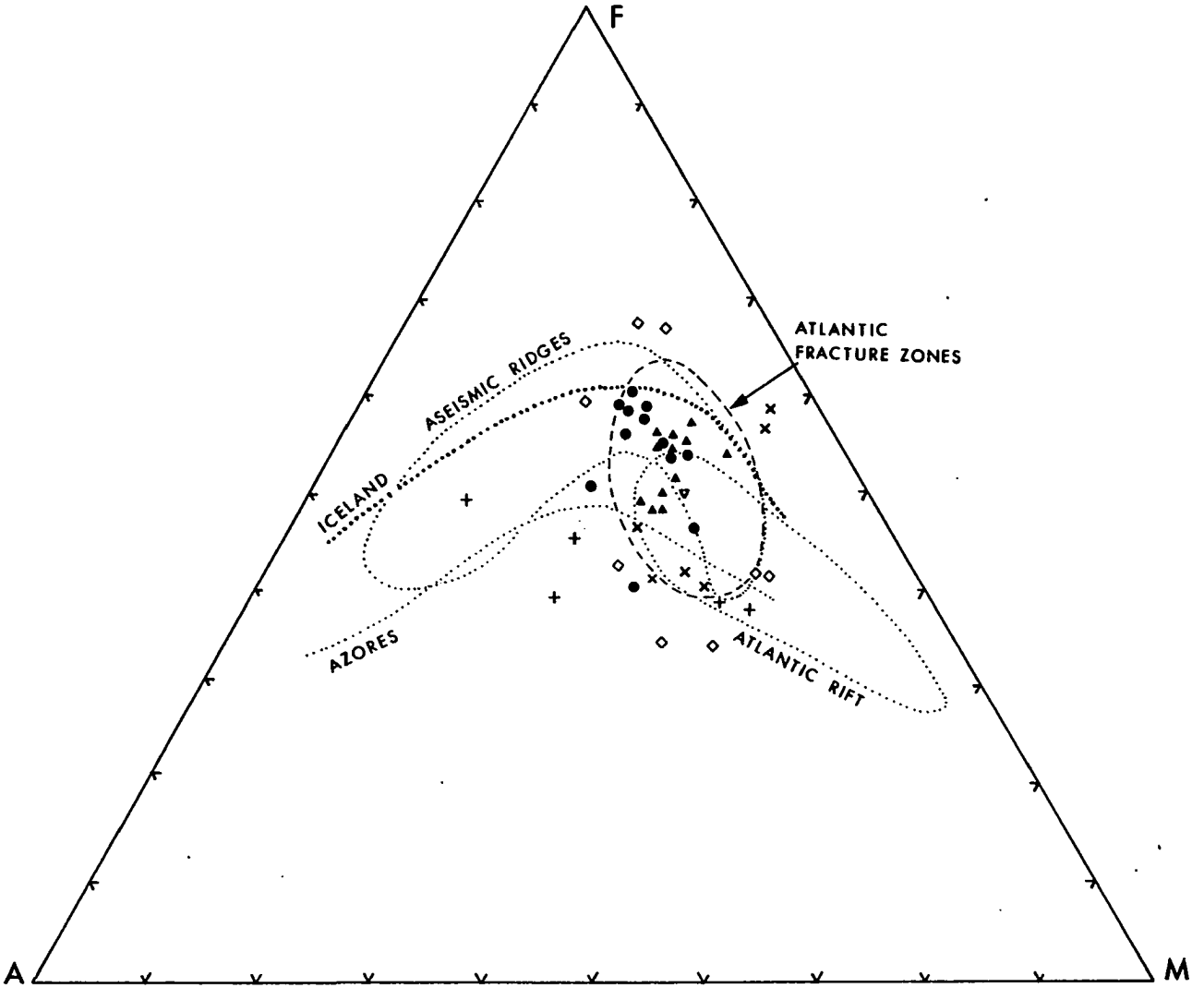

(Glennie et al., 1974) is also shown on Figure 50 for comparison with the Bela basalts.

Ti:Cr Diagram (Fig. 51): Selected trace element data (Appendix 10B) for the Bela basalts are plotted on discriminant diagrams using immobile elements in an attempt to further test the oceanic affinity of these rocks.

The Ti:Cr diagram (Pearce, 1975), which distinguishes between the island arc tholeiites and the ocean floor basalts, shows that all six samples of the Bela basalts fall in the ocean floor field (Fig. 51).

Ti/Cr:Ni Diagram: Another diagram which distinguishes between the same two tectonic environments is the Ti/Cr:Ni plot (Beccaluva et al., 1979); see Figure 52. It also shows that all four Bela basalt samples fall in the field of the ocean floor tholeiites (2 samples could not be plotted because the Ni content was below the detection limit). Four samples from the Indian Ocean fracture zone basalts (Engel and Fisher, 1975) are also plotted on the Ti/Cr:Ni diagram. These basalts are lower in TiO_2 as compared to the Bela basalts.

Hf-Ta-Th Data: Wood et al. (1979, Fig. 3) proposed a triangular diagram based on Hf, Ta and Th data that distinguishes mid-oceanic ridge and within plate basalts (e.g., ocean island like Azores and continental rift like E. African rift) from each other and from Ta-depleted basalts erupted at converging plate margins (e.g., Andean and Western Pacific type magmatic arcs).

Figure 53 shows the Hf, Ta and Th plot for the Bela basalts. Five samples plot in the field of E-type mid-oceanic ridge basalt; the Th content of sixth sample was below the detection limit (< 0.58 ppm) and for

Figure 51. Ti-Cr plot for Bela volcanics and intrusives.

▲ = basalts

● = diabase-gabbro sills

Diagram from Pearce, 1975.

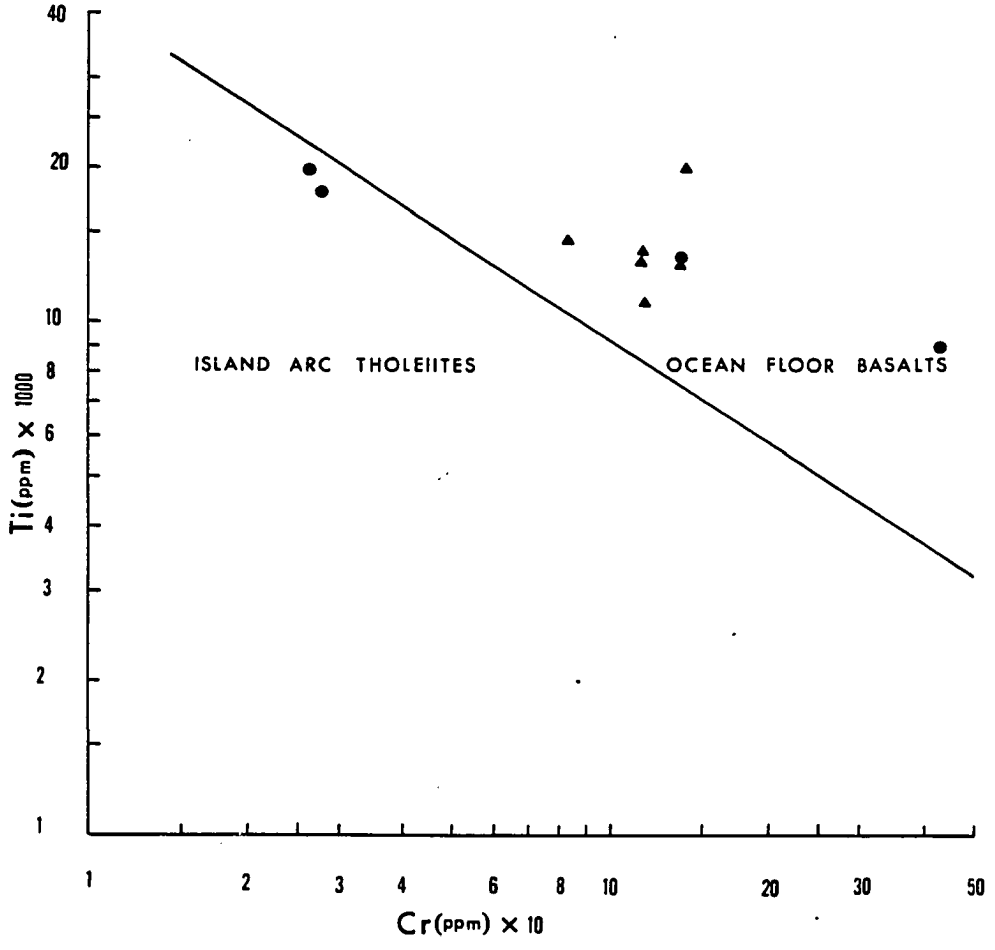

Figure 52. Ti/Cr-Ni plot for the Bela volcanics and intrusives.

▲ = basalts (sample numbers Sr-16-79, Sr-99-79, Sr-104-79 and 78-SR-42).

● = diabase-gabbro sills (sample numbers SR-14-79 and SR-73-79).

□ = Indian Ocean fracture zone basalts (data from Engel and Fisher, 1975).

Samples: ANTP-95-7
ANTP-99-1
ANTP-131-2
CIRCE-106-A

Diagram from Beccaluva et al. (1979).

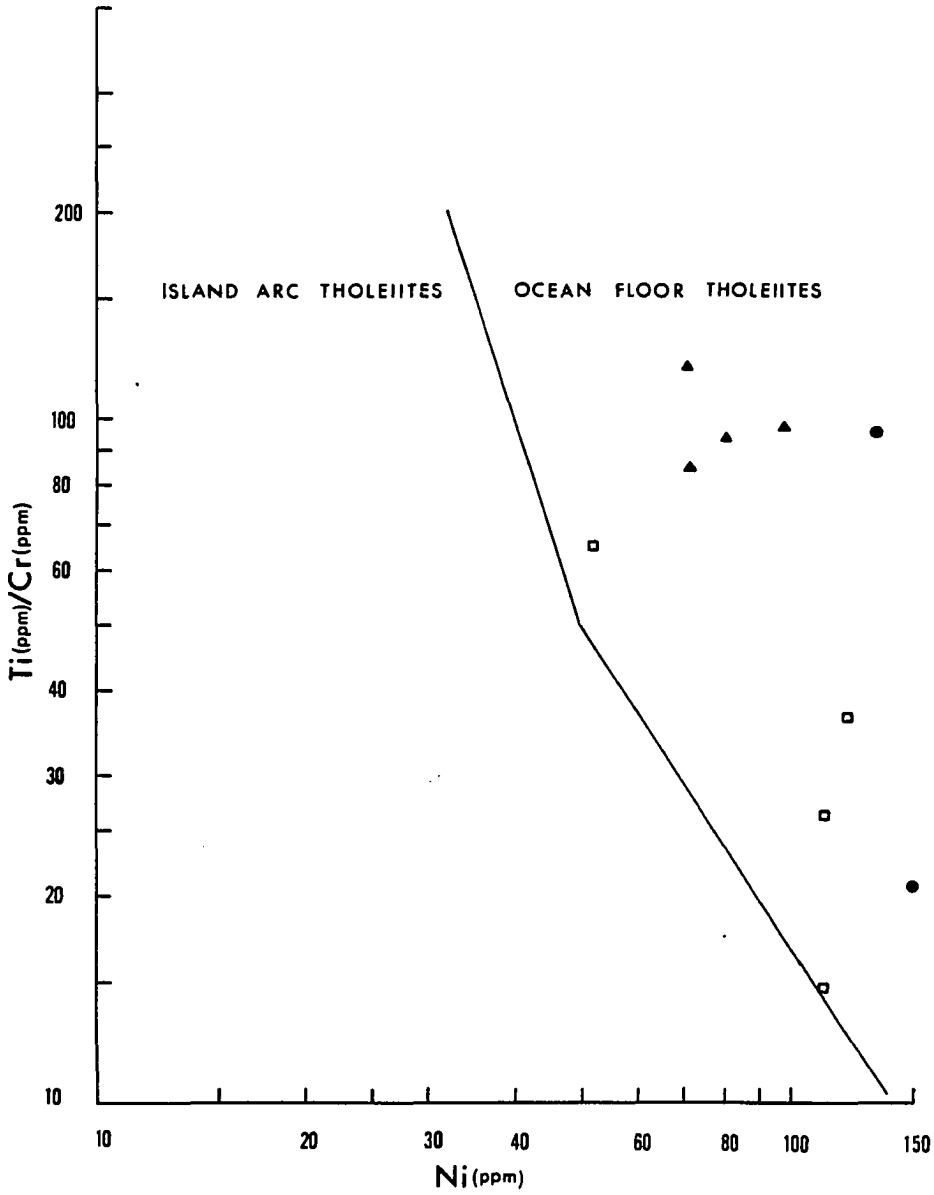

Figure 53. Hf/3Th-Ta plot for the Bela volcanics, Porali Conglomerate volcanic clasts and the Deccan basalts.

● = Bela volcanics (sample numbers: Sr-16-79, SR-30-79, SR-88-79, SR-99-79, SR-104-79, and 78-SR-42). Th content of sample 16 was below the detection limit.

△ = Porali clasts (sample numbers: SR-1-79, SR-3-79, SR-7-79, and SR-81-79).

■ = Deccan basalts (data from Alexander and Gibson, 1977; (Table 1, samples number OA/D3 and from OA/D-17 - OA/D37).

Diagram from Wood *et al*. (1979).

MORB = Mid-Oceanic Ridge basalt

N-type = normal
E-type = enriched
WPB = within plate basalts

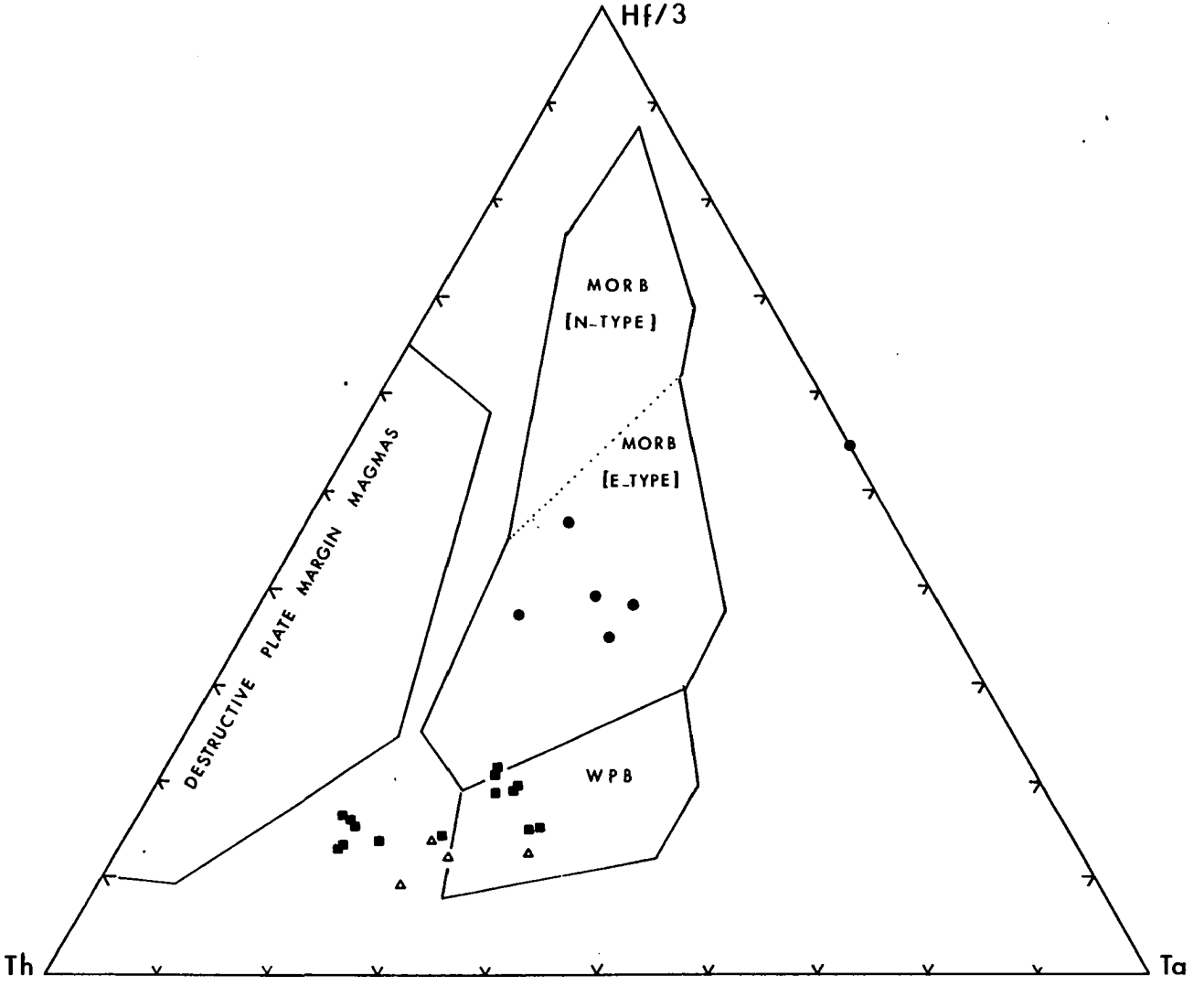

this reason only its Hf and Ta content has been considered.

Wood et al. (1979) have divided the mid-oceanic ridge basalts into three categories:

1. N-type MORB: These basalts are erupted from the so-called normal ridge segments and show very low abundances of some hygromagmatophile elements (elements with large ionic radii. These elements are partitioned into liquid during partial melting and into residual liquid of a crystallizing magma, e.g., Cs, Rb, K, U, Th, Ta, Nb, Ba, La and Ce). They also have very low Rb/Sr (Ca < 0.01), Th/U (Ca ~ 2), La/Ta (Ca ~ 15) and Hf/Ta (Ca > 7) ratios.

2. E-type MORB: These basalts are erupted along the so-called anamolous ridge-segments (e.g., hot spot like Azores, Schilling, 1975) of the oceanic ridge and are usually enriched in the hygromagmatophile elements listed above. They also show greater variation in hygromagmatophile elements and radiogenic isotope ratios than N-type MORB (Rb/Sr ~ 0.04 and Hf/Ta < 7 but > 2) with La/Th about 10 and Th/U about 4.

Thus the distinguishing criteria between the N-type and E-type MORB are:

	(La/Ta)	(Hf/Ta)	(Th/U)
N-Type MORB =	~ 15	> 7	~ 2
E-Type MORB =	~ 10	< 7	~ 4

The E-type MORB can also be distinguished from the basalts erupted at ocean islands (i.e., off-axis WPB) by their higher Hf/Ta ratios (> 2).

3. T-Type MORB: These basalts are transitional between the N and E type MORB.

For the Bela basalts, the Hf/Ta (2.9-5.7) ratio is consistent with the E-type MORB; however, the La/Ta ratio (9.62-18.04) includes the range of both the E and N type MORB. The Th/U ratio for the Bela basalts is not known because the U content is below the detection limit.

Thus for the Bela basalts

Hf/Ta = similar to E-type ridge basalts

La/Ta = much higher than both E and N type ridge basalts.

Therefore, the Bela basalts, although of anomalous (E-type) chemical character, are somewhat different from the ridge generated basalts.

REE Distribution: The REE distribution patterns for six samples of the Bela basalts are shown in Figure 54 and the data is given in Table 5. The REE distribution in the Bela basalts displays several interesting features.

1. They are enriched in the light rare earth elements (LREE; i.e., La, Ce and Nd) compared to the heavy ones (HREE; i.e., Yb and Lu):

$[La/Sm]^N$ = 1.04-1.27

$[La/Yb]^N$ = 3.1-4.25

$[Ce/Yb]^N$ = 2.4-3.7 (3.49-3.7, for 5 out of 6 samples)

The La/Sm and La/Yb ratios are like those of the enriched type oceanic tholeiites (e.g., Azores, Hawaii, Iceland; Jacques et al., 1978; Sun et al., 1979).

2. Compared to chondrites, the Bela basalts are (34-41) times enriched in La and (11-13.9) times enriched in Lu.

3. REE enrichment from Lu to La is not uniform but shows two distinct negative anomalies at Yb and Sm and two sharp positive anomalies

Figure 54. REE distribution patterns for the Bela basalts.

Analyzed samples:

A = SR-88-79

B = SR-99-79

C = SR-104-79

D = SR-16-79

E = SR-30-79

F = 78-SR-42

Nd content in 5 out of 6 samples is below the detection limit (see Appendix 10B).

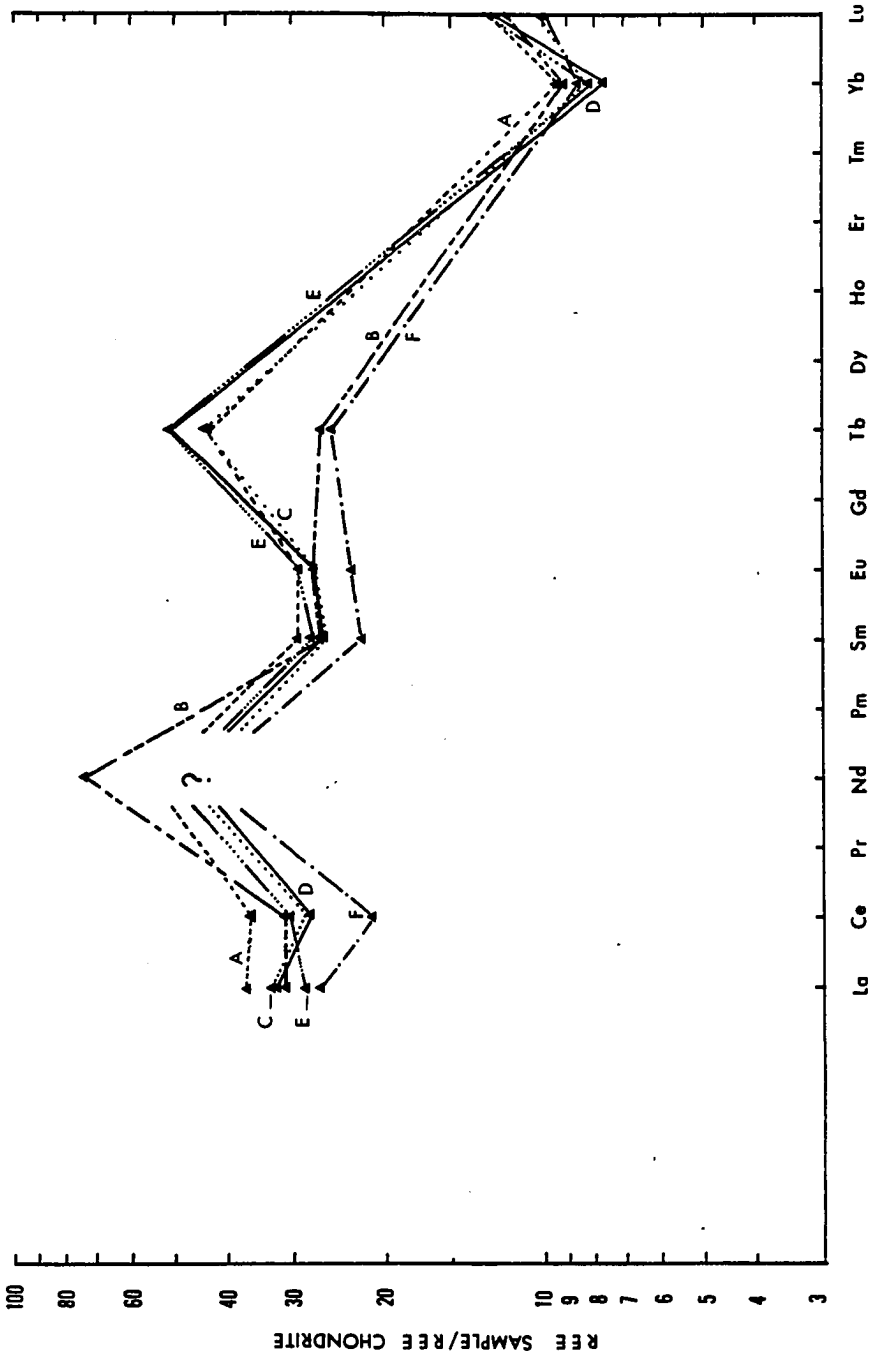

at Tb and Nd. The Nd content of five samples was below the detection limit (see Appendix 10B); therefore, it is not known whether all six samples show positive Nd anomaly. The same anomaly, however, is present in three out of five sills associated with the lavas.

4. The Yb and Tb anomalies are of variable intensity in different samples.

5. All samples except one (SR-99-79) follow identical distribution patterns and a consistent LREE enrichment trend; however, compared to chondrites, the lavas appear to be much more enriched in Tb and Nd than in LREE (La and Ce).

The Nd and Tb anomalies in the Bela basalts and diabase sills are difficult to explain. According to Wedepohl (1978), Nd and Tb are concentrated in apatite in both mafic and felsic igneous rocks. Apatite is present in the sills; however, it was not detected in the basalts.

Comparison of REE patterns of the Bela basalts with REE patterns of modern basalts from different tectonic settings and other ophiolites:

Figure 55 shows REE patterns of basalts from major ocean basins, oceanic islands, marginal basins and a fracture zone from the Atlantic Ocean. The LREE depleted pattern of mid-oceanic ridge basalts (MORB, Fig. 55) is by far the most common pattern observed both in the major basins and the island-arc tholeiites (Kay and Senechal, 1976, Sun et al., 1979; Suen et al., 1979). Except for this, only LREE enriched patterns are shown (Fig. 55) which are known from various sections of major oceanic spreading centers (Nicols and Islam, 1971; Shibata et al., 1979), plume type or ocean island basalts (e.g., Azores, Hawaii; Sun et al., 1979), marginal basins (Ashley et al., 1979) and oceanic fracture zones (Shibata,

Figure 55. Example of LREE-enriched and LREE-depleted patterns in basalts from different modern ocaenic tectonic environments.

1-2 = Range for oceanic fracture zone basalts at latitude 43°N in the Atlantic (Shibata et al., 1979; Fig. 7B).

3 and 4 = two samples from a western Pacific-type marginal basin (Lau Basin) (Samples 98-3 and 103-3 of Ashley et al., 1979).

5 = oceanic island (Kilauea tholeiite, USGS standard BHVO-1; data from Sun et al., 1979).

6-7 = range for LREE enriched tholeiites from some parts of the Mid-Atlantic Ridge (data from Shibata et al., 1979, Fig. 8).

8-9 = range for common LREE depleted or normal type Mid-Oceanic Ridge basalt (MORB) (Sun et al., 1979).

LREE depleted patterns are common also in tholeiites from the marginal basin (e.g., Lau Basin, Hawkins, 1977), from the island arcs and fall within the range of MORB (Ashley et al., 1979).

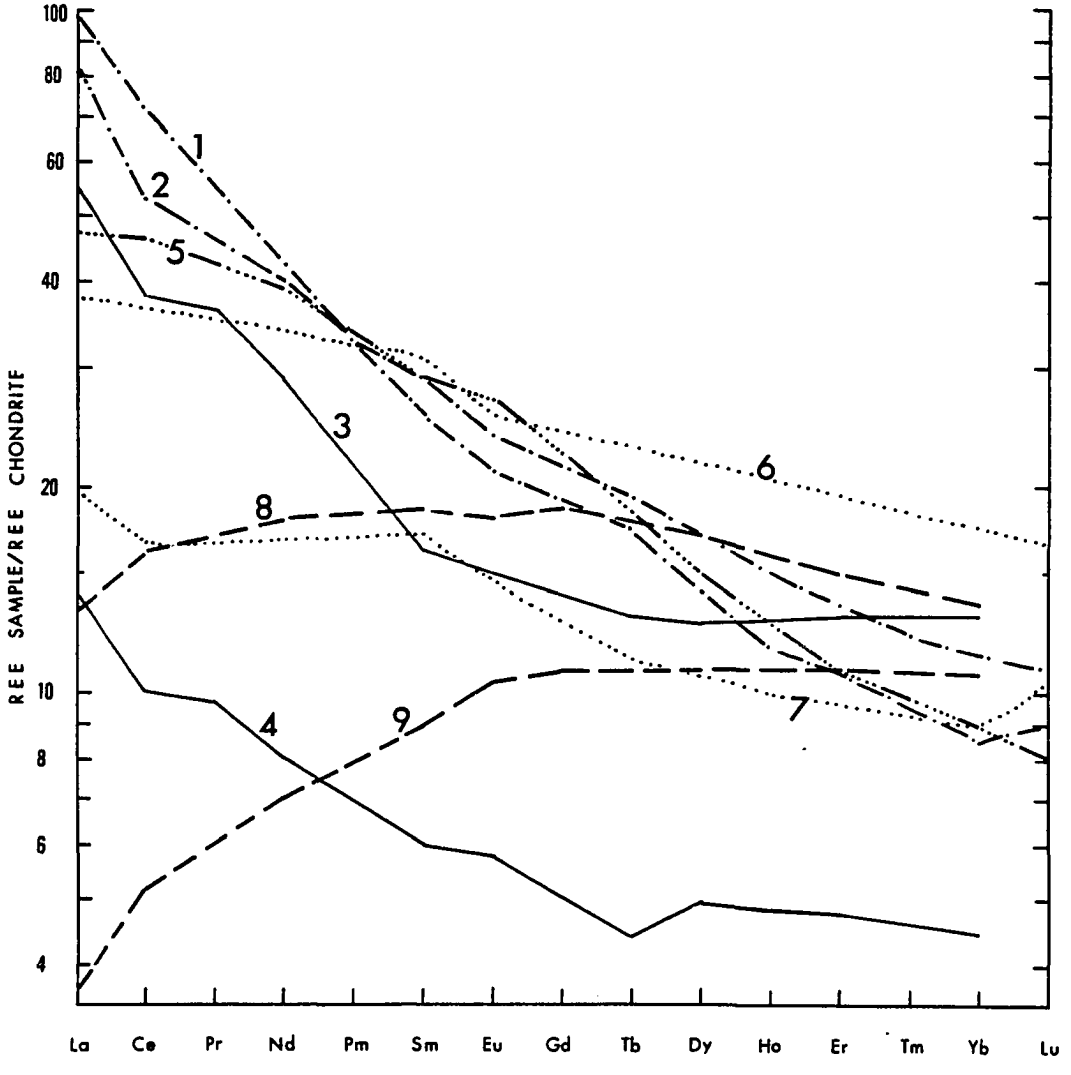

et al., 1979). Besides, LREE enriched basalts are also found in aseismic oceanic ridges.

A comparison of the REE patterns of the Bela basalts with the above indicates that they are unlike the normal type MORB and the island-arc tholeiites. Several other patterns are like those of the Bela basalts; however, some Bela basalts are different in having sharp positive Tb and Nd anomalies. It is not known whether these anomalies are primary in origin or a result of alteration. Since LREE enriched basalts occur in a number of different tectonic environments, it is not possible to say which of these is more suitable for the Bela basalts.

Figure 56 shows REE patterns of basalts from several ophiolites for comparison with those of the Bela Ophiolites. It is shown that the ophiolitic basalts exhibit a range of LREE depleted to LREE enriched patterns very similar to those from the various modern oceanic tectonic settings (Fig. 55). Thus, based on the REE patterns (i.e., depletion or enrichment in LREE) no definite conclusions can be reached about the original tectonic setting of ophiolites (Kay and Senechal, 1976; Lewis and Bloxam, 1977; Coish and Church, 1979; Ashley et al., 1979; Suen et al., 1979).

Sills (Bela Intrusives):

Like the petrographic features, the chemistry of the Bela Intrusives is also much like that of the Bela basalts.

Alkali-SiO_2 Diagram (Fig. 45) and K_2O:SiO_2 Diagram (Fig. 46): The 12 samples of Bela Intrusives fall in equal numbers in the alkaline and subalkaline fields. One of these plots in the strongly alkaline field. Similarly on the K_2O:SiO_2 plot, they fall in the fields of both low-K subalkaline and alkaline rocks.

Figure 56. Examples of LREE enriched and LREE depleted patterns in ophiolite basalts.

A = A Caradocian tholeiite of the Girvan Ballantrae Ophiolite, Ayrshire, Scotland (Lewis and Bloxam, 1977) (Sample, Varr 130).

B = Coolac ophiolite basalt, southern New South Wales (sample MU 3973 from Ashley et al., 1979).

C = Tholeiitic basalt (sample 549) from the Marum ophiolite complex, northern Papua, New Guinea (Jaques et al., 1978).

D = Balagne basalts REE range, Corsican ophiolite, W. Mediterranean (Venturelli et al., 1979, Fig. 5).

E = REE range for Troodos basalts and diabases (Kay and Senechal, 1970). The pattern is similar to that for normal MORB. Vourinos and Bay of islands ophiolite lavas also show a similar pattern.

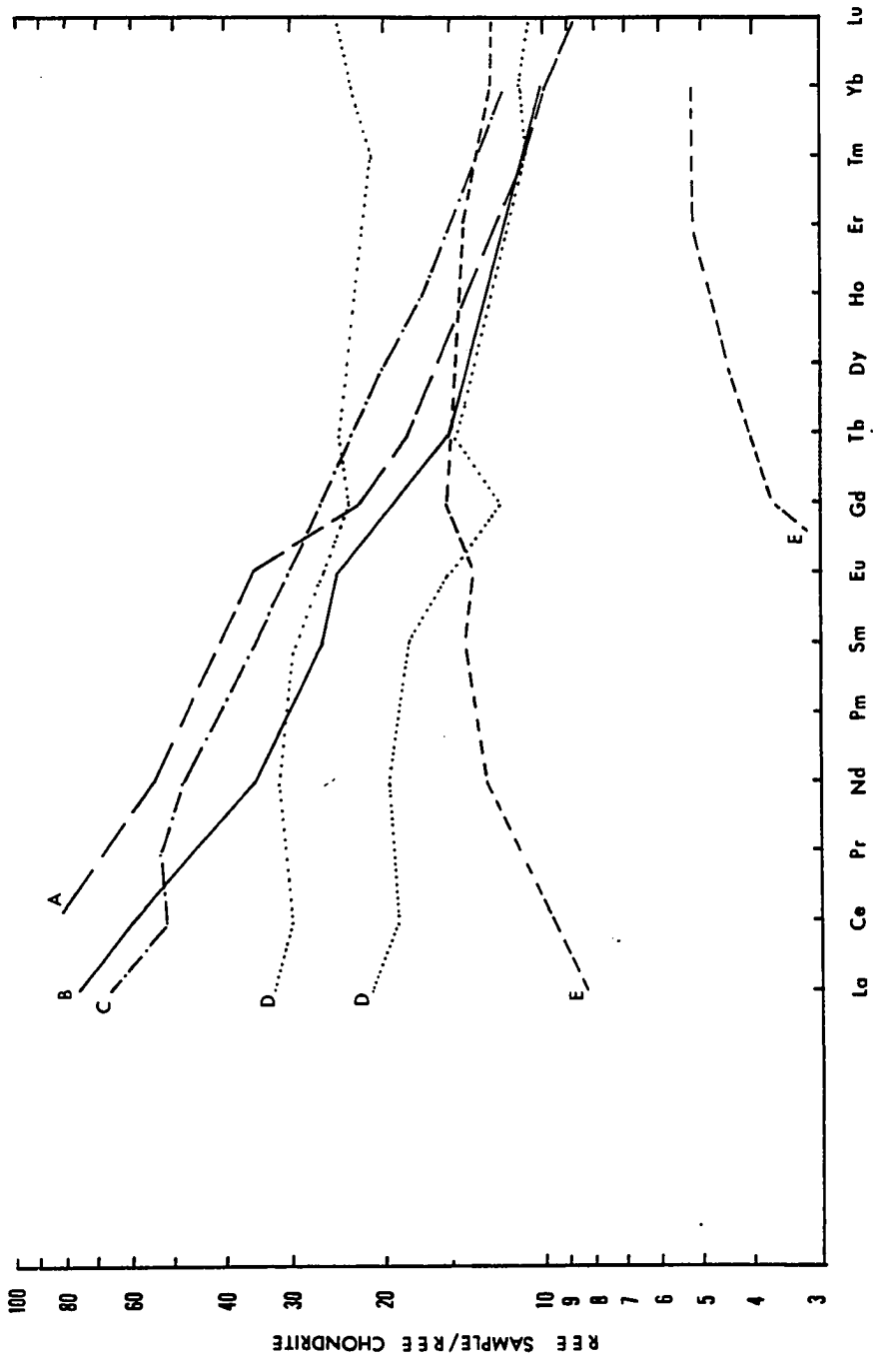

SiO_2:Fe/Mg Diagram (Fig. 47): All samples, like those of the Bela basalt, plot in the tholeiitic field of IAT and MORB.

Fe:Fe/Mg Diagram (Fig. 48): On this plot, 11 out of 12 samples fall in the tholeiitic field and, like the Bela basalts, follow the MORB trend. The Fe-rich character of the sills with respect to the lava flows is apparent. The Fe/Mg ratio for the sills is (1.5-313), versus (1.9-2.7) for the lava flows.

TiO_2:FeO/MgO Diagram (Fig. 49): On the TiO_2:FeO*/MgO diagram, the Bela Intrusives range higher than the Bela basalts and abyssal tholeiitic basalts. The greater range of TiO_2 (1.1-3.4) and other oxides in the Bela Intrusives versus the Bela basalts could be due to advanced fractional crystallization in the intrusives (cf., Miyashiro, 1975). It is interesting to note that the Bela basalts and intrusives as a group are more TiO_2 and Fe-enriched than the modern OFB. A distinct feature of the tholeiitic rock series is that the magma shows increase in TiO_2 with a maximum during fractional crystallization (Miyashiro, 1973, Fig. 2; 1975, p. 258). This is clearly shown by the Bela Intrusives (Fig. 49). The calc-alkaline rocks on the other hand, show decrease in TiO_2 during fractionation (Miyashiro, 1973; 1975). The calc-alkaline rocks also have lower TiO_2 than the abyssal tholeiites, however low TiO_2 abyssal rocks do occur. According to Church and Coish (1976, p. 10) for the arc tholeiites, TiO_2 = 0.4% at FeO(total)/MgO = 0.9. All the Bela lavas and intrusives are much higher than this and thus not calc-alkaline.

Note that roughly linear variation of TiO_2 versus FeO/MgO in the Bela lava/intrusive sequence probably indicates primary differentiation

control (cf., Miyashiro, 1975, p. 266). The trend parallels the tholeiitic trend of the modern OFB, as also seen in Fe:Fe/Mg plot (Fig. 48), but is more advanced.

AFM Diagram (Fig. 50): On the AFM plot, the Bela Intrusives behave much like the Bela basalts and plot mostly in the field of the Atlantic fracture zone basalts, which partly overlaps with the fields of the aseismic ridge and Atlantic rift basalts. However, the more iron and alkali enriched character of some of the intrusives is apparent. Two samples of the Bela Intrusives fall outside the fields of the rift valley and fracture zone basalts. Similar behavior is observed for the gabbroic rocks of the Kane and Romanche fracture zones (Fig. 50; Hekinian and Thompson, 1976). It is remarkable to note that like the Atlantic fracture zone basalts and gabbros, the Bela basalts, diabases and gabbros also show a greater range of FeO/MgO ratio and TiO_2 compared to the ridge generated (rift) basalts.

REE Distribution: The REE distribution pattern for the Bela Intrusives is shown in Figure 57. It broadly resembles the REE pattern of the Bela volcanics (Fig. 54), however, there are also certain differences as follows:

1. Like the lavas the sills are also enriched in LREE, however, the REE contents are generally higher in sills. Compared to chondrites, the sills are (32-86) times enriched in La and (12-20.4) times enriched in Lu. For sills:

$$\left[\frac{La}{Sm}\right]^{N} = 1.14\text{-}1.56$$

Figure 57. REE distribution patterns for the Bela Intrusives. Analyzed samples are marked by:

A = SR-34-79

B = SR-21-79

C = SR-73-79

D = SR-45-79

E = SR-14-79

In sample D the Nd and Tb content is below the detection limit (< 32.5 ppm and < 2.8 ppm, respectively).

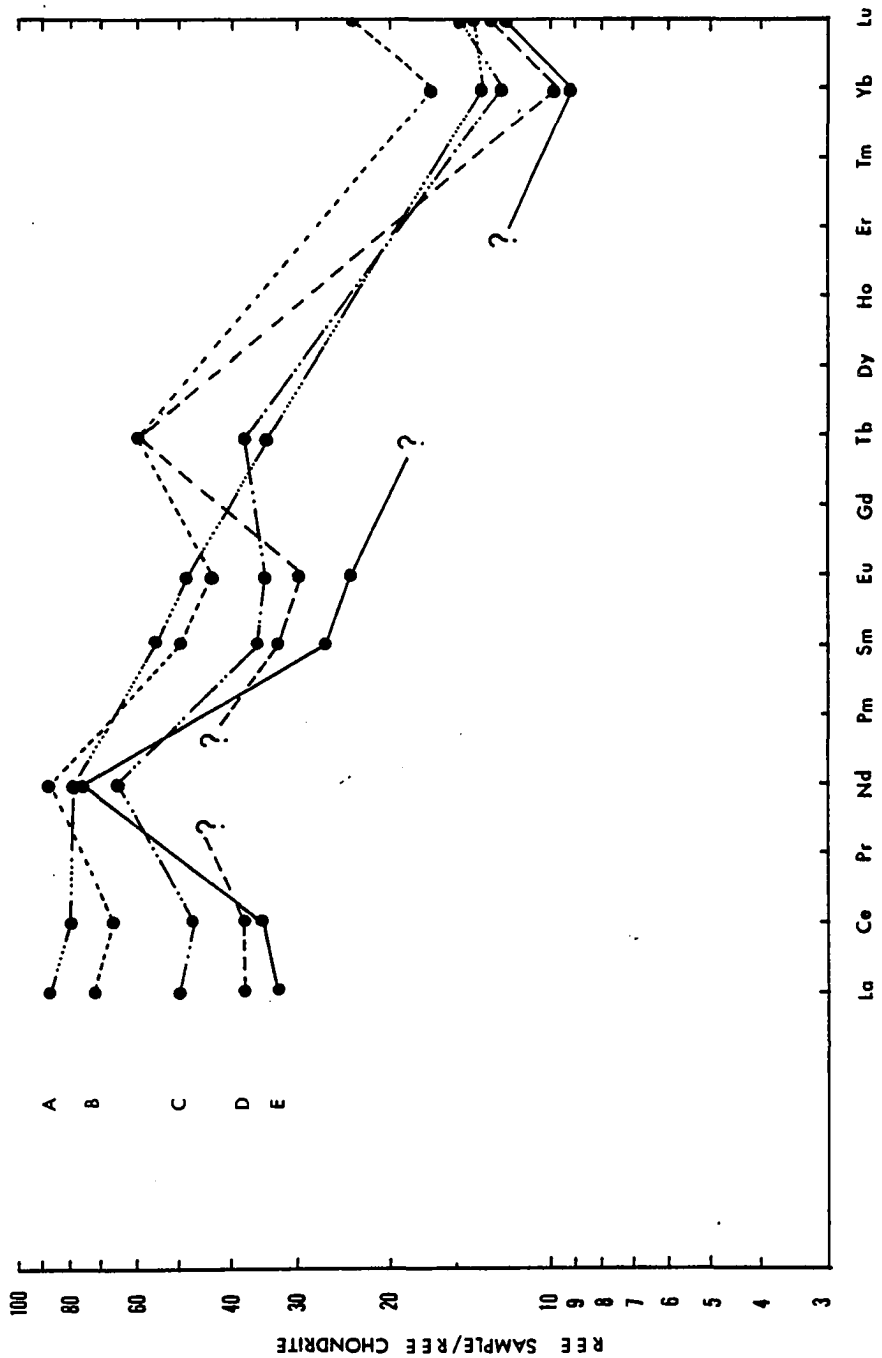

$$\left[\frac{La}{Yb}\right]_N = 3.8\text{-}6.42$$

$$\left[\frac{Ce}{Yb}\right]_N = 3.7\text{-}5.9$$

However, like the lavas, Tb and Nd enrichment seems to exceed LREE enrichment.

2. Like the lavas, all sill samples show a negative Yb anomaly but there is no Sm anomaly. Two samples (SR-21-79 and SR-73-79) from the sills show a marked negative Ce anomaly and three others (SR-21-79, SR-45-79 and SR-73-79) show a noticeable negative Eu anomaly, which is absent in the lavas. The positive Tb anomaly is well marked in three samples, whereas it is absent in one sample (SR-34-79). In sample SR-14-79, Tb was below the detection limit (see Appendix 10B). Three samples show a sharp positive Nd anomaly, whereas one sample (SR-34-79) does not show any. In one sample (SR-45-79), Nd was below the detection limit (see Appendix 10B).

3. The sample (SR-34-79) shows only a negative Yb anomaly and none of the others observed in the remaining four samples. It also follows a much more uniform LREE enriched pattern which is different from the other sill samples. Except for sample (SR-34-79), the overall REE patterns for the sills and lavas broadly mimic each other.

Enriched character of Bela Intrusives versus Bela volcanics: Chemical data (Appendix 10B, Table 6) show that the Bela Intrusives tend to be more enriched in several elements than the lava flows they intrude. Table 6 shows that, with respect to the lava flows, the intrusives are enriched in Hf, Th, Ta, Cs, and Ba. Also the intrusives show higher

range of some major elements (e.g., SiO_2, Na_2O, K_2O, Fe_2O_3, Al_2O_3, and TiO_2). Several of these (e.g., Hf, Ti, Th, and Ta) are large ion lithophile (LIL) elements that are considered to be immobile during post-solidification alteration processes (e.g., sea floor weathering, low-grade metamorphism, spilitization etc.; Wood et al., 1976; Jaques et al., 1978; Coish and Church, 1979). Therefore, it appears that the enriched character of the Bela Intrusives versus the Bela basalts is a primary feature. Since the LIL elements are partitioned into residual fractions of a crystallizing magma (Wood et al., 1979), their enrichment in the Bela Intrusives means that they (as a group) are more fractionated or evolved than the associated basalts.

The relative REE enrichment of the Bela Intrusives versus basalts is also consistent with the above idea (compare Figures 57 and 54).

The post-solidification behavior of the REE is somewhat controversial. A number of workers are of the opinion that the REE are essentially immobile during such processes as sea floor weathering, spilitization and green schist metamorphism (Lewis and Bloxam, 1977; Coish and Church, 1979; Venturelli et al., 1979; Vance et al., 1980). However, some others are in favor of a limited mobility (e.g., Wood et al., 1976; Menzies et al., 1980). In the case of the Bela Ophiolites, certain observations suggest that the LREE enriched trend and the relative enrichment of REE in the sills versus lava flows are probably original magmatic features:

1. LREE enrichment is a feature common to all samples of sills and lava flows. If this were due to some secondary process, one would expect to find at least some departure from the rule.

2. In most samples the REE pattern of the sills is similar to that of the lava flows.

3. LREE enriched patterns are not exotic and are known from other ophiolites as well as parts of the present-day oceanic crust (Figs. 55 and 56).

The broad similarities between the REE distribution pattern of lavas and sills (except for sample SR-34-79 of a sill) and the fact that the sills intrude the lava-sedimentary rock sequence, combined with identical petrographic features, already indicate that these rocks were derived from the same mantle source. However, the more enriched nature of some sills indicate that they may represent late fractionated melts. If these sills fed any lava flows, such flows are either missing in the study area or were not sampled.

The sample (SR-34-79) comes from a ±200 ft thick sill and shows LREE enriched patterns which, unlike the other sill and lava samples, is devoid of any Tb and Nd anomalies. Although its HREE content falls within the range for sills, it shows the highest LREE enrichment factor with respect to its HREE content (i.e., $[La/Yb]^N$ = 6.42 compared to $[La/Yb]^N$ = 3.4-4.29 for other sills). Its Ba and K content and FeO(total)/MgO ratio is also higher than most sills and lavas. On the basis of these observations it appears that this sill was derived from a still more enriched or fractionated melt than the other sills.

Summary of Petrographic and Chemical Features of Mafic Rocks:

1. The Bela Volcanics are hypocrystalline to holocrystalline rocks texturally more varied than the associated Bela Intrusives. The Volcanics

show equigranular, porphyritic, glomeroporphyritic, subophitic-ophitic, intersertal and trachytic textures. They are mostly spilitic basalts and less commonly keratophyres and basaltic andesites.

2. The Bela Intrusives are mostly fine to coarse grained diabases and diabasic gabbros with ophitic and porphyritic type textures. They also exhibit spilitic mineralogical features. However, some may be classed as dioritic diabases. A single plagiogranite (quartz keratophyre) dike is also present.

3. The Bela Volcanics are mostly like low-K tholeiites with an alkaline tendency. However, compared to the ridge generated basalts the Bela basalts are more Fe and TiO_2 enriched and, in this respect resemble the Atlantic fracture zone basalts. Some trace element data (Ta, Th and Hf) indicates that the Bela Volcanics are like some enriched (E-type) basalts erupted along anomalous segments of oceanic ridges (e.g., hot spots); however, the tange of La/Ta ratio of the Bela Volcanics is different both from the E-type and other (normal; N-type) baslalts erupted along ridges.

4. The Bela Volcanics exhibit an LREE enriched pattern which is different from the LREE depleted patterns of normal MORB and arc-tholeiites. The LREE enriched basalts are known from certain anomalous oceanic environments such as parts of spreading centers (hot spots), ocean islands, fracture zones and aseismic ridges. Thus, in a few words, the Bela Volcanics are spilitic tholeiites, low in K but enriched in certain major and trace elements (e.g., Fe, TiO_2, LREE) that were probably formed in an anomalous oceanic tectonic setting.

5. The diabase-gabbro sills (Bela Intrusives) are also chemically similar to the associated lava flows. However, they tend to be more enriched (e.g., in alkalis, Fe, TiO_2, REE, Hf, Th, Ta, Cs, Ba etc.). This suggests that some sills represent more fractionated late melts.

6. Field relations, petrographic and chemical similarities between the lava flows and the sills indicate that they were derived from a common magmatic source.

Petrography of Other Ophiolite Rocks:

This section is concerned with the serpentinites, serpentinite-carbonate breccias (ophicalcite), detrital serpentinites and some exotic rocks found in the melange horizons within the Bela Ophiolite sequence; many of these, however, are also found in the Kanar Melange, as described elsewhere. Following is an outline of the petrographic characters of these rocks; more detailed information is presented in Appendices 6-9.

Serpentinites: These are variably deformed and almost totally serpentinized peridotites, harzburgites and pyroxenites of mottled green, gray, brownish gray or black color. Serpentine pseudomorphs after pyroxene (bastite ?; Fig. 58) are quite common, however, those after olivine are rare. Relicts of fresh pyroxene are occasionally present but fresh olivine was not observed. Among others, opaque minerals (magnetite, hematite) are always present and may be locally abundant. Chlorite, tremolite-actinolite, biotite and carbonate are also occasionally present.

Serpentine-Carbonate breccias (ophicalcite; Abbate et al., 1972): These consist largely of angular serpentinite clasts embedded in a carbonate matrix (Fig. 59). The serpentinite is very similar to that described

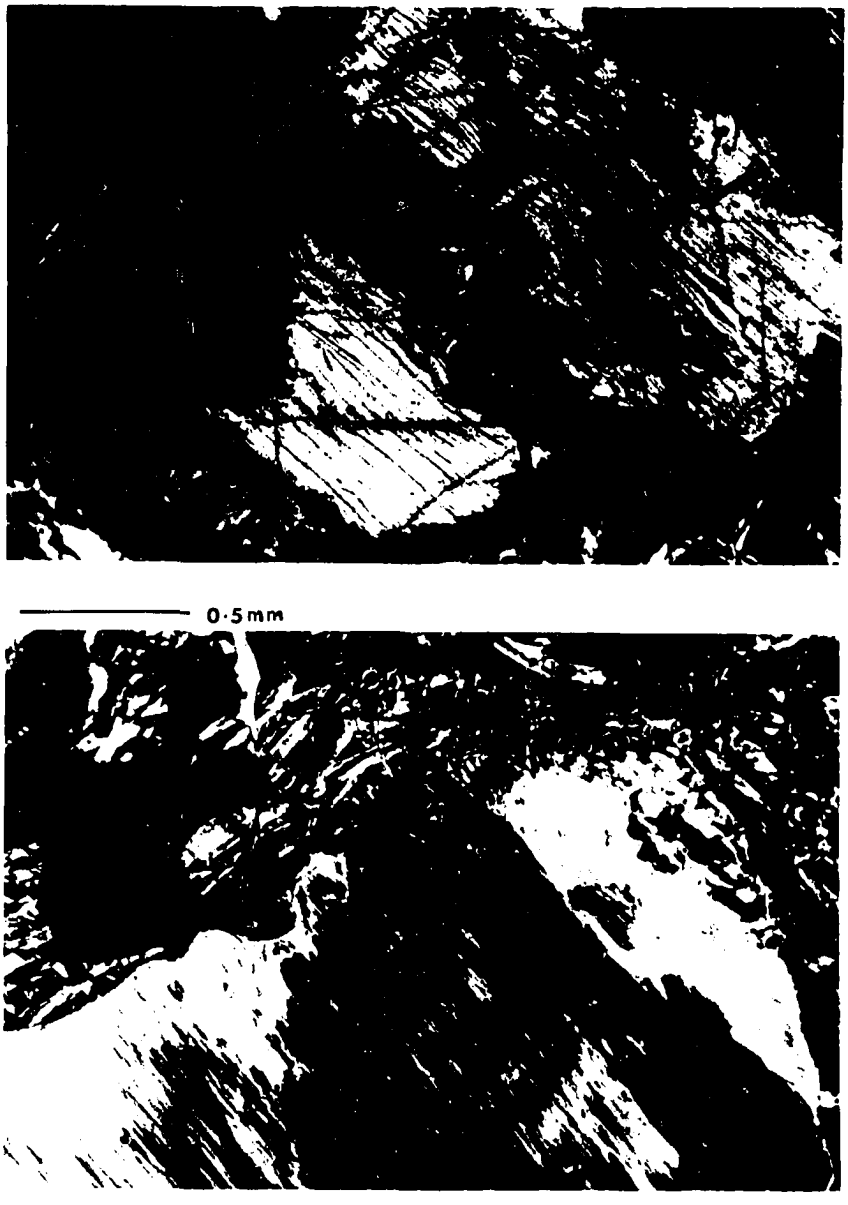

Figure 58. Serpentine pseudomorphism after pyroxene (note cleavage; bastite ?) and a few hematite grains in serpentinite. Note deformed cleave traces (cross nicols).

(Sample Nos. 78-SR-54 and SR-29-79)

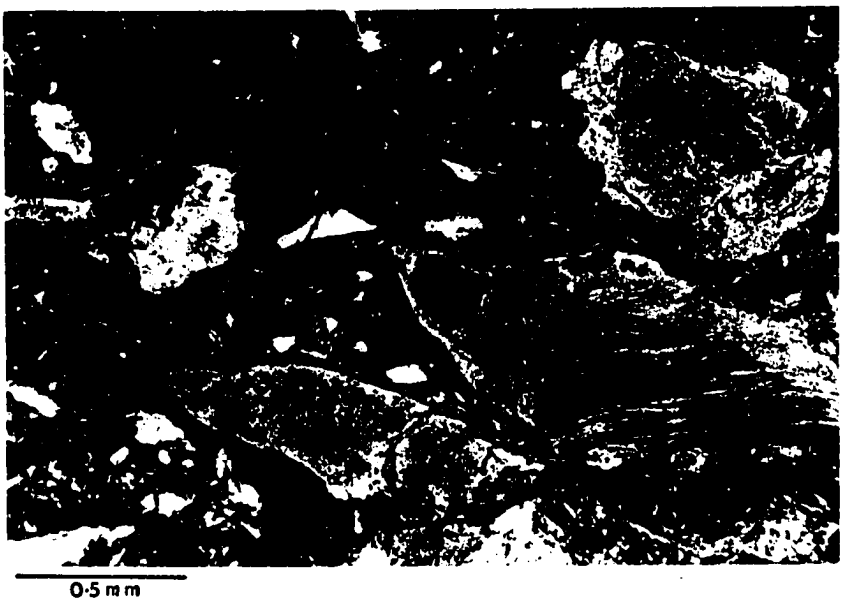

Figure 59. Ophicalcite showing poorly aligned, angular to subrounded clasts of serpentinite set in a calcite matrix. Note a serpentine pseudomorph after pyroxene (deformed cleavage traces) (cross nicols).

(Sample No. 78-SR-28)

above. However, some breccias consist of highly carbonatized serpentinite with calcite and serpentinite filled fractures. Clasts of opaque minerals (magnetite, hematite), tremolite, nephrite(?), calcite, phlogopite (rare) and rock clasts (reworked host rock, chert, altered basalt ?) are also occasionally present. The matrix is mostly formed by calcite (rarely dolomite) and some finer serpentinite and clay material. Presence of certain features (e.g., calcite-coated serpentinite clasts, tiny globular aggregates and pelloids of possibly organic calcite, deformed clasts embedded in undeformed matrix) suggests that a tectonic origin cannot be argued for all breccias and some are probably of sedimentary origin (see Appendix 7 for details).

Detrital Serpentinites: These rocks include some serpentinite-carbonate sandstones (Fig. 60) and pebble/boulder beds.

These rocks are light greenish gray to brown in color and consist of texturally and compositionally immature material. That is, sorting and bedding characters are poorly defined and most clasts consist of serpentinite. Clasts of other types such as altered mafic minerals, opaques, calcite, reworked host rock, limestone, chert and altered basalt are occasionally present. The clasts are embedded in dominantly micritic calcite matrix.

Exotic Rocks: Among these are included some metasedimentary and meta-igneous rocks occasionally formed as small blocks in the melange belts within the Bela Ophiolites (e.g., marble, schistose clastic rock, meta-gabbro, metabasalt and amphibolite; Fig. 61).

Figure 60. Lithic sandstone with clasts of serpentinite (dark) and calcite (light) set in a calcite matrix. Some clasts are coated with dark iron oxide (arrows); the large one consists of a core of serpentinite grown over by radially disposed calcite (cross nicols).

(Sample No. SR-19-79)

Figure 61. Amphibolite showing poorly oriented hornblende grains with deformed cleavage. White areas are anhedral plagioclase grains; some chlorite is also present (cross nicols).

(Sample No. SR-62-79)

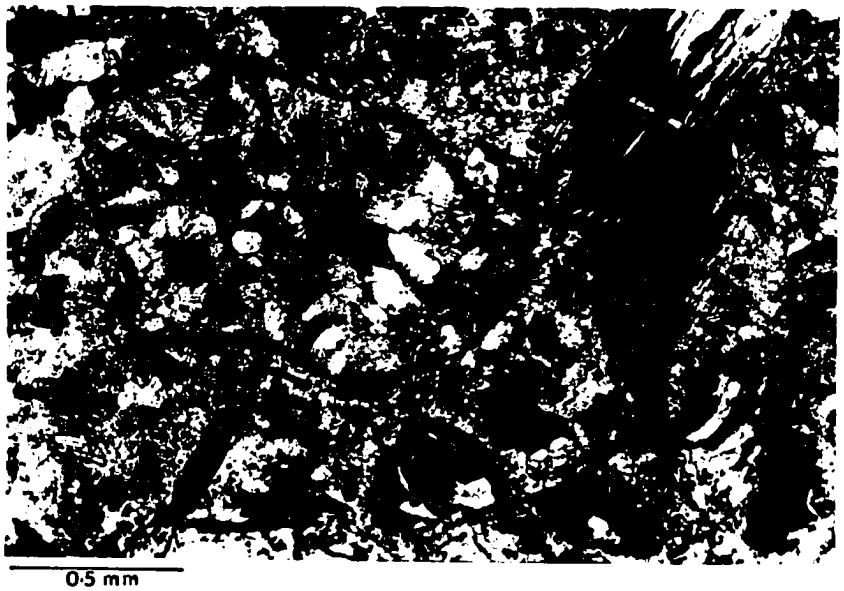

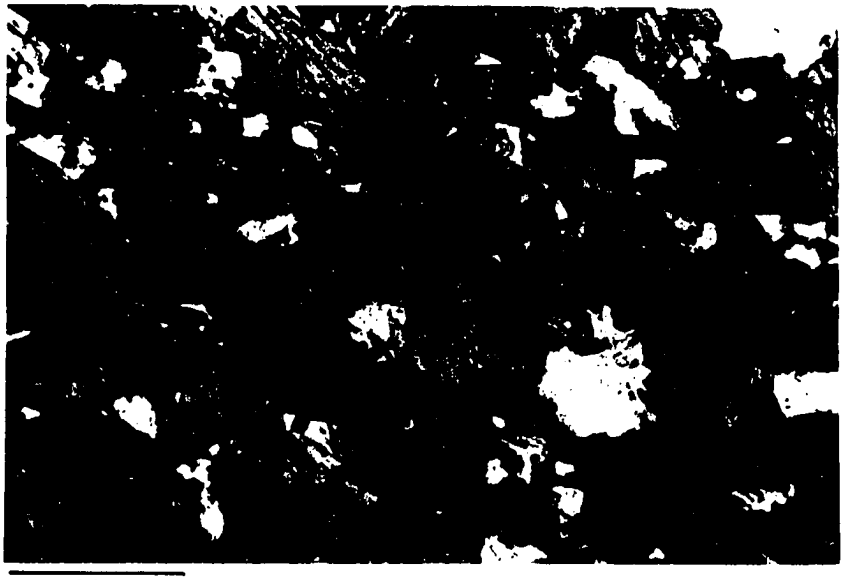

Metamorphic Features of the Bela Ophiolites:

Rocks showing metamorphic features in the Bela Ophiolites can be divided into three groups:

A. Bela volcanics and Bela intrusives (lava flows and sills)

B. Rocks found in melanges within the ophiolites (e.g., serpentinite)

C. Contact metamorphic rocks (along sills)

These groups exhibit contrasting metamorphic features as follows:

The Bela volcanics and intrusives show typical igneous textures (e.g., ophitic, porphyritic, trachytic etc.), however, their spilitic mineral assemblage resembles that of green schist facies (chlorite-lower amphibolite) metamorphic rocks. For example, the clinopyroxene is considerably uralitized to amphibole (hornblende, tremolite-actinolite) and chlorite aggregate. The plagioclase feldspar is variably saussuritized. Chlorite veining and replacement of feldspar is present. Magnetite or ilmenitomagnetite also shows alteration to leucoxene and sphene. Also hematite is present and could possibly have been derived from primary iron minerals. Quartz, calcite, and zeolites also occur.

The igneous texture and secondary looking mineralogy of the Bela volcanics and sills is similar to the spilitic rocks found elsewhere around the world. These rocks are the subject of a great controversy as to their magmatic and/or metamorphic origin (see Appendix 1). The Bela volcanics and sills exhibit petrographic features that have been used to claim a primary or secondary origin for spilites elsewhere. Among those for a primary origin are the preservation of delicate igneous textures, e.g., ophitic intergrowths of clinopyroxene, plagioclase and opaque

minerals; myrmekitic intergrowth of plagioclase and quartz; texture involving plagioclase and colloform chlorite (Patwardhan and Bhandari, 1974). Among those for a secondary origin are the various alteration products mentioned in the previous paragraph.

Such conflicting features are typical of the spilitic suite in general, therefore, the origin of the spilitic nature of the Bela volcanics and sills is probably as unclear as that of other spilites. However, following the arguments of those in favor of a secondary origin (see Appendix 1), a metamorphic origin for the spilitic nature of the Bela volcanics and sills is favored here. Also, green schist-amphibolite grade mafic igneous rocks, similar to those of the Bela Ophiolites, are known from other ophiolites where they have been interpreted as oceanic crust metamorphosed along a spreading ridge (Dewey and Bird, 1970; Gass and Smewing, 1977; Coleman, 1977; Liou and Ernst, 1979). Similar rocks have also been dredged from the modern ocean bottoms including fracture zones (Cann, 1969; Bonatti, 1976, 1978; Bonatti and Honnorez, 1976; Bonatti et al., 1971, 1974; DeLong et al., 1979).

Lack of oriented tectonic fabrics in the Bela volcanics and sills indicate that they were metamorphosed under static conditions. Also, the absence of any regional metamorphism in the autochthonous sequence that underlies the ophiolites, suggests that the Bela volcanics and sills were metamorphosed before the ophiolites were emplaced, i.e., the metamorphism had taken place in the oceanic regime.

The metamorphosed rocks found in the melanges within the ophiolite sequence pose a different problem. These include such rocks as serpentinite, ophicalcite breccia, metagabbro, amphibolite and marble. They

occur as clasts of different sizes and, unlike the Bela volcanics and sills, show a variable but distinct tectonic overprint (e.g., foliation). The presence of such deformed rocks cannot be accounted for by the static metamorphism alone; however, it can be easily explained within the framework of an oceanic fracture zone model discussed elsewhere (see Fig. 65, p. 176). According to this model, the debris of deformed metamorphic rocks may be periodically released from dynathermally metamorphosed zones in a fracture zone.

Contact metamorphic effects along the Bela Intrusives are negligible in the lava flows and limited in the sedimentary rocks. The argillaceous rocks are baked, silicified or hornfelsized and converted to a dense resistant material only for a few centimeters; the limestones show more pronounced effects (e.g., development of calc-silicates), but again just along the contacts (Figs. 62-63).

Figure 62. Epidote hornfels showing euhedral porphyroblasts of epidote (zoisite ?) set in a calcite matrix (cross nicols).

(Sample No. SR-69-79)

Figure 63. Pyroxene hornfels showing radial blades of hedenbergite porphyroblasts and recrystallized calcite (arrow). Finer material consists of plagioclase feldspar, quartz, hedenbergite, tremolite and calcite.

(Sample No. SR-96-79)

ORIGIN OF THE BELA OPHIOLITES

Introduction

According to the concepts of plate tectonics ophiolites represent lithospheric materials formed in four different tectonic settings:

1. Major ocean basins of the Atlantic type (Gass, 1968; Coleman, 1971; Moore and Vine, 1971; Laurent, 1975, 1979).
2. Small marginal basins of the western Pacific type (Karig, 1970, 1971; Matsuda and Uyeda, 1971; Dewey, 1974; Dalziel et al., 1974; Upadhyay and Neale, 1979; Hawkins, 1977, 1979; Sinton, 1980).
3. Island arcs (or inter-arc basins) (Miyashiro, 1973, 1975a and b; Beccaluva, 1979; Brunn, 1979; Gealy, 1979; Menzies et al., 1980).
4. Fracture zones of a major basin (transform fault including its inactive trace) (Gianelli and Principi, 1977; Tysdal et al., 1977; Saleeby, 1977, 1979; Simonian and Gass, 1978; Karson and Dewey, 1978; DeLong et al., 1979).

It is generally believed that ophiolites are emplaced on destructive continental plate margins (Dewey and Bird, 1970, 1971; Dewey, 1976; Gass, 1977; Coleman, 1971, 1977; Brookfield, 1977). In this sense ophiolites are allochthonous by definition. However, an autochthonous marginal basin origin has recently been suggested for certain Chilean ophiolites (Dalziel et al., 1976; Saunders et al., 1979).

Aside from the above, a few other ideas are: Maxwell (1973, 1974) proposed that the Tethyan and some Franciscan ophiolites formed by diapiric intrusion/extrusion of mantle material. Muratov (1977, p. 125) suggested a "protrusion" of upper mantle "into the bottoms of the troughs" to explain the Alpine-Hercynian ophiolites. Brunn (1979) maintained that some ophiolites originated by oceanization of downwarped continental platforms - a view held by many Soviet workers to explain the origin of ocean basins (see Muratov, 1977, p. 157).

Determination of initial tectonic setting of ophiolites

The determination of the initial tectonic setting of ophiolites is tedious and requires a detailed study of their field relations, lithostratigraphic and structural features combined with relevant plate tectonic considerations (e.g., Glennie et al., 1974). Better preserved ophiolites (e.g., Troodos, cyprus) are not common, therefore, the desired structural, sedimentological or petrological evidence may be absent.

In such cases chemical discriminants between basaltic rocks from differing tectonic environments have been increasingly used in an attempt to characterize the original tectonic setting of ophiolites (e.g., Pearce and Caan, 1973; Pearce, 1975, 1976, and in press; Pearce et al., 1975, 1976, 1977; Pearce and Gale, 1977; Venturelli et al., 1979). A host of major and trace elements have been used for this purpose (e.g., Ti, K, P, Si, Al, Fe, Ca, Na, Sr, Nb, Cr, Zr, Ba, La, Hf, Y, and the rare earths). It has been claimed that the proposed discrimination diagrams can distinguish basaltic rocks of the following tectonic environments: ocean ridge, ocean island, island arc and continent. However, as yet there is

no consensus on the distinction between basalts from major and marginal arc-related basins (Hawkins, 1977; Saunders et al., in press). Also, to this writer's knowledge, little has been published on the chemical discrimination of basaltic rocks erupted in a fracture zone from similar rocks formed elsewhere. Another major problem with the above approach is the lack of or poor understanding of the theoretical bases (e.g., Pearce et al., 1975; Wood et al., 1979; Saunders et al., in press). Usually the results are accepted as empirical facts and little explanation is offered. Therefore, many workers have even questioned the basic validity of the technique itself (e.g., Gass et al., 1975, and the references therein; U.S. National Report, 1975-1978, p. 807).

Previous Views on the Origin of Bela Ophiolites

The earliest view on the origin of basaltic rocks in the Bela area was that they were an extension of the Deccan plateau basalts of west-central India (Vredenburg, 1909; Wadia, 1953). Later the Hunting Survey (1960, p. 382-385) suggested that the Kirthar-Sulaiman orogenic belt which includes the Bela Ophiolites, originated in the same way as modern island arc systems. The Hunting Survey included the volcanic rocks of the Bela Ophiolites in their Bela Group which represented undifferentiated Cretaceous marine sedimentary and volcanic rocks of the southern Kirthan Range. The gabbroic and ultramafic rocks of the ophiolites were named Porali intrusives and thought to have been emplaced in the Bela Group during Late Cretaceous-Early Eocene time (Hunting Survey, 1960; Bakr and Jackson, 1964).

Subsequently, the Pakistani ophiolite belt (Fig. 1), including the Bela Ophiolites, was interpreted as obducted fragments of the Tethyan

lithosphere (Gansser, 1966; Farah, 1972; Stocklin, 1977; Sillitoe, 1975, 1979; Assrarullah et al., 1979; Abbas and Ahmed, 1979; Powell, 1979). Gansser (1979) and DeJong and Subhani (1979) recognized the tectonic emplacement of the Bela Ophiolites. DeJong and Subhani (1979) also suggested that the Bela Ophiolites represented sea mounts formed at a distance from a spreading center, and that the Porali Agglomerate (Porali Conglomerate of this study) represented debris of a late Cretaceous island arc located on the margin of the Indo-Pakistan subcontinent. This arc was later overthrust by the Bela Ophiolites.

Discussion

Chemical Considerations

Chemical features of the Bela basalts and their comparison with similar rocks from known tectonic environments have been described in a previous section. A summary of the more interesting points, intended to supplement the present discussion, is as follows:

1) The Bela basalts are spilitic and mostly low K-tholeiites with an alkaline tendency; they are not calc-alkaline.

2) They resemble the modern abyssal tholeiites in their general character (Table 6). However, compared to normal ridge-generated basalts, they are more like certain basalts erupted along anomalous sections of the oceanic crust as explained below:

A. They are more enriched in TiO_2, Fe, and, in this respect, compare well with the Atlantic fracture zone basalts (Fig. 39).

B. Ta, Th, and Hf data (Fig. 53) indicate that the Bela basalts are like some enriched basalts erupted along anomalous segments of

oceanic ridges (e.g., hot spots); however, their La/Ta ratio is different from both the normal and anomalous ocean ridge basalts.

3) The Bela basalts are enriched in LREE as compared to HREE and thus differ from both the normal oceanic ridge and arc-basalts which are LREE depleted.

4) The LREE enriched pattern of the Bela basalts is broadly similar to those erupted along the various anomalous tectonic settings within a large basin (Figs. 54-55) such as fracture zones, ocean islands, aseismic ridges and even some parts of the oceanic ridges.

The above observations clearly demonstrate the difficulty of making an unbiased choice from several widely different oceanic environments as the most likely setting for the Bela Ophiolites. However, it is clear that the Bela basalts are low K-spilitic-tholeiites (enriched in TiO_2, Fe, LREE and some other trace elements), that were probably erupted in some anomalous oceanic tectonic setting. Some chemical features such as the strongly alkaline nature of aseismic ridge basalts (Fig. 50) seem to set them apart from the Bela basalts. The Bela basalts also have a much higher Hf/Ta ratio (2.9-5.7) as compared to those from the ocean islands (< 2).

Field Considerations: Marginal basin-island arc and major basin origin.

A comparison of the Bela ophiolite sequence with those of major (Atlantic type) and small marginal (western Pacific type) basins is presented in Table 7. It shows that the Bela ophiolite sequence is unlike that of the marginal basin-island arc environment, e.g., the volcanogenic flysch piles found in the marginal basins (Dewey and Bird, 1971; Dietrich et al., 1978; Hawkins, 1979; Sigurdsson et al., 1980) are absent in the

Table 7. Comparison of the Bela Ophiolite Sequence with Those Formed in Different Oceanic Tectonic Settings.

Variables	Major Basins (Atlantic type)	Marginal Basins (Western Pacific type)
Tectonic Setting	Spreading oceanic ridge (8,9) basins overlying accretion zones. Tension (7.18) > compression > shear.	Inter-arc/back-arc spreading basins overlying subduction zones (8,9,15). Tension (7-10) > compression > shear.
Basin Shape	Multiple, narrow elongate rift basins/horsts parallel to ridge (1,3,16).	Multiple, linear enechelon rift basins (9)/ horsts roughly parallel to flanking arc(s).
Basin Relief	Irregular, tectonically controlled; up to 2 km(?) (16).	Irregular, tectonically controlled (1,9-12, 15); ±1-4 km (9).
Generalized Stratigraphic Sequence	1: Lava flows and interbedded/overlying sedimentary rocks: Mainly pillowed basalt + deep-sea pelagic-siliceous muds (limestone + argillite + chert) (12,13,15) + locally derived volcaniclastics (turbidites, talus deposits, slide blocks) (1,3,4,10,12,15, 17). 2: Sheeted dikes (diabase-gabbro) (11,14). 3: Cumulate gabbroic rocks (11,12,14). 4: Cumulate/tectonite ultramafic rocks (9,11, 14) (minor intermediate-felsic intrusive/ extrusive rocks (3); e.g., plagiogranite) [occasional (?) diapir-derived serpentinite debris (2,5,6,12)].	1: Lava flows and interbedded/overlying sedimentary rocks: Pillowed basalt (7,15) + andesite-dacite (6,9) + deep-sea sedimentary rocks (9-10) + locally and arc-derived volcaniclastics (turbidites, flysch aprons/wedges, talus deposits, slide blocks, agglomerate, tuff, ash beds) (3-6, 8-10,12,16). 2: Sheeted dikes (diabase-gabbro) (14). 3: Cumulate gabbroic rocks (14). 4: Cumulate/tectonite ultramafic rocks (13, 14) (num erous intermediate-felsic intrusives) (6,9,14); (serpentine diapirs ?).
Thickness	Variable (14); sedimentary rocks = 350 m (13); basalts = 1.7 km (11).	Variable (2,8); sedimentary/volcanic rocks = 2-3 km (1,11,12).
Metamorphic Features of Oceanic Origin	Greenschist-amphibolite facies (8-9) (primary features commonly preserved); cataclasites (2, 10) (minor ?); tectonite ultramafic rocks (14,19).	Like major basins (3,14,15).
Distinctive Features	Underlined above.	Underlined above; additional; Sedimentary-volcanic sequence may overlap flanking continental blocks or interfinger with island-arc sequence (15); it may also include elements of rifted arc (3).

Table 7. (continued)

Variables	Oceanic Fracture Zones [Large transform faults (Romanche Fracture Zone)]	Bela Ophiolites
Tectonic	Ridge-ridge or ridge-trench transform faults (25) of intraplate and plate-boundary setting. Shear (6,17,23) > tension (9) - compression (3,6).	Not known.
Basin Shape	Multiple, linear, narrow, V-shaped fault block bound troughs (3,5,9); width = up to 30 kms (3,5); depth = up to ±5 km (5); length = up to several hundred km (15). Width of trough/block domain up to several tens of kms; length up to a few thousand kms (3,5,15,26).	Not known; probably tectonically controlled, deep, linear fault block bound troughs.
Basin Relief	Highly irregular (5); tectonically controlled; up to 5 km (3,5,18).	Not known; probably highly irregular.
Generalized Stratigraphic Sequence	Highly variable (5,19,14,17). 1: Lava flows and interbedded/overlying sedimentary rocks; mainly pillowed basalt (5,13) + deep-sea sedimentary rocks (5,9,15) + locally derived debris of oceanic rocks (turbidites (7,9,21); chaotic slide deposits/blocks (2,9,11,17,20,21); tectonic breccia (6). Includes large proportion of serpentinite debris (1,5,7,8,16) and other oceanic rocks (5). 2: Diabase-gabbro sills/dikes within and below volcanic/sedimentary sequence (14,17). 3: Gabbroic rocks (14,17). 4: Ultramafic rocks (9,14,17) (minor intermediate-felsic intrusive (13)/extrusive rocks, e.g., plagiogranite) (serpentinite diapirs extensive and abundant) (3,4,9,14,17).	Highly variable. Mainly basaltic pillow lavas and interbedded/interfingered pelagic limestone-chert-argillite intruded by diabase-gabbro sills and a few dikes (1,2); includes several horizons of locally derived chaotic debris (melanges) and blocks of oceanic rocks, e.g., abundant serpentinite, ophicalcite, mafic rocks and sedimentary rocks. Tectonic breccias (1,2); includes minor felsic intrusives (plagiogranite).
Thickness	Variable 99,14,17); sedimentary/volcanic rocks = 2.5 km (15).	±3 - ±5 km.

Table 7. (continued)

Variables	Oceanic Fracture Zones) [Large transform faults (Romanche Fracture Zone)]	Bela Ophiolites
Metamorphic Features of Oceanic Origin	Green schist-amphibolite facies (5,8,13,15, 18,21) (primary features locally destroyed). Includes highly deformed blocks of metasedimentary/igneous rocks, e.g., marble, gneissic gabbro, foliated/brecciated serpentinite, ophicalcite (3,10,13,17,19,21,22).	Greenschist (2)-amphibolite facies rocks; marble (2); cataclastic-penetrative fabric common in melange belts (1,2) and individual slide blocks.
Distinctive Features	Underlined above; additional; A - deformation at high angles or perpendicular to sheeted dikes (22). B - recurrent tectonism ± mafic intrusive/extrusive activity during sedimentation (9,17,20,21). Type of evidence: 1 - blocks with refolded/refoliated fabric embedded in undeformed sedimentary rocks. 2 - different crustal levels locked up against each other (17) and blanketed by sedimentary/volcanic rocks. 3 - undeformed/mildly deformed sills/dikes in folded/foliated rocks.	Evidence for recurrent tectonic and magmatic activity during sedimentation.

Table 7. References.

Major Basins

1. ARCYANA, 1975
2. Aumento and Loubat, 1971
3. Ballard et al., 1975
4. Bezrukov et al., 1975
5. Bonatti, 1976
6. Bonatti and Honnorez, 1976
7. Daignieres et al., 1975
8. Dewey and Bird, 1971
9. Dewey and Bird, 1970
10. Dimitriev and Sharas'kin, 1975
11. Gass, 1977
12. Hall and Robinson, 1979
13. Maxwell et al., 1970
14. Moore and Jackson, 1974
15. Robinson et al., 1980
16. Rona et al., 1976
17. Smewing et al., 1977
18. Sykes, 1967
19. Thayer, 1979

Marginal Basins

1. Broin et al., 1977
2. Dewey, 1974
3. Dewey and Bird, 1971
4. Dickinson and Suczek, 1979
5. Dickinson and Valloni, 1980
6. Gill, 1976
7. Hawkins, 1979
8. Hawkins, 1974
9. Karig, 1970
10. Karig and Moore, 1975
11. Ravenne et al., 1977A
12. Ravenne et al., 1977B
13. Ridley et al., 1979
14. Saunders et al., 1979
15. Dietrich et al., 1978
16. Upadhyay and Neale, 1979

Fracture Zones

1. Abbatte et al., 1972
2. ARCYANA, 1975
3. Bonatti, 1978
4. Bonatti, 1976
5. Bonatti and Honnorez, 1976
6. Bonatti et al., 1974
7. Bonatti et al., 1973
8. Bonatti et al., 1971
9. DeLong et al., 1979
10. Dewey and Bird, 1971
11. Dewey and Bird, 1970
12. Dietrich et al., 1978
13. Engel and Fisher, 1975
14. Fox et al., 1979
15. Fox et al., 1976
16. Gianelli and Principi, 1979
17. Karson and Dewey, 1978
18. Melson and Thompson, 1971
19. Prinz et al., 1976
20. Saleeby, 1979
21. Saleeby, 1977, 1978
22. Smewing, 1979
23. Sykes, 1967
24. Varet and Choukroune, 1979
25. Wilson, 1965
26. Wilson and Williams, 1979

Bela Ophiolites

1. DeJong and Subhani, 1979
2. Gansser, 1979

Bela Ophiolites. Also the absence of blue schist/eclogite-bearing melange, intermediate-felsic volcanic piles and plutons in the Bela region indicates that subduction apparently did not occur along this continental margin, making it unlikely that a marginal basin existed. Further paleogeographic reconstructions (e.g., McKenzie and Sclater, 1971; Powell, 1979) have shown that the western margin of the Indian Plate, on which the Bela Ophiolites were obducted, has generally been a transform margin since the late Cretaceous.

Some sedimentary rock types and mafic rocks of the Bela Ophiolites are similar to rocks occurring in the layers 1 and 2 of the ridge-generated oceanic crust of the major basins. However, the sequence of these rocks and the frequently present interlayered melange horizons are different (Table 7; Fig. 64).

Fracture zone Origin

A comparison of the internal features of the Bela Ophiolites with those ascribed to fracture zone complexes (Table 7) indicates several resembling aspects. These are further discussed as follows:

Most significant is the frequent presence of serpentinite-bearing melange horizons within the sedimentary rock-pillow lava-sill sequence (Figs. 18-23, 64, Plate I). These melanges consist of debris of oceanic rocks and were formed on the ocean floor. This requires deep level exposures of the oceanic lithosphere which mostly occur along the large fracture zones or transform faults (Bonatti et al., 1971; Melson and Thompson, 1971; Fox et al., 1976; Bonatti and Honnorez, 1976; Bonatti, 1978; DeLong et al., 1979). Large fracture zones are often marked by prominent high

Figure 64. Schematic rock sequence of typical ridge-generated ocean crust (A, modified after Dewey and Bird, 1971; Gass, 1977) and the Bela Ophiolites (B) as seen in the Wayaro Quadrangle.

1 - chert, argillite, pelagic limestone

2 - pillow lava

3 - sheeted dikes

4 - mafic cumulates

5 - ultramafic cumulates

6 - diabase-gabbro sills

7 - melange - mainly slivers of deformed serpentinite and serpentinite-carbonate-mudstone breccia; less commonly with blocks of massive and pillowed basalt, diabase, gabbro, amphibolite, metagabbro, chert, limestone, marl and detrital* beds with variable amounts of argillaceous matrix.

*Includes detrital serpentinite, lithic sandstone, pebble beds, etc.

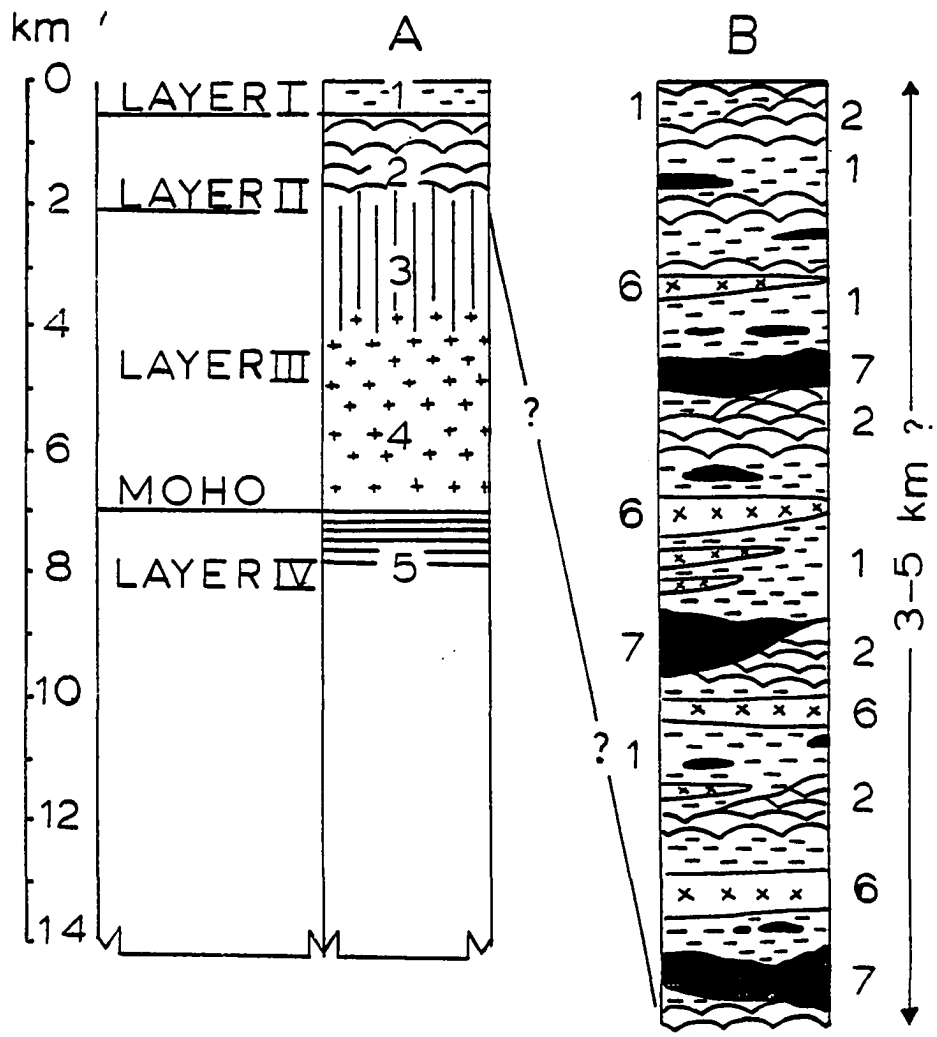

ridges (horsts) and deep elongate troughs, and expose thick sections of all oceanic rocks, serpentinized ultramafic rocks being the most abundant (Thompson and Melson, 1972; Bonatti and Honnorez, 1976; Fox et al., 1976; Bonatti, 1978) (see Fig. 65). The ultramafic rocks are derived from the mantle as protrusions (solid diapirs) along faults and some may possibly extrude on the ocean bottom (Thompson and Melson, 1972; Bonatti, 1976, 1978). However, some dredging and deep crustal drilling data from the North Atlantic Ridge indicates that occasionally a similar process may also take place along median rifts of spreading centers (Aumento and Loubat, 1971; Hall and Robinson, 1979). All rocks in the fracture zone domain are subject to both vertical and horizontal (strike-slip) movements, which involve tension, compression, and shear along the various segments of fracture zones (Bonatti, 1978; DeLong et al., 1979). Serpentinization of ultramafic rocks occurs during their ascent (Bonatti, 1976, 1978) and tectonic fabrics are imposed to a variable degree on all rocks involved in fracture zones (Bonatti, 1976, 1978; DeLong et al., 1979). Rocks exposed along the ridge flanks and troughs are subject to erosional processes, and contribute debris of all sizes (Fig. 65). The results are large slide blocks, talus fans, debris flows and turbidites (Saleeby, 1977; DeLong et al., 1979); these deposits are incorporated in any existing sedimentary and/or volcanic deposits in the fracture zone domain. Lockwood (1971, 1972) has suggested that certain "Alpine type" serpentinite bodies and sedimentary serpentinites could be explained by diapiric emplacement and gravity induced processes, respectively.

The common occurrence and most features of the melanges within the Bela Ophiolites can be explained by the above tectonic, erosional, and

Figure 65. Schematic diagram of a large oceanic fracture zone showing a cross sectional view of its upper crust and some complex geological relations.

P = pillow lava mound.

T = talus deposits.

 = shale, mudstone, marl, pelagic limestone and cherts, with or without metalliferous deposits.

 = detrital deposits and/or large blocks of rock types exposed along troughs, e.g., serpentinite, serpentinite-carbonate breccias, basalt, gabbro, sedimentary and metamorphic rocks; the latter consist of cataclastics and/or dynamothermally metamorphosed materials released from the tectonically active zones.

 = basaltic pillow lavas

 = diabasic-gabbroic rocks: shallow intrusives and/or uplifted layer-3 material; the former may also include minor felsic rocks, e.g., plagiogranites.

 = serpentinite protrusions.

 = shear zone.

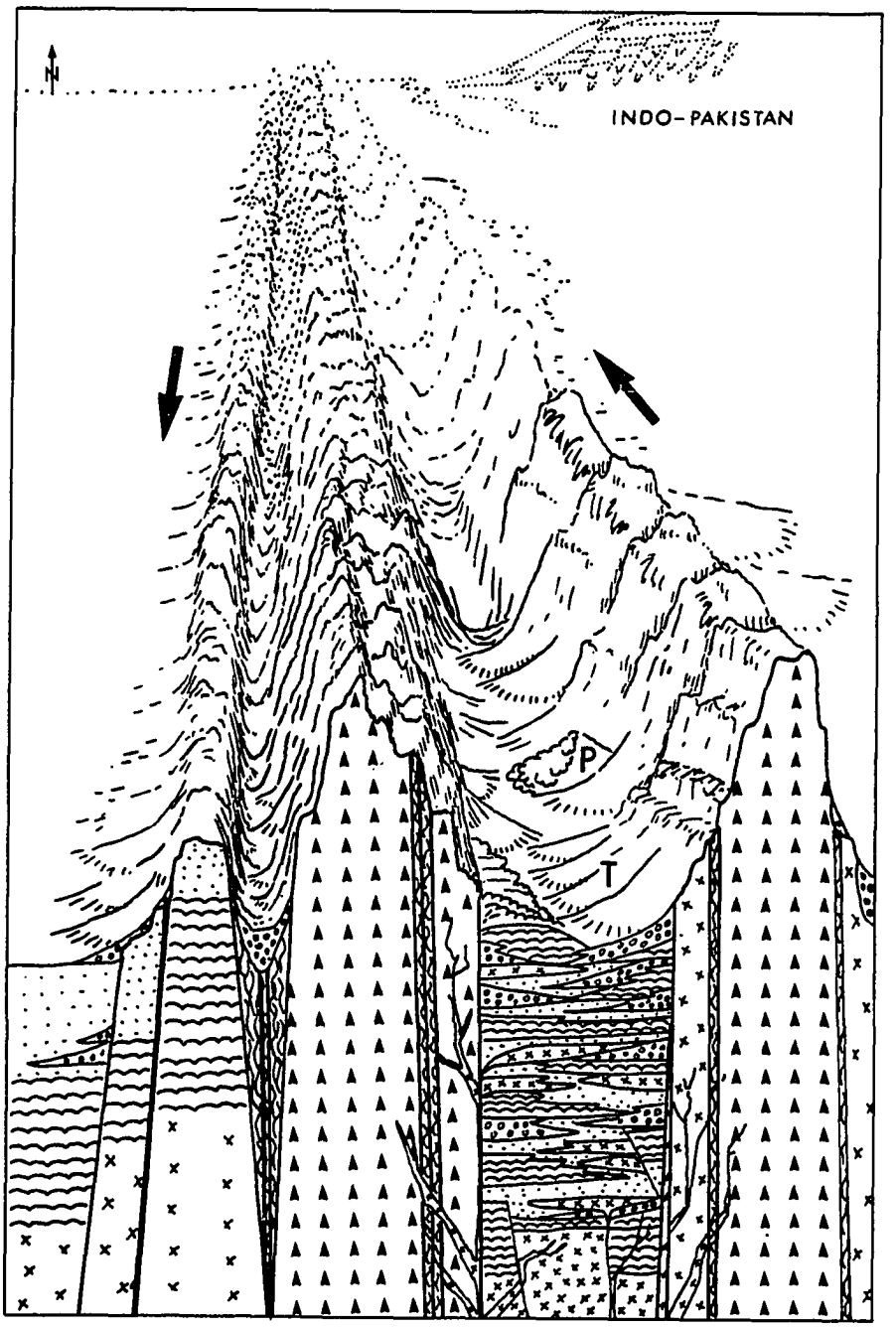

sedimentary processes of the fracture zones. Serpentinite-carbonate breccias and detrital serpentinite strikingly similar to those of the Bela Ophiolites (Fig. 22), have been dredged from the Romanche and Vema fracture zones in the equatorial Atlantic (Bonatti et al., 1973; 1974).

The fracture zone origin of inter-ophiolite melange horizons requires that the enclosing pillow lavas, sills and sedimentary rocks were also formed within or adjacent to the same domain. There is evidence that oceanic crust is accreted within certain fracture zones, such as Vema and Oceanographer fracture zones of the Atlantic (Thompson and Melson, 1972; Fox et al., 1976). The process has been explained as due to changes in the direction of relative plate motion (Menard and Atwater, 1968; Van Andel et al., 1969; Fox et al., 1976). Thus large fracture zones involve both old ridge generated and new self-generated oceanic crust and have a complex diachronous evolution (Fox et al., 1976; Karson and Dewey, 1978).

The above discussion shows that the internal features of the Bela Ophiolites appear to be more consistent with a fracture zone environment than with any other tectonic setting.

Relation Between Bela Ophiolites and Certain Fracture Zones of the Arabian-Indian-Tethyan Oceans

A. Owen Fracture Zone: The present-day plate tectonic framework of the South Asian-Arabian Sea region is shown in Figure 66. As shown, the Bela Ophiolite Belt is aligned with the Murray Ridge-Owen Fracture Zone boundary of the Indian Plate (Barker, 1966; Mathews, 1966; Bonatti, 1978a, b). The Murray Ridge is a topographic feature (Barker, 1966) and not like the spreading centers. It is part of the Owen Fracture Zone

Figure 66. Present-day plate tectonic sketch map of the South Asian-Arabian Sea region. Toothed lines in the northern Arabian Sea and northern India represent the Makran subduction zone and the Himalayan collisional belt, respectively. The western tectonic boundary of the Indian Plate is marked by the Owen Fracture Zone-Murray Ridge-Ornach-Nal-Chaman Fault. Note the position of the Bela Ophiolite belt with respect to the above plate boundary, and the location of the Chagos-Laccadive Ridge. See text for discussion (modified after Jacob and Quittmeyer, 1979).

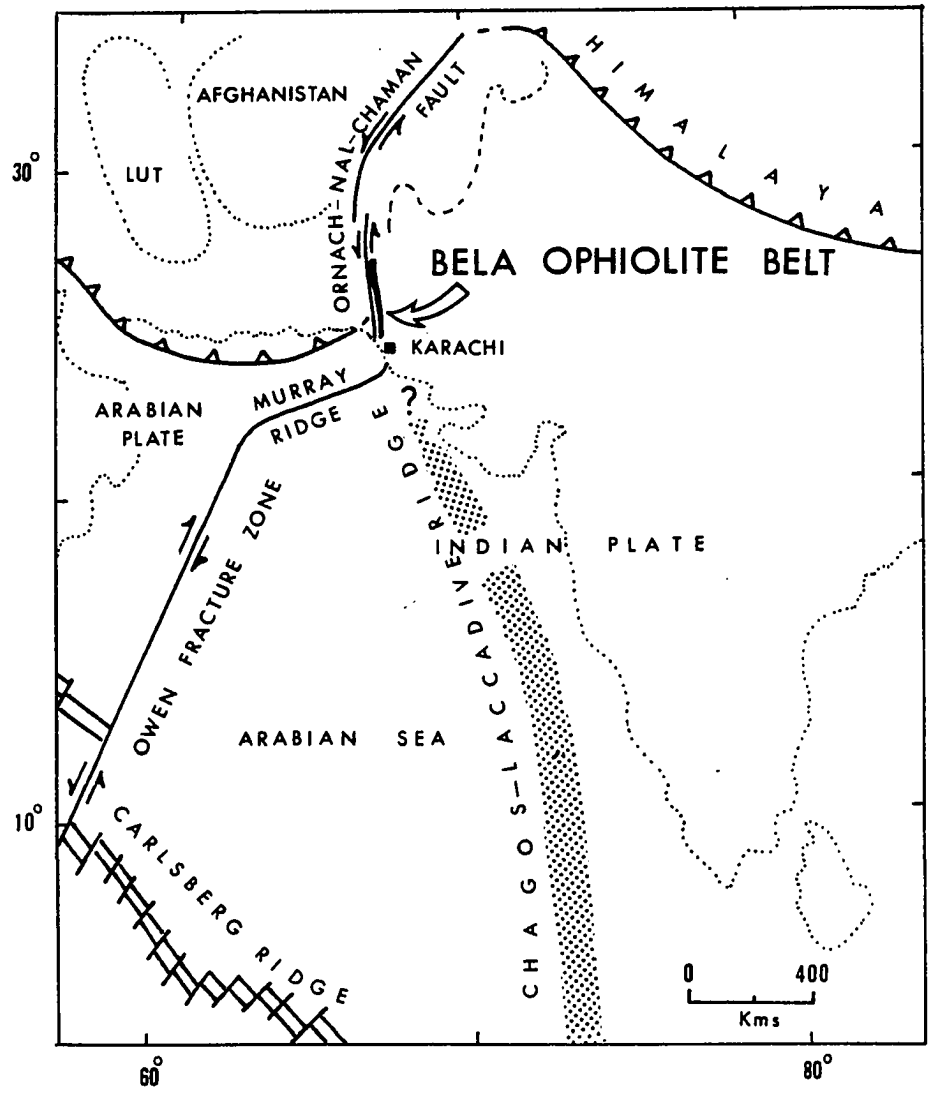

transform boundary between the Arabian and the Indian Plates, and somehow owes its origin to the differential movement between the two plates (McKenzie and Sclater, 1971; Jacob and Quittmeyer, 1979).

The alignment of the Bela Ophiolite Belt with the Owen Fracture Zone makes it tempting to suggest that the former possibly represents a segment of obducted oceanic crust of the latter (proto-Owen Fracture Zone, Powell, 1979). However, there are two major problems with this idea:

1) The proto-Owen Fracture Zone probably formed after the late Cretaceous separation of India from Madagascar (Powell, 1979; 80-90 Ma, Norton and Sclater, 1979). The Bela Ophiolites, as we now know, are of Cretaceous (Aptian-Maestrichtian) age, and thus older than the Owen Fracture Zone.

2) At the time of obduction of the Bela Ophiolites (Paleocene-early Eocene, Allemann, 1979), the Owen Fracture Zone was separated from the western edge of the Indo-Pakistan subcontinent by a vast stretch of oceanic crust as indicated by plate tectonic reconstructions (e.g., McKenzie and Sclater, 1971; Powell, 1979; Norton and Sclater, 1979; see Fig. 67).

If the observations (1) and (2) are valid, there is probably no genetic connection between the Bela Ophiolites and the Owen Fracture Zone. The present alignment of the two features is then fortuitous and probably a result of the Late Cenozoic counterclockwise rotation of India (see Powell, 1979; Klootwijck et al., 1981).

B. Chagos Fracture Zone: Plate tectonic reconstructions for late Cretaceous-Eocene time (Fig. 67) indicate that a vast stretch of the Tethys Ocean north and northwest of the Indian Shield was being subducted under the Eurasian blocks (McKenzie and Sclater, 1971; Powell, 1979).

Figure 67. Tectonic sketch map of the Indian Plate and surroundings 75-70 m.y. ago relative to Africa in its present position. The western active boundary of the Indian Plate is defined by the Owen Fracture Zone (OFZ) and the Chagos Fracture Zone (CFZ) that are separated by the Carlsberg Ridge (CR). The Chagos Fracture Zone links the Carlsberg Ridge with the Mid-Indian Ocean Ridge (MIOR). The eastern active plate boundary is formed by the Ninety East Fracture Zone (NEFZ). Barbed line marks north-dipping subduction zone where the Tethyan oceanic crust (Paleozoic and Mesozoic) is being consumed under Eurasia (CI and A represent the microcontinents of central Iran and Afghanistan). Modified after McKenzie and Sclater (1971) and Powell (1979).

MD = Madagascar

M = Mozambique basin

S = Somali basin

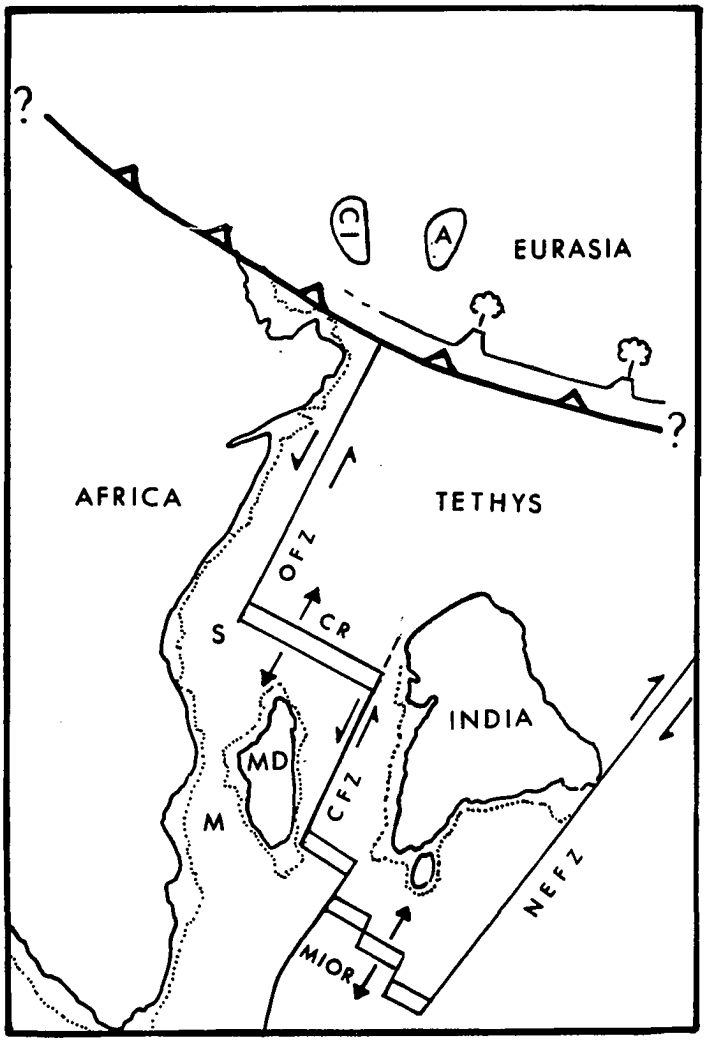

Offset of marine magnetic anomalies suggest that during late Cretaceous to Paleocene time, a large north-south oriented fracture zone existed adjacent to the western margin of the Indian Shield (McKenzie and Sclater, 1971). This is the 'Chagos Fracture Zone' (Fig. 67) which served as a left-lateral transform boundary (McKenzie and Sclater, 1971; Fisher et al., 1971). The Chagos Fracture Zone was ancestral to the present-day Chagos-Laccadive aseismic ridge, which is a north-south oriented elongate feature adjacent to the western margin of the Indian Shield (Fig. 66). It has been suggested that this ridge is volcanic and continues northward (under the Indus cone) along the Indian coast right up to Karachi (Narain et al., 1968; Closs et al., 1974). Based on abrupt changes in sediment thickness, it has also been suggested that a fault system parallels the western coast of India (Closs et al., 1974; Rao, 1976).

The possibility that the Chagos Fracture Zone was ancestral to the Bela Ophiolite also has some problems. This fracture zone developed in the oceanic crust that formed between India and Madagascar (Figs. 66-68) after their late Cretaceous separation (80-90 Ma, Norton and Sclater, 1979; Powell, 1979). Therefore, like the Owen Fracture Zone, it is probably also younger than the Bela Ophiolites and of little interest for our purpose. Also the fracture zone origin of the Chagos-Laccadive Ridge is controversial: for example, Whitmarsh (1974) has proposed a hot spot origin.

C. Tethyan Fracture Zone: Norton and Sclater (1979) have suggested that India and Madagascar, acting as a single coherent unit, separated from Africa sometime between middle-upper Jurassic. The break occurred along a large transform and ridge/transform system parallel to the

Figure 68. Early Cretaceous reconstruction of the southern continents. Note the Tethyan basin between India and Africa (after Norton and Sclater, 1979).

Figure 69. Reconstruction of the initial position of the southern continents before Gondwana breakup (after Norton and Sclater, 1979).

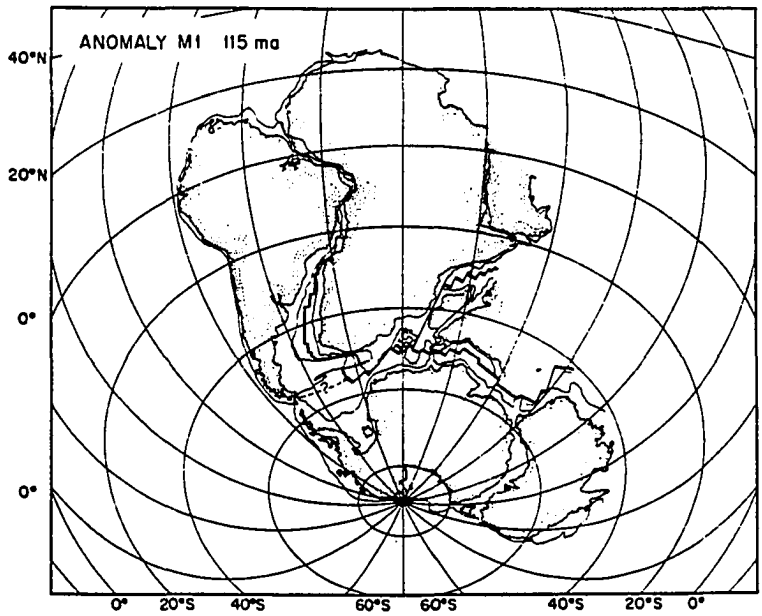

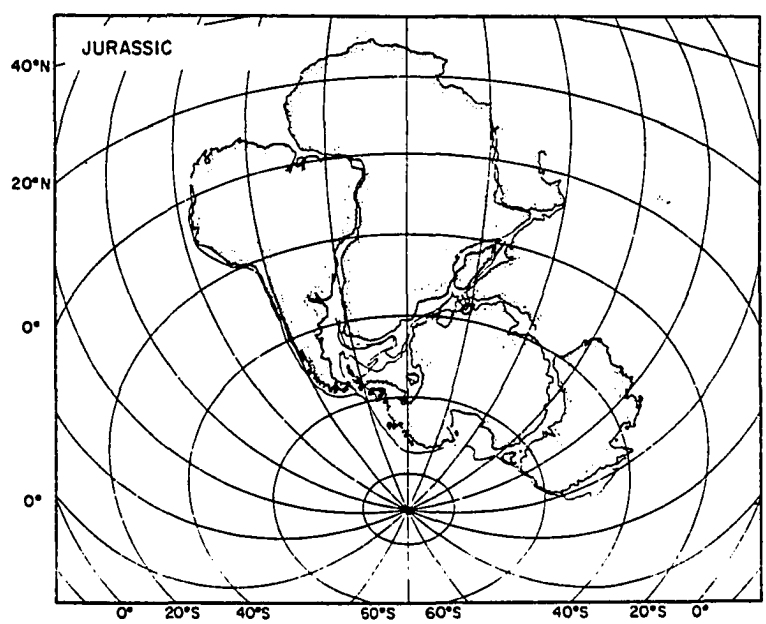

African coast, and an oceanic basin (Neo-Tethys ?) was formed (Figs. 68, 69).

The hypothetical fracture zone, most likely to be the ancestor to the Bela Ophiolites, evolved in the Cretaceous and was probably located in the Tethyan basin adjacent to the western margin of Indo-Pakistan. It is possible that such a fracture zone existed in the oceanic basin which opened between Indo-Pakistan and Africa (Fig. 68). This fracture zone was destroyed during the Paleocene-Early Eocene when the ophiolites were emplaced.

The Problem of Emplacement of the Bela Ophiolites: According to the prevailing general opinion, the Pakistani ophiolites are believed to have been emplaced as a result of collision between the Indo-Pakistan and surrounding Eurasian blocks. The ophiolites represent lithospheric fragments of the Tethyan basin which was closed by this collision (Sillitoe, 1976; Stocklin, 1977; Powell, 1979; Abbas and Ahmed, 1979). This general idea, however, is not valid for the emplacement of the Bela Ophiolites.

No collision has yet occurred along this part of the continental margin. The Bela Ophiolites are still at least 200 kilometers away from the Afghan block with which the northwestern edge of the Indo-Pakistan subcontinent has already collided. According to Karig and Farhoudi (1977) and White (1979), the Bela Ophiolite belt is presently bound to the west by oceanic crust (of the Arabian Plate; Fig. 66) which is buried under the Makran arc-trench complex.

During Paleocene-Early Eocene, the time of the ophiolite emplacement (Allemann, 1979), India was located farther to the south and its Bela margin was nowhere close to any of the Eurasian blocks, assuming they were

in their present position (Fig. 3, Powell, 1979). If this is valid, then a continental collision obviously was not a cause for the emplacement of the Bela Ophiolites.

As discussed previously, the Bela Ophiolites originated in a Cretaceous oceanic fracture zone probably located adjacent to the continental margin. It is possible that the cause of the ophiolite obduction was an oblique convergence between the Indo-Pakistan subcontinent and this fracture zone (Fig. 70). Fitch (1972) has proposed a model of convergence in which slip that is oblique to the plate margin is at least partially decoupled between parallel zones of transcurrent faulting and underthrusting (Fig. 70). The model has been applied to certain southeast Asian arc-trench complexes (Brookfield, 1977). The cause of oblique convergence could be a change in the direction of motion of India induced by the Paleocene-Early Eocene collision of its northern edge with the Eurasian blocks (Powell, 1979).

Figure 70. A possible genetic model for the Bela Ophiolites.

A = Schematic plan view of a zone of oblique convergence between plates x and y. Slip (long arrows) oblique to the plate boundary is partially decoupled between parallel zones of transcurrent faulting (F) and thrusting (T).

B = Block diagram showing cross section along line a-a' (modified after Fitch, 1972).

C = Schematic diagram showing Late Cretaceous-Early Eocene oblique convergence between the Indo-Pakistan block and an oceanic plate (Tethys ?) along a transform zone F. F is destroyed and elements of its crust are obducted on the deformed continental margin along thrust belt T (based on Fitch's model AOB).

D-E = Schematic diagrams showing progressive deformation along the continental margin, development of the Kanar Melange and obduction of the Bela Ophiolites (Late Cretaceous-Early Eocene).

F = Present-day scenario. Note synclinal structure of the Bela Ophiolites and the Piaro Ridge thrust mass. The Nal limestone represents the neoautochthonous rocks deposited on top of the ophiolites (after their obduction) in the Middle Eocene-Oligocene (Allemann, 1979).

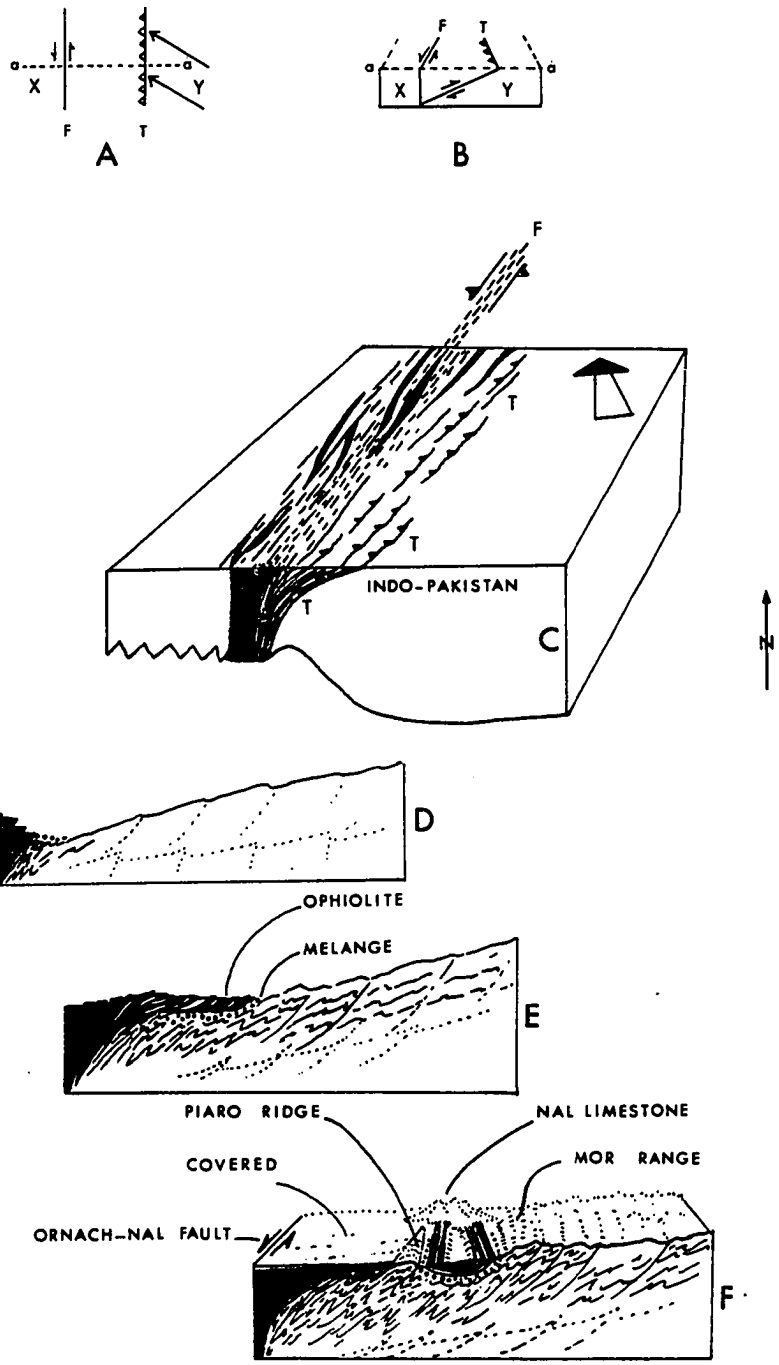

ORIGIN OF VOLCANIC CLASTS OF THE PORALI CONGLOMERATE

(1) Petrographic and Chemical Comparison of the Mor Intrusives, Porali Conglomerate Volcanic Clasts, and Bela Volcanics:

The Mor Intrusives consist of altered ultramafic to mafic alkaline rocks such as limburgites and basalts. Petrographic comparison has shown that similar rocks are also present among the volcanic clasts of the Porali Conglomerate (see Table 8). Some differences are also present (e.g., the presence of accessory quartz in the groundmass of some intrusives and its absence in the clasts). However, as shown in Table 8, the resemblance between the two groups of rocks is considerable.

Both the Mor Intrusives and the Porali clasts are petrographically different from the Bela volcanics as can be easily judged from Table 8.

A chemical comparison of the above three groups of rocks (Table 9) indicates that both the Mor Intrusives and the Porali Conglomerate are different from the Bela Volcanics. As shown, the former two groups are poorer in SiO_2, Cr, Ni, and higher in alkalis, TiO_2, trace elements, and the ratios: FeO/MgO, $[La/Yb]^N$, $[La/Sm]^N$, and $[Ce/Yb]^N$.

The REE distribution patterns for both the Bela Volcanics and the Porali clasts exhibit LREE enriched patterns; however, the conglomerate is far more LREE enriched and also follows a different and more uniformly enriched pattern than the Bela Volcanics (e.g., no Tb and Nd anomalies in the former). Also the conglomerate is less enriched in HREE (e.g., Lu) than the Bela volcanics as shown in Figures 34 and 54; the above

Table 8. Comparison of Certain Petrographic Features of the Bela Volcanics, Porali Conglomerate Volcanic Clasts, and Mor Intrusives.

Variables	Bela Volcanics	Porali Conglomerate	Mor Intrusives
Rock Types	Spilitic basalts some keratophyres and basaltic andesite (Tholeiitic series)	Augitic limburgite, altered alkaline basalts, somewhat like the Mor Intrusives (Alkaline series)	Augitic limburgite, altered alkali basalts (Alkaline series)
Common Texture	Ophitic-trachytic some porphyritic	Porphyritic varieties	Porphyritic varieties
Amygdules/ Cavities	Filled with chlorite, calcite, glass, quartz, and zeolite	Filled with chlorite, calcite amorphous SiO_2 (rare quartz) and occasional sodic plagioclase	Veinlets of chlorite and calcite
Feldspar	Always present (Alb-olig; some andes)	May be absent; sodic (alb-andes)	May be absent; sodic (alb-andes)
Clinopyroxene	Diopside; some augite; ophitically intergrown with plagioclase; occasionally zoned; normal interf. colors	Titanaugite; similar to that of Mor Intrusives	Titanaugite; no ophitic relation; frequently zoned; (hour-glass and concentric zoning); anomalous bluish interf. colors
Quartz	Relatively more common	Rare - absent	Rare - absent
Hornblende	Commonly greenish-brown uralitic variety	Occasional; strongly pleochroic brown variety; greenish in one sample	Similar to Porali samples
Brown Biotite	Very rare - absent	Occasionally present	Occasionally present

Table 9. Comparison of Certain Chemical Features of Bela Volcanics, Porali Conglomerate Volcanic Clasts, and Mor Intrusives.

	Bela Volcanics	Porali Conglomerate	Mor Intrusives
SiO_2%	44.5 - 52.8	43.2 - 46.5 (68.1 in one sample)	37.5 - 47.3
$Na_2O + K_2O$%	2.2 - 3.9	3.22- 6.18	1.5 - 6.3
TiO_2%	1.8 - 2.7	1.2 - 3.8	2.5 - 3.5
FeO*/MgO	1.48- 1.99	1.79- 2.51	1.15- 1.8
Cs (ppm)	< 0.4	0.4 - 4.84	< 0.4 - 3.98
Rb (ppm)	< 35	32.9 - 36.67	< 30.5 - 43.78
U (ppm)	< 0.5	1.8 - 4.4	1.18- 3.03
Th (ppm)	0.58- 0.95	9.01- 16.9	6.73- 12.5
Ta (ppm)	0.59- 0.98	4.34- 8.25	2.67- 4.82
Ba (ppm)	<138 -225.9	464.17-1121.7	<124.3 -892.6
La (ppm)	8.85- 10.9	63.6 - 110.12	41.4 - 88.75
Ce (ppm)	18.7 - 31.9	128.08- 219.32	60.76-170.4
Cr (ppm)	81.3 -142.3	8.26- 61.34	246 -524
Ni (ppm)	71 - 98	< 51 - 76	84 -173
$[La/Yb]^N$	3.1 - 4.25	12.0 - 19.6	15.3 - 23.1
$(La/Sm]^N$	1.0 - 1.27	2.87- 4.34	2.75- 3.8
$(Ce/Yb]^N$	2.47- 3.7	9.5 - 14.6	8.43- 17.31

* = Total iron

Figures preceded by sign "<" represent the lower detection limits for the corresponding elements (see Appendix 10B).

considerations indicate that the Porali clasts are different and were probably not derived from the Bela volcanics.

A chemical comparison of the Porali Conglomerate with the Mor Intrusives indicates that, although both are alkaline, the former shows a higher range of total alkalis, SiO_2 (Fig. 26), TiO_2, Cs, Rb, U, Th, Ba, except for Cr and Ni, there is a large overlap in the element contents. In other words, the Porali clasts appear to be more fractionated than the Mor Intrusives.

A comparison of the REE distribution patterns of the two groups of rocks (Figs. 29, 34) reveals that they show remarkably similar trends. Both the Mor Intrusives and the Porali clasts show LREE enriched patterns with a large overlap in $[La/Yb]^N$, $[La/Sm]^N$, $[Ce/Yb]^N$ ratios with the latter showing more enrichment in LREE as well as HREE. This observation substantiates the idea that the Porali clasts represent more fractionated rocks than the Mor Intrusives. It also agrees well with the higher range of other incompatible elements (e.g., Cs, Rb, U, Th, Ba and K), and Ta, TiO_2, SiO_2 and FeO/MgO (Figs. 26, 27, 28, Table 9) in the clasts, and their lower Cr and Ni content. The two groups appear to be chemically related.

(2) Case for a Continental Origin:

Considering the overall petrographic (Table 8) and chemical observations (Table 9), it appears that the Bela Volcanics are different from the Porali clasts and, therefore, can be safely ruled out as their source rocks. On the other hand, both petrographic and chemical data indicate that there are several identical features between the Mor Intrusives and

the Porali clasts (e.g., the presence of similar titanaugite and similar REE patterns in both groups). Therefore, it is likely that the Porali Conglomerate was possibly derived from some volcanic equivalents of the Mor Intrusives. In other words, the Porali volcanic clasts were of continental origin and not of oceanic origin.

This hypothesis can be further tested. Wood et al. (1979, Fig. 3) have proposed a triangular diagram utilizing Hf, Ta, and Th data that distinguishes mid-ocean ridge and within-plate basalts (except for Hawaii) from each other and from Ta-depleted basalts erupted at converging plate margins. This diagram has been successfully tested by Wood and Cole (1980) in the identification of certain Late Paleozoic metabasalts from Sierra Nevada (California) as island-arc volcanics. Accordingly, Figure 53 presents Hf, Ta, and Th data for four Porali clasts. As shown, the conglomerate clasts plot in the within-plate basalt (WPB) field and between WPB and the field of destructive plate margin magmas (calc-alkaline and crustal silicic rocks). This means that the sample plotting in the WPB field (Sample 3) represents uncontaminated material produced by within-plate parent magma, as suggested by the reasoning of Wood et al. (1979). Sample 81, plotting at the edge of the WPB field, represents within-plate parent magma somewhat contaminated by crustal rocks, again following Wood et al. (1979). Thus the conglomerate samples represent within-plate volcanism possibly contaminated by continental crustal material which is consistent with the idea of continental margin volcanism.

Six samples from the Bela volcanics are also plotted on the Hf, Ta, and Th diagram (Fig. 53); they plot in the MORB field and, therefore, are genetically different from the Porali clasts.

For comparison with the Porali Conglomerate, 14 samples of the Deccan Basalts (Alexander and Gibson, 1977), which are known to be of continental rift origin (Raju et al., 1972; Ghose, 1976) are also plotted (Fig. 53). Most of these also plot in the same fields as the Porali samples and, therefore, possibly include both contaminated and uncontaminated WPB lavas.

The LREE enriched pattern of the Porali clasts also somewhat resembles that of the Deccan Basalts and certain other plateau basalts (e.g., Columbia River Basalts) as shown in Figure 34. However, the conglomerate is more LREE enriched than these lavas (e.g., for the Porali Conglomerate $[Ce/Yb]^N$ = 9.56-14.65 as compared to $[Ce/Yb]^N$ = 4.85-7.71 for Deccan Basalts; Alexander and Gibson, 1977).

(3) Conclusion:

Considering the overall information presented above, it can be concluded that the Porali Conglomerate was most probably derived from certain continental volcanics. It is also likely that both the volcanics and the Mor Intrusives were fed by the same magmatic sources.

(4) Time of Igneous Activity on the Western Margin of Indo-Pakistan Subcontinent:

Little is known about the timing of the alkaline igneous activity that took place on the continental margin and was responsible for the Mor Intrusives, the Porali source volcanics, and the dikes that cut the conglomerate mass. It, however, appears that this activity took place before the final obduction of the Bela Ophiolites (Paleocene-Early Eocene, Allemann, 1979). This is based on the observation that the Mor

Intrusives are apparently confined to the autochthonous sequence only (Shirinab Formation, Sembar Formation, Kanar Melange). No such intrusives were observed in the ophiolite nappe which tectonically overlies the Kanar Melange.

Some evidence for a Maestrichtian volcanic episode near the study area is provided by the occurrence of intermediate-mafic (possibly alkaline) volcaniclastic material in the Moghul Kot Formation and Pab Sandstone of the southern Kirthar Range (White, 1981). It is possible that this volcaniclastic material was derived from the same source as the Porali Conglomerate.

It also appears that several episodes of igneous activity took place on the continental margin as suggested by the following observations:

A. Blocks consisting of volcanic debris (Porali Conglomerate occur in the Kanar Melange (Fig. 13).

B. Several large blocks of Shirinab-type rocks in the Kanar Melange contain mafic sills and dikes. These intrusives were emplaced before the incorporation of blocks in the melange (Fig. 13).

It is not known when this igneous activity started and what its cause was. Alkaline igneous activity is generally associated with the continental rifting (Bailey, 1974). Therefore, it is likely that the alkaline activity in the Bela area was heralded by the rifting of eastern Gondwana (Middle-Late Jurassic, Powell, 1979), and continued episodically during the Late Cretaceous-Early Eocene convergence of the Indo-Pakistan subcontinent with the Eurasian blocks.

According to Ghose (1976), the Deccan rift volcanism in west-central India took place between 65-37 m.y. (Late Cretaceous-Late Eocene/earliest Oligocene) and was related to Gondwana breakup. It is, therefore, possible that the igneous activity, both in the continental interior and at the margin was partly coeval.

STRUCTURE

Introduction

The regional structure of the Wayaro area is defined by a large NNW-SSE trending syncline. The ophiolite nappe lies in the core of the syncline whereas the autochthonous sequence forms the limbs (Fig. 4A and Plate I). North of the Wayaro area, the syncline continues for 45 kilometers to the Porali River and to an unknown distance beyond that. South of the area, the western limb of the syncline is buried under the alluvium and only the eastern limb is exposed. The structures within the syncline vary widely in complexity and in deformation style in different types of rocks. The ophiolites, especially the lava flows and the sills, exhibit an intricate transverse fault and fracture pattern with only local development of folds. On the other hand, the autochthonous sequence is deformed principally by means of folds (Plate I).

Regional Syncline

The regional syncline is an open, bowl-shaped structure with a sinuous axial trace which is broadly concave toward the east (Plate I and Fig. 4A). The sinuosity of the axial trace is rather peculiar, and probably reflects the curved, concave to the east, disposition of the ophiolitic rock units along the eastern limb of the syncline (Fig. 4A). These rock units are truncated by the Basal Ophiolite Thrust (BOT) which marks the contact between the ophiolite nappe and the underlying autochthonous sequence. This truncation indicates that the curvature of the ophiolitic

units is older than the BOT, i.e., the units were already curved when the ophiolites were emplaced.

Another peculiar feature is that, the V-shaped outcrop pattern of the ophiolitic unit 4, which lies in the core of the syncline, apparently indicates that the syncline has a northward plunge (Fig. 4A and Plate I). This is probably not the case because the units underlying unit 4 do not show any plunge. An alternative explanation is that the apparent plunge of unit 4 is caused by its northward tilt relative to the underlying units, i.e., unit 4 overlies a north-sloping surface of unconformity defined by its contact. This unconformable contact is very irregular in the west but does seem to have a northward slope in the east (Fig. 4A, Plate I).

Thrust Faults

Two major thrust faults are recognized in the area: the Basal Ophiolite Thrust (BOT) along which the ophiolite nappe was emplaced, and the Piaro Thrust, which lies along the western limb of the syncline.

The Basal Ophiolite Thrust separates the ophiolites from the Kanar Melange and is exposed at both limbs of the syncline. Along the southern part of the eastern limb of the syncline, the outcrop width of the Kanar Melange is much less than it is further north (Fig. 4A). This may be the result of a decrease in the thickness of the melange. Another possible explanation is that the upper part of the melange was tectonically removed by overthrusting of the Bela Ophiolites. The curved, convex to the east, trace of the BOT in this area, and the fact that the melange reappears as a wide belt south of the mapped area (Figs. 2, 4A; Plate I), favor the second explanation. Thus the BOT cuts obliquely into the Kanar Melange.

The thrust is also discordant to the overlying ophiolite units as shown along both limbs of the syncline (Plate I). In the field, the thrust is also marked by a variably developed shear or rubble zone.

Along the Piaro Thrust, which cuts the western limb of the syncline, a large mass of the Shirinab Formation has moved eastward and is brought up against the Sembar Formation and the Kanar Melange (Figs. 2 and 4A). This upthrust mass of Shirinab Formation forms a 55 kilometers long topographic feature called Piaro Ridge. The thrust lies along the eastern edge of the ridge and dips to the west. The Piaro Thrust overlies the Sembar Formation in the north and the Kanar Melange in the south. The stratigraphic throw on the fault decreases northward and becomes zero at about 10 kilometers north of the map area near the Kulri stream, where Piaro Ridge plunges beneath the Sembar Formation without a tectonic break (DeJong and Subhani, 1979, Fig. 2). In the northern part of the map area, the Piaro thrust fault is marked by severe brecciation of a few meters of the Shirinab limestone and all the Sembar shales which dip westward under Piaro Ridge due to overturning. This can be seen along the Bhampani stream cut (see Plate I). Along the thrust the Sembar rocks are tightly folded and are cut by a steep and strong cleavage that parallels the thrust. South of the Bhampani stream the thrust is generally concealed except at the southeastern part of Piaro Ridge.

In the northwestern part of Piaro Ridge orthoquartzitic sandstones are overthrust by a dominantly limestone/shale sequence. The thrust fault dips to the east within the mapped area, but in the adjacent area to the west, it dips to the west. It is marked by a tectonically produced rubble zone. Just north of the study area, near the Gajri stream, several west-

dipping, low angle or subhorizontal thrust faults are well exposed. The faults separate sandstones from limestone/shale units. The existence of such faults may indicate that the Piaro fault itself is a low angle thrust, which locally becomes steeper (e.g., in Bhampani stream gorge).

Relation Between Geology of Piaro Ridge and Mor Range

Both Piaro Ridge and the Mor Range consist of the Shirinab Formation of Triassic and Jurassic age. Along the western flank of the Mor Range, the Shirinab Formation underlies the Sembar Formation, whereas along the eastern flank of Piaro Ridge the Shirinab Formation is thrust over the Sembar Formation and the Kanar Melange (Fig. 4A). Two interpretations are possible to explain the relation between Piaro Ridge and the Mor Range:

(1) The Mor Range and Piaro Ridge represent "two superimposed overthrust sheets" (DeJong and Subhani, 1979). They base their interpretation on the distribution of the Porali Agglomerate (Porali Conglomerate of this report): West of the Mor Range the agglomerate occurs above the Sembar Formation and east of the Kulri Range (Piaro Ridge of this report) the agglomerate appears to occur in a "tectonic window" below the Sembar shales (DeJong and Subhani, 1979). This suggested to them that the rocks of Piaro Ridge form a higher tectonic unit than those of the Mor Range (Fig. 3).

(2) The Piaro Ridge represents an upthrust antiform of the autochthonous or para-authochthonous Jurassic rocks that underlie the ophiolites (Kulri uplift of Gansser, 1979; p. 207-211, Figs. 28-31). Thus he appears to believe that before their overthrusting (on the Sembar Formation and the Kanar Melange), the rocks of Piaro Ridge

occupied the same tectonic position as the Mor Range (both below the ophiolites).

As previously described, the Porali Conglomerate does not occur as a regular stratigraphic horizon but as blocks embedded in the Kanar Melange, as seen in the Wayaro area. It probably occurs in the same fashion also in the Kanar area east of Piaro Ridge and not in a tectonic window as thought by DeJong and Subhani (1979). The thrusting of the Shirinab Formation of Piaro Ridge over the Sembar Formation and the Kanar Melange occurred only south of the Kulri stream (latitude 26°25', Fig. 3). North of the Kulri stream the Shirinab Formation underlies the Sembar Formation without a tectonic break, as it does also in the western Mor Range. Therefore, Gansser's view, that Piaro Ridge is an upfolded and partly upthrust mass of the same unit as the Mor Range, is more appealing.

Folds

Folds may be poorly developed or well developed in the various rock units exposed in the study area. As a general rule, the ophiolitic rocks (with the exception of the serpentinite and the breccia of the interophiolite melange) are far less deformed than the rocks of the Shirinab and Sembar formations. The lava flows and sills may show occasional gentle flexures. However, locally the associated sedimentary rocks do show folds of small wave length which plunge within a few tens of meters. The folds may be upright, or asymmetrical with round or angular hinges. An example of this is shown in Figure 71.

The folds in the Sembar Formation vary from gentle flexures to open or tight folds of small wavelength (a few tens of meters). They are

generally parallel asymmetric folds with a long gentle dipping western flank and a steeper short eastern flank. Most plunge either northward or southward within a few hundred meters. Some are doubly plunging. The folds in the upper part of the Shirinab Formation in the western Mor Range, are similar to those of the Sembar Formation. However, farther to the east, where limestone beds are thicker, the folds have much larger wavelength and axial extent.

The rocks of Piaro Ridge are strongly deformed and exhibit highly asymmetrical, overturned, and isoclinal folds (Figs. 72 and 73). They are also locally disharmonic. The folds generally have round hinges, but chevron folds are also present, especially in the sandstone. The folds are generally small with wavelength of less than 10 meters, however large ones up to a few tens of meters in wavelength are also present. Folds are commonly fractured or cleaved. At least three phases of deformation can be recognized, two of these by means of folds alone (Figs. 72, 74). Folding has occurred along axes ranging between northwest and north-northeast directions (Fig. 75). Most axial planes of folds dip toward the west, but several have been rotated to face eastward. This has produced a late generation of larger folds (Figs. 72, 74, 75; see Plate I also).

Relation Between the Regional Syncline and Smaller Folds

An important question from the structural point of view is that whether the folds in the rocks of the autochthonous sequence and the ophiolites were formed at the same time as the regional syncline. Folds occurring on the limbs or in the closure of larger folds are referred to as parasitic folds with respect to the larger structures (de Sitter, 1958;

Figure 71. View of plunging (to the bottom left of observer) chevron folds in thin-bedded red marls associated with pillow lavas. Such folds are uncommon and lie near and parallel to the major synclinal axis (e.g., in Bhampani and Porar streams). The length of view along the top of the hill is about 35 meters.

(Location 71, Figure 4A; photograph by S. Ghazanfar Abbas)

Figure 72. Some fold styles observed in Piaro Ridge.

a. Overturned isoclinal folds developed on eastern limb of a large anticline. Note the gradual development of folds and increased tilting of their axial planes in a west-east direction. Rocks are dominantly limestone with subordinate interbedded sandstone and shale of the Shirinab Formation (Location 72a, Fig. 4A).

b. Tight overturned and recumbent folds in interbedded limestone and sandstone. Note gradual rotation of axial planes of folds in a west-east direction (Location 72b, Fig. 4A).

c. Sharp hinged overturned folds in limestone with minor shale and sandstone interbeds (Location 72c, Fig. 4A).

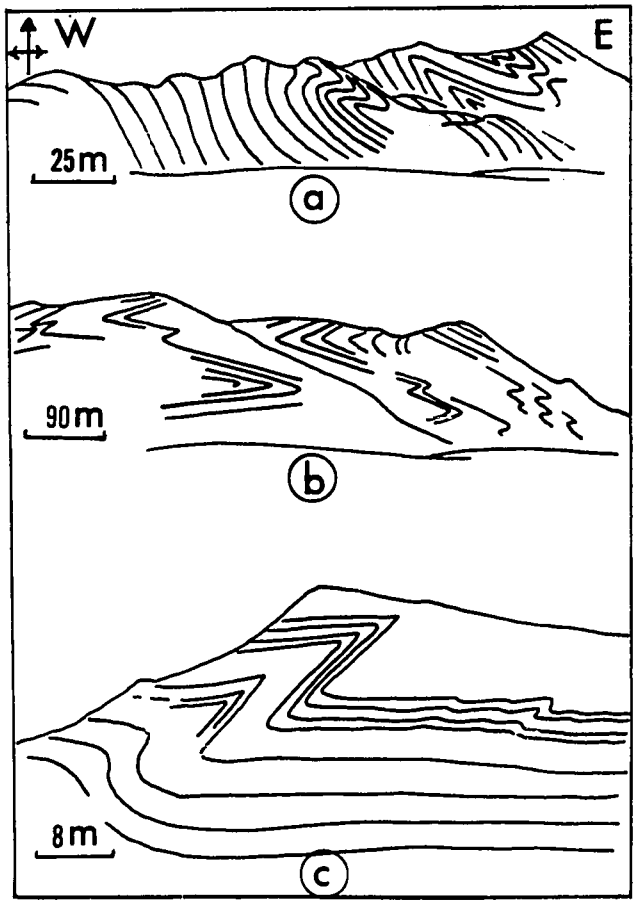

Figure 73. View of a tightly folded recumbent syncline in Shirinab limestone of Piaro Ridge. Note axial plane cleavage and hammer for scale.

(Location 73, Fig. 4A; sketch of photograph)

Figure 74. Refolded isoclinal fold* in a bed of the Shirinab limestone. F1 is roughly along SSW axis and F2 along N-S axis; both axes plunge away from observer. Note axial plane cleavage is related to F2 and dips 75°W.

(View looking south; Location 74, Fig. 4A)

* = 

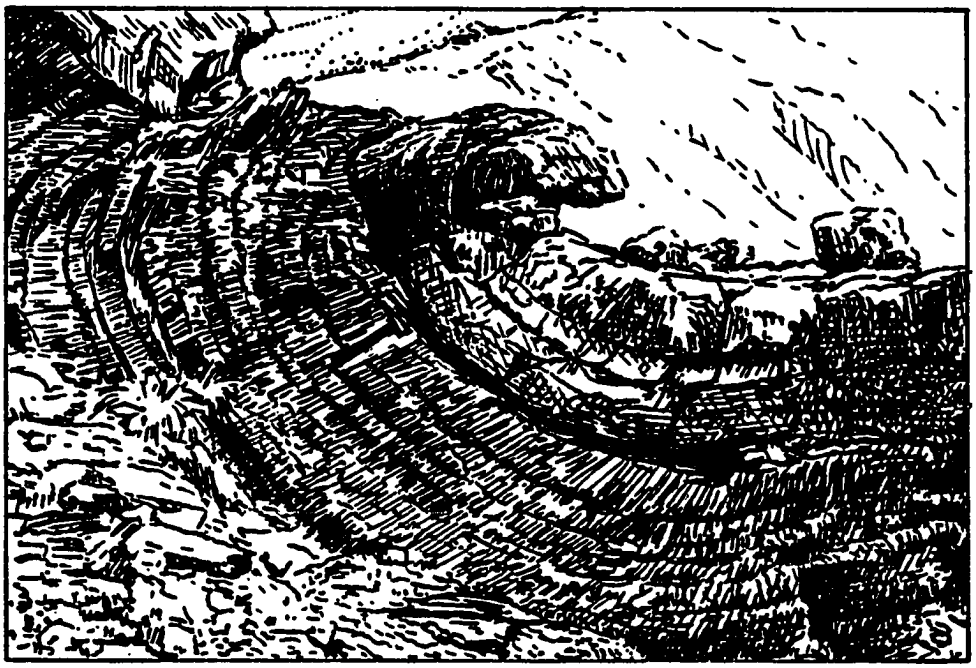

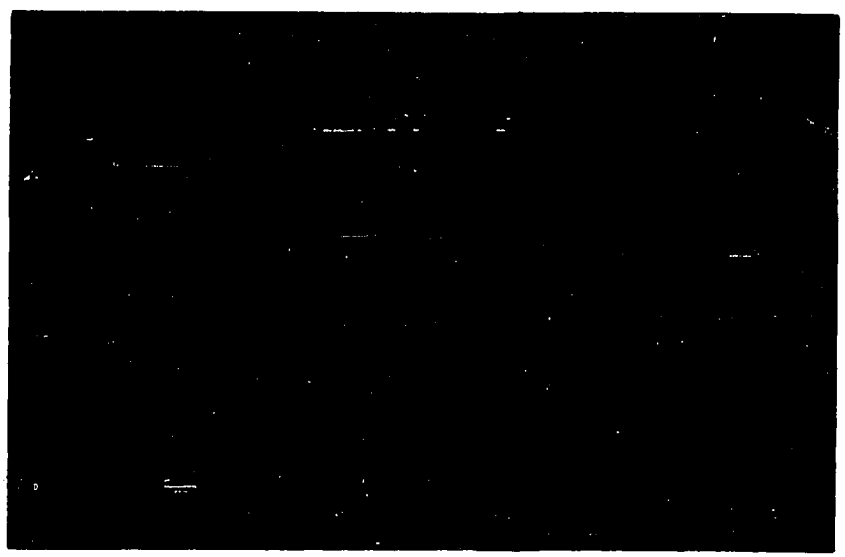

Figure 75. Structural data from Piaro Ridge plotted on a Schmidt equal area net (lower hemisphere). Solid circles represent (40) fold axes; open circles mark poles to (41) axial planes or axial plane cleavage of folds. Note plunging fold axes and their NW to NNE strike. Also note that most axial planes of folds dip SW, W or NW. Axial planes dipping E or NE are few and believed to have been rotated in this position by repeated folding (see Fig. 72).

(Data collected in Piaro Ridge between Sukkan and Gajri streams)

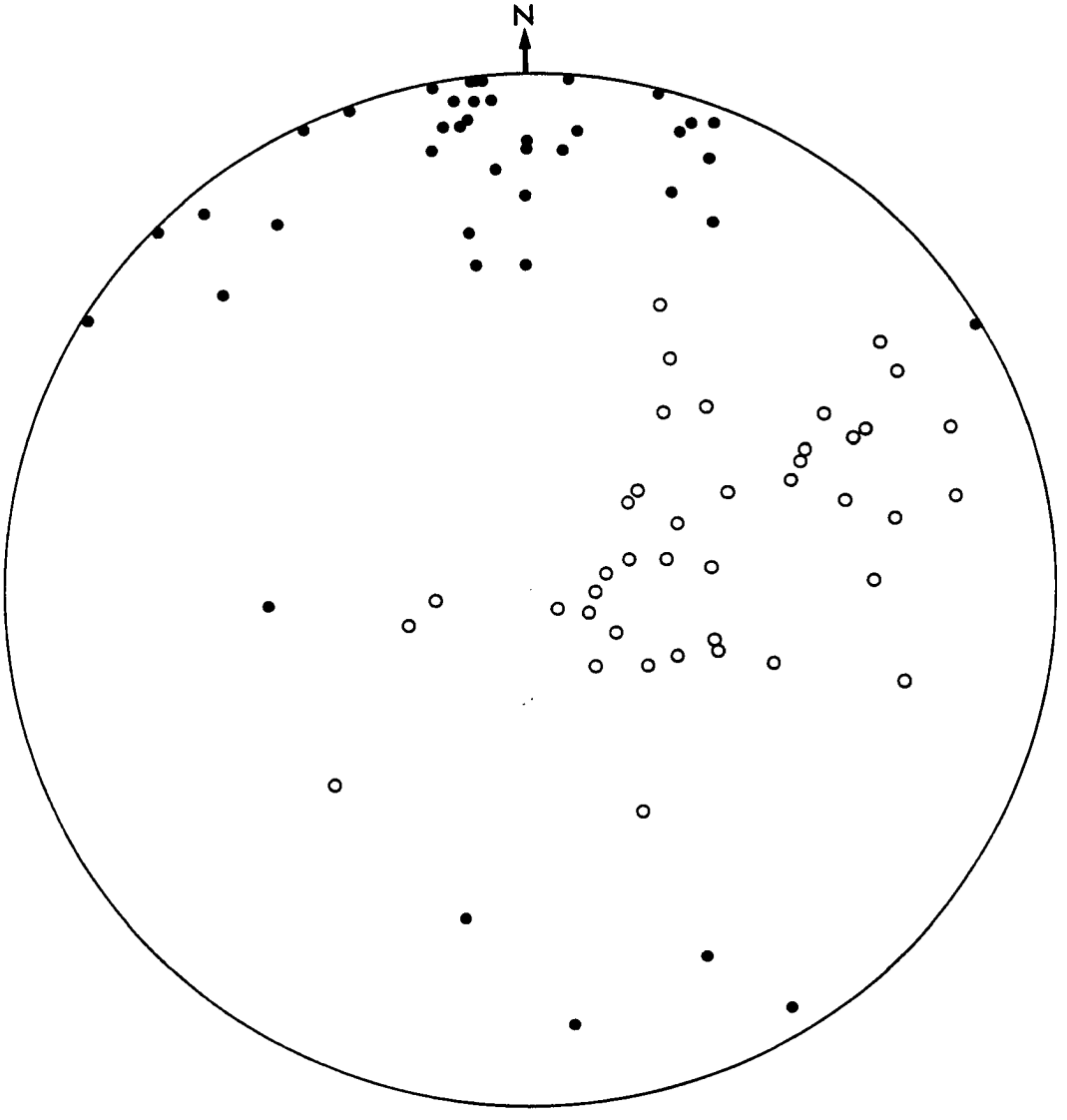

Whitten, 1966; Hobbs et al., 1976). Parasitic folds on the opposite limbs of a large structure are commonly asymmetrical and have opposite vergence (clockwise and counter-clockwise, Fig. 76A). Such parasitic folds are thought to have formed at the same time as the major structure (Whitten, 1966; Hobbs et al., 1976).

The folds in the rocks of the autochthonous sequence (excluding Piaro Ridge) are parasitic to the regional syncline; however, they have the same (clockwise) vergence along both limbs of the syncline (Fig. 76C). This means that the parasitic folds were not formed at the same time as the regional syncline. An alternative explanation is that they were formed before the syncline was formed. The fact that the ophiolites are far less strongly folded than the autochthonous sequence, indicates that the sequence was folded before and/or during the ophiolite emplacement. The clockwise vergence of folds in the autochthonous sequence indicates eastward tectonic transport. This agrees well with the idea that these folds probably originated as drag folds under the ophiolite nappe which was emplaced from the west (Fig. 76B). This hypothesis also explains why the autochthonous sequence is so strongly folded and the ophiolites are not. The autochthonous sequence was folded at least twice: first, before or during the ophiolite emplacement, and second, after the ophiolite emplacement, when the regional syncline was formed (Fig. 76B, C).

The parasitic folds within the ophiolites tend to occur in the innermost part of the regional syncline (Plate I). Therefore, it is possible that these folds were formed during the second phase of folding when the ophiolite nappe was folded into a syncline (Fig. 76C).

The folds in the Shirinab Formation of the Piaro Ridge allochthon

Figure 76. A. Schematic cross section of a large syncline and anticline showing smaller asymmetrical parasitic folds in a thick bed. Note that asymmetry (vergence) of parasitic folds is variable and opposite on the limbs of the larger folds. Folds in the limb 'y' are said to have a dextral or clockwise vergence whereas those in the limbs 'x' and 'z' have a sinistral or counter-clockwise vergence.

B. Schematic diagram showing formation of drag folds (with a dextral or clockwise vergence) in the autochthonous sequence caused by emplacement of the Bela Ophiolite Nappe.

C. Sketch showing regional synclinal structure of the Wayaro area. Note that parasitic folds in the autochthonous sequence have dextral or clockwise vergence on both limbs of the syncline. The ophiolite nappe also shows some parasitic folds along the axial trace of the syncline.

(See text for discussion)

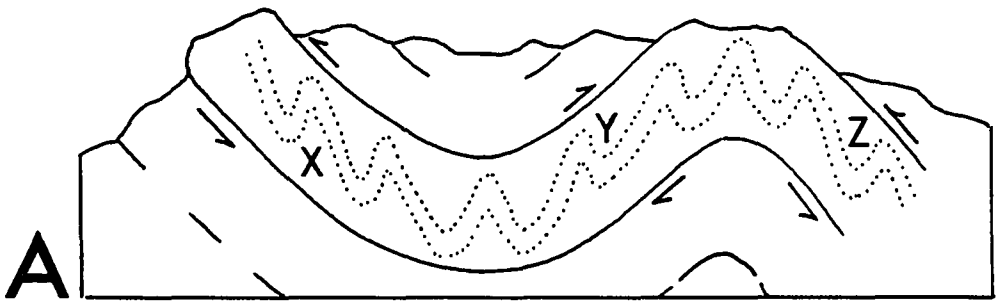

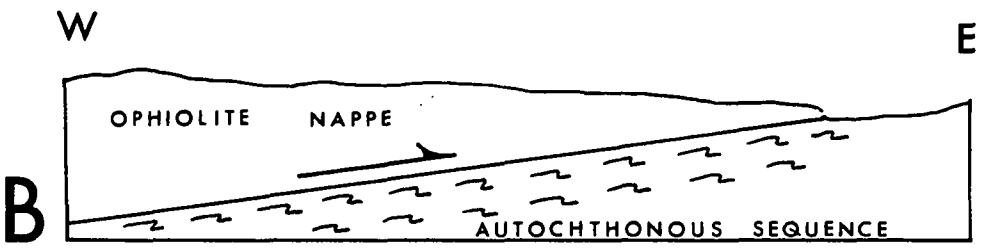

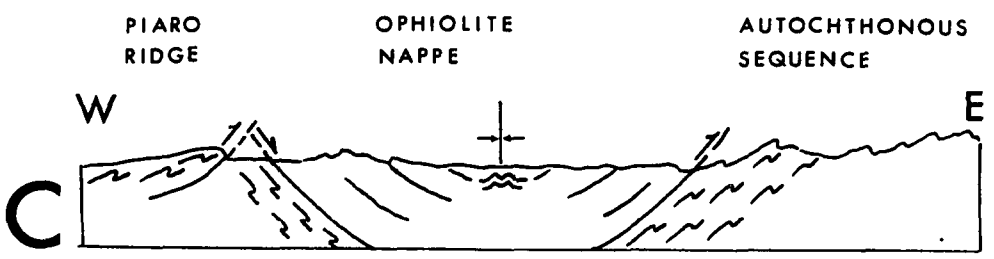

are clearly of several generations (Figs. 72, 74, 75). Three possibilities are considered to speculate on the origin of these folds:

1. The folds have the same origin as those of the autochthonous sequence that underlies the ophiolite nappe, i.e., drag folds formed during the ophiolite emplacement which took place before the formation of the regional syncline and the Piaro thrust.

2. The folds formed at the same time when the regional syncline was formed.

3. The folds formed at the time (or after) when the Piaro thrust was formed.

The first possibility probably accounts for the initial folding because, before upthrusting, the rocks of the Piaro Ridge occupied an autochthonous position, and must have been deformed by the emplacement of the ophiolite nappe (Fig. 76B). The fact that the folds in the Piaro Ridge generally have the same vergence as those in the autochthonous sequence, seems to favor this idea (Fig. 76C).

The second possibility fails to explain why the rocks of the Piaro Ridge are so intensely deformed and folds so asymmetrical whereas the regional syncline is an open and rather symmetrical structure. Similarly, the third possibility does not explain why the folds in Piaro Ridge are not confined only to the vicinity of the Piaro thrust, if they were caused by this fault. It is admitted, however, that the rocks are more intensely folded and fractured near the fault than away from it.

Therefore, it is more likely that the rocks of Piaro Ridge were folded first at the time of ophiolite nappe emplacement. Subsequent

formation of the syncline and the Piaro thrust might have caused additional deformation which is responsible for the complex fold pattern in Piaro Ridge.

Transverse Faults and Fractures

These features are transverse to the regional strike of the rocks and are best developed in the ophiolites, with the lava flows exhibiting the highest fracture density.

Transverse faults and fractures were studied to learn about their origin, age and relationship (if any) with the major syncline in the area (Fig. 4A). Studies of fracture pattern in ophiolitic rocks may also be of economic significance. It was recently shown that fractures in ophiolites and oceanic crust could be related to sulphide mineralization (e.g., Rona, 1976; Bonatti et al., 1976; Smewing et al., 1977).

Several sets of faults and fractures are present and at places are arranged in a conjugate pattern. Both faults and fractures can be up to several kilometers in length though the former are generally longer. As these features are much more striking on aerial photographs (1:40,000) than on the ground, it was decided that a photoscale study would be more useful. On the ground the transverse faults and fractures are generally defined by streams and gullies. Usually an offset of layering of juxtaposition of contrasting rock types is present where a sequence of lavas, sedimentary rocks and sills is faulted. However, no offset is apparent if the fracture is confined to a single rock type. Slickensides are generally absent because of erosion by streams that have followed structurally

weak zones. Drag features are also not common and were observed only along a few large faults (Fig. 16).

Three areas were selected for photo-scale fracture analyses (Fig. 4A). The selection was governed by the availability of good quality aerial photographs. The fractures, as seen with the unaided eye were traced on transparent Mylar overlays directly from the aerial photographs (scale 1:40,000). Fractures less than 100 meters in length were not plotted to avoid overcrowding and to fix an arbitrary lower size-limit for photo-scale fractures. Observations were confined to the central parts of photographs to avoid distortion effects. Figures 77-79 show the fracture pattern in the three selected areas.

McQuillan's approach was followed in the treatment of fracture data (McQuillan, 1974). The three chosen areas represent three structural realms, each with a unique fracture pattern. The southern area was further divided into three domains based on significant differences in the fracture pattern. All fractures were classified into eighteen azimuth classes each of 10°, and the length of each fracture in each azimuth class was also noted. The total number of fractures (N) in each azimuth class was also noted. The total length (L) was calculated. For the purpose of plotting the length- and azimuth-distribution diagrams, the values of length percentage and number percentage for all azimuth classes were also calculated as:

$L_1\% = [L_1/L_1+L_2+L_3 \ldots L_{18}] \times 100$, and so on for all azimuth classes.

Similarly for azimuth class 1 the number percentage is calculated as:

$N_1\% = [N_1/N_1+N_2+N_3 \ldots N_{18}] \times 100$, and so on for all azimuth classes.

The calculated length and number percentages are plotted on polar

Figure 77. Aerial photo-scale fracture pattern in a selected northern part of Wayaro Quadrangle (see location on Figure 4A).

BOT = Basal Ophiolite Thrust

Figure 78. Aerial photo-scale fracture pattern in a selected western part of Wayaro Quadrangle (see location on Figure 4A).

KF = Kanilo fault

VF = Vatrari fault

WF = Watri fault

BOT = Basal Ophiolite Thrust

Inset - (P = general direction of principal folding stress;
A = average direction of acute bisectrices of conjugate fractures).

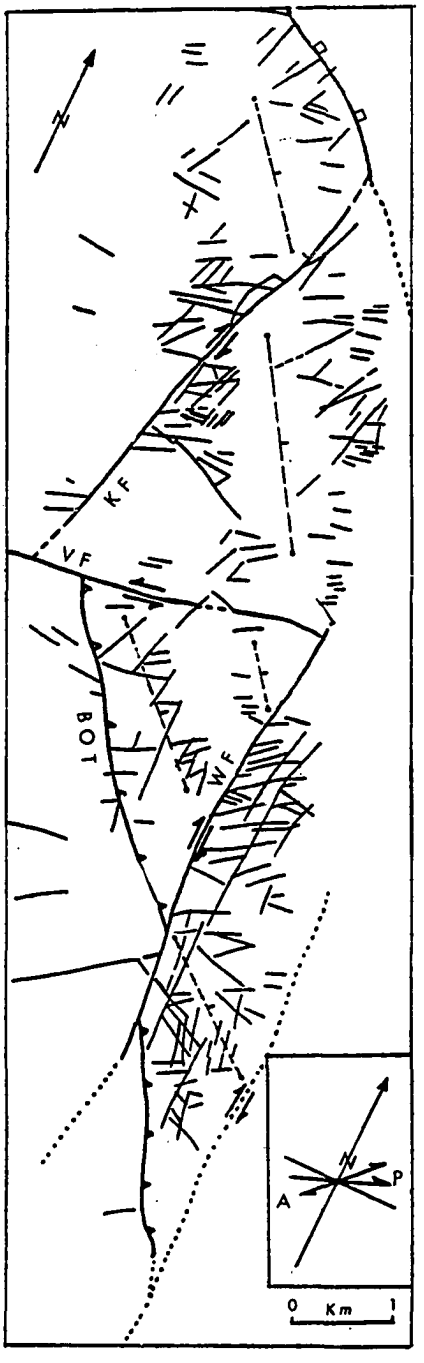

Figure 79. Aerial photo-scale fracture pattern in a selected southern part of Wayaro Quadrangle (see location on Figure 4A).

BOT = Basal Ophiolite Thrust

Based on differences in fracture density and attitudes, the area is divided into three domains:

1, 2, and 3 - Domain boundaries are marked by faults T-T-T and T'-T'-T'.

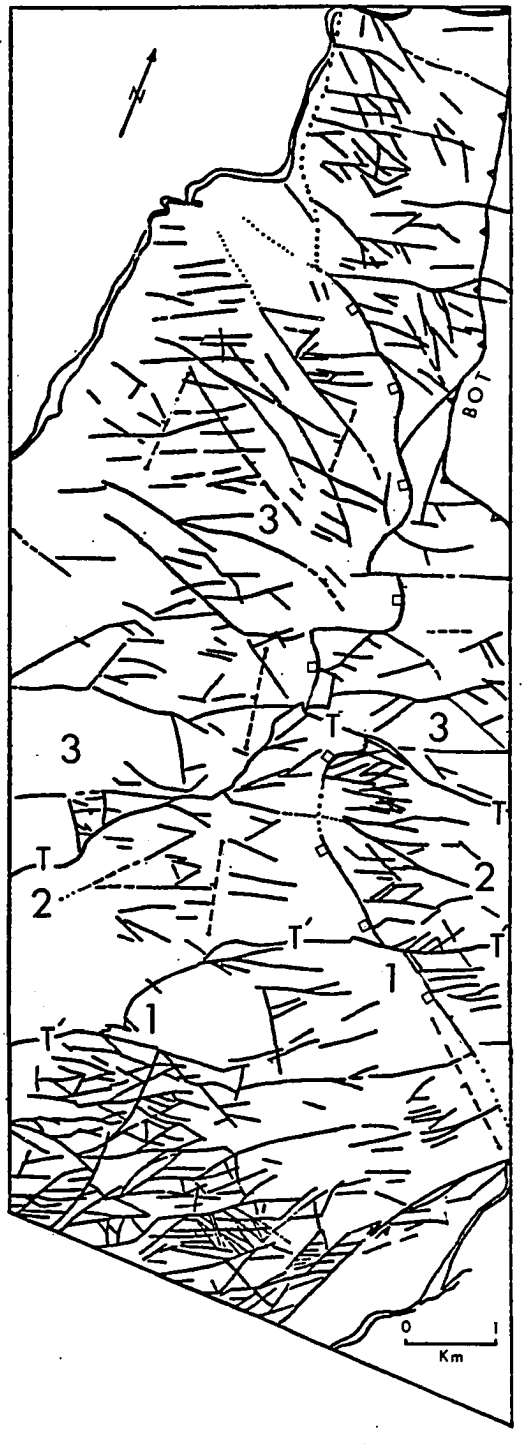

diagrams divided into 10° azimuth classes (Fig. 80A). Circles of various radii on the diagrams represent percentage intervals. These diagrams bring out the directional relations of fracture sets. Length percentages are plotted in the upper half of the circles whereas number percentages are plotted in the lower half. Polar diagrams for the areas studied are shown in Figures 80-85. The length and number percentages are plotted in graphic form in Figures 86-91. These plots give a better idea of the distribution than is given by the Polar diagrams, and help in recognition of significant trends or systems. In Figures 86-91 length percentages are plotted as histograms and number percentages as curves.

The results of the study are presented separately for the selected areas:

Northern Area: The number and length percentages in Figures 77, 80 and 86 show that there is no clearly dominant fracture set. There are four sets more or less equally developed (two each in NW-SE and NE-SW quadrants). A fifth set (ESE-WNW) is most prominent because it includes the longest faults and fractures of the area. No well defined conjugate pattern is present; the relative ages of the various sets are also conflicting.

Western Area: This area shows a well developed conjugate fracture pattern as is evident from Figures 79, 81 and 87. Most fractures are oriented either ENE or NNE, and the acute bisectrices point in a general SW direction. The pattern also includes three prominent transverse faults

Figure 80. A. Equal area Polar net used in the construction of Figures 80B-85. Eighteen azimuth classes used to classify fractures are indicated. Length percentages (L%) and number percentages (N%) calculated for each azimuth class (see text) are to be plotted in upper and lower halves of the circles. Percentage intervals are shown on inner circles.

B. Polar diagram for the fracture pattern shown in Figure 77, indicating fracture length (L) and number (N) percentages.

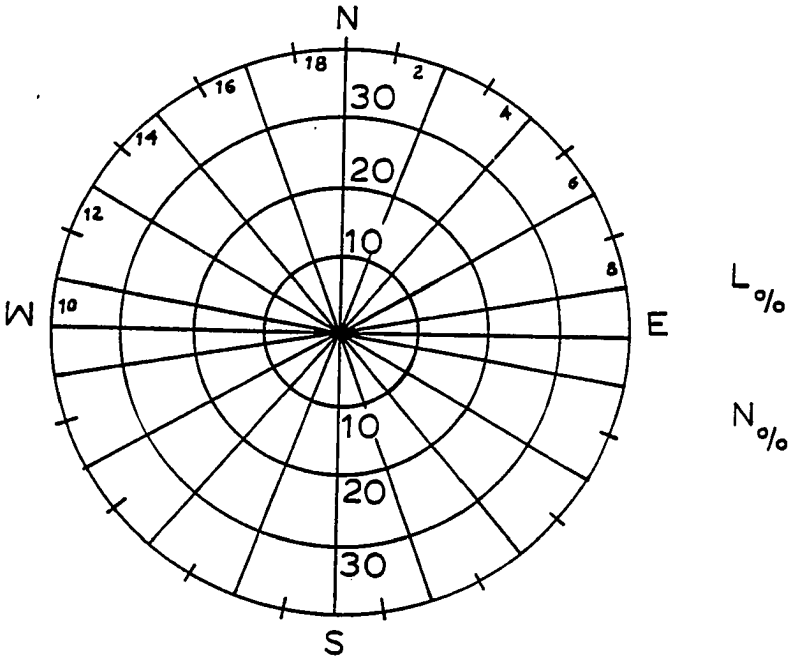

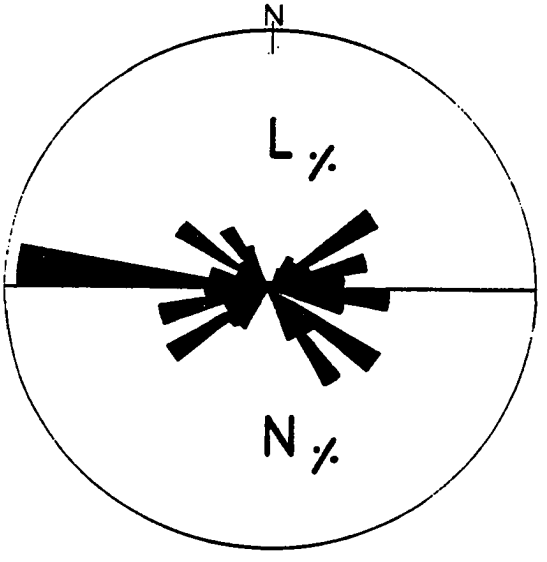

Figure 81. Polar diagram for the fracture pattern shown in Figure 78, indicating length (L) and number (N) percentages.

Figure 82. Polar diagram for the fracture pattern shown in Figure 79, indicating length (L) and number (N) percentages.

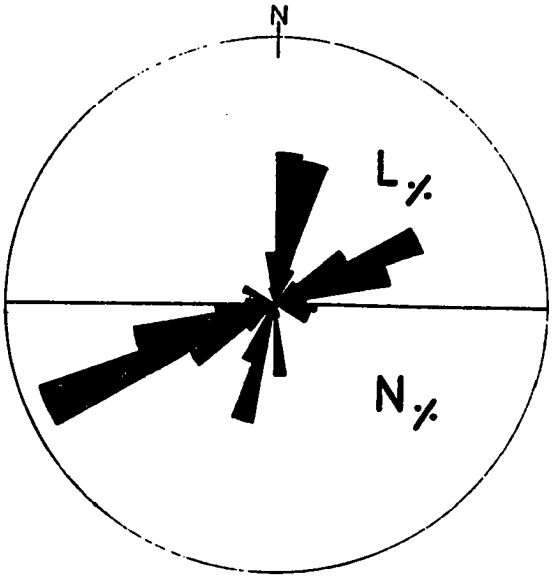

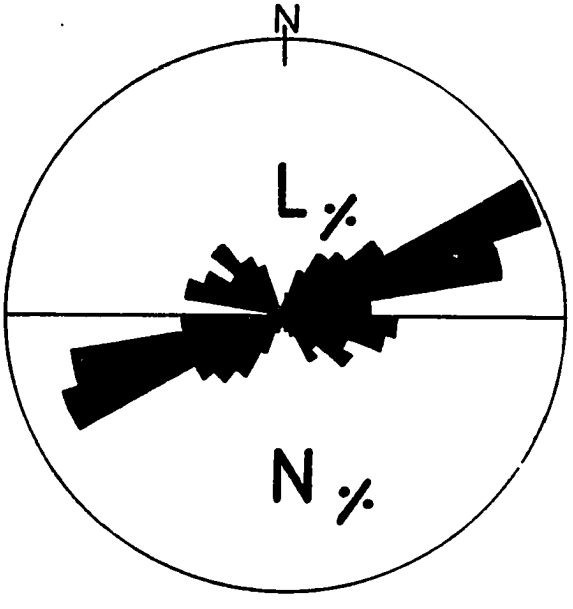

Figure 83. Polar diagram for the fracture pattern in domain 1 of Figure 79, indicating length (L) and number (N) percentages. Compare with Figures 84-85.

Figure 84. Polar diagram for the fracture pattern in domain 2 of Figure 79, indicating length (L) and number (N) percentages. Compare with Figure 83 and 85.

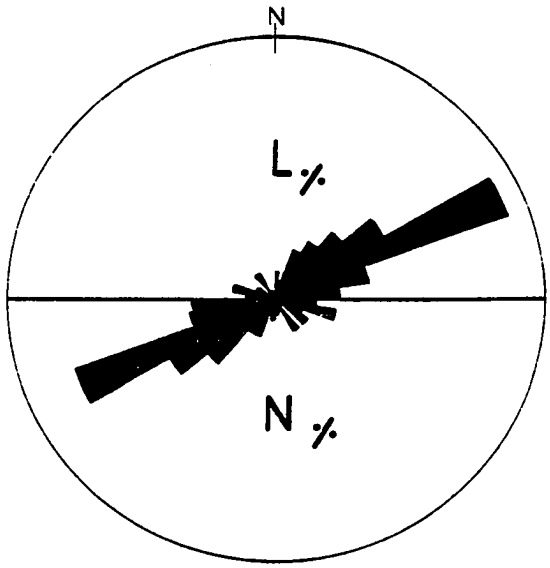

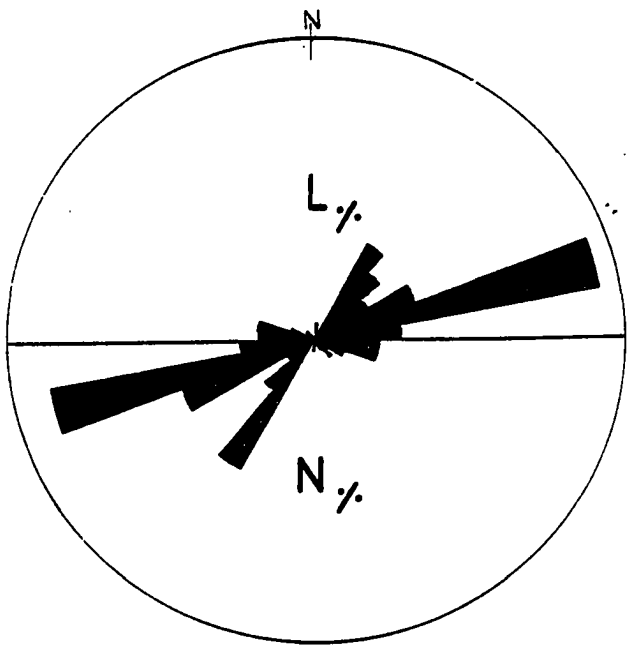

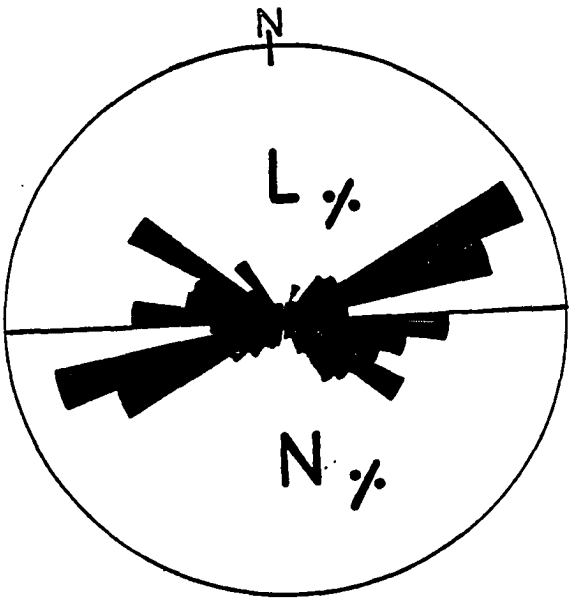

Figure 85. Polar diagram for the fracture pattern in domain 3 of Figure 79 indicating length (L) and number (N) percentages. Compare with Figures 83 and 84.

of the area (Fig. 79). A third fracture set oriented WNW is only poorly developed.

It is tempting to suggest that the well developed conjugate fracture pattern could have been caused by the principal folding stress. However, there are problems with this explanation. First of all, there is a significant discrepancy between the direction of the acute bisectrix of the conjugate pattern (which is SW-NE) and that of the principal folding stress (perpendicular to the averaged direction of the synclinal axis, which appears to be WSW-ENE; see inset in Fig. 78). Other difficulties arise from age and movement considerations of the three major transverse faults (Watri, Vatrari, and Kanilo faults in Fig. 78). These faults, all members of a conjugate system, cut across the Kanar Melange, BOT and the lower part of the ophiolite sequence. The faults are truncated, upsection by a serpentinite bearing melange horizon (base of ophiolite unit 4, Figure 4A), and also downsection by the Piaro thrust. Drag associated with the three major faults indicates lateral movement along them (e.g., in Fig. 16). Such movement along the Watri and Vatrari faults seems to explain the separation of the BOT, which obviously took place after the emplacement of ophiolites on top of the Kanar Melange. However, other features (such as sequence of lava flows, asedimentary rocks and sills in unit 2) of the walls cannot be matched. Similar reasoning can be applied to the Kanilo fault. This indicates that these faults involve unknown previous movements that cannot be accounted for at present by the apparent lateral movement mentioned above. In other words, they are old features that were present in the ophiolites at the time of obduction. Post obduction reactivation, which explains the present separation of the

BOT, caused extension of these faults into the underlying Kanar Melange. If this view is correct, then there is no simple relation between folding and the conjugate fractures; it only reactivated them.

Upsection truncation of the three faults can be explained by the unconformity at the base of the serpentinite-bearing melange horizon in the ophiolite unit 4 (Fig. 4A). A better example of upsection truncation of a fault by an unconformity is a NW-SE trending fault located at Longitude 66°39' and Latitude 26°9' (Plate I). Along this fault, a block of pillow lava is juxtaposed against a diabase sill bearing block. The fault is buried under a serpentinite/argillite melange horizon which forms the base of the ophiolite unit 2 (Plate I).

Downsection truncation of the Vatrari and Watri faults by the Piaro thrust can be explained by late movement of Piaro Ridge (Plate I, Fig. 4A), which took place after the regional syncline was formed.

Southern Area: Figures 79 and 83-85 show the fracture pattern and the plots for rocks lying between the Sukkan and the Gacheri streams. This area has been divided into three structural domains because of changes in the fracture pattern in a N-S direction (Figs. 79, 83-85 and 89-91). As evident, the southernmost area (domain 1) shows a dense and intricate pattern with dominant ENE orientation (Figs. 79, 83, 89). No generalization can be made about the relative ages of various fracture sets.

In domain 2 (Figs. 79, 84, 90), the ENE fracture set is dominant. However, a second set, trending NE, has clearly manifested itself. The NE set might be younger than the ENE set as several of the NE fractures terminate against the ENE fractures. It is interesting that there is a

Figures 86-91. Graphs and histograms of fracture number and length percentages for the fracture data shown in Figures 80-85, respectively.

Graph = Number %

Histogram = Length %

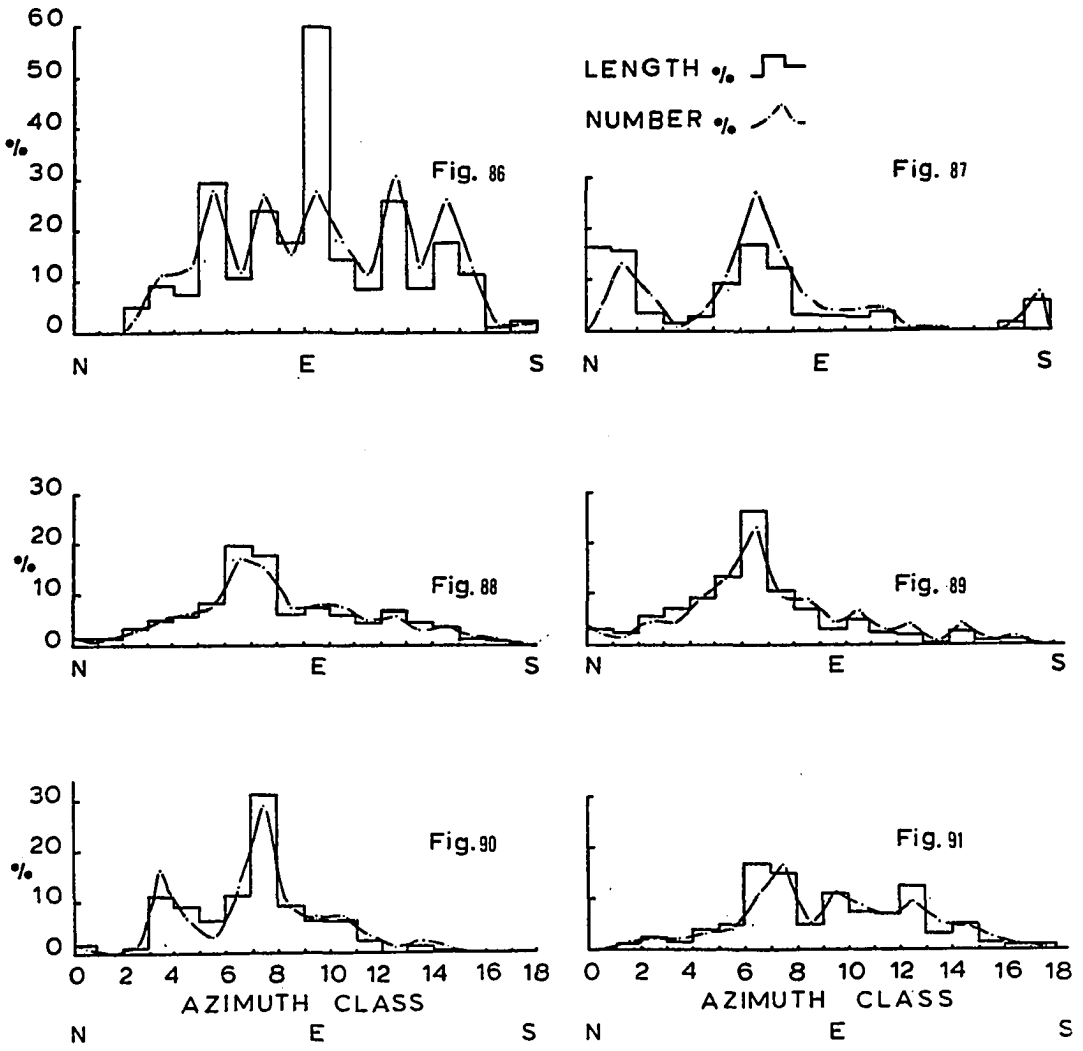

difference of 10° between the azimuths of best developed fracture sets in domains 1 and 2 (Figs. 79, 83, 84, 89-90). Also the difference between the strike of rock formations in domains 1 and 2 is noticeable. These differences appear to be due to bending in plan and rotation of the two domains relative to each other. The cause of bending and rotation is not known.

In domain 3 (Figs. 79, 85, 91), the ENE fracture set is still dominant, but two other sets (NW and WNW oriented) are also notably developed (contrast with NE set of domain 2). Neither the relative ages of these sets nor their relation with the folding stress is clear. Certain fractures, confined only to unit 1 and abutting against the basal thrust of the overlying unit 2, could possibly be older than the unconformity between the two units (Figs. 4A, 79). Those cutting across the unconformity may be younger.

Age and Origin of the Fracture Pattern: From the above it can be seen that the fracture pattern varies in different parts of the study area, and appears to involve several generations of fractures. Due to discrepancies between the orientation of the principal folding stress and the acute bisectrices of the various fracture sets, a direct relationship between the two cannot be established. Further, some faults are probably old features that were formed in the oceanic regime. There is additional evidence (presented later) that suggests that certain joints, in the sedimentary rocks associated with diabase sills, were also formed in the oceanic regime.

Crustal rocks are subject to deformation in the oceanic regime just as they are on the continents. Horizontal compressional and tensional

stresses are present within the oceanic crust across ridges and fracture zones (Sykes and Sbar, 1973; Eittreim and Eving, 1975; Collette, 1974; Bonatti and Honnorez, 1976; Bonatti, 1978). According to Bonatti (1978), compressional and tensional horizontal stresses, created mainly due to small changes in the direction of spreading, are the main cause of vertical tectonism in the fracture zones. Initial fracturing and faulting within the Bela Ophiolites can perhaps be attributed to such stresses in the oceanic regime.

It is also plausible that additional disruption of the Bela Ophiolites might have occurred during thrusting at the time of obduction. Likewise certain fractures could have been caused by the post-obduction regional folding. The Piaro Ridge thrust is younger than the several transverse faults that approach obliquely toward it from the east (e.g., Kanilo and Watrari faults, Fig. 4A). However, Piaro Ridge is offset by a NNE trending dextral strike-slip fault that follows the Gajri stream just outside the NW corner of the mapped area. Therefore, it is concluded that the present fracture pattern of the area is a sum total of several periods of disruption which commenced in the oceanic regime. Tectonic activity in the area is still going on.

Joints and Cleavage

A variety of joints and cleavage are displayed by the various rock types within the study area. Because of lack of time, no detailed study was possible. Therefore, only a short description is given here and no attempt is made to relate the joints and cleavage with larger structures

in the rocks. Some data on the axial plane cleavage of folds in the Piaro Ridge is given in Figure 75.

The mudstones and shales of the folded Sembar Formation show two interesting joint and cleavage combinations. In the mudstones, a set of orthogonal or conjugate joints, developed at a high angle to bedding, is intersected by a bedding cleavage. This results in the tabular weathering fragments characteristic of the Sembar mudstones. The less coherent shales show a bedding cleavage intersected by another cleavage which is strike-parallel but at high angle to bedding. The two cleavages are cut by a set of regularly spaced vertical joints parallel to dip direction of beds. The result is that the beds are broken into a stack of "sticks," each with rectangular or rhombic cross section. This type of cleavage, observed elsewhere, has been termed "pencil lineation or pencil cleavage" by the Hunting Survey (1960, Fig. 231).

The dolerite-gabbro sills may show various joint patterns such as columnar, rectangular or irregular. Columnar joints are generally crudely formed in the medium to coarse grained thick sills. However, at one locality (Kunjeji stream gorge) excellent columnar joints were seen in a fine-grained basaltic sill.

The pillow lavas may show excellent polygonal tensional joints on pillow surfaces. Besides, pillows are generally cut by a network of irregular closely spaced joints; for this reason the flows are more weathered and friable than the sills. The unpillowed, massive lavas exhibit a close polygonal or rectangular block-joint pattern. Besides the above, all lava flows show a well developed and complex regional fracture pattern already discussed in a previous section.

The sedimentary rocks associated with the lava flows and the sills may show a tabular, rectangular or irregular joint pattern. Also, bedding cleavage may be more or less well developed. The argillites, may exhibit a strong slaty cleavage, especially near sills. Also in some inter-sill argillites, some polygonal joints were observed which stand out as 'ribs' or low ridges on the bedding planes. Each 'rib' is actually a thin border of hardened rock along both sides of the joint which itself is marked by a median groove. The rib is, therefore, more resistant to weathering than the unaffected argillaceous material away from the fracture, which is more easily removed. The hardening along joints was probably a result of thermal and/or metasomatic activity related to the emplacement of the sills, which might have caused the jointing itself. At one locality well developed columnar joints were seen in cherts that were intruded by a gabbro sill.

In Piaro Ridge, well developed axial plane cleavage is often associated with the folds (Fig. 73). On the southern part of the ridge (north of the Sukkan stream), it was noted that the axial plane cleavage accompanied the second generation of folds (Fig. 74). This, however, could not be established elsewhere because of the lack of proper exposure. In extreme cases, shearing along the axial plane cleavage may completely obliterate the true bedding. The shears parallel the general strike of the rocks and are probably related to thrusting. The cleaved rocks release a debris of sharp-edged roughly platy or tabular clasts. Beds of limestone and sandstone may show rectangular joints.

GEOLOGICAL HISTORY

The present knowledge of the area is far from complete and permits only a tentative outline of its geological history:

I. Triassic and Jurassic:

Platform type sedimentation of the Shirinab Formation. Rifting of the Gondwana in Middle-Upper Jurassic with India still attached to Madagascar (Norton and Sclater, 1979; Powell, 1979). The Neotethys Ocean lies to the north and northwest of India (Powell, 1979)

II. Cretaceous:

Deposition of Sembar Formation reflecting development of a distinct slope environment (White, 1981) off the rifted margin. A large fracture zone (ancestral to the Bela Ophiolites) lies near the northwestern margin of the Indo-Pakistan subcontinent (Fig. 70). Late Cretaceous separation of India from Madagascar and formation of the proto-Owen and Chagos transform boundaries at the western margin of the Indian Plate as it moves northward, subducting Neotethys under the Iran-Afghanistan-Eurasian Blocks (McKenzie and Sclater, 1971; Powell, 1979; Norton and Sclater, 1979). Alkaline igneous activity, possibly heralded by the Gondwana rifting, takes place on the western margin of Indo-Pakistan (the Mor Intrusives and Porali Conglomerate volcanics).

III. Paleocene-Eocene:

Following subduction of the Neotethys, the Indian Plate collides with the continental blocks to the north in Late Paleocene-Early Eocene (McKenzie and Sclater, 1971); by Middle Eocene the Pakistani ophiolites are emplaced, the Indus Suture (Gansser, 1964) is closed, and collision is complete (Powell, 1979).

Within the study area, large slide blocks and debris of ophiolitic and Mesozoic continental rocks (Kanar Melange) were laid down on top of the Sembar Formation. This was followed by the emplacement of ophiolites, which were probably derived from a fracture zone located adjacent to the continental margin. Initial folding of the autochthonous sequence, probably related to ophiolite nappe emplacement, also takes place. The alkaline igneous activity ceases with the emplacement of ophiolites.

Formation of the Kanar Melange, some continental margin igneous activity, and ophiolite emplacement, all seem to have taken place during the latest Cretaceous-Early Eocene time.

IV. Eocene-Oligocene:

Marine transgression and deposition of neo-autochthonous carbonates on top of the ophiolites (Lower Middle Eocene-Oligocene, Allemann, 1979). These are exposed near Kanar 50 kilometers north of the mapped area (Figs. 2, 70F).

There is no evidence within the mapped area to indicate the time of post-emplacement folding of the ophiolites. It appears that marine sedimentation continued in the Bela area through the Oligocene (Hunting Survey, 1980; Allemann, 1979). Whether

it was accompanied by folding is not established, although it would be expected from the compression caused by the counter-clockwise rotation and renewed northward motion of the Indian Plate which still continues (Powell, 1979).

V. Neogene:

Marine regression and uplift of the Bela area (Allemann, 1979), probably caused by compression of the continental margin is presently going on. The formation of the regional synclinal fold of the Bela Ophiolites and eastward thrusting of Piaro Ridge have possibly occurred during this period. Major tectonic features along the Kirthar-Sulaiman Belt developed during this time (Hunting Survey, 1960; Powell, 1979; Sarwar and DeJong, 1979).

ECONOMIC GEOLOGY

Several showings of copper, iron and manganese are known from the ophiolitic rocks of the study area (see Plate I). The minerals are associated mainly with the lava flows and the interflow sedimentary rocks as primary constituents. Disseminated pyrite is visible in several lava flows and sills. Occasionally impregnations and veinlets of pyrite, possibly of secondary origin, are also observed. The sulphides of copper and iron are generally oxidized as indicated by infrequent malachite-stained flows and small limonitic gossans. Small concentrations of manganese may occur with jasperoid and other siliceous sedimentary rocks. Despite drilling (by the Pakistani Geological Survey and private prospectors) no viable deposit of any of the above minerals has yet been found. Manganese, however, has been exploited in small quantity by some local tribesmen.

Many small occurrences of Mississippi Valley type barite with minor base metal sulphides (Sillitoe, 1978) are also known from the Shirinab Formation of the Mor Range, Piaro Ridge and several olistoliths of similar rocks in the Kanar Melange (see Plate I). Galena is associated with barite in subordinate to minor amounts, while pyrite, chalcopyrite and sphalerite(?) are present in traces. Fluorite may also be occasionally seen in trace amounts. The mineralization is epigenetic and occurs as partial replacement of certain limestone beds and also as cavity fillings. The presence of barite and sulphides within some allochthonous limestone

blocks of the melange clearly suggests that the mineralization is of pre-Kanar Melange age. According to Sillitoe (1978), it could have been an event related to the Gondwana rifting. The mineralization occurs in an extensive belt from Quetta in the north to the Las Bela region in the south. South of Quetta veins and rich stratabound bodies of fluorite are known from Kohi Maran and Dilband in the Kalat Plateau (Bakr, 1962; Mohsin and Sarwar, 1974). Further south in the Khuzdar-Las Bela region several barite and barite-galena deposits of similar type are known from the Triassic-Jurassic limestone sequence. Some of these deposits are being mined on a small scale. Exploration by the Pakistani Geological Survey (currently in progress) and drilling has indicated the presence of zinc and silver also, besides the usual barium and lead.

Besides the above, the pelagic limestone and serpentinite-bearing rocks are quarried by the local tribesmen on a small scale. The material is transported to Karachi and used for building purposes.

CONCLUSIONS

(1) The Bela Ophiolites were obducted in the Paleocene-Early Eocene (Allemann, 1979) on the Mesozoic sedimentary sequence of the northwest paleo-margin of the Indo-Pakistan subcontinent. The ophiolites form a north-south belt adjacent to the Oranch-Nal-Chaman fault zone which forms the present northwest transform (left-lateral) margin of the Indo-Pakistan subcontinent. Field work in the Wayaro and adjacent areas revealed that the autochthonous sequence below the ophiolites consists of the following units: The Kanar Melange (Paleocene-Early Eocene ?), Sembar Formation (Cretaceous argillaceous rocks) and Shirinab Formation (Triassic-Jurassic carbonate and clastic rocks).

(2) The Kanar Melange is a sedimentary complex of assorted debris of mainly older continental and ophiolitic (oceanic) rocks that was deposited on top of the Sembar Formation. It mainly consists of olistostromes, and olistoliths. The melange was laid down in a deep linear trough on the continental margin, and its formation was accompanied by strong tectonic movements. Based on the presence of certain Maestrichtian microfauna in some boulders found in the melange, its stratigraphic and tectonic position, and constitution, it has been suggested that the Kanar Melange was formed during Paleocene-Early Eocene time. Its formation, therefore, was largely coeval with the ophiolite emplacement. The Kanar Melange can be correlated with the Gidar-Dhor Group, Thar Formation, and the Bad Kachu Formation of the northern Bela Ophiolite Belt and vicinity.

(3) Several episodes of alkaline ultramafic and mafic intrusive activity and at least one of extrusive activity (Porali Conglomerate source volcanics) took place on the continental margin. The time of the earliest intrusive activity is not known but was possibly linked with the rifting of eastern Gondwana (Middle-Late Jurassic ?). The extrusive activity took place before the melange formation, because its reworked material (Porali Conglomerate) was incorporated in the Kanar Melange. The intrusive activity apparently ceased after the melange formation but before the final emplacement of the ophiolites as indicated by the lack of such intrusives in the ophiolites. No igneous activity took place after the ophiolite emplacement.

(4) The Bela Ophiolites consist of a sequence of basaltic pillow lavas, interlayered deep-sea sedimentary rocks (chert, pelagic limestone, marl, argillite) and diabase-gabbro sills. The sequence also includes several melange horizons which consist of assorted debris of typical oceanic rocks. The most common rocks are deformed serpentinite slivers (up to several hundred meters long) and breccias of serpentinite-carbonate material with or without clasts of limestone, chert, mudstone, and basalt; less commonly boulders and blocks of peridotite, gabbro, pillow lava, chert, limestone, lithic sandstone and occasionally their metamorphic equivalents are also found. The matrix is formed by argillites and subordinate coarser detrital material involving serpentinite and other rocks mentioned above. Isolated slivers and slabs of deformed serpentinite and breccias (up to a few tens of meters) are also irregularly distributed throughout the ophiolite sequence.

(5) A large oceanic fracture zone is the most suitable tectonic setting to explain the origin of the Bela Ophiolites. This is mainly based on the following observations (see also number 8 and 9 below):

A. The melange horizons including the isolated bodies are best interpreted as intermittently and locally derived debris in a tectonically controlled fault block-trough oceanic environment. The debris is deposited in a deep-sea sedimentary-basaltic lava sequence which is intruded by mafic sills. This indicates that tectonic, sedimentary and igneous processes were simultaneous in nature (Fig. 65).

B. Serpentinite is abundant and forms the most common component of the melange material. Most serpentinite exposures occur in the fracture zones (Bonatti, 1976).

C. Deformed rocks commonly occur in the melange material, e.g., the serpentinite is generally foliated; breccias and foliated breccias are common; also other metamorphic rocks such as amphibolite clasts are found. Such deformed rocks can be attributed to the shear zones.

(6) Pelagic fauna indicates that the age of the Bela Ophiolites is Aptian-lower Maestrichtian (Upper-Lower Cretaceous-Upper Cretaceous).

(7) Petrographically, the Bela lavas are spilitic basalts, and, less commonly, keratophyres, and basaltic andesites. The associated sills are diabases and gabbros of broadly similar petrographic features.

(8) Chemically the Bela lavas are low K-tholeiites with an alkaline tendency, and enriched in Fe, TiO_2, and LREE. A comparison with the modern oceanic basalts revealed that the Bela basalts are chemically different from basalts erupted along the mid-oceanic ridges, but somewhat similar to those erupted in anomalous tectonic settings: e.g., fracture zones, aseismic ridges, oceanic islands, etc.

(9) The diabase-gabbro sills are also chemically similar to the associated lavas. However, they tend to be more enriched in alkalis, Fe, TiO_2, LREE and generally exhibit a greater range of constituent elements. Therefore, the diabases and gabbros are more fractionated than the lava flows they intrude. However, their generally similar petrographic and chemical features and field relations clearly suggest that both the lava flows and the diabase-gabbro sills were derived from the same magmatic source, which apparently changed in chemistry with time.

(10) The fracture zones of the Arabian-NW Indian Oceans (e.g., Owen and Chagos fracture zones) developed in Cenozoic oceanic crust (Powell, 1979; Norton and Sclater, 1979). Therefore, they are younger than the Bela Ophiolites (Cretaceous), and cannot be related to them.

(11) The Bela Ophiolites evolved during the Cretaceous in a Tethyan fracture zone which probably lay adjacent to the Bela margin of the Indo-Pakistan subcontinent.

(12) The ophiolite emplacement in Pakistan is generally attributed to collision between the Indo-Pakistan and the Eurasian blocks (Powell, 1979). This is not valid for the Bela Ophiolites because no collision

has yet occurred along this part of the continental margin. Instead, it is more plausible that the emplacement of the Bela Ophiolites was related to an oblique convergence between the Indo-Pakistan subcontinent and the adjacent fracture zone. The convergence probably took place during Paleocene-Early Eocene time; it resulted in the destruction of the fracture zone and emplacement of its crustal material (ophiolites) on the continental margin.

(13) The earliest tectonic activity in the area probably commenced with the rifting of eastern Gondwana (Middle-Late Jurassic, Powell, 1979), and might have continued through the Cretaceous along with the alkaline igneous activity (Mor Intrusives; Porali volcanism). However, it is only in the Paleocene-Early Eocene that strong tectonic movements are clearly evidenced (formation of Kanar Melange, and emplacement of Bela Ophiolites). Initial folding of the autochthonous sequence was probably related to the emplacement of the ophiolite nappe. The tectonic activity has probably been continuing since then as several observations suggest: The whole area was folded and an open NNW-SSE trending syncline, which is the major structure of the Wayaro-Kanar area, was formed. Further deformation resulted in thrusting along the western limb of the syncline. This produced Piaro Ridge which is a tightly folded upthrust mass of the Shirinab Formation that was brought against the Kanar Melange. Tilted terraces of subrecent gravel attest to the present-day tectonic activity.

(14) The autochthonous sequence of the area was mainly deformed by folding. On the other hand, the ophiolites were deformed mainly by fracturing. This is clearly visible on aerial photographs (1:40,000). A

geometric analysis of the photo-scale fracture pattern revealed that it probably developed during several episodes, and was partly inherited from the oceanic regime.

(15) Several showings of Cu, Mn, and Fe occur in the pillow lava/ sedimentary sequence of the ophiolites. This mineralization is probably of hydrothermal-exhalative type and directly linked with the associated mafic igneous activity.

(16) Small occurrences of Mississippi Valley type Ba-Pb deposits occur in the Shirinab limestone of the Mor Range, Piaro Ridge, and several large blocks in the Kanar Melange. These deposits were certainly formed prior to the melange formation. Their exact age is not known, however, they have been linked with the eastern Gondwana rifting (Sillitoe, 1975).

PROBLEMS FOR FURTHER RESEARCH

1. The formation of the Kanar Melange was accompanied by strong tectonic movements as attested by the abundant olisoliths of continental rocks which were severely deformed before their emplacement in the melange. What kind of tectonic movements were they? How did this tectonic activity affect the Sembar basin which became the Kanar basin?

2. The Kanar basin was probably a linear north-south trending trough. Some idea of its depth can be gained by the shear size of certain olistoliths in the Kanar Melange (several cubic kilometers, e.g., the Porali Conglomerate block, Fig. 4A). What were the processes involved in the formation of this melange? How far does it continue northward and how does it end? Are there any comparable rocks east of the Mor Range?

3. The Mor Intrusives and the Porali Conglomerate represent the alkaline magmatism that took place on the continental margin before the ophiolites were obducted. When and how was this igneous activity initiated and why it apparently ceased (at least in the Wayaro area and vicinity) with the ophiolite emplacement? It appears that the alkaline magmatism was widespread in the Kirthar-Sulaiman Mountains. Its extent and the details about its nature need to be further documented. It should be kept in mind that it was partly coeval with the Deccan

volcanism of west-central India. Also trap rocks are known to occur in the subsurface Cretaceous sequence of the Karachi-Hyderabad region east of the Mor Range (Kadri and Khan, 1973).

4. The ophiolitic material in the Kanar Melange was probably released from the nappes of oceanic material encroaching from the west toward the continental margin. Many ophiolitic olistoliths in the melange measure in kilometers. Does it mean that the emplacement of the ophiolite nappe was also gravity induced? Gravity induced emplacement has been suggested for other ophiolite nappes, e.g., the Semail Ophiolites, Oman (Glennie et al., 1974); see also Coleman (1977) and references therein.

5. So far the Bela Ophiolites have been partly mapped on a scale of 1:50,000 (DeJong and Subhani, 1979; and this study). More mapping is needed, especially in the northern part of the ophiolite belt which is as yet practially untouched. Also, the scale 1:50,000 does not show the details of the sedimentary, igneous and structural relations of the ophiolites so vividly exposed. Mapping on a larger scale (at least 1:20,000) of a selected segment of the belt will bring out such detail and greatly help in the understanding of the evolution of a very interesting type of oceanic crust not commonly observed in other ophiolite complexes.

6. The petrographic and chemical nature of the Bela Ophiolite needs to be further documented elsewhere along the belt. Its basaltic rocks exhibit chemical traits resembling those erupted in anomalous tectonic

settings (e.g., fracture zones, aseismic ridges) of modern large oceans. This is significant and should be pursued further.

7. Though no viable ore deposits have yet been found, the Bela Ophiolite belt still has considerable economic potential. Small showings of Fe, Mn and Cu minerals do exist in the ophiolites. It is suggested that, within the context of the oceanic fracture zone model, fracture-controlled mineralization is likely to occur along old features (e.g., Rona et al., 1976; Smewing et al., 1977). The aerial photo-scale fracture pattern can be utilized from this point of view.

8. Besides the above the Mississippi Valley type barite/base metal sulphide prospects of the Shirinab Formation are important. Field work in the Wayaro and Kanar areas has indicated that the mineralization apparently follows several horizons in the Shirinab Formation of Piaro Ridge and the western part of the Mor Range. The Mor Range is more important because of its already known deposits and the extensive outcrop of the Shirinab limestone. However, structural complexities will be encountered. It is emphasized that the exploration by the Geological Survey or any other group must include mapping and detailed structural studies of at least the more prospective parts of the Mor Range.

REFERENCES

Abbas, S. G., and Ahmad, Z., 1979, The Muslimbagh Ophiolites, in Farah, A., and DeJong, K. A., Eds., Geodynamics of Pakistan: Geological Survey of Pakistan, Quetta, 1979, p. 243-350.

Abbate, E., Bortolotti, V., and Passerini, P., 1972, Paleogeography and tectonic considerations on the ultramafic belts in the Mediterranean area: Boll. Soc. Geol. Ital., v. 91, p. 239-282.

Abbey, S., 1973, Studies in 'Standard Samples' of silicate rocks and minerals - Part 3: 1973 extension and revision of 'useable' values: Geol. Surv. Can. Paper 73-36, 25 p.

Allemann, F., 1979, Time of emplacement of the Zhob Valley ophiolites and Bela ophiolites, in Farah, A., and DeJong, K. A., Eds., Geodynamics of Pakistan: Geological Survey of Pakistan, Quetta, 1979, p. 215-242.

Alexander, P. O., and Gibson, I. L., 1977, Rare earth abundances in Deccan trap basalts: Lithos, v. 10, no. 2, p. 143-147.

Amstutz, G. C., 1968, Spilites and spilitic rocks, in Basalts: the Poldervaart Treatise on Rocks of Basaltic Composition, Hess, H. H., and Poldervaart, A., Eds.: Interscience, Wiley, New York, p. 737-753.

Amstutz, G. C., and Patwardhan, A. M., 1974, A reappraisal of the textures and the composition of the spilites in the Permo-Carboniferous Verrucano of Glarus, Switzerland, in Amstutz, G. C., Ed., Spilites and Spilitic Rocks: Springer-Verlag, p. 71-82.

ARCYANA, 1975, Transform fault and rift valley from bathyscaph and diving saucer: Science, v. 190, no. 4210, p. 108-116.

Ashley, P. M., Brown, P. F., Franklin, B. J., Ray, A. S., and Scheibner, E., 1979, Field and geochemical characteristics of the Coolac ophiolite suite and its possible origin in a marginal sea: J. Geol. Soc. Austral., v. 26, Parts 1-2, p. 45-60.

Asrarullah, Ahmad, Z., and Abbas, S. G., 1979, Ophiolites in Pakistan: an introduction, in Farah, A., and DeJong, K. A., Eds., Geodynamics of Pakistan: Geological Survey of Pakistan, Quetta, 1979, p. 181-192.

Aumunto, F., and Loubat, H., 1971, The Mid-Atlantic Ridge near 45°N. SVI. Serpentinized ultramafic intrusions: Can. J. Earth Sci., v. 8, p. 631-663.

Bailey, D. K., 1974, Continental rifting and alkaline magmatism, in The Alkaline Rocks, Sorensen, H., Ed.: John Wiley and Sons, p. 148-159.

Bakr, A., 1962, Fluorspar deposits in the northern part of Koh-Maran Range: Recs. Geol. Surv. Pakistan, v. 9, pt. 2, 7 p.

Bakr, M. A., and Jackson, R. O., 1964, Geological map of Pakistan (1:2,000,000): Geol. Surv. Pakistan, Quetta, Pakistan.

Ballard, R. D., Bryan, W. B., Heirtzler, J. R., Keller, G., Moore, J. G., and VanAndel, Tj., 1975, Manned submersible observations in the Famous area: Mid-Atlantic Ridge: Science, v. 190, no. 4210, p. 103-108.

Barker, P. F., 1966, A reconnaissance survey of the Murray Ridge: Phil. Trans. R. Soc. London, v. 259, p. 187-197.

Battey, M. H., 1974, Spilites as weakly metamorphosed tholeiites, in Spilites and Spilitic Rocks, Amstutz, G. C., Ed.: Springer-Verlag, p. 365-372.

Beccaluva, L., 1979, The Vourinos ophiolitic complex has been created in an island arc setting: Evidences from petrographic and geochemical features, in Abstr. Inernatl. Ophiol. Symp., Nicosia, Cyprus, p. 16.

Beccaluva, L., Ohnenstetter, D., Ohnenstetter, M., and Venturelli, G., 1977, The trace element geochemistry of Corsican ophiolites: Contr. Min. Pet., v. 64, p. 11-31.

Bezrukov, P. L., Bodganor, Yu, A., Murdmaa, I. O., and Romankevich, E. A., 1975, Bottom sediments of the Indian Ocean rift zone, in Rift Zones of the World Ocean, Vinogradov, A. P., and Udintsev, G. B., Eds.: Eng. Trans. published by John Wiley & Sons, p. 205-229.

Bonatti, E., 1978, Vertical tectonism in oceanic fracture zones: Earth and Planet. Sci. Lett., v. 37, p. 369-379.

Bonatti, E., 1976, Serpentinite protrusions in the oceanic crust: Earth and Planet. Sci. Lett., v. 32, p. 107-113.

Bonatti, E., Emiliani, E., Ferrara, G., Honnorez, J., and Rydell, H., 1974, Ultramafic-carbonate breccias from the equatorial mid-Atlantic Ridge: Marine Geol., v. 16, p. 83-102.

Bonatti, E., and Honnorez, J., 1976, Sections of Earth's crust in the equatorial Atlantic: J. Geophy. Res., v. 81, p. 4104-4116.

Bonatti, E., Honnorez, J., and Ferrara, G., 1971, Peridotite-gabbro-basalt complex from the equatorial mid-Atlantic Ridge: Phil. Tr. Roy. Soc. London, Ser. A., v. 268, p. 385-402.

Bonatti, E., Honnorez, J., and Gartner, S., Jr., 1973, Sedimentary serpentinites from the mid-Atlantic Ridge: J. Sed. Petrol., v. 43, p. 728-735.

Broin, C. E., Aubertin, F., and Ravenne, C., 1977, Structure and history of the Solomon-New Ireland regime, in Int. Symp. Geodynamics in Southwest Pacific, North Caledonia, 1976, Editions Technip, Paris, p. 37-50.

Brookfield, M. E., 1977, The emplacement of giant ophiolite nappes, 1. Mesozoic-Cenozoic examples: Tectonophy, v. 37, p. 247-303.

Brunn, J. H., 1979, Ophiolites, Origin of orogens and oceanization, in Abstr. Interntl. Ophiol. Symp. Nicosia-Cyprus, p. 107-108.

Caan, J. R., 1969, Spilites from the Carlsberg Ridge, Indian Ocean: J. Petrol., v. 16, p. 1-19.

Caan, J. R., 1971, Major element variations in ocean-floor basalts: Phil. Tr. Roy. Soc. London, v. 268-A, p. 495-505.

Carmichael, I. S. E., Turner, F. J., and Verhoogen, J., 1974, Igneous Petrology: McGraw Hill, 739 p.

Church, W. R., and Coish, R. A., 1976, Oceanic versus island-arc origin of ophiolites: Earth and Planet. Sci. Lett., v. 31, p. 8-14.

Closs, H., Narain, H., and Garde, S. C., 1974, Continental margins of India, in The Geology of Continental Margins, Burk, C. A., and Drake, C. L., Eds.: Springer-Verlag, p. 629-640.

Coish, R. A., and Church, W. R., 1979, Igneous geochemistry of mafic rocks in the Betts Cove ophiolites, Newfoundland: Contrib. Mineral. Petrol., v. 70, p. 29-39.

Coleman, R. G., 1977, Ophiolites: Springer-Verlag, 229 p.

Coleman, R. G., 1971, Plate tectonic emplacement of upper mantle peridotites along continental edges: J. Geophy. Res., v. 76, p. 1212-1222.

Collette, B. J., 1974, Thermal contraction joints in a spreading floor as origin of fracture zones: Nature, v. 251, p. 299-300.

Coombs, D. S., 1974, On the mineral facies of spilitic rocks and their genesis, in Spilites and Spilitic Rocks, Amstutz, G. C., Ed.: Springer-Verlag, p. 373-386.

Cowan, D. S., 1978, Origin of blueschist-bearing chaotic rocks in the Franciscan complex, San Simeon, California: Geol. Soc. Amer. Bull., v. 89, p. 1415-1523.

Cowan, D. S., and Page, B. M., 1975, Recycled Franciscan material in Franciscan Melange west of Paso Robles, California: Geol. Soc. Amer. Bull., v. 86, p. 1089-1095.

Daignieres, M., Courtillot, V., Bayer, R., and Tapponnier, P., 1975, A model for the evolution of the axial zone of mid-ocean ridges suggested by Icelandic tectonis: Earth and Planet. Sci. Lett., v. 26, p. 222-232.

Dalziel, I. W. D., de Wit, M. J., and Palmer, K. F., 1974, Fossil marginal basin in the southern Andes: Nature, v. 250, p. 291-294.

Davis, G. H., Phillips, M. P., Reynolds, S. J., and Varga, R. J., 1979, Origin and provenance of some exotic blocks in lower-Mesozoic red bed basin deposits, southern Arizona: Geol. Soc. Amer. Bull., v. 90, p. 376-384.

DeJong, K. A., and Subhani, A. M., 1979, Note on the Bela Ophiolites with special reference to the Kanar area, in Farah, A., and DeJong, K. A., Eds., Geodynamics of Pakistan: Geological Survey of Pakistan, Quetta, 1979, p. 263-270.

DeLong, S. E., Dewey, J. F., and Fox, P. J., 1979, Topographic and geologic evolution of fracture zones: J. Geol. Soc. London, v. 136, p. 303-310.

Dewey, J. F., 1976, Ophiolite obduction: Tectonophy, v. 31, p. 93-120.

Dewey, J. F., 1974, Continental margins and ophiolite obduction: Appalachian Caledonian system, in The Geology of Continental Margins, Burk, C. A., and Drake, C. L., Eds.: Springer-Verlag, p. 933-952.

Dewey, J. F., and Bird, J. M., 1971, Origin and emplacement of the ophiolite suite: Appalachian ophiolites in Newfoundland: J. Geophy. Res., v. 76, p. 3179-3206.

Dewey, J. F., and Bird, J. M., 1970, Mountain belts and the new global tectonics: J. Geophy. Res., v. 75, p. 2625-2647.

Dickinson, W. R., and Suczek, C. A., 1979, Plate tectonics and sandstone compositions: Amer. Assoc. Petrol. Geol. Bull., v. 63, no. 12, p. 2164-2182.

Dickinson, W. R., and Valloni, R., 1980, Plate settings and provenance of sands in modern ocean basins: Geology, v. 8, p. 82-86.

Dietrich, V., Emmermann, R., Oberhansli, R., and Puchelt, H., 1978, Geochemistry of basaltic and gabbroic rocks from the West Mariana Basin and the Mariana Trench: Earth and Planet. Sci. Lett., v. 39, p. 127-144.

Dmitriev, L. V., and Sharas'kin, A. Ya., 1975, Petrography and petrochemistry of bedrock from the Arabian-Indian Ridge, in Rift Zones of the World Ocean, Vinogradov, A. P., and Udintsev, G. B., Eds.: English transl. published by John Wiley and Sons, p. 393-430.

Eittreim, S., and Ewing, J., 1975, Vema fracture zone transform fault: Geology, v. 3, p. 555-558.

Elter, P., and Trevisan, L., 1973, Olistostromes in the tectonic evolution of the northern Appennines, in DeJong, K. A., and Scholton, R., Eds., Gravity and Tectonics: John Wiley and Sons, New York, 502 p.

Engel, C. G., and Fisher, R. L., 1975, Granitic to ultramafic rock complexes of the Indian Ocean ridge system, western Indian Ocean: Geol. Soc. Amer. Bull., v. 86, p. 1553-1578.

Farah, A., 1972, Preliminary statement on initiation of Geodynamics Project in Pakistan: Rept. no. 3, Prog. Devel. Inter-Union Commiss. on Geodyn., p. 237-241.

Farhoudi, G., and Karig, D. E., 1977, Makran of India and Pakistan as an active arc system: Geology, v. 5, p. 664-668.

Fiala, F., 1974, Some notes on the problem of spilites, in Spilites and Ophiolitic Rocks, Amstutz, G. C., Ed.: Springer-Verlag, p. 9-22.

Fisher, R. L., Scalter, J. G., and McKenzie, D. P., The evolution of the Central Indian Ridge, Western Indian Ocean: Geol. Soc. Amer. Bull., v. 82, p. 553.

Fitch, T. J., 1972, Plate convergence, transcurrent faults and internal deformation adjacent to southeast Asia and the western Pacific: J. Geophy. Res., v. 77, p. 4432-4460.

Fox, P. J., Schreiber, E., Rowlett, H., and McCamy, K., 1976, The geology of the oceanographer fracture zone: A model for fracture zone: J. Geophy. Res., v. 81, p. 4117-4128.

Fox, P. J., Detrick, R., and Purdy, M., 1979, Evidence for crustal thinning near fractures zones: implications for ophiolites, in Abstr. Int. Ophiol. Symp., Nicosia, Cyprus, p. 114.

Gansser, A., 1979, Reconnaissance visit to the ophiolites in Baluchistan and the Himalaya, in Farah, A., and DeJong, K. A., Eds., Geodynamics of Pakistan: Geological Survey of Pakistan, Quetta, 1979, p. 193-214.

Gansser, A., 1974, The ophiolitic melange, a worldwide problem on Tethyan examples: Eclogae Geol. Helv., v. 67, p. 497-507.

Gansser, A., 1966, The Indian Ocean and the Himalayas: Eclogae Geol. Helv., v. 59, p. 831-848.

Gansser, A., 1964, The Geology of the Himalayas: Interscience, New York, 289 p.

Gass, I. G., 1977, Origin and emplacement of ophiolites, in Volcanic Processes in Ore-genesis: Geol. Soc. London Spec. Publ., no. 7, p. 72-76.

Gass, I. G., 1968, Is the Troodos massif of Cyprus a fragment of Mesozoic ocean floor? Nature, London, v. 220, p. 39-42.

Gass, I. G., and Smewing, J. D., 1973, Intrusion, extrusion and metamorphism at constructive margins: evidence from the Troodos massif, Cyprus: Nature, v. 22, p. 26-29.

Gealy, W. K., 1979, Ophiolite obduction mechanism, in Abstr. Interntl. Ophiol. Symp. Nicosia, Cyprus, 1-8 April, 1979, p. 114.

Gerasimovsky, V. I., 1977, Trace elements in selected groups of alkaline rocks, in The Alkaline Rocks, Sorensen, H., Ed.: John Wiley and Sons, p. 402-412.

Ghose, N. C., 1976, Composition and origin of Deccan basalts: Lithos, v. 9, no. 1, p. 65-73.

Gill, J. B., 1976, Composition and age of Lau Basin and Ridge volcanic rocks: Implications for evolution of an interarc basin and remnant arc: Geol. Soc. Amer. Bull., v. 87, p. 1384-1395.

Gianelli, G., and Principi, G., 1977, Northern Apennine ophiolite: An ancient transcurrent fault zone: Boll. Soc. Geol. Italy, v. 96, p. 53-58.

Glennie, K. W., Boeuf, M. G. A., Clarke, M. W. H., Stuart, M. M., Pilaar, W. F. H., and Reinhardt, B. M., 1974, Geology of the Oman Mountains: Verh. K. Ned. Geol. Mijnbouwkd. Genoot., part 1, 423 p.

Gucwa, P. R., 1975, Middle to Late Cretaceous sedimentary melange, Franciscan Complex, northern California: Geology, v. 3, p. 105-108.

Hall, J. M., and Robinson, 1979, Deep crustal drilling in the North Atlantic Ocean: Science, v. 204, no. 4393, p. 573-586.

Haskins, L. A., Haskin, M. A., Frey, F. A., and Wilderman, T. R., 1968, Relative and absolute terrestrial abundances of the rare earths, in Origin and Distribution of the Elements, Ahrens, L., Ed.: Pergamon Press, Oxford, Int. Ser. Mon. Earth Sci., v. 30, p. 889-912.

Hawkins, J. W., 1979, Geology of marginal basins and their significance to the origin of ophiolites, in Abstr. Interntl. Ophiol. Symp. Nicosia, Cyprus, 1-8 April, 1979, p. 119.

Hawkins, J. W., Jr., 1977, Petrologic and geochemical characteristics of marginal basin basalts, in Island Arcs, Deep Sea Trenches and Back-Arc Basins, Talwani, M., and Pitman, W. C., III, Eds., Maurice Ewing Series 1, Amer. Geophy. Union, Washington, D.C., p. 355-366.

Hawkins, J. W., Jr., 1974, Geology of the Lau Basin, a marginal sea behind the Tonga Arc, in The Geology of Continental Margins, Burk, C. A., and Drake, C. L., Eds.: Springer-Verlag, p. 505-520.

Hekinian, R., and Aumento, F., 1973, Rocks from the Gibbs fracture zone and the Minia seamount near 53°N in the Atlantic Ocean: Marine Geol., v. 14, p. 47-72.

Hekinian, R., and Thompson, G., 1976, Comparative geochemistry of volcanics from rift valleys, transform faults and aseismic ridges: Contrib. Mineral. Petrol., v. 57, p. 145-162.

Hobbs, B. E., Means, W. D., and Williams, P. F., 1976, An outline of structural geology: John Wiley and Sons, Inc., 571 p.

Hsu, K. J., 1974, Melanges and their distinction from olistostromes, in Dott, R. H., and Shaver, R. H., Eds., Modern and Ancient Geosynclinal Sedimentation: Soc. Econ. Paleont. and Mineral., Spec. Publ., no. 19, p. 321-333.

Hunting Survey, 1960, Reconnaissance geology of part of West Pakistan: A Colombo Plan Co-operative Project: Government of Canada, Toronto, 550 p.

Hutchison, C. S., 1974, Laboratory Handbook of Petrographic Techniques: John Wiley and Sons, 527 p.

Hyndman, D. W., 1972, Petrology of Igneous and Metamorphic Rocks: McGraw Hill, 533 p.

Jacob, K. H., and Quittmeyer, R. C., 1977, The Makran region of Pakistan and Iran: Trench-arc system with active plate subduction, in Farah, A., and DeJong, K. A., Eds., Geodynamics of Pakistan: Geological Survey of Pakistan, Quetta, 1979, p. 305-318.

Jaques, A. L., Chappell, B. W., and Taylor, S. R., 1978, Geochemistry of LIL-element enriched tholeiites from the Marum ophiolite complex, northern Papua, New Guinea: BMR J. Austral. Geol. and Geophy., v. 3, p. 297-310.

Karig, D. E., 1971, Origin and development of marginal basins in the western Pacific: J. Geophy. Res., v. 76, p. 2542-2561.

Karig, D. E., 1970, Ridges and basins of the Tonga-Kermadec Island arc system: J. Geophy. Res., v. 75, p. 239-254.

Karig, D. E., and Moore, G. F., 1975, Tectonically controlled sedimentation in marginal basins: Earth and Planet. Sci. Lett., v. 26, p. 233-238.

Karson, J., and Dewey, J. F., 1978, Coastal complex, western Newfoundland: An Early Ordovician oceanic fracture zone: Geol. Soc. Amer. Bull., v. 89, p. 1037-1049.

Kay, R. W., and Senechal, R. G., 1976, The rare-earth geochemistry of the Troodos ophiolite complex: Tr. Geophy. Res., v. 81, p.964-969.

Kazmi, A. H., 1979A, The Bibai and Gogai nappes in the Kach-Ziarat area of northeastern Baluchistan, in Farah, A., and DeJong, K. A., Eds., Geodynamics of Pakistan: Geological Survey of Pakistan, Quetta, 1979, p. 333-340.

Kazmi, A. H., 1979B, Active fault systems in Pakistan, in Farah, A., and DeJong, K. A., Eds., Geodynamics of Pakistan: Geological Survey of Pakistan, Quetta, 1979, p. 285-294.

Klootwijk, C. T., Nazirullah, R., DeJong, K. A., and Ahmad, H., 1981, A paleomagnetic reconnaissance of northeastern Baluchistan, Pakistan: J. Geophy. Res., v. 87, no. B1, p. 289-306.

Kuno, H., 1959, Origin of Cenozoic petrographic provinces of Japan and surrounding areas: Bull. Volcanologique, v. 20, p. 37-76.

Laurent, R., 1979, Environment of formation, evolution and emplacement of the Appalachian ophiolites from Quebec, in Abstr. Interntl. Ophiol. Symp. Nicosia, Cyprus, 1-9 April, p. 95.

Laurent, R., 1975, Occurrences and origin of the ophiolites of southern Quebec, northern Appalachians: Can. J. Earth Sci., v. 12, p. 443-455.

Lawrence, R. D., and Yeats, R. S., 1979, Geological reconnaissance of the Chaman fault in Pakistan, in Farah, A., and DeJong, K. A., Eds., Geodynamics of Pakistan: Geological Survey of Pakistan, Quetta, 1979, p. 351-358.

Lensch, G., Mihm, A., and Tehrani, N. A., 1977, Petrography and geology of the ophiolite belt north of Sabzevar/Khorassan, Iran: N. Jb. Miner. Abh., v. 131, no. 2, p. 156-178.

Lewis, A. D., and Bloxam, T. W., 1977, Petrotectonic environments of the Girvan-Ballantrae lavas from rare-earth element distribution: Scott. J. Sci., v. 13, p. 211-222.

Leonov, M. G., 1976, Tectonic conditions in periods of olistostrome development: Geotectonics, Eng. ed., v. 40, p. 169-177.

Liou, J. G., and Ernst, W. G., 1979, Ocean ridge metamorphism of the east Taiwan ophiolite: Contrib. Mineral. Petrol., v. C8, p. 335-348.

Lockwood, J. P., 1972, Possible mechanisms for the emplacement of the Alpine-type serpentinite: Geol. Soc. Amer. Memoir 132, p. 273-287.

Lockwood, J. P., 1971, Sedimentary and gravity slide-emplacement of serpentinite: Geol. Soc. Amer. Bull., v. 82, p. 919-936.

Macdonald, G. A., and Katsura, T., 1964, Chemical composition of Hawaiian lavas: J. Petrol., v. 5, p. 82-133.

Matsuda, T., and Uyeda, S., 1971, On the Pacific-type orogeny and its models: Extension of the paired belts concept and possible origin of marginal seas: Tectonophy, v. 11, p. 5-27.

Matthews, D. H., 1966, The Owen fracture zone and the northern end of the Carlsberg Ridge: Phil. Tr. Roy. Soc. London, v. 259, p. 172-186.

Maxwell, J. C., 1974, Anatomy of an orogen: Geol. Soc. Amer. Bull., v. 85, p. 1195-1204.

Maxwell, J. C., 1973, Ophiolites - old oceanic crust or internal diapirs? in Symp: Ophiolites in the Earth's Crust, Moscow, Acad. Sci., USSR, p. 71-73.

Maxwell, A. E., Herzen, R. P. V., Hsü, K. J., Andrews, J. E., Saito, T., Percival, S. F., Milow, E. D., and Boyce, R. E., 1970, Deep sea drilling in the south Atlantic: Science, v. 168, p. 1047-1059.

Mayere, M. D., Marcoux, J., Parrot, J. F., and Poisson, A., 1977, Modéle d'evolution Mesozoique de la Paleo-Marge Tehysienne au niveau des nappes radiolaritiques et ophiolitiques du Taurus Lycien, d'Antalya et du Baer-Bassit, in Interntl. Symp. on the Structural History of the Mediterranean basins, Split (Yugoslavia), Oct., 1976, Biju-Duval, B., and Montadirt, L., Eds., Editions Technip, Paris, p. 79-94.

McKenzie, D., and Sclater, J. G., 1971, The evolution of the Indian Ocean since the Late Cretaceous: J. Geophy. Res., v. 25, p. 437-528.

McQuillan, H., 1974, Fracture pattern on Kuh-e Asmari anticline, southwest Iran: Amer. Assoc. Petrol. Geol. Bull., v. 58, p. 236-246.

Medlin, J. H., Suhr, N. H., and Bodkin, J. B., 1969, Atomic absorption analysis of slicates employing $LiBO_4$ fusion: Atomic Absorb. Newsletter 8, p. 25-29.

Melson, W. G., and Thompson, G., 1971, Petrology of a transform fault zone and adjacent ridge segments: Phil. Tr. Roy. Soc. London, Ser. A., v. 263, p. 423-442.

Menard, H. W., and Atwater, T. M., 1968, Changes in direction of sea floor spreading: Nature, v. 19, p. 463-467.

Menzies, M., Blanchard, D., and Xenophontes, C., 1980, Genesis of the Smartville arc-ophiolite, Sierra Nevada foothills, California: Amer. J. Sci., v. 280-A, p. 329-344.

Middlemost, E. A. K., 1975, The basalt clan: Earth Sci. Rev., v. 11, p. 337-364.

Miyashiro, A., 1978, Nature of alkalic volcanic rock series: Contrib. Mineral. Petrol., v. 66, p. 91-104.

Miyashiro, A., 1975(A), Origin of the Troodos and other ophiolites: A reply to Hynes: Earth and Planet. Sci. Lett., v. 25, p. 217-222.

Miyashiro, A., 1975(B), Classification, characteristics, and origin of ophiolites: J. Geol., v. 83, p. 249-281.

Miyashiro, A., 1973, The Troodos ophiolitic complex was probably formed in an island arc: Earth and Planet. Sci. Lett., v. 19, p. 218-224.

Mohsin, S. I., and Sarwar, G., 1974, Geology of Dilbund fluorite deposits: Geonews, v. 4, p. 24-30.

Moiseyev, N., 1970, Late serpentinite movements in the California Coast Ranges: New evidence and its implications: Geol. Soc. Amer. Bull., v. 81, p. 1721-1732.

Moores, E. M., 1973, Geotectonic significance of ultramafic rocks: Earth Sci. Rev., v. 9, p. 241-258.

Moores, E. M., and Jackson, E. D., 1974, Ophiolites and oceanic crust: Nature, v. 250, p. 136-138.

Moores, E. M., and Vine, F. J., 1971, The Troodos massif, Cyprus and other ophiolites as oceanic crust: evaluation and implications: Phils. Trans. Roy. Soc., v. A268, p. 443-466.

Muratov, M. V., 1977, The Origin of Continents and Ocean Basins: Mir Publishers, Moscow, 191 p.

Narain, H., Kaila, K. L., and Verma, R. K., 1968, Continental margins of India: Can. J. Earth Sci., v. 5, p. 1051-1065.

Nicols, G. D., and Islam, M. R., 1971, Geochemical investigations of basalt and associated rocks from the ocean floor and their implications: Phil. Tr. Roy. Soc. London, v. 268A, p. 469-486.

Norton, I. O., and Sclater, J. G., 1979, A model for the evolution of the Indian Ocean and the breakup of Gondwanaland: J. Geophy. Res., v. 84, no. 12, p. 6803-6830.

Pamic, J., 1974, Middle Triassic spilite-keratophyre association of the Dinarides and its position in Alpine magmatic-tectonic cycle, in Spilites and Spilitic Rocks, Amstutz, G. C., Ed.: Springer-Verlag, p. 161-174.

Patwardhan, A. M., and Bhandari, 1974, Petrogenesis of spilites occurring at Mandi, Himachal Pradesh, India, in Spilites and Spilitic Rocks, Amstutz, G. C., Ed.: Interntl. Union Geol. Sciences Ser. A., no. 4: Springer-Verlag, p. 175-190.

Pearce, J. A., in press, Geochemical evidence for the genesis and eruptive setting of the Tethyan ophiolites: preprint Proc. Interntl. Ophiol. Symp., Nicosia, Cyprus, 1979.

Pearce, J. A., 1976, Statistical analysis of major element patterns in basalts: J. Petrol., v. 17, p. 15-43.

Pearce, J. A., 1975, Basalt geochemistry used to indicate past tectonic environments on Cyprus: Tectonophy., v. 25, p. 41-67.

Pearce, J. A., and Caan, J. R., 1973, Tectonic setting of basic igneous rocks determined using trace element analysis: Earth and Planet. Sci. Lett., v. 19, p. 290-300.

Pearce, J. A., and Gale, 1977, Identification of ore deposition environments from trace element geochemistry of associated igneous rock hosts, in Volcanic Processes in Ore Genesis: Spec. Pub. Geol. Soc. London, no. 7, p. 14-24.

Pearce, T. H., Gorman, B. E., and Birkett, T. C., 1975, The TiO_2-K_2O-P_2O_5 diagram: A method of discriminating oceanic and non-oceanic basalts: Earth and Planet. Sci. Lett., v. 24, p. 412-426.

Pearce, T. H., Gorman, B. E., and Birkett, T. C., 1976, Tectonic setting inferred from chemistry of Cenozoic and Archean volcanics: EOS, Tr. Amer. Geophy. Union, v. 57, p. 343-344.

Pearce, T. H. Gorman, B. E., and Birkett, T. C., 1977, The relationship between major element chemistry and tectonic environment of basic and intermediate volcanic rocks: Earth and Planet. Sci. Lett., v. 26, p. 121-132.

Pennington, W. D., 1979, A summary of field and seismic observations of the Pattan earthquake, 28 December, 1974, in Farah, A., and DeJong, K. A., Eds., Geodynamics of Pakistan: Geological Survey of Pakistan, Quetta, 1979, p. 143-148.

Powell, C. M., 1979, A speculative tectonic history of Pakistan and surroundings: Some constraints from the Indian Ocean, in Farah, A., and DeJong, K. A., Eds., Geodynamics of Pakistan: Geological Survey of Pakistan, Quetta, 1979, p. 5-24.

Prinz, M., Keil, K., Green, J. A., Reid, A. M., Bonatti, E., and Honnorez, J., 1976, Ultramafic and mafic dredge samples from the equatorial Mid-Atlantic Ridge and fracture zone: J. Geophy. Res., v. 81, no.23, p. 4087-4103.

Quittmeyer, R. C., Farah, A., and Jacob, K. H., 1979, The seismicity of Pakistan and its relation to surface faults, in Farah, A., and DeJong, K. A., Eds., Geodynamics of Pakistan: Geological Survey of Pakistan, Quetta, 1979, p. 271-284.

Raju, A. T. R., Chaube, A. N., and Chaudhary, L. R., 1972, Deccan traps and the geologic framework of the Cambay Basin: Bull. Volcanologique, v. 35, no. 3, p. 521-538.

Rao, D. G., 1976, A preliminary interpretation of two marine gravity profiles on the continental shelf margin west of Bombay, India: Marine Geol., v. 22, p. M31-M35.

Ravenne, C., de Broin, C. E., Dupont, J., Lapouille, A., and Launay, J., 1977A, New Caledonia Basin-Fairway Ridge: Structural and sedimentary study, in Int. Symp. Geodyn. in SW Pacific, New Caledonia, 1976, Technip, Paris, p. 145-154.

Ravenne, C., Pascal, G., Dobois, J., Dugas, F., and Montadert, L., 1977B, Model of a young intra-oceanic arc: New Hebrides Island-arc, in Int. S-mp. Geodyn. SW Pacific, New Caledonia, 1976, Editions Technip, Paris, p. 63-78.

Reinhardt, B., 1974, The relationships between spilites and other members of the Oman Mountains ophiolite suite, in Spilites and Spilitic Rocks, Amstutz, G. C., Ed.: Springer-Verlag, p. 207-228.

Rona, P. A., Harbison, R. N., Bassinger, B. G., Scott, R. B., and Nalwalk, A. J., 1976, Tectonic fabric and hydrothermal activity of Mid-Atlantic Ridge crest (Lat. 26°N): Geol. Soc. Amer. Bull., v. 87, p. 661-674.

Ridley, W. I., Dalziel, I. W. D., Elthon, D., and Allen, R., 1979, The evolution of the Rocas Verdes ophiolite complex, a Mesozoic back-arc basin in southern Chile, in Abstr. Int. Ophiol. Symp. Nicosia, Cyprus, p. 66-67.

Robinson, P. T., Flower, M. F. J., Swanson, D. A., and Standigel, H., 1980, Lithology and eruptive stratigraphy of Cretaceous oceanic crust, Western Atlantic Ocean: Initial Reports DSDP, v. 51-53, Pt. 2, Legs 51-53, p. 1535-1546.

Rupke, N. A., 1976, Large-scale slumping in a flysch basin, southwestern Pyrenees: J. Geol. Soc. London, v. 132, p. 121-130.

Saleeby, J., 1979, Kaweah serpentinite melange, southwest Sierra Nevada foothills, California: Geol. Soc. Amer. Bull., v. 90, p. 29-46.

Saleeby, J., 1978, Kings River ophiolite, southwest Sierra Nevada foothills, California: Geol. Soc. Amer. Bull., v. 89, p. 617-636.

Saleeby, J., 1977, Fracture zone tectonics, continental margin fragmentation, and emplacement of the Kings-Kaweah ophiolite belt, southwest Sierra Nevada, California, in North American Ophiolites: Bull. 195, Dept. Geol. Miner. Indust., p. 141-159.

Sarwar, G., and DeJong, K. A., 1979, Arcs, orocline, syntaxes: the curvatures of mountain belts in Pakistan, in Farah, A., and DeJong, K. A., Eds., Geodynamics of Pakistan: Geological Survey of Pakistan, Quetta, 1979, p. 341-350.

Saunders, A. D., Tarney, J., and Marsh, N. G., (in press), Ophiolites as oceanic crust or marginal basin crust: a geochemical approach: Preprint, Proc. Int. Ophiol. Symp., Nicosia, Cyprus, 1979.

Saunders, A. D., Tarney, J., Stern, C. R., Dalziel, I. W. D., 1979, Geochemistry of Mesozoic marginal basin floor igneous rocks from southern Chile: J. Geol. Soc. Amer. Bull., v. 90, p. 237-258.

Schilling, J. G., 1975, Azore mantle blob - Rare earth evidence: Earth and Planet. Sci. Lett., v. 25, p. 103-115.

Schwarzer, R. R., and Rogers, J. J. W., 1974, A worldwide comparison of alkali olivine basalts and their differentiation trends: Earth and Planet. Sci. Lett., v. 23, p. 286-296.

Shah, S. M. I., 1977, Stratigraphy of Pakistan: Mems. Geol. Surv. Pakistan, v. 12, 138 p.

Shearman, D. J., 1976, The geological evolution of southern Iran: The report of the Iranian Makran Expedition: The Geogr. Journal, v. 142, Pt. 3, p. 393-413.

Shibata, T., DeLong, S. E., and Walker, D., 1979, Abyssal tholeiites from the oceanographer fracture zone: Contrib. Mineral. Petrol., v. 70, p. 89-102.

Sigurdsson, H., Sparks, R. S. J., Carey, S. N., and Huang, T. C., 1980, Volcanogenic sedimentation in the Lesser Antilles arc: J. Geol., v. 88, p. 523-540.

Sillitoe, R. H., 1975, Metallogenic evolution of a collisional mountain belt in Pakistan: a preliminary analysis, Rocs. Geol. Surv. Pakistan, v. 34, 16 p.

Simonian, K. O., and Gass, I. G., 1978, Arakapas fault belt, Cyprus: A fossil transform fault: Geol. Soc. Amer. Bull., v. 89, p. 1220-1230.

Sinton, J. M., 1980, Petrology and evolution of the Red mountain ophiolitic complex, New Zealand: Amer. J. Sci., v. 280-A, p. 298-328.

Smewing, J. D., 1979, An upper Cretaceous ridge-transform intersection in the Oman ophiolite, in Abstr. Int. Ophiol. Symp. Nicosia, Cyprus, p. 73-74.

Smewing, J. D., Simonian, K. O., Elboushi, I. M., and Gass, I. G., 1977, Mineralized fault zone parallel to the Oman ophiolite spreading axis: Geology, v. 5, p. 534-538.

Smith, R. E., 1974, The production of spilitic lithologies by burial metamorphism of flood basalts from the Canadian Keweenawan, Lake Superior, in Spilites and Spilitic Rocks, Amstutz, G. C., Ed.: Springer-Verlag, p. 403-416.

Smith, G. W., Howell, D. G., and Ingersoll, R. V., 1979, Late Cretaceous trench-slope basins of central California: Geology, v. 7, p. 303-306.

Sorensen, H., 1974, Glossary of alkaline and related rocks, in Sorensen, H., Ed., The Alkaline Rocks: John Wiley and Sons, p. 558-577.

Stocklin, J., 1977, Structural correlation of the Alpine range between Iran and central Asia: Mem. h. Ser. Soc. Geol. Fr., no. 8, p. 333-353.

Sturt, B. A., 1979, The Karmoy ophiolite, southwest Norway: Geology, v. 7, p. 316-320.

Spooner, E. T. C., and Fyfe, W. S., 1973, Sub-sea floor metamorphism, heat and mass transfer: Contr. Mineral. Petrol., v. 42, p. 287-304.

Subbaro, K. V., Kempe, D. R. C., Reddy, V. V., Reddy, G. R., and Hekinian, R., 1977, Review of the geochemistry of Indian and other oceanic rocks, in Origin and Distribution of the Elements, Ahrens, L. H., Ed.: Pergamon Press, Oxford, p. 367-400.

Suen, C. J., Frey, F. A., and Malpas, J., 1979, Bay of islands ophiolite suite, Newfoundland: Petrological and geochemical characteristics with emphasis on REE geochemistry: Earth and Planet. Sci. Lett., v. 45, no. 2, p. 337-348.

Sukheswala, R. N., 1974, Gradation of tholeiitic Deccan basalt into spilite, Bombay, India, in Spilites and Spilitic Rocks, Amstutz, G. C., Ed.: Springer-Verlag, p. 229-252.

Sun, S., Nesbitt, R. W., and Sharaskin, A. Y., 1979, Geochemical characteristics of mid-ocean ridge basalts: Earth and Planet. Sci. Lett., v. 44, p. 119-138.

Sykes, L. R., 1967, Mechanism of earthquakes and nature of faulting on the mid-ocean ridges: J. Geophy. Res., v. 72, p. 2131-2153.

Sykes, L. R., and Sbar, M. L., 1973, Intraplate earthquakes, lithospheric stresses and the driving mechanisms of plate tectonics: Nature, v. 245, p. 298-302.

Thayer, T. P., Lipin, B. R., and Eugin, T., 1979, Are podiform chromite deposits in tectonite harzburgite introduced or indigenous? in Abstr. Interntl. Ophio. Symp. Nicosia, Cyprus, 1979, p. 145-146.

Thompson, G., and Melson, W. G., 1972, The petrology of oceanic crust across fracture zones in the Atlantic Ocean: Evidence of a new kind of sea-floor spreading: J. Geol., v. 80, p. 526-538.

Travis, R. B., 1955, Classification of rocks: Quarterly of the Colorado School of Mines, v. 50, no. 1, 98 p.

Tysdal, R. G., Case, J. E., Winkler, G. R., and Clark, S. H. B., 1977, Sheeted dikes, gabbro, and pillow basalt in flysch of coastal southern Alaska: Geology, v. 5, p. 377-383.

Upadhyay, H. D., and Neale, E. R. W., 1979, On the tectonic regimes of ophiolite genesis: Earth and Planet. Sci. Lett., v. 43, p. 93-102.

U. S. National Report, 1975-1978, 17th General Assembly, International Union Geodesy and Geophy., Canberra, Australia, Dec. 2-15, 1979: Pub. Amer. Geophy. Union, 1980.

Vallance, T. G., 1974, Pyroxenes and the basalt-spilite relation, in Spilites and Spilitic Rocks, Amstutz, G. C., Ed.: Springer-Verlag, p. 59-70.

Van Andel, T. H., Phillips, J. D., and Von Herzen, R. P., 1969, Rifting origin for the Vema fracture zone in the North Atlantic: Earth and Planet. Sci. Lett., v. 5, p. 293-300.

Vance, J. A., Dungan, M. A., Blanchard, D. P., and Rhodes, T. M., 1980, Tectonic setting and trace element geochemistry of Mesozoic ophiolitic rocks in western Washington: Amer. J. Sci., v. 280-A, p. 359-388.

Varet, J., and Choukroune, P., 1979, Study of tectonic deformation in sediments interlayered with the basalts from hole 412A, IPOD Leg 49, in Initial Rept. DSDP, v. 49, p. 427-431.

Venturelli, G., Capedri, S., Thorpe, R. S., and Potts, P. J., 1979, Rare-earth and other element distribution in some ophiolitic metabasalts of Corsica, western Mediterranean: Chem. Geol., v. 24, p. 339-353.

Vredenburg, E. W., 1909, Report on the geology of Sarwan, Jhalwan, Makran, and the State of Las Bela: India Geol. Surv. Recs., v. 38, p. 182-215.

Wadia, D. N., 1953, Geology of India: Macmillan and Co., Ltd., London, 531 p.

Wedepohl, K. H., 1978, Handbook of Geochemistry, v. 2/5, Springer-Verlag.

White, H. J., 1981, The stratigraphy of the southern Pab Range, Pakistan: Unpublished Ph.D. Thesis, Iowa State University, 170 p.

White, R. S., 1979, Deformation of the Makran continental margin, in Farah, A., and DeJong, K. A., Eds., Geodynamics of Pakistan: Geological Survey of Pakistan, Quetta, 1979, p. 295-304.

Whitmarsh, R. B., 1974, Summary of general features of Arabian Sea and Red Sea Cenozoic history based on Leg 23 cores, in Initial Repts. DSDP, v. XXIII, p. 1115-1123.

Whitten, E. H. T., 1966, Structural geology of folded rocks: Rand McNally and Co., Chicago, 663 p.

Williams, M. D., 1959, Stratigraphy of the lower Indus basin, West Pakistan: World Petrol. Congr., 5th, New York, Proc., Sec. 1, Paper 19, p. 377-390.

Williams, H., Turner, F. J., and Gilbert, C. M., 1954, Petrography: W. H. Freeman and Co., San Francisco, 406 p.

Wilkinson, J. F. G., 1967, The petrography of basaltic rocks, in Hess, H. H., Ed., Basalts, v. 1: Interscience Publ., p. 163-214.

Wilson, J. T., 1965, A new class of faults and their bearing on continental drift: Nature, v. 207, p. 343-347.

Wilson, R. C. L., and Williams, C. A., 1979, Oceanic transform structures and the development of Atlantic continental margin sedimentary basins - a review: J. Geol. Soc. London, v. 136, p. 311-320.

Wood, D. A., Gibson, I. L., and Thompson, R. N., 1976, Elemental mobility during zeolite facies metamorphism of the Tertiary basalts of eastern Iceland: Contrib. Mineral. Petrol., v. 55, p. 241-254.

Wood, D. A., Joron, J. L., and Treuil, M., 1979, A reappraisal of the use of trace-elements to classify and discriminate between magma series erupted in different tectonic settings: Earth and Planet. Sci. Lett., v. 45, p. 325-336.

APPENDIX 1

DEFINITIONS

Ophiolite:

According to its current definition (Penrose Ophiolite Symposium, Geotimes, Dec., 1972), an ophiolite is a distinctive pseudostratigraphic assemblage of ultramafic and mafic rocks, a complete assemblage being as shown by the following sequence:

Basic volcanics (commonly pillowed)

. . . merging into . . .

Sheeted dike complex

Trondjemites

Gabbros

Olivine gabbros (layered cumulates)

Ultramafic rocks (commonly serpentinized)

Associated sedimentary rocks typically include radiolarian chert, shale and limestone. They are generally considered to be overlying the pillow lavas and are excluded from the definition of ophiolites (Penrose Conference, 1972; Moores, 1973; Coleman, 1977; Gass, 1977). In several ophiolites, however, sedimentary rocks are interlayered with the pillow lavas, e.g., the Eastern Papus ophiolite, New Guinea (Coleman, 1977), Karmoy ophiolite, Norway (Sturt et al., 1979), upper lavas of Semail ophiolite, Oman (Glennie et al., 1974), Antalyan ophiolite, southern Turkey (Mayere et al., 1977), Troodos upper lavas, Cyprus (Moores and Vine, 1971)

and some Iranian ophiolites (Lensch et al., 1977). The Bela ophiolites also belong to this category.

A complete ophiolite sequence may not be present or it may be dismembered and metamorphosed (Coleman, 1977, p. 7).

Spilite (occurrence and origin):

Spilites are analogous to basalts in mode of occurrence and broad fabric elements, but differ from them in consisting largely of green schist facies minerals such as sodic plagioclase (albite-oligoclase), chlorite, epidote, pumpellyite, prehnite, carbonates, quartz, Fe-Cu oxides and sulphides (Amstutz, 1968; Fiala, 1974; Vallance, 1974). Common mineral assemblages are

Albite + Clinopyroxene + Chlorite

Albite + Chlorite

Albite + Chlorite + Epidote ± Calcite

Albite + Chlorite + Pumpellyite + Calcite

Albite + Calcite

Albite + Amphibole + Epidote

Albite + Amphibole + Chlorite

Like basalts, spilites occur as lava flows and shallow intrusives (Fiala, 1974). They are known from the continental flood basalts (Smith, 1974; Patwardhan and Bhandari, 1974), and frequently occur in geosynclinal piles. A characteristic association is spilite-keratophyre-quartz Keratophyre-serpentinite (Hyndman, 1972). Several ophiolites include spilitic rocks where they may occur with other basaltic rocks (e.g., Reinhardt, 1974; Glennie et al., 1974; Coleman, 1977).

Compared to basalts, spilites are generally high in H_2O, Na_2O, Fe^{+3} and low in K_2O, MgO and CaO (Fiala, 1974; Battey, 1974).

Origin:

Due to their typical igneous textures but mineralogy resembling that of green schist facies metamorphic rocks, the origin of spilitic rocks has been a subject of debate for over 150 years. Amstutz (1968, 1974) has listed eight different theories that have been advanced to explain the origin of spilites. These theories fall in two categories briefly outlined as follows:

A. Theory of Primary Nature of Spilites. - According to this view, spilites are igneous rocks, just like basalts, and were crystallized from hydrous silica and alkali rich magmas that may have evolved (fractionated) from other basaltic magmas (e.g., tholeiitic, Amstutz and Patwardham, 1974; Reinhardt, 1974; Sukheswala, 1974; and several others listed in Amstutz, 1968, 1974). Reinhardt (1974) believes that in the case of the Oman ophiolites, high oxygen fugacity encouraged the formation of Fe-Ti oxides at the expense of silicates (Fe-rich olivine and pyroxene), and thus caused silica enrichment in the residual melt. Water sources may be either endogenic or exogenic. Albite is explained as due to Na enrichment caused by earlier removal of Ca-feldspar or its continuous reaction. Excess Ca in residual liquids explains the presence of calcite and zeolites (Sukheswala, 1974). Clinopyroxene survives (metastably) but gives way to hydrous phases such as chlorite at lower temperature (Sukheswala, 1974). Some of the major arguments proposed in favor of a primary origin for spilites are:

1) Preservation of magmatic fabric, e.g., fluidic textures, ophitic intergrowths between albite, clinopyroxene, opaques, and chlorite, chlorite inclusions in albite etc. (Amstutz and Patwardhan, 1974; Patwardhan and Bhandari, 1974; Sukheswala, 1974).

2) Spilites transitional to rocks that show clear secondary features (Amstutz and Patwardhan, 1974).

3) Presence of magmatic carbonate as indicated by isotopic study (Amstutz and Patwardhan, 1974).

4) No trace of albitization of calcic plagioclase, and spilites associated with normal subalkaline rocks, both having similar textures (Pamic, 1974; Sukheswala, 1974).

5) Presence of primary coloform chlorite with albite and chlorite (Patwardhan and Bhandari, 1974).

6) Field evidence suggesting derivation of spilitic magma by differentiation of normal basaltic magma (Reinhardt, 1974).

B. Theory of Secondary Nature of Spilites. - Spilites are produced by subsolidus adjustment of basaltic material (e.g., tholeiites) under hydrous conditions. Emphasis is placed on the various deuteric autometasomatic changes or Na-metasomatism due to reaction with sea water (trapped or circulating) during subsequent low grade burial metamorphism (Amstutz, 1968, 1974; Carmaichael et al., 1974; Coleman, 1979). Spilitic rocks are widespread within the upper parts of several ophiolites where they show a vertical metamorphic facies zonation from zeolite facies on top to green schist-lower amphibolite facies at the bottom (Dewey and Bird, 1970, 1971; Gass and Smewing, 1973; Coleman, 1977). Such metamorphism affects the pillow lavas, sheeted dikes, and upper parts of gabbroic rocks. Under

the assumption that most ophiolites form at a spreading center under a high heat flow, the spilitic metamorphism results from hot circulating sea water within the upper parts of the newly formed oceanic crust (Spooner and Fyfe, 1973; Coleman, 1977). The process transforms the original basalt minerals of plagioclase, clinopyroxene and olivine to secondary minerals such as zeolites, epidote, chlorite, albite, actinolite, sphene, quartz, calcite etc. (Liou and Ernst, 1979).

Some of the major arguments in favor of a secondary origin for the spilitic rocks are:

1) Presence of metamorphic mineral assemblages. According to Coombs (1974) the stability fields of spilitic minerals (such as zeolites, prehnite, pumpellyite etc.) are well below the crystallization temperature of basalts.

2) Pseudomorphs (e.g., of chlorite and epidote after pyroxene, olivine and feldspar) and other textural evidence for replacement (e.g., relict calcic plagioclase, and veinlets of secondary minerals) in spilites (Battey, 1974).

3) The amount of water locked in the hydroxyl-bearing minerals of spilites far exceeds that retained by rapidly cooling basaltic lavas and shallow intrusives. Thus the water involved is not magmatic (Coombs, 1974).

4) Spilite mineral assemblages may be present in the sedimentary rocks associated with the spilites where they can be ascribed to burial metamorphism (Coombs, 1974).

5) Partial to complete spilitization of basaltic lava flows has been observed in the Canadian Keweenawan Series of the Lake Superior (Smith, 1974).

6) If the spilites crystallize from a melt at low temperature (± 350°C) to allow the formation of the hydroxyl-bearing minerals, their textures should not mimic so closely that formed in normal basalts at 1100°C (Caan, 1969).

7) Spilites are rare in young (Cenozoic) lavas, i.e., lavas that have not been buried (Battey, 1974).

APPENDIX 2

Petrographic Description of the Mor Intrusives

Altered Limburgite(?)

Sample No.: 77-SA-4

Structure: Dike in Shirinab Formation

Location: 1, Figure 6.

Color: Light greenish gray

Texture: Fine-grained with a few pseudomorphs of (serpentine + chlorite + calcite) after (olivine-pyroxene?) set in a groundmass consisting of carbonate, clay mineral/serpentine and opaque minerals.

Minerals: serpentine - pseudomorphs (up to 4-5 mm) after (olivine + pyroxene) as judged by subhedral-euhedral crystal forms; also in the groundmass.

Calcite + chlorite - replace phenocrysts, groundmass and form veinlets

Biotite - brown, flaky, highly pleochroic, occurs in groundmass.

Opaque minerals - (magnetite ?) occurs as dust, needles and irregularly shaped grains. Serpentine pseudomorphs after olivine are choked with opaque dust.

Zeolite(?) - in cavities.

Relative Proportion: Carbonate > opaque minerals > serpentine

Sample No.: 77-SA-4A.

Structure: Dike in Shirinab Formation

Location: 1, Figure 3.

Color: Light greenish gray

Texture: Fine grained; equigranular.

Minerals: Highly altered rock, similar to 77-SA-4 in mineralogy, and consists of carbonate, clay minerals, serpentinite (pseudomorphous after olivine + pyroxene?), black opaque minerals and some brown pleochroic biotite.

Altered Porphyritic Limburgite

Sample No.: 77-SA-6

Structure: Dike in Shirinab Formation, western flank of Mor Range

Location: 2, Figure 3.

Color: Gray

Texture: Glomeroporphyritic with relatively fresh phenocrysts of clinopyroxene and altered olivine set in a fine-grained groundmass of glass, carbonate and mafic minerals.

Minerals: Titanaugite - Brownish subhedral phenocrysts (up to 4-5 mm, average ±1 mm); some show hourglass structure and anomalous blue interference color; highly fractured; also occurs in groundmass as small tabular crystals.

Olivine pseudomorphs - subhedral-euhedral crystals with typical olivine-like shape and fractures;

totally replaced by a mixture of serpentine ± calcite, talc and clay minerals.

Biotite - Brown-reddish brown flakes in groundmass; highly pleochroic.

Opaque minerals - magnetite; occurs as dust in groundmass; fractures and edges of olivine pseudomorphs are lined with red iron oxide.

Felspathoid(?) - suspected in groundmass.

Glass - some in groundmass; amorphous silica and calcite form some fracture fillings.

Relative Proportion: Pyroxene > olivine pseudomorphs > biotite > opaque minerals

Altered Basalt

Sample No.: 77-SA-24

Structure: Dike in Shirinab Formation

Location: 6, Figure 3.

Color: Greenish gray

Texture: Holocrystalline, fine grained.

Minerals: Feldspar - brownish, cloudy and tightly interwoven laths; twinned (albite, carlsbad); extinction angle on some albite twins (± 10°) suggests presence of albite; largely replaced by calcite and some clay minerals.

Olivine and pyroxene(?) - serpentine ± calcite pseudomorphs; some with olivine-like fractures.

Calcite - replaces feldspar and forms some cavity fillings.

Quartz - interstitial to feldspar laths, also forms some cavity fillings.

Apatite - tiny needles in feldspar and quartz-filled cavities.

Opaque minerals - reddish brown hematite; forms grains, needles and skeletal masks; some gray translucent high relief material is probably sphene.

Relative Proportion: carbonatized feldspar > opaque minerals > serpentine > quartz > apatite

Altered Plagioclase Basalt

Sample No.: SA-77-26

Structure: Sill in Shirinab Formation

Location: 7, Figure 3.

Color: grayish green

Texture: Fine grained; porphyritic; with altered feldspar phenocrysts set in a mafic groundmass.

Minerals: Plagioclase - occurs as phenocrysts and in groundmass; the phenocrysts are twinned (albite and some carlsbad type) laths 1-4 mm in length. Extinction angle on albite twins indicates the presence of oligoclase-andesine; however, some zoned phenocrysts are present. Feldspar microliths in groundmass are apparently similar to the phenocrysts. All feldspar is more or less sericitized and chloritized.

Chlorite - green, replaces feldspar.

Quartz - tiny round grains in groundmass; accessory.

Opaque minerals - magnetite occurs as anhedral grains, needles, irregularly shape masses (up to 1 mm) and dust in groundmass; some hematite also present.

Calcite - forms tiny veinlets.

Relative Proportion: Plagioclase > chlorite > magnetite > quartz

Altered Porphyritic Basalt

Sample No.: SR-5-79

Structure: Sill in Sembar Formation

Location: 21, Figure 4B.

Color: Light greenish gray

Texture: Porphyritic, with pseudomorphs of carbonate/chlorite after plagioclase and pyroxene/olivine(?) set in a groundmass of calcite and opaque minerals.

Minerals: Calcite - patchy and mosaic calcite (± chlorite) replaces phenocrysts (up to 8 mm) of subhedral-euhedral zoned plagioclase and groundmass. Calcite pseudomorphs rimmed by opaque dust. Some calcite pseudomorphs have opaque/chlorite inclusions. These were probably formed after olivine or, less likely, pyroxene, as suggested by the crystal shapes. Calcite also forms some veinlets and fills amygdules.

Chlorite - replaces phenocrysts with calcite.

Opaque minerals (Magnetite?) - occurs as dust, and needles in groundmass.

Glass - some in groundmass.

Relative Proportion: Calcite > chlorite > opaque minerals > glass

Porphyritic Plagioclase Basalt

Sample No.: SR-9-79

Structure: Dike in the matrix of Kanar Melange

Location: 21, Figure 4B.

Color: Greenish gray

Texture: Porphyritic, with phenocrysts of plagioclase and altered mafic minerals set in a glassy groundmass.

Minerals: Plagioclase - subhedral-euhedral laths, twinned (albite type); extinction (13-17°) on albite twins indicates presence of albite; some phenocrysts are partly replaced by chlorite ± calcite.

Chlorite - green; replaces phenocrysts of feldspar and some mafic minerals (olivine-pyroxene); opaque dust occurs as rims and inclusions in chlorite.

Calcite - replaces feldspar and apatite; also forms veinlets.

Apatite - euhedral laths; partly replaced by calcite.

Opaque minerals (magnetite) - occurs as dust and small grains and skeletal masses in groundmass, some associate with chlorite; some gray translucent material is probably leucoxene.

Altered Porphyritic Basalt

Sample No.: SR-11-79

Structure: Sill in Sembar Formation

Location: 24, Figure 4B.

Color: Greenish gray

Texture: Porphyritic, with large (up to 5 mm) calcite pseudomorphs after pyroxene(?) and plagioclase phenocrysts (± 1 mm) set in a fine grained groundmass of plagioclase microliths, patchy calcite and opaque material.

Minerals: Calcite - cloudy, brownish calcite pseudomorphs subhedral-euhedral pyroxene(?) and some plagioclase. Also occurs as veinlets, specks and patchy replacement in groundmass.

Chlorite - occurs with calcite in and around pseudomorphs after pyroxene(?).

Plagioclase - occasional zoned laths as phenocrysts and as a network of microliths in groundmass; shows albite type twins, partly replaced by calcite.

Opaque minerals (hematite) - reddish with translucent edges; occurs as dust in and around calcite pseudomorphs and as grains, needles and irregularly shaped masses in the groundmass.

Relative Proportions: Carbonate > chlorite > feldspar > opaque minerals

Altered Basalt (Greenstone)

Sample No.: SR-56-79

Structure: Sill in Sembar Formation.

Location: 45, Figure 4B.

Color: Brownish green

Texture: A compact mass of chlorite and chlorite-calcite mixture.

Minerals: Chlorite - light green, light pale-greenish gray, sheaf-like, radiating or plumose aggregates.

Unidentified - small tabular, high relief, high birefringence (3° colors); extinction uneven or does not extinct.

Biotite - brown, accessory.

Calcite - irregular areas associated with chlorite; also forms veinlets.

Opaque minerals (magnetite) - occurs as dust in chlorite and small equant to irregularly shaped grains in groundmass.

Relative Proportion: Chlorite > unidentifed mineral > calcite > opaque minerals > biotite

Altered Porphyritic Basalt

Sample No.: SR-71-79

Structure: Sill in Sembar Formation

Location: 50, Figure 4B.

Color: Grayish green

Texture: Porphyritic, with phenocrysts of plagioclase (up to 2 mm) and chlorite patches (pseudomorphs after pyroxene?) set in a fine-grained groundmass of plagioclase microliths, chlorite, calcite, opaque minerals and glass.

Minerals: Plagioclase - subhedral-euhedral laths; cloudy, partly replaced by patchy calcite, twinned (albite type), extinction on twins (10°-14°) indicates presence of albite; however, some zoned phenocrysts are present.

Chlorite - green-brown, occurs as patches and irregular replacement of groundmass; also forms veinlets.

Calcite - patchy-mosaic type; occurs as partial replacement of feldspar and as veinlets.

Opaque minerals (magnetite) - occurs as dust, needles, grains in groundmass; also as dust in chlorite; some brownish material may be hematite.

Relative Proportion: Plagioclase > calcite > chlorite > opaque minerals

Porphyritic Basalt

Sample No.: SR-82-79

Structure: Dike in Sembar Formation

Location: 55, Figure 4B.

Color: Greenish gray

Texture: Porphyritic with phenocrysts of clinopyroxene (up to 6 mm long) and plagioclase (up to 2 mm long) set in a groundmass

of plagioclase microliths, chlorite, calcite and opaque minerals.

Minerals: Plagioclase - subhedral-euhedral laths of rather irregular outline; twinned (albite, carlsbad type); some zoned; groundmass feldspar is acicular-feathery and also twinned; partly replaced by calcite.

Clinopyroxene - subhedral-euhedral, fractured grains; chloritized along fractures and rimmed by opaque minerals; some partly replaced by calcite; zoned.

Calcite - clear-brownish, mosaic type; pseudomorphs some pyroxene and replaces groundmass feldspar in patches.

Chlorite - green; fills fractures in pyroxene; fills interstices between feldspar laths in groundmass and also occurs with calcite.

Opaque minerals (magnetite) - tiny to large, equant to irregularly shaped grains in groundmass, some leucoxene.

Apatite(?) - accessory, with chlorite.

Relative Proportion: Feldspar > chlorite > calcite > opaque > pyroxene

Greenstone

Sample No.: SR-95-79

Structure: Dike in Sembar Formation

Location: 59, Figure 4B.

Color: Grayish green

Texture: Porphyritic, with altered phenocrysts of pyroxene and feldspar(?) set in a dense groundmass of chlorite, calcite, biotite and opaque minerals.

Minerals: Calcite-chlorite - replace phenocrysts; calcite also forms veinlets.

Biotite - brown, strongly pleochroic flakes in groundmass associated with opaque material; partly replaced by chlorite.

Opaque minerals (magnetite) - occurs as dust, needles irregular-skeletal masses in groundmass; also as dust in and around phenocrysts.

Relative Proportion: Calcite > chlorite > opaque minerals > biotite

APPENDIX 3

A. Petrograhpic Summary of the Minerals Forming the Porali Conglomerate Volcanic Clasts

Clinopyroxene (Titanaugite): neutral-brownish or purplish, fractured; occurs both as subhedral-euhedral phenocrysts (1-7 mm) and in groundmass; phenocrysts are zoned (concentric and less commonly hourglass structure); twinned and may include acicular apatite; may be fresh or partly replaced by chlorite along fractures, occasionally partly replaced by brown hornblende and biotite. Sometimes phenocrysts are replaced by a mixture of chlorite, biotite, calcite and opaques. The groundmass pyroxene is also similar in color and appearance and occurs as tiny subhedral-euhedral granules; it may be resorbed in glass. The groundmass and phenocryst pyroxenes both show a characteristic purplish or brownish blue interference color which is anomalous. This indicates that they are probably similar in composition. Optical data (Bxl^{+}, $c\Lambda z$ angles) and color indicates the presence of titanaugite.

Plagioclase (albite-andesite?): The plagioclase may also occur both as phenocrysts and in groundmass; however, no feldspar was seen in 4 out of 9 samples examined. The phenocrysts are anhedral to euhedral; cloudly, twinned (albite, carlsbad and pericline) and are more or less replaced by chlorite and calcite. Calcite may actually be seen as pseudomorphs after plagioclase. In groundmass the plagio-

clase occurs as tiny laths and may show albite twins. Sodic plagioclase (albite-oligoclase) was also noted in amygdules and veinlets; it occurs as clear-cloudy radiating laths with sharp albite and carlsbad-type twins and is associated with chlorite and some calcite. Feldspar composition was optically determined.

Calcite: occurs as partial replacement of pyroxene; it also replaces plagioclase and may completely pseudomorph it; also occurs as patchy replacement of groundmass and in amygdules with or without chlorite and sodic plagioclase.

Chlorite: colorless-green; replaces feldspar and pyroxene phenocrysts along fractures and occasionally pseudomorphs the latter; also replaces biotite and groundmass; forms amygdaloidal fillings with or without calcite and sodic plagioclase.

Glass: clear, brown to gray material in groundmass.

Opaque Minerals: magnetite; as dust, tiny granules, needles, or irregularly shaped masses (up to 2 mm); dispersed in groundmass and associated with altered pyroxene; some red to brown hematite also occurs as grains and as stain in groundmass; occasional gray translucent tiny grains of sphene and leucoxene also occur.

Amphibole: Two varieties of hornblende; one is pale green and was seen as phenocrysts in a lava; the other one is brown, strongly pleochroic and was seen as tiny (1/2 mm) euhedral prisms in the groundmass. This one is either basaltic hornblende or probably sodic amphibole(?).

Biotite: (trace), brown, replaces pyroxene and also as small flakes in groundmass.

Apatite: Acicular, as tiny euhedral laths in feldspar, chlorite and amphibole.

Quartz: Trace of mosaic quartz is occasionally present in amygdules and is associated with amorphous silica, chlorite and zeolites.

Zeolites: radiating acicular masses in some amygdules and veinlets.

B. Petrographic Descriptions of Porali Conglomerate

Volcanic Clasts

Augitic Limburgite

Sample No.: SR-1-79

Occurrence: Boulder

Location: 17, Figure 4B.

Color: Gray

Texture: Hypocrystalline, seriate-porphyritic, with titanaugite phenocrysts set in a felted groundmass of glass, plagioclase microliths and tiny clinopyroxene grains.

Minerals: Titanaugite - neutral-slightly purplish in color, relatively fresh, subhedral-euhedral phenocrysts (up to 1.5 mm long) and tiny grains in groundmass, twinned and zoned (concentric and hour-glass); shows anomalous 1° blue interference color.

Plagioclase - tiny laths in groundmass, twinned (albite type), accessory.

Biotite - Brown, tiny fibrous grains in groundmass; pleochroic; some replaces pyroxene; accessory.

Felspathoid(?) - colorless, low relief short prisms in groundmass; possibly nepheline(?); accessory.

Opaque minerals - magnetite and occasional brown hematite; occurs as small discrete grains in groundmass; a few large (± 2 mm) grains of irregular shape are associated with pyroxene, some sphene and leucoxene.

Olivine(?) - tiny round grains in groundmass; accessory.

Glass - clear-brownish, forms groundmass.

Relative Proportion: Pyroxene > glass > opaque minerals > other.

Augitic Limburgite (Augitite)

Sample No.: SR-3-79

Occurrence: Boulder

Location: 9, Figure 4B.

Color: Gray

Texture: Hypocrystalline, porphyritic with titanaugite phenocrysts (up to 1.5 mm) set in a glassy groundmass; a xenolith (6 mm) consisting of pyroxenite crystals is included; a few amygdules.

Minerals: Titanaugite - similar to that of SR-1-79

Opaque minerals - dust and irregularly shaped grains dispersed through groundmass.

Glass - grayish groundmass.

Calcite - occurs in amygdules with or without other minerals listed below.

Chlorite - green-brown; occurs in amygdules, veinlets, and occasionally replaces pyroxene; chlorite in amygdules is of colloform type.

Amorphous silica - occurs in amygdules with chlorite; also colloform.

Zeolite - occurs in amygdules with other minerals listed above.

Augitic Limburgite

Sample No.: SR-4-79

Structure: Dike

Location: 20, Figure 4B.

Color: Light gray

Texture: Hypocrystalline, glomeroporphyritic, with titanaugite phenocrysts and hornblende set in a glassy groundmass.

Minerals: Titanaugite - purplish brown phenocrysts (0.5-3 mm long) and tiny grains in groundmass; zoned (concentric and hourglass) and shows 1° anomalous blue color.

Hornblende - brown, strongly pelochroic; replaces pyroxene.

Opaque minerals - magnetite; small grains and skeletal masses in groundmass; some sphene.

Calcite - forms patches and irregular replacement of groundmass glass; also fills cavities.

Chlorite - light green; replaces pyroxene and hornblende and also fills cavities with calcite.

Olivine(?) - a few tiny anhedral grains in groundmass.

Zeolites - occaionally found in cavities.

Felspathoids(?) - tiny prisms in groundmass.

Glass - forms groundmass; some shard-like masses that turn isotropic in cross nicols are probably also glass.

Relative Proportion: Glass > pyroxene > opaque minerals > calcite > chlorite > felspathoid > hornblende > zeolite

Altered Basalt

Sample No.: SR-7-79

Occurrence: Boulder

Location: 22, Figure 4B.

Color: Gray

Texture: Porphyritic, with a few altered feldspar and pyroxene phenocrysts (up to 1.5 mm long) set in a fine-grained groundmass of chloritized and carbonatized material.

Minerals: Plagioclase - cloudy laths; twinned (carlsbad, albite, pericline ?), extinction angle (6°-26°) on albite twins indicates the presence of albite-andesine; partly chloritized and carbonatized.

Clinopyroxene - phenocrysts; largely replaced by a mixture of chlorite, calcite, biotite and opaque material.

Chlorite - colorless-green; replaces groundmass and phenocrysts.

Calcite - patchy, replaces groundmass and phenocrysts.

Biotite - brown, strongly pleochroic; replaces pyroxene.

Apatite - tiny laths and elongated tabular crystals; occurs in association with chlorite and feldspar.

Opaque minerals - magnetite; forms discrete equant grains, needles and irregularly shaped grains in

groundmass; also associated with pyroxene; some sphene and leucoxene.

Relative Proportion: calcite > feldspar > opaque > chlorite > biotite > pyroxene > others

Amygdaloidal Basalt

Sample No.: SR-79-79

Occurrence: Block

Location: 52, Figure 4B.

Color: Gray

Texture: Intersertal, with poorly oriented feldspar and hornblende phenocrysts set in an amygdaloidal glassy groundmass.

Minerals: Plagioclase - anhedral-euhedral laths (up to 1.2 mm); some curved; twinned (albite, carlsbad), partly chloritized; extinction angle (5°-19°) on seven albite twins indicates presence of albite-oligoclase(?); occasionally partly replaced by chlorite.

Clinopyroxene - occasional relicts, resorbed in glass; not observed with hornblende.

Hornblende - two varieties (1) occasional phenocrysts (up to 4.5 mm); pale-greenish, strongly pleochroic anhedral-subhedral grain with excellent cleavage; deformed; (2) fibrous, uralitic(?), partly replaced by chlorite; includes apatite.

Opaque minerals - magnetite, sphene-leucoxene; equant and irregularly shaped grains in groundmass, sometimes associated with mafics.

Apatite - tiny tabular grains in felspar and hornblende.

Glass - in groundmass.

Amygdules - silica; mosaic quartz and amorphous; chlorite, green-brown; zeolite.

Relative Proportion: Feldspar > glass > amygdules > hornblende > apatite > pyroxene > others

Augitic Limburgite

Sample No.: SR-81-79

Occurrence: Boulder

Location: 54, Figure 4B.

Color: Gray

Texture: Hypocrystalline, sub-porphyritic with small pyroxene phenocrysts set in a groundmass of glass, pyroxene, amphibole and opaque material.

Minerals: Titanaugite - similar to that of Sample SR-1-79.

Amphibole - brown, strongly pleochroic; elongated needles and prisms (± 0.5 mm); occurs in groundmass; probably sodic (barkevikite(?), kaesutite(?)).

Olivine(?) - some tiny grains in groundmass.

Glass - gray groundmass; also in some cavities.

Chlorite - green; replaces some groundmass; also occurs in amygdules.

Calcite and zeolite - occur in veinlets and amygdules.

Relative Proportion: Glass > amphibole > pyroxene > opaque minerals > others

Altered Augitic Limburgite

Sample No.: SR-90A-79

Occurrence: Boulder

Location: 53, Figure 4B.

Color: Gray

Texture: Vitrophyric, with phenocrysts of titanaugite set in a glassy groundmass; shows abundant amygdules.

Minerals: Titanaugite - subhedral-euhedral grains (up to 2.2 mm) neutral-brownish; zoned (concentric-hourglass); twinned; also in groundmass as tiny anhedral-euhedral grains.

Plagioclase - occurs mainly in amygdules and cavities as clear-cloudy twinned laths; extinction angles on albite twins indicate presence of albite-oligoclase. Also occurs as microliths in groundmass.

Chlorite - green, vermicular growths lining amygdules with or without feldspar; also partly replaces groundmass and some pyroxene phenocrysts along fractures.

Epidote(?) - pistachio green; trace in a cavity.

Opaque minerals - tiny grains and some skeletal magnetite masses in groundmass; trace of red hematite in a cavity.

Glass - gray groundmass.

Relative Proportion: Glass > feldspar (in amygdules) > pyroxene > chlorite > opaques

Altered Porphyritic Basalt

Sample No.: SR-90B-79

Occurrence: Boulder

Location: 53, Figure 4B.

Color: Dark gray

Texture: Hypocrystalline; porphyritic with large phenocrysts of pyroxene and altered feldspar(?) set in a glassy groundmass; a few amygdules.

Minerals: Titanaugite - forms phenocrysts (up to 7 mm long) similar to that of Sample SR-1-79, partly replaced by chlorite along fractures.

Calcite - occurs as pseudomorphs after feldspar(?) phenocrysts (as judged from crystal shapes) and in amygdules.

Chlorite - occurs in amygdules with or without calcite.

Plagioclase - occurs as tiny microliths in groundmass; also in amygdules with calcite and chlorite.

Opaque minerals - magnetite; forms tiny grains in groundmass; also associated with pyroxene; some leucoxene.

Glass - dark gray groundmass.

Relative Porportion: Glass > pyroxene > calcite > chlorite > feldspar > opaque minerals

Altered Basalt

Sample No.: SR-92-79

Structure: Dike in Porali Conglomerate

Location: 53, Figure 4B.

Color: Gray

Texture: Holocrystalline, fine grained, with a dense framework of elongated prisms of some unidentified mineral, chlorite and opaques and other minerals; a few amygdules.

Minerals: Unidentified - gray turbid-translucent and occasionally clear-transparent; fibrous long prismatic grains, 1 cleavage; low 1° interference color; parallel extinction; biaxial^{+}; partly replaced by chlorite. (Epidotized plagioclase ?)

Titanaugite - purplish brown; fractured; euhedral; occasionally twinned.

Olivine(?) - tiny equant subhedral grains.

Chlorite - pale greenish-reddish green; occurs in cavities; also fibrous-colloform masses interstitial to pyroxene which it partly replaces.

Zeolite - in cavities with or without chlorite.

Opaque minerals - discrete small equant grains of magnetite, evenly distributed in groundmass; some sphene(?).

Biotite - reddish brown flakes, accessory.

Clay minerals - colorless, high birefringence; in cavities with chlorite.

Augitic Limburgite

Sample No.: SR-110-79

Occurrence: Boulder

Location: 67, Figure 4B.

Color: Gray

Texture: Hypocrystalline; porphyritic, with phenocrysts of pyroxene set in a glassy groundmass; a few amygdules.

Minerals: Titanaugite - neutral-brownish, subhedral-euhedral grains (up to 2.2 mm long); zoned (concentric) and twinned; relatively fresh; also occurs in groundmass as tiny grains.

Chlorite - occurs as partial to total replacement of pyroxene and possibly olivine(?); also in amygdules.

Apatite - inclusions in pyroxene.

Opaque minerals - magnetite; dust and small to large grains in groundmass; associated with pyroxene; some red iron oxide stains groundmass.

Calcite - occurs with chlorite in groundmass.

Glass - gray groundmass.

Relative Proportion: Pyroxene > glass > opaque > chlorite > calcite

APPENDIX 4

A. Petrographic Summary of Minerals Forming the Bela Volcanics

Plagioclase: The plagioclase occurs as cloudy, subhedral to euhedral phenocrysts and also as acicular or needle-like microliths or feathery dendritic sheaf-like bunches in the groundmass; some groundmass feldspar is tiny moss-like; some microliths may be curved. Both the phenocryst and groundmass feldspar may be twinned, showing albite and carlsbad type twins. Combined albite/carlsbad twins were occasionally identified only in the phenocrysts. The phenocrysts may show normal or undulose extinction; some are zoned. They may also be fractured and show corroded edges. Among the minerals seen as inclusions in the plagioclase phenocrysts of different samples are: plagioclase, chlorite, opaque, sphene, epidote and pyroxene.

The feldspar is variably altered; the phenocrysts may be more or less sausuritized. Chlorite and epidote group minerals may occur along fractures and cleavage traces and occasionally form pseudomorphs. They may also replace the groundmass feldspar in a patchy or irregular fashion. The groundmass feldspar may also be fused with glass and occasionally iron stained. Calcite may partly or wholly replace some feldspar phenocrysts.

Optical data (on twins) indicates that the phenocryst feldspar is albite-oligoclase and occasionally andesine; the composition of groundmass

feldspar is not known, but appears to be the same.

Clinopyroxene (diopside): The clinopyroxene may also occur both as subhedral-euhedral phenocrysts and as tiny xenomorphic grains in the groundmass. The latter may occasionally occur as tiny feathery prisms. The pyroxene is commonly neutral to brownish in color and may have dark borders; some groundmass pyroxene, however, may be brownish gray. The phenocrysts may be twinned and occasionally zoned. They were generally somewhat uralitized though fresh pyroxene was seen in one sample. Therefore chlorite-uralite are the common replacement products. Also inclusions of feldspar, chlorite and opaque may be present in phenocrysts.

Opaque minerals (magnetite-ilmenito-magnetite?, hematite): The opaque minerals occur as black, reddish or brownish gray granules, dust, tiny needles, and skeletal masses in the matrix. Some occur as occasional tiny inclusions in feldspar phenocrysts and also as moss-like intergrowth with the matrix feldspar and glass. Some opaque material is clearly interstitial to groundmass feldspar. Leucoxene and sphene are occasionally present. The opaque minerals are generally associated with the mafics.

Glass: forms matrix in variable amounts; it is generally brownish, greenish or gray. Occasional glass spherules also occur.

Chlorite: replaces feldspar and mafic minerals to a variable degree. It also replaces groundmass and occurs in veinlets and amygdules with or without quartz, carbonate and zeolites; some appears to be colloidal.

Accessory minerals: Epidote group minerals replace feldspar and may occur in cavities occasionally.

Biotite - brown flakes; associated with other mafics, very rare.

Hornblende - fibrous, sheaf-like uralite of light brown or greenish color in groundmass and with pyroxene; may be replaced by chlorite and rarely by biotite.

Quartz - tiny anhedral grains in groundmass and also as cavity fillings with chlorite, epidote and opaque minerals.

Calcite - replaces some feldspar phenocrysts to a variable degree; also occurs as patchy replacement of groundmass. May form veinlets with chlorite and epidote.

Zeolite(?) - in amygdaloidal cavities.

B. Petrographic Description of the Bela Volcanics

Porphyritic Spilitic Basalt

Sample No.: 77-SA-14A

Occurrence: Unpillowed lava flow with vesicled top.

Location: 4, Figure 3.

Color: Grayish green

Texture: Holocrystalline, porphyritic, with plagioclase and a few pyroxene phenocrysts set in a groundmass of tiny feldspar laths, pyroxene and other minerals.

Minerals: Plagioclase - cloudy, euhedral laths; phenocrysts are twinned (carlsbad and albite type); occasionally zoned; optical data indicates albitic composition for

both the phenocrysts and the groundmass feldspar.

Clinopyroxene - neutral, anhedral-subhedral; small grains in groundmass and few phenocrysts; highly fractured and partly altered to amphibole. c∧z angles indicate presence of diopside.

Amphibole - green, nonpleochroic-highly pleochroic; fibrous and elongated deformed prisms; probably tremolite-actinolite with some hornblende.

Opaque minerals - magnetite (or ilmenito-magnetite), anhedral-irregularly shaped grains in groundmass. Trace of pyrite.

Chlorite - occurs as partial replacement of feldspar, pyroxene and as fillings in amygdules and other cavities.

Calcite - occasional replacement of feldspar; also in groundmass and in veinlets.

Quartz - trace in groundmass and in cavities.

Counts (200): Plagioclase, 60; clinopyroxene, 24; opaque minerals, 6; other, 10.

Altered Porphyritic Basalt

Sample No.: 77-SA-14B

Occurrence: Unpillowed lava with vesicled top.

Location: 4, Figure 3.

Color: Grayish green

Texture: Porphyritic with chlorite pseudomorphs after plagioclase phenocrysts embedded in a dense groundmass formed by plagioclase, pyroxene and opaques.

Minerals: Plagioclase - as phenocrysts (replaced by chlorite) and tiny twinned laths in groundmass.

Clinopyroxene -

Opaques - magnetite, hematite (red); trace of pyrite.

Other minerals - similar to 77-SA-14A.

Spilitic Basalt

Sample No.: 78-SR-42

Occurrence: Pillow lava

Location: 12, Figure 4B.

Color: Greenish gray

Texture: Fine grained; subophitic-intersertal, with plagioclase laths defining a network and interstitial pyroxene set in a somewhat glassy groundmass.

Minerals: Plagioclase - cloudy, elongated laths (up to 2.5 mm long); twinned (albite, carlsbad); extinction generally undulose, however, extinction angles on sharp albite twins in two laths indicate presence of albite-oligoclase; somewhat sericitized, also occurs in groundmass.

Clinopyroxene - (diopside ?); neutral-brownish in color; xenomorphic-subhedral grains (up to 2.5 mm) subophitically intergrown with plagioclase; contains inclusions of plagioclase, chlorite(?)

and opaque material; occasionally twinned; generally fresh but grains are uralitized.

Chlorite - light green; partly replaces plagioclase.

Hornblende (Uralite) - brownish green to dark green; replaces pyroxene; associated with some biotite and chlorite.

Opaque minerals - dust and tiny needles and skeletal masses in groundmass; some sphene.

Quartz - tiny grains in groundmass; trace.

Glass - groundmass.

Counts (360): Plagioclase, 51; clinopyroxene, 29; opaque minerals, 9; chlorite, 6; glass, 4; hornblende, 1.

Altered Porphyritic Basalt

Sample No.: SR-2-79

Occurrence: Pillow lava

Location: 18, Figure 4B.

Color: Dark gray

Texture: Vitrophyric, with phenocrysts of pyroxene and altered plagioclase set in a glassy groundmass.

Minerals: Clinopyroxene - (diopside ?), subhedral-euhedral phenocrysts up to 6 mm long), twinned and occasionally zoned.

Calcite - mosaic type; pseudomorphs plagioclase(?) phenocrysts as judged from crystal shapes; also forms patchy areas in groundmass, forms veinlets and fills amygdules with chlorite and zeolites.

Plagioclase - tiny cloudy laths in groundmass.

Chlorite - replaces some groundmass and pyroxene grains along fractures; also occurs in amygdules as colloform masses.

Opaque minerals - (magnetite, ilmenito-magnetite) form network of tiny needles and small grains in groundmass; also occurs as tiny inclusions in pyroxene and as patches in calcite pseudomorphs; some sphene and leucoxene.

Zeolite - in amygdules with chlorite.

Glass - in groundmass.

Relative Proportion: Groundmass (glass + chlorite + opaque minerals) > calcite > clinopyroxene.

Spilitic Basalt

Sample No.: SR-16-79

Occurrence: Pillow lava

Location: 28, Figure 4B.

Color: Greenish gray

Texture: Dense, holocrystalline, with interwoven microliths of plagioclase and pyroxene grains forming a felted texture; a few amygdules and veinlets.

Minerals: Plagioclase - cloudy disoriented and occasionally curved, partly chloritized microliths; twinned (carlsbad, albite) with generally undulose extinction; however, extinction in sharp albite twins in 3 grains indicate presence of albite-oligoclase.

Clinopyroxene - (diopside ?) small, xenomorphic-subhedral grains, neutral-brownish in color and with dark borders; twinned; fractured.

Opaque minerals - magnetite-ilmenito-magnetite(?) forms small needles and irregularly shaped grains dispersed in groundmass; associated with mafic minerals; a few grains coated with leucoene; some sphene granules also present.

Calcite, Zeolite, Quartz and Chlorite - occurs in veinlets and cavities; chlorite also occurs as partial replacement of feldspar.

Counts (235): Clinopyroxene, 32; Plagioclase, 31; Chlorite, 22; Opaque Minerals, 11; others, 4.

Spilitic Basalt

Sample No.: SR-30-79

Occurrence: Pillow lava

Location: 33, Figure 4B.

Color: Grayish green

Texture: Hypocrystalline, glomeroporphyritic, with bunches of feldspar phenocrysts (< 1 mm - 2 mm) set in a groundmass of glass, feldspar, pyroxene.

Minerals: Plagioclase - clear to mostly cloudy, grayish subhedral-euhedral phenocrysts; also as tiny acicular, radiating sheaf-like or dendritic masses set in groundmass glass. Both feldspars are twinned

(albite, carlsbad); phenocrysts occasionally zoned and show wavy extinction making identification very difficult. They are also partly replaced by chlorite and occasionally by red epidote (piedmontite ?) and carbonate; the groundmass plagioclase is stained by iron oxide at places.

Clinopyroxene - tiny xenomorphic-subhedral grains in groundmass; also occurs as occasional twinned phenocrysts.

Chlorite - colorless, brownish or green; partly replaces feldspar and also occurs in veinlets.

Calcite - occasionally replaces feldspar and also occurs with chlorite in veinlets.

Glass - occurs in groundmass.

Opaque minerals - translucent, red-black hematite; occurs as needles and skeletal masses. It is interstitial to and intergrown with feldspar in groundmass; also forms veinlets. Also magnetite occurs as tiny inclusions in feldspar phenocrysts.

Counts (242): Feldspar; Clinopyroxene, 16; Glass, 10; Opaque minerals, 8; Chlorite-calcite, 10.

Spilitic Basalt

Sample No.: SR-36-79

Occurrence: Pillow lava

Location: 36, Figure 4B.

Color: Greenish to brownish gray

Texture: Holocrystalline; subporphyritic, with a few phenocrysts (up to 1.3 mm long) of plagioclase and clinopyroxene set in a groundmass of smaller plagioclase laths, sub-ophitically intergrown clinopyroxene, chlorite and other minerals.

Minerals: Plagioclase - cloudy, subhedral-euhedral laths; occurs both as phenocrysts and in groundmass; corroded; somewhat sericitized; groundmass feldspar is twinned (albite, carlsbad); optical data indicates the presence of albite-oligoclase in groundmass.

Clinopyroxene - (diopside); xenomorphic-subhedral prisms; neutral-brownish in color; variably uralitized twinned.

Chlorite - green, fibrous; replaces both the feldspars and pyroxene.

Opaque minerals - (magnetite, ilmenito-magnetite ?) form needles, rectangular and irregularly shaped grains in groundmass.

Hornblende, biotite, calcite, quartz and apatite(?) - occur in lesser amounts.

Counts (152): Feldspar, 42; Clinopyroxene, 19; Chlorite, 26; Opaque minerals, 9; Ciotite/uralite, 2; quartz, 2.

Plagioclase Basalt or Keratophyre (?)

Sample No.: SR-37-79

Occurrence: Pillow lava.

Location: 37, Figure 4B.

Color: Brownish gray

Texture: Hypocrystalline, porphyritic with altered feldspar phenocrysts (up to 2 mm) set in a groundmass of tiny moss-like network of glass, feldspar microliths and opaque minerals.

Minerals: Plagioclase - occurs as cloudy, subhedral-euhedral, twinned phenocrysts and as moss-like masses in groundmass. Most phenocrysts completely replaced by calcite-chlorite; sometimes only an unreplaced feldspar rim is left suggesting that the feldspar was zoned and only selectively replaced.

Calcite - pseudomorphs plagioclase phenocrysts; also occurs with chlorite.

Chlorite - occurs as partial replacement of feldspar.

Zoisite(?) - replaces some feldspar; shows berlin blue interference color.

Opaque minerals - (magnetite ilmenito-magnetite ?) occur as dust, needles, skeletal masses and moss-like growths in groundmass; also occurs as inclusions in feldspar phenocrysts; some sphene/leucoxene also present.

Glass - forms groundmass.

Relative Proportion: Feldspar > opaque minerals > glass > calcite > other

Plagioclase Basalt or Keratophyre(?)

Sample No.: SR-42-79

Occurrence: Pillow lava

Location: 40, Figure 4B.

Color: Brownish gray

Texture: Hypocrystalline, subporphyritic with a few phenocrysts of euhedral plagioclase set in a subtrachytic groundmass consisting of plagioclase microlites and gray glass.

Minerals: Plagioclase - occurs as clear stubby lath-like phenocrysts and as microlites in groundmass; laths are zoned, twinned (albite-carlsbad), partly chloritized, and resorbed in glass; also occurs with chlorite and quartz in a few amygdules.

Chlorite -

Quartz -

Opaque minerals - fine dust and a few small grains in groundmass; similar to SR-37-79.

Relative Proportion: Glass >> plagioclase > opaque > chlorite.

Spilitic Basalt

Sample No.: SR-43-79

Occurrence: Pillow lava

Location: 40, Figure 4B.

Color: Grayish green.

Texture: Holocrystalline, fine grained, with subophitically intergrown plagioclase laths (up to 2.5 mm) and clinopyroxene (up to 2.4 mm) forming a loose framework, filled with plagioclase

microliths, tiny clinopyroxene grains, opaques and chlorite.

Minerals: Plagioclase - cloudy laths and small acicular microliths, twinned (carlsbad, albite); with undulose extinction; somewhat sausuritized.

Clinopyroxene - neutral-brownish; interstitial to plagioclase, however, also poikilitically enclosed within plagioclase; partly replaced by chlorite along fractures, cleavage and twin lamellae.

Chlorite - green, occurs as inclusions in feldspar and replaces pyroxene; also occurs in groundmass, and with quartz in cavity fillings.

Opaque minerals - (magnetite, ilmenito-magnetite); occur as tiny grains, needles, skeletal masses; associated with mafic minerals; leucoxene/sphene occurs as tiny translucent high relief grains of turbid gray or reddish brown color.

Quartz - forms veinlets and also in groundmass.

Zeolites - colorless, acicular; fibrous radial aggregates; associated with quartz.

Counts (270): Pyroxene, 26; feldspar, 45; chlorite, 15; quartz, 2; opaque minerals, 11; other, 1.

Amygdaloidal Basalt

Sample No.: SR-68-79

Occurrence: Pillow lava

Location: 48, Figure 4B.

Color:

Texture: Hypocrystalline; fine grained; subporphyritic with phenocrysts of plagioclase and pyroxene set in a glassy groundmass; amygdules (up to 3 mm) of round-irregular shape are filled with chlorite and calcite.

Minerals: Plagioclase - occurs both as phenocrysts and in groundmass; the phenocrysts (± 1 mm long) are cloudy, subhedral, corroded laths; twinned (albite type); undulose extinction; groundmass feldspar occurs as disoriented microliths.

Clinopyroxene - occurs as subhedral-euhedral phenocrysts and as tiny grains in groundmass.

Chlorite - mainly in amygdules as lining; also replaces some groundmass.

Calcite - fills amygdules with chlorite.

Opaque minerals - granules and needles in groundmass.

Glass - forms gray groundmass.

Relative Proportion: Plagioclase > glass > pyroxene > opaque minerals > chlorite > calcite.

Basaltic Andesite

Sample No.: SR-88-79

Occurrence: Pillow lava

Location: 57, Figure 4B.

Color: Grayish green

Texture: Hypocrystalline; glomeroporphyritic with bunches of feldspar phenocrysts (up to 1.5 mm long but one is 5 mm) set in a groundmass of glass, feldspar microliths and pyroxene; the groundmass is subtrachytic - intersertal.

Minerals: Plagioclase - the phenocrysts are laths with inclusions of early plagioclase and some oriented opaque granules; the groundmass plagioclase may be acicular and feathery masses arranged in dendritic bunches: they are also curved. Both feldspars are twinned (albite type) and extinction angles indicate the presence of andesine.

Clinopyroxene - forms tiny xenomorphic to subhedral grains in groundmass.

Opaque minerals - occur as dust, tiny needles and small skeletal masses in groundmass.

Epidote - (Piedmontite) yellow, orange; reddish brown in color, pleochroic; forms partial replacement of feldspar along fractures and also irregularly.

Glass - forms groundmass.

Relative Proportion: Feldspar > glass > opaque minerals > pyroxene > other

Keratophyre

Sample No.: SR-99-79

Occurrence: Pillow lava

Location: 61, Figure 4B.

Color: Grayish green

Texture: Hypocrystalline, porphyritic - glomeroporphyritic, with plagioclase phenocrysts set in a trachytic groundmass.

Minerals: Plagioclase - occurs as lath-like phenocrysts (up to 1.3 mm long); twinned (albite, carlsbad) occasionally zoned; optical data indicates presence of albite-andesine; fractured and partly replaced by chlorite along fractures; also occasionally sausuritized; the groundmass microliths are also twinned.

Chlorite - occurs in amygdules and partly replaces plagioclase.

Clinopyroxene - tiny xenomorphic grains and prisms in glass.

Hornblende - brownish; minute fibrous grains.

Zeolite - radiating acicular prisms in amygdules.

Opaque minerals - occur as dust and tiny grains associated with feldspar, chlorite and in groundmass.

Glass - dark gray groundmass.

Relative Proportion: Glass > feldspar > opaque minerals > chlorite > other

Keratophyre

Sample No.: SR-104-79

Occurrence: Pillow lava

Location: 63, Figure 4B.

Color: Grayish brown

Texture: Hypocrystalline, with altered plagioclase phenocrysts set in an intersertal-trachytic groundmass.

Minerals: Plagioclase - occurs as a few chloritized and sausuritized phenocrysts (up to 1.5 mm long) and tiny needles in groundmass where it is fused with glass.

Clinopyroxene - tiny, brown-brownish gray grains and feathery prisms in groundmass.

Chlorite - colorless, green-brown; occurs mainly as patchy replacement of feldspar and some groundmass; also forms veinlets.

Opaque minerals - occur as fine dust and skeletal masses in glass.

Hornblende - light brown; trace.

Glass - grayish brown groundmass.

Keratophyre

Sample No.: SR-105-79

Occurrence: Pillow lava

Location: 64, Figure 4B.

Color: Dark gray

Texture: Hypocrystalline, glomeroporphyritic, with altered plagioclase phenocrysts set in a trachytic matrix. A few amygdules filled with glass; chlorite and calcite.

Minerals: Plagioclase - occurs as phenocrysts (up to 2.2 mm) and in groundmass; the former are cloudy laths; partly chloritized and sausuritized twinned (carlsbad, albite); the groundmass feldspar occurs as acicular microliths.

Clinopyroxene(?) - occasional tiny grains in glass.

Opaque minerals - magnetite, hematite and some sphene/leucoxene(?). Black-reddish in color; occur as dust, and tiny grains in glass; also as inclusions in feldspar.

Chlorite - green; partly replaces feldspar and occurs in amygdules and veinlets.

Calcite/zeolite - occasionally occur in amygdules.

Relative Proportion: Feldspar > glass > chlorite > opaque > pyroxene > other

Basaltic Andesite

Sample No.: SR-114-79

Occurrence: Pillow lava

Location: 70, Figure 4B.

Texture: Hypocrystalline; porphyritic with plagioclase phenocrysts set in an intersertal groundmass.

Minerals: Plagioclase - occurs as lath-like phenocrysts (1.2 mm long) and feathery microliths in groundmass; phenocrysts are twinned (carlsbad, albite and combination); optical data indicates presence of oligoclase-andesine(?); some phenocrysts are, however, zoned; some are also epidotized (iddingsite).

Clinopyroxene - small xenomorphic grains in groundmass; uralitized.

Hornblende - (uralite); fibrous sheaf-like aggregates in groundmass.

Opaque minerals - tiny grains, needles and skeletal masses in groundmass.

Chlorite - partly replaces glass and fills some fractures in feldspar.

Glass - forms groundmass.

Relative Proportion: Plagioclase > clinopyroxene > opaque minerals > hornblende > glass > epidote > chlorite

APPENDIX 5

A. Petrographic Summary of Minerals Constituting the Bela Intrusives

Plagioclase: The plagioclase feldspar is the most abundant mineral found in the diabases and gabbros of the Bela Intrusives. As framework feldspar in the ophitic-subophitic rocks - the most common type, it is intergrown with the clinopyroxene. It also occurs as a groundmass phase and commonly forms phenocrysts in the porphyritic varieties. Feldspar commonly occurs as subhedral-euhedral, cloudy or grayish laths (up to 3 mm), and as smaller acicular, feathery grains; it is frequently twinned. Albite and carlsbad type twins are common; less commonly, pericline and combined albite/carlsbad twins are also present. Extinction is generally undulose; however, where possible, optical determination in laths showing sharp albite-type twins indicates that most feldspar falls in the albite-oligoclase, and, less commonly, the andesine range. More calcic feldspar was not positively identified; however, plagioclase (excluding groundmass) is clearly of multigeneration origin in a few samples. The younger feldspar occurs as overgrowths on the older one or as laths surrounding corroded grains of the older feldspar. Some plagioclase phenocrysts are zoned and, therefore, could not be optically identified. Thus at present the existence of calcic plagioclase in the diabasic rocks cannot be ruled out. The groundmass feldspar occurs as tiny laths, acicular or needle-like grains and occasionally as spherules. The feldspar generally shows variable

alteration involving sericitization, chloritization or sausuritization. Inclusions of pyroxene, amphibole, opaque minerals, and clay minerals are also present. Veinlets of chlorite may also cut across feldspar grains.

Clinopyroxene: The clinopyroxene occurs as xenomorphic to euhedral, elongated (up to 5 mm) or feathery prisms sub-ophitically intergrown with the plagioclase; it also occurs as phenocrysts and also in groundmass. The pyroxene is neutral, greenish or brownish in color and is commonly twinned. Optical data (c∧z extinction angle) indicate the presence of both augite (titanaugite ?) and diopside. Like the feldspar, the pyroxene is also variably altered; the products being uralitic hornblende, tremolite-actinolite, chlorite, biotite and opaque material. Alteration may proceed along grain-edges, fractures, cleavage traces or be irregular. In one sample, relict olivine(?) was observed within pyroxene grains (Fig. 43). Except for this, olivine was not observed either in the Bela Intrusives or in the Bela Volcanics.

Amphiboles: Brownish or greenish fibrous hornblende (uralite) is frequently seen to replace pyroxene. Besides, accessory amounts of strongly pleochroic brown or green hornblende are found as tabular grains; it is interstitial to pyroxene and feldspar. Occasionally tremolite-actinolite have also been observed to replace pyroxene. Probably both magmatic and secondary hornblendes are present; however, it is difficult to tell them apart. Amphiboles may be replaced by biotite and chlorite.

Chlorite: Chlorite occurs as colorless, greenish to brownish vermicular or scaly masses and radiating crystals. It usually replaced other mafic

minerals and plagioclase; replacement may proceed along fractures, cleavage traces or grain edges. Cores of some plagioclase phenocrysts have been chloritized. Chlorite also occasionally pseudomorphs some pyroxene grains. Penninite was identified in two samples. Chlorite also occasionally occurs as patchy replacement of groundmass, as cavity fillings and veinlets (with or without calcite) and also within myrmekitic quartz-plagioclase intergrowths.

Opaque minerals: (Magnetite-ilmenito-magnetite(?) and hematite). The opaque minerals occur as black to brownish black dust, granules, needles, skeletal and irregularly shaped masses in the groundmass and associated with the mafic minerals. Pyroxene and hornblende grains may show opaque dust and needles oriented along cleavage traces. Some magnetite (or ilmenito-magnetite) occurs as large skeletal masses subophitically intergrown with plagioclase and pyroxene. Opaque material also occurs in some chlorite-filled cavities. Some opaque grains appear to be coated with grayish translucent leucoxene.

Quartz: It occurs as xenomorphic grains intersitial to feldspar and pyroxene grains, in myrmekitic intergrowths with plagioclase, and in veinlets and cavities with chlorite and calcite. However, not all diabase samples contain quartz.

Accessory Minerals:

Apatite - occurs as tiny euhedral, short or elongated prismatic grains associated with feldspar, chlorite, and myrmekite.

Epidote-clinozoisite - some associated with feldspar and myrmekite.

Calcite - occurs with chlorite and quartz in veinlets and cavities. In one sample calcite occurs as a few euhedral hezagonal phenocrysts which appear to be pseudomorphs after olivine(?).

Zeolites - occur as tiny radiating prisms in cavities with chlorite and myrmekite.

Sphene - occurs as minute, wedge-like, round or irregularly shaped grains.

Biotite - trace; occurs as brown or green curved flakes; associated with other mafic minerals.

Pyrite - occurs as euhedral grains (a few mm long) disseminated through rock and tiny veinlets; observed only in a few samples.

B. Petrographic Description of Bela Intrusives

Diabase

Sample No.: 77-SA-7

Structure: Sill

Location: 3, Figure 3.

Color: Grayish green

Texture: Subophitic; medium grained.

Minerals: Plagioclase - (albite-oligoclase) occurs as laths and anhedral corroded grains of cloudy appearance with a few clear patches; twinned (albite, carlsbad type); includes some pyroxene grains and their alteration products.

Clinopyroxene - (augite) anhedral-subhedral grains; twinned; bariably altered.

Amphibole - green to brown hornblende occurs as replacement of pyroxene around grain edges; some tremolite-actinolite is also associated; amphiboles are partly altered to chlorite and some biotite.

Quartz - clear; granular and myrmekitic intergrowths with feldspar and chloritic material.

Opaque minerals - magnetite-ilmenito-magnetite(?) occur as irregularly shaped or skeletal masses associated with pyroxene and its alteration products.

Apatite - trace in feldspar.

Counts (240): Feldspar, 51; pyroxene, 17; green minerals, 15; opaque minerals, 10; quartz, 7.

Diabase

Sample No.: 77-SA-17

Structure: Sill

Location: 5, Figure 3.

Color: Brownish gray to gray.

Texture: Medium grained; subophitic-ophitic, with elongated feldspar laths intergrown with pyroxene grains set in a grayish matrix of feldspar microliths, chlorite and opaque minerals.

Minerals: Plagioclase - (oligoclase ?) occurs as large framework laths (up to 3 mm) and tiny microliths in groundmass; the laths are cloudy, twinned (albite, carlsbad), and often show undulatory extinction; some laths have corroded edges; partly chloritized; groundmass feldspar is too small for identification.

Clinopyroxene - neutral; occurs as large xenomorphic-subhedral grains (up to 1.2 mm) and some tiny grains in groundmass; twinned; fractured and partly uralitized; includes some relict olivine.

Chlorite - green, partly replaces feldspar, pyroxene and groundmass; some hornblende is also associated.

Opaque minerals - magnetite-ilmenito-magnetite(?); occur as small grains in groundmass and as large

irregular-skeletal grains intergrown with feldspar and pyroxene.

Relative Proportion: Feldspar > pyroxene > chlorite > opaque minerals > other.

Diabase

Sample No.: 78-SR-29

Structure: Sill

Location: 10, Figure 4B.

Color: Grayish green

Texture: Medium grained, subophitic-ophitic.

Minerals: Plagioclase - cloudy, fused laths; partly sericitized and chloritized; some are twinned with undulose extinction.

Clinopyroxene - (diopside) xenomorphic; interstitial to plagioclase and poikilitically including it in ophitic fasion; partly uralitized.

Hornblende - colorless, light brown; replacement of pyroxene.

Biotite - greenish brown-brown; radiating curved flakes; replacement of hornblende.

Chlorite - green, vermicular; replaces other mafic minerals and feldspar.

Opaque minerals - magnetite-ilmenito-magnetite; occurs as irregular-skeletal grains, occasionally coasted with leucoxene also occurs as dust along hornblende cleavage.

Apatite - tiny laths and elongated prisms.

Epidote(?) - pistachio-green; trace with feldspar.

Calcite - trace.

Relative Proportion: Feldspar > pyroxene > green minerals > opaque minerals > apatite > calcite.

Diabase

Sample No.: SR-78-46

Structure: Sill

Location: 13, Figure 4B.

Texture: Medium grained; subophitic-ophitic; with elongated feldspar laths forming a framework with interstitial pyroxene; the remaining space is filled with feldspar microliths, small pyroxene grains and other minerals.

Minerals: Plagioclase - (albite-oligoclase) occurs as large (up to 3 mm) clear-cloudy laths and microliths; laths are twinned (albite, carlsbad) and somewhat sericitized; the groundmass feldspar is locally intergrown with quartz.

Clinopyroxene - (diopside) occurs as xenomorphic grains and euhedral elongated prisms (up to 5 mm long); also occurs in groundmass; partly uralitized.

Hornblende - green, pelochroic; occurs as partial replacement of pyroxene and also as separate small-large fibrous grains.

Opaque minerals - magnetite-ilmenito-magnetite(?) occur as needles and skeletal masses associated with

mafic minerals; occasionally coated with leucoxene.

Quartz - occurs as tiny grains with feldspar microliths, chlorite, and hornblende; accessory; also occurs in a few cavities.

Chlorite - trace.

Counts (150): Feldspar, 63, pyroxene, 20; opaque, 11; hornblende, 6.

Plagiogranite (Quartz Keratophyre)

Sample No.: 78-SR-50A

Structure: Dike in a diabase sill (of Bela Intrusives)

Location: 14, Figure 4B.

Color: Light greenish gray

Texture: Fine-medium grained; porphyritic, with feldspar laths set in a fine-grained groundmass of quartz, feldspar, mafic minerals and glass.

Minerals: Plagioclase - (albite-oligoclase) occurs as lath-like phenocrysts (2 mm long) and in myrmeketic intergrowths with quartz in groundmass; laths are cloudly-brownish in color, twinned (albite, carlsbad, pericline types), and include quartz and some biotite; sometimes partly replaced by chlorite.

Quartz - occurs mainly in groundmass as tiny grains and intergrowths with feldspar; grains are generally xenomorphic, however a few euhedral crystals were noted.

Chlorite - bright green, vermicular masses; associated with feldspar, quartz and biotite; accessory.

Opaque minerals - magnetite-ilmenito-magnetite (?), occurs as equant-rod-like grains.

Biotite - tiny flakes in groundmass, accessory.

Epidote(?) - green, high relief; accessory.

Apatite (?) - trace.

Relative Proportion: Plagioclase > quartz > (chlorite + biotite) > opaque minerals

Plagioclase + quartz, ±75-80%.

Diabase

Sample No.: 78-SR-52

Structure: Sill

Location: 15, Figure 4B.

Color: Greenish gray

Texture: Porphyritic, with plagioclase and pyroxene phenocrysts set in a dense fine-grained groundmass formed by interwoven microliths of plagioclase, pyroxene and other minerals.

Minerals: Plagioclase - occurs as phenocrysts and in groundmass; the phenocrysts are of two generations; one includes the other; they are cloudy, zoned and twinned (albite, carlsbad type) and are partly replaced by chlorite. The groundmass plagioclase consists of feathery, bent and twinned (albite type) microliths; it shows subophitic relation with groundmass pyroxene.

Clinopyroxene - (diopside) occurs as occasional phenocrysts (0.2 mm) and mostly in groundmass as small grains; the phenocrysts may poikilitically include feldspar; they have corroded edges.

Chlorite - green, vermicular flakes; partly replaces feldspar and clinopyroxene; also fills a cavity.

Opaque minerals - magnetite-ilmenito-magnetite(?), forms tiny grains, needles and skeletal masses.

Quartz - tiny grains in groundmass; accessory.

Counts (150): Plagioclase, 52; pyroxene, 27; chlorite, 11; opaque minerals, 10.

Gabbro

Sample No.: 78-SR-55

Structure: Sill

Location: 16, Figure 4B.

Color: Grayish green

Texture: Subophitic-ophitic; coarse grained.

Minerals: Plagioclase - cloudy laths; ophitically intergrown with pyroxene; twinned (albite, carlsbad); extinction undulose, occasionally zoned; has late clear overgrowths; at least two generations; laths of first generation are bigger, have corroded edges and are surrounded by younger feldspar. Composition not known.

Clinopyroxene - (diopside); neutral-brownish in color; may occur in clumps; partly altered.

Hornblende - uralitic, light green-brownish in color; pleochroic; partly replaces pyroxene.

Biotite - brown, curved flakes; alteration of pyroxene.

Chlorite - light green; tiny vermicular radiating flakes, partly replaces feldspar and pyroxene; also occurs in groundmass.

Opaque minerals - magnetite-ilmenito-magnetite(?); irregular-skeletal grains; associated with mafic minerals; some sphene is present.

Apatite - euhedral elongated prisms; accessory.

Counts (240): Feldspar, 56; pyroxene, 20; opaque minerals, 8; chlorite, 9; others, 7.

Diabase

Sample No.: SR-10-79

Structure: Sill

Location: 23, Figure 4B.

Color: Gray

Texture: Fine-grained; porphyritic, with laths of plagioclase of phenocrysts set in a groundmass formed by a mesostasis of feldspar microliths, pyroxene and other minerals.

Minerals: Plagioclase - (oligoclase-andesine ?) occurs as euhedral phenocrysts (up to 1 mm) and as microliths in groundmass; phenocrysts are twinned (albite, carlsbad, pericline ?) with undulose extinction; some are zoned; composition of groundmass feldspar is not known.

Clinopyroxene - grayish-brownish in color; occurs mostly in groundmass as anhedral-euhedral prisms and is subophitically grown with feldspar.

Opaque minerals - magnetite-ilmenito-magnetite(?) occurs as irregularly shaped grains in groundmass, as needles along cleavage in pyroxene and in a veinlet with chlorite.

Chlorite - occurs as alteration of pyroxene and feldspar and also forms veinlets.

Quartz - occurs as tiny grains; also in a veinlet.

Calcite - occurs in a veinlet with quartz; also pseudomorphs a few grains of what possibly was olivine.

Counts (160): Feldspar, 54; pyroxene, 29; chlorite, 14; opaque minerals, 12; other, 1.

Diabase

Sample No.: SR-13-79

Structure: Sill

Location: 26, Figure 4B.

Color: Grayish green

Texture: Fine-medium grained; subophitic.

Minerals: Plagioclase - (albite-oligoclase), cloudy, elongated laths; intergrown with pyroxene and some quartz; twinned (albite, carlsbad); partly sericitized.

Clinopyroxene - (augite), anhedral-subhedral grains and elongated prisms; neutral-brownish in color.

Hornblende - green.

Chlorite - green, partly replaces feldspar, pyroxene and occurs with quartz.

Quartz - occurs in myrmekitic intergrowths with feldspar and quartz.

Opaque minerals - magnetite; occurs as skeletal masses; some sphene also present.

Epidote(?) - bright green, trace.

Diabase

Sample No.: SR-14-79

Structure: Sill

Location: 26, Figure 4B.

Color: Grayish green

Texture: Fine-medium grained; seriate; with plagioclase laths (up to 1 mm long) defining a framework filled with other minerals.

Minerals: Plagioclase - (oligoclase-andesine ?), clear-cloudy, twinned (albite-carlsbad type) laths; somewhat sericitized and slightly replaced by calcite.

Clinopyroxene - neutral-brownish, anhedral-subhedral; subophitically intergrown with feldspar; fractures partly replaced by chlorite.

Chlorite - green-brownish green; small vermicular aggregates and tabular grains (up to 0.5 mm) mostly occurs in groundmass; may show fine intergrowths with feldspar and quartz.

Opaque minerals - magnetite-ilmenito-magnetite; small grains.

Quartz - accessory.

Counts (130): Feldspar, 50; clinopyroxene, 25; chlorite, 13; opaque minerals, 12.

Diabase

Sample No.: SR-15-79

Structure: Sill

Location: 27, Figure 4B.

Color: Grayish green.

Texture: Medium grained; subophitic.

Minerals: Plagioclase - (albite-oligoclase) cloudy euhedral laths (up to 2.3 mm); twinned (carlsbad, albite and combined; also some pericline type).

Clinopyroxene - (augite ?) brownish, xenomorphic to subhedral elongated prisms; interstitial to plagioclase and also included in it, twinned, mostly altered to uralite.

Amphibole - (actinolite-hornblende) green-brownish green; mainly alteration of pyroxene along cleavage and edges; form long prismatic grains.

Quartz - forms irregular areas interstitial to feldspar and mafic minerals (e.g., chlorite); also forms myrmekitic intergrowths.

Chlorite - occurs in a mixture of uralite.

Opaque minerals - mostly hematite; occurs as anhedral, irregular or skeletal masses associated with

mafic minerals; some magnetite-ilmenito-magnetite; sphene also occurs as tiny round grains in accessory amounts.

Apatite - occurs as tiny elongated slender prisms associated with chlorite, fledspar and myrmekite.

Biotite - trace with uralite.

Zeolite(?) - small radial dendritic material.

Counts (230): Plagioclase, 45; quartz + myrmekite, 14; amphibole, 13; chlorite, 16; pyroxene, 4; opaque minerals, 6; other, 2.

Diabase

Sample No.: SR-21-79

Structure: Sill

Location: 31, Figure 4B.

Color: Grayish green

Texture: Fine-medium grained subophitic-ophitic.

MInerals: Plagioclase - cloudy, elongated laths (up to 2.2. mm) twinned (albite, carlsbad); partly sericitized; apparently of multi-generation.

Clinopyroxene - (diopside, some augite) occurs as xenomorphic-euhedral, feathery and irregularly shaped grains; interstitial to feldspar; partly uralitized.

Hornblende - light green-greenish brown; mostly alteration of pyroxene.

Chlorite - green, radiating crystals; associated with myrmekite and other mafic minerals.

Quartz - occurs as anhedral grains interstitial to feldspar and myrmeketic intergrowths.

Opaque minerals - magnetite-ilmenito-magnetite(?); occur as dust and skeletal grains; some sphene.

Apatite - acicular elongated needles; accessory.

Zeolite(?) -

Counts (130): Plagioclase, 45; pyroxene, 21; quartz/myrmekite, 15; hornblende, 7; chlorite, 6; opaque minerals, 6.

Diabase

Sample No.: SR-23-79

Structure: Sill

Location: 31, Figure 4B.

Color: Grayish green.

Texture: Fine-medium grained; seriate-glomeroporphyritic; mafic minerals occur in clumps.

Minerals: Plagioclase - (albite oligoclase ?), cloudy twinned (albite type) lath-like phenocrysts; also occurs in groundmass, partly chloritized.

Clinopyroxene - brownish, xenomorphic; occurs both as phenocrysts and in groundmass; subophitically intergrown with feldspar; twinned; partly uralitized augite and diopside.

Hornblende - light green; alteration of pyroxene.

Chlorite - green-greenish brown; tiny vermicular radiating crystals; replaces feldspar and pyroxene.

Biotite - brown curved flakes; associated with pyroxene; accessory.

Opaque minerals - (hematite; magnetite-ilmenito-magnetite ?); occur as grains and skeletal masses.

Glass - some in groundmass.

Diabase

Sample No.: SR-33-79

Structure: Sill

Location: 34, Figure 4B.

Color: Greenish gray

Texture: Subporphyritic; consists of a fine-grained mesostasis of plagioclase and pyroxene in subophitic intergrowth with occasional phenocrysts of both minerals.

Minerals: Plagioclase - cloudy twinned laths.

Clinopyroxene - brownish grains.

Hornblende - fibrous; uralitic.

Chlorite - green; partly replaces feldspar and pyroxene; some chlorite is penninite (berlin-blue interference color).

Biotite - green-brown; alteration of pyroxene.

Opaque minerals - needles and rods dispersed through rock.

Quartz - clear; interstitial to feldspar and pyroxene.

Gabbro

Sample No.: SR-34-79

Structure: Sill

Location: 34, Figure 4B.

Color: Grayish green

Texture: Medium-coarse grained; subophitic-ophitic, defined by a framework of plagioclase laths with interstices filled with pyroxene and other minerals.

Minerals: Plagioclase - (sodic) cloudy stubby to elongated laths with corroded edges; partly sericitized; twinned (albite-carlsbad).

Clinopyroxene - neutral; partly uralitized; alteration products are the following:

Hornblende

Biotite

Chlorite

Opaque minerals - magnetite-ilmenito-magnetite.

Apatite - tiny needles; accessory.

Relative Proportion: Plagioclase > pyroxene > alteration products of pyroxene > opaque minerals

Gabbro

Sample No.: SR-45-79

Structure: Sill

Location: 41, Figure 4B.

Color: Greenish gray

Texture: Medium to coarse grained; mafic minerals tend to occur in clumps.

Minerals: Plagioclase - mostly forms groundmass; occurs as small tightly interwoven laths subophitically

with pyroxene; cloudy; partly sericitized; twinned.

Clinopyroxene - (diopside; some augite) neutral, brownish to greenish; anhedral-irregularly shaped grains.

Chlorite - green; partly replaces feldspar and pyroxene; also forms patchy replacement of groundmass.

Hornblende - light greenish to brownish; occurs as alteration of pyroxene and also as separate grains.

Opaque minerals - magnetite-ilmenito-magnetite(?) forms skeletal masses associated with mafic minerals.

Apatite - tiny clear prisms.

Counts (140): Plagioclase, 57; pyroxene, 26; chlorite, 7; opaque minerals, 7; hornblende, 3.

Gabbro

Sample No.: SR-47A-79

Structure: Sill

Location: 42, Figure 4B.

Color: Grayish green

Texture: Coarse grained, subophitic-ophitic.

Minerals: Plagioclase - (oligoclase-andesine) small to large, anhedral-subhedral grains; twinned (albite type); poikilitically includes corroded pyroxene grains; partly sericitized.

Clinopyroxene - (diopside) neutral; anhedral-irregularly shaped grains; partly uralitized.

Chlorite - light green; partly replaced feldspar and pyroxene; also forms veinlets; some chlorite is penninite.

Hornblende - pale brown-green; partly replacement of pyroxene; also occurs as separate large grains.

Biotite - brown; replacement of pyroxene.

Opaque minerals - magnetite-ilmenito-magnetite.

Calcite - occurs in veinlets with chlorite; occasional.

Relative Proportion: Feldspar > pyroxene > chlorite > biotite > hornblende > opaque minerals > calcite.

Diabase

Sample No.: SR-52A-79

Structure: Sill

Location: 43, Figure 4B.

Color: Grayish green

Texture: Medium grained; subophitic.

Minerals: Plagioclase - (andesine - clear-cloudy laths (2 mm), twinned (carlsbad, albite and combined); partly sericitized.

Clinopyroxene - (diopside) neutral; anhedral-subhedral; twinned; partly uralitized.

Opaque minerals - magnetite-ilmenito-magnetite; occurs as irregularly shaped and skeletal masses; interstitial to feldspar and pyroxene; some leucoxene and sphene also present.

Hornblende - chlorite-biotite = alteration of pyroxene; chlorite also partly replaces plagioclase.

Epidote - trace.

Calcite - trace.

Counts (210): Feldspar, 59; pyroxene, 28; uralite, 8; opaque minerals, 4; other, 1.

Diabase

Sample No.: SR-52B-79

Structure: Sill

Location: 43, Figure 4B.

Color: Grayish green

Texture: Medium grained; subophitic.

Minerals: Plagioclase -

Clinopyroxene -

Hornblende -

Chlorite -

Biotite -

Opaque minerals -

Apatite -

Quartz -

The minerals are similar to sample SR-34-79; however, clinopyroxene is somewhat more uralitized and quartz is occasionally present.

Basalt

Sample No.: SR-73-79

Structure: Sill

Location: 51, Figure 4B.

Color: Grayish green

Texture: Fine grained; holocrystalline; subporphyritic with a few small (< 1 mm) corroded phenocrysts of plagioclase and clinopyroxene aset in a dense groundmass formed by the above two and other minerals.

Minerals: Plagioclase - occurs as lath-like phenocrysts and as microliths in groundmass; the latter is altered to grayish chloritic material.

Clinopyroxene - occurs as phenocrysts and tiny anedral grains in groundmass.

Opaque minerals - magnetite-ilmenito-magnetite(?) occurs as dust and small equant grains in groundmass.

Chlorite - occurs as replacement of pyroxene phenocrysts and groundmass.

Calcite - occasionally occurs with chlorite.

Relative Proportion: Plagioclase > pyroxene > opaque minerals > chlorite

Diabase

Sample No.: SR-89-79

Structure: Sill

Location: 58, Figure 4B.

Color: Grayish green.

Texture: Fine to medium grained; subophitic with densely bunched plagioclase laths (up to 1.5 mm long) enclosding large (± 2.5 mm) areas filled with clinopyroxene.

Minerals: Plagioclase - (sodic) cloudy, partly sericitized; twinned (albite type) laths.

Clinopyroxene - anhedral, twinned; partly replaced by uralitic mixture of hornblende and chlorite.

Opaque minerals - magnetite-ilmenito-magnetite; occur as small needles and irregular skeletal masses.

Hornblende -

Chlorite -

Apatite - needles; accessory.

Quartz - anhedral grains; accessory.

Relative Proportion: Plagioclase > clinopyroxene > uralitic mixture > opaque minerals > other.

C. Two Examples of Contact Metamorphic Rocks

Epidote Hornfels

Sample No.: SR-69-79

Occurrence: Inter-flow limestone intruded by a diabase sill; sample comes from 1/3 meter away from the contact.

Location: 49, Figure 4B.

Texture: Porphyroblastic.

Description: Consists of euhedral porphyroblasts of some epidote group mineral (epidote ?, zoisite ?) set in a fine-grained carbonate matrix (Fig. 62).

Pyroxene Hornfels

Sample No.: SR-96-79

Occurrence: Inter-flow limestone intruded by a diabase sill; sample comes exactly from the contact.

Location: 60, Figure 4B.

Texture: Porphyroblastic.

Description: Consists of large elongated radiating prisms of hedenbergite (green, twinned) set in a matrix consisting of small grains of plagioclase, tremolite-actinolite, diopside(?), epidote, quartz and coarse calcite (Fig. 63).

APPENDIX 6

Petrographic Summary of the Serpentinized Ultramafic Rocks Found in the Bela Ophiolites (based on 12 samples)

The commonly found ultramafic rocks (found as isolated masses or in melange horizons) are peridotite, harzburgite and pyroxenite. Often the rock is almost totally serpentinized and appears mottled, light green to dark green, greenish to brownish gray or black in color. It consists of a dense mesh or net-structured antigorite and/or serpophite (lizardite) with or without chrysotile veinlets. Serpentine also occurs as large (up to 1 cm), light green perfect pseudomorphs after pyroxene (bastite ?, see Fig. 58). Such grains show a silky appearance in hand specimen and also well preserved pyroxene cleavage. Relict pyroxene is occasionally present. Both clinopyroxene (diopside ?) and orthopyroxene (enstatite) are present though the latter was only rarely seen in the examined samples.

No relicts of fresh olivine were observed; however, serpentinized pseudomorphs with well preserved olivine fracture pattern are occasionally present.

Opaque material is ubiquitous and may be locally abundant. It may appear as fine dust sprinkled through the rock or form streaks, small veinlets, irregular nets, skeletal masses, patches and clusters. Most of it appears to be secondary magnetite and less commonly hematite; no chromite was positively identified.

Among other minerals found in the serpentinites, chlorite, tremolite-actinolite, biotite, and carbonate may be mentioned. Chlorite occurs as fine aggregate structures, flakes, or radiating fan-like fibrous bunches. In some chrysotile veinlets chlorite occurs along the edges. Tremolite-actinolite are occasionally observed as irregular areas in serpentinite and may be replaced by it. Biotite is rare. Carbonate is also rare and appears to accompany hematite in irregular fracture fillings.

APPENDIX 7

Petrographic Summary and Sedimentary Versus Tectonic Origin of the Serpentinite-Carbonate Breccias (Ophicalcite)

The ophicalcites consist largely of angular serpentinite clasts (up to a few meters long) embedded in a dominantly carbonate matrix.

Clasts

Serpentinite: These clasts are colorless to mottled green in color and subrounded, angular or irregular in shape; however, angular clasts are by far the most common; some clasts occur as platy chips, shards and rod-like masses. The clasts are made of antigorite-serpophite material with or without chrysotile veinlets; chrysotile clasts are also present. Commonly, clasts may be choked with opaque dust or a patchy network (hematite, magnetite), imparting a reddish-brown color to the rock in hand specimens. Calcite (mircrite/sparite) may replace serpentinite along fractures and grain edges; some clasts are totally replaced by calcite and heavily bordered by hematite; rarely talc also replaced serpentinite in fibrous aggregates.

Some reddish brown breccias and dense reddish gray rocks associated with them consist entirely of thoroughly carbonated serpentinite, and may show anostomosing network of fractures filled with serpentine and sparry calcite; the calcite veinlets may be up to 6 mm thick. In such rocks, despite thorough replacement, serpentine structure has been preserved and

is marked by a mosaic of small closely spaced triangular or polygonal areas occupied by hematite; the mosaic is defined by criss-crossing serpentine-calcite veinlets.

Pyroxene: Occasionally occurs as small (up to 0.4 mm long) relicts with serpentinite clasts and also separately; serpentinite pseudomorphs after pyroxene frequently exhibit well preserved cleavage. Most are probably after clinopyroxene as its relicts are relatively more common than those of orthopyroxene.

Opaque Minerals: Occur as angular irregularly shaped clasts (up to 1 mm in size) occasional.

Tremolite-nephrite(?): Occur as small rectangular clasts; tremolite was also seen to replace pyroxene in a few clasts; occasional.

Calcite: Sparry variety; clasts range up to a few millimeters in size.

Phlogopite(?): Elongated fibrous clasts; rare.

Rocks: Among these are included clasts of chert, altered basalt(?) and composite clasts of serpentinite + calcite + opaque material.

Matrix: The matrix consists mostly of carbonate material with minor clay and serpentinite particles; most carbonate is calcite which may be clear, reddish brown or grayish in color and mostly of non-ferrous variety; however, locally some ferroan calcite and minor dolomite also occurs as revealed by Dickinson's staining technique (see Hutchison, 1974; p. 25). Both micritic and sparry calcite is common and their mutual proportion is

variable. Some calcite occurs as tiny globular masses, aggregates and pelloids possibly of organic origin. Rarely, tiny forms, resembling those of foraminiferal tests may be present. The contacts between serpentinite clasts and matrix are usually sharp; however, calcite replacement may occur along clast edges. Both matrix and clasts may be cut by veinlets of opaque (hematite, magnetite) material, calcite, serpentinite and zoned calcite-serpentine veinlets.

Tectonic versus sedimentary origin: The serpentinite-carbonate breccias apparently give the impression of tectonically produced breccias, especially where they are deformed (i.e., subfoliated, foliated). Even the undeformed ones lack any convincing sedimentary feature (e.g., lamination, bedding, size sorting). However, such features are crudely developed and were occasionally observed in outcrop. This suggests that at least some breccias are of sedimentary origin; certain microscopic features also support this idea. In several cases, deformed serpentine clasts are embedded in totally undeformed calcite matrix as indicated by undisturbed cleavage traces and twin lamellae. Also some serpentinite clasts are coated by a thin calcite layer, itself enhanced by a dark border. The occurrence of carbonate material of probable biogenic origin in the matrix has already been mentioned. Therefore, it is concluded that some of these breccias are of sedimentary origin. The dominance of serpentinite clasts and their commonly angular shape indicates that such breccias are talus deposits.

Petrographic Description

Sample No.: 78-SR-28

Occurrence: Block in melange within ophiolites.

Location: 9, Figure 4B.

Consists of subrounded-angular clasts (mostly of serpentinite; up to several cm) set in a carbonate matrix.

Clasts: Serpentinite - mottled green or reddish brown in hand specimen; colorless-greenish in thin section; mainly mesh-textured antigorite and some serpophite with a few chrysotile and calcite veinlets; clasts include pseudomorphs after pyroxene (bastite ?); some clasts are partly replaced by calcite; clasts are fractured and heavily patched with and outlined by opaque material (hematitic).

Hematite - brown black; mostly within serpentinite clasts; also forms small clasts.

Pyroxene - relict orthopyroxene; occasional clast; relict clinopyroxene was observed in serpentinite clast.

Tremolite - nephrite(?); replace pyroxene and form a few rectangular clasts.

Matrix - mostly calcite with minor dolomite and some tiny clastic serpentinite; calcite is mostly micrite with some sparite; tiny globular masses of calcite and pelloids also present; veinlets of sparry calcite cut the rock; calcite also replaces serpentine clasts along edges.

Sample No.: 78-SR-38

Occurrence: Block in melange within ophiolites.

Location: 11, Figure 4B.

Consists of rounded to angular clasts (mostly of serpentinite; up to 1 cm long) set in a micritic carbonate matrix; most clasts are, however, angular.

Clasts: Serpentinite - similar to sample 78-SR-28; some clasts are made of cross-fiber chrysotile; relict orthopyroxene in one clast.

Opaque minerals - brown hematite and some magnetite occur as small grains (up to 0.5 mm) within serpentinite clasts; also occur as occasional angular or irregularly shaped clasts.

Calcite - sparry; clasts up to a few mm.

Matrix - consists mostly of grayish micritic and some sparry calcite with minor dolomite; some calcite is of ferroan variety; contains a few veinlets of sparry calcite.

Sample No.: SR-27-79

Occurrence: Block in melange within ophiolites.

Location: 32, Figure 4B.

Similar to above two samples; serpentinite clasts are up to several cm long and the matrix consists mostly of sparry calcite; some serpentinite clasts are totally replaced by calcite of reddish brown color; these are also choked with hematite; serpentinite structure is still preserved; hematite also forms a few small clasts (up to 1 mm long).

Sample No.: SR-28-79

Occurrence: Block in melange with ophiolites.

Location: Near 32, Figure 4B.

Color: Reddish brown

Consists of dense serpentinite (mainly chrysotile with some antigorite) cut by an intricate closely spaced polygonal network of thin calcite veinlets. Each polygon has black or brown core of hematite rimmed by chrysotile. The cores may have hollows filled with micritic calcite. Veinlets of hematite, calcite and serpentine also cut the rock.

Sample No.: SR-86-79

Occurrence: Boulder in melange within ophiolites.

Location: 56, Figure 4B.

Consists of clasts of serpentinite and (serpentinite + calcite + opaque material) set in a matrix of sparry calcite. Veinlets of calcite and zoned calcite/serpentine cut across the matrix and some clasts; also a single veinlet of talc(?) was noticed.

Clasts: Serpentinite - clasts (up to 1 cm) consist of mesh-textured antigorite and dense almost isotropic serpophite cut by chrysotile veinlets. Hematite dust and patchy network occurs in msot clasts; some clasts are coated with a thin calcite layer enhanced by a dark border.

Pyroxene - a few clasts of serpentinite pseudomorphs after pyroxene (bastite ?) with well preserved cleavage; relict orthopyroxene (enstatite) clast (0.4 mm)

also present.

Calcite - sparry variety; a few clasts.

Phlogopite(?) - a single clast (0.5 mm long).

Matrix - exclusively of calcite; mostly sparite with some globular aggregates and pelloids; one form showed chambers like a foraminiferal test; tiny chips of serpentinite and granules of opaque material are also present in matrix.

Sample No.: SR-101-79

Occurrence: Block in melange within ophiolites.

Location: 62, Figure 4B.

Consists of a highly fractured mass of thoroughly carbonated serpentinite with fractures filled with serpentine and sparry calcite (up to 6 mm thick) similar to sample SR-28-79.

APPENDIX 8

Petrographic Summary and Description of the Sedimentary (detrital) Serpentinites

Summary

These rocks consist of sandstones, pebble and boulder beds of greenish gray, reddish brown or brown color. They are texturally immature, i.e., poorly sorted and poorly bedded; some graded beds are apparent in outcrop; however, in thin section grading and lamination are poorly defined. Compositionally, these rocks are also immature and consist dominantly of serpentinite clasts and subordinate amounts of other minerals and rock clasts set in a carbonate matrix.

Clasts

Serpentinite: Brownish or grayish green in outcrop; in thin section colorless - brownish green, green or reddish brown; the latter probably due to iron oxide inclusions or pigment; may have mottled appearance. Clasts may be of clay/sand size (up to 2 mm) in fine-coarse grained lithic beds; (however, pebble-block size clasts also are abundant in outcrop). Clast shape commonly angular-subrounded; shards, rod-like, platy and irregularly shaped clasts also present. Mineralogically, mesh structured or fibro-lamellar antigorite most common with subordinate serpophite (lizardite); chrysotile veinlets may or may not be present. Opaque minerals (magnetite, hematite) occur as dust, trains, patches and veinlets

in serpentinite clasts. Some clasts may be heavily choked with opaques. Clasts may also be partly or wholly replaced by calcite and occasionally some unidentified clay minerals; replacement usually starts along clast edges or fracture fillings of calcite; some clasts, totally replaced by calcite, have left only ghosts marked by opaque material. Serpentinite clasts may be fractured or subfoliated.

Bastite(?): Serpentinite pseudomorphs after subhedral-euhedral pyroxene, often with well preserved cleavage occur either within serpentinite clasts or separately as individual clasts of tabular-rod-like shape; often sprinkled with opaque dust.

Unaltered pyroxene: Occasional relicts of ortho- and clinopyroxene found as anhedral or irregularly shaped grains.

Olivine: Rare. Found only as serpentine or calcite pseudomorphs of anhedral shape with preserved olivine-fracture pattern; occurs either within the serpentine clasts or as separate clasts.

Opaque minerals: Occur usually in serpentinite clasts or as irregularly shaped grains (up to 2 mm) in matrix; mostly magnetite and hematite; the latter may be reddish brown-black in color and is translucent or opaque. Some chromite grains also suspected but not confirmed.

Tremolite-actinolite: Occasional elongated tabular clasts.

Chlorite: Occasional fibrous, platy clasts.

Carbonate: Calcite (micrite and sparite) clasts of angular-subrounded and irregular shapes (± 1 mm size); hard to distinguish from

matrix unless edges coated with dark iron oxides; calcite also occurs as tiny (0.15 mm) globular aggregates possibly of organic origin; calcite and some dolomite occurs as tiny grains in fine equigranular beds.

Rock fragments: Occasional; may be up to a few mm in size and angular, subrounded or irregular outline; following types observed.

a) limestone - mixed micrite and sparite.

b) clasts of (serpentine/carbonate) rock, probably reworked material of host rock.

c) occasional angular clasts (up to 0.5 mm) of altered basalt and chert.

Matrix: Mostly micritic calcite; some replaced by sparite; colorless, grayish, reddish or brownish in color. Staining (Dickinson's method, Hutchison, 1974, p. 25) revealed that most calcite is nonferrous variety; however, ferroan calcite is locally present; sparite crystals may include tiny serpentine clasts; some serpentinite clasts may show a thin coating of crystalline calcite which itself is augmented with opaque border. Some micritic matrix appears to be an aggregate of tiny granules stained with iron oxides. Fine clasts of serpentinite also occur in the matrix. Veinlets of micritic-sparry calcite and occasionally chrysotile may cut across the matrix as well as clasts.

Petrographic Description

Lithic Sandstone

Sample No.: SR-19-79

Occurrence: Lenticular bed in a melange horizon within ophiolites.

Location: 29, Figure 4B.

Consists of serpentinite and other clasts (< 3 mm long) set in a calcite matrix.

Clasts: Serpentinite - colorless, brownish, greenish; up to 2.5 mm long; consist of antigorite and serpophite; may be partly replaced by calcite and clay minerals, especially along edges; some clasts are clustered with magnetite-hematite which also outline the clasts and fill fractures in them.

Pyroxene - occurs as serpentinized pseudomorphs (bastite ?) in serpentinite clasts; bastite also occurs as tabular rod-like clasts; clasts may be bent and show cleavage traces lined with opaque dust; fresh pyroxene occurs as occasional tiny clasts.

Opaque minerals - hematite and magnetite; occur as dust and small irregularly shaped clasts in matrix; some sphene.

Olivine(?) - clast of serpentinized material with olivine-like fractures.

Chlorite - occasional; small green clasts.

Tremolite-actinolite - elongated tabular clasts of green-brownish color.

Rock clasts - (a) limestone; micrite-sparite;
(b) reworked host rock; serpentinite + calcite clasts; some coated with iron oxide (Fig. 60).

Matrix - mainly calcite; silt-sand size; calcite also forms veinlets.

Relative Proportion: Clasts (mainly serpentinite), ± 40%
Matrix, ± 60%.

Lithic Sandstone

Sample No.: SR-20-79

Occurrence: Thin lenticular bed in melange horizon within ophiolites.

Location: 30, Figure 4B.

Consists of serpentinite and other clasts set in a fine-grained matrix of calcite; similar to sample SR-19-79.

Clasts: Serpentinite - up to 2.2 mm long.

Calcite - (± 1 mm long).

Bastite(?) - rod-like; with excellent cleavage traces.

Opaque minerals _ (0.5 mm long); hematite-magnetite.

Matrix - micritic calcite; some iron oxide stained. Calcite also boasts some serpentinite clasts; the coating is itself outlined by a dark border.

Lithic Sandstone

Sample No.: SR-35-79

Occurrence: Lenticular bed in melange horizon with ophiolites.

Location: 35, Figure 4B.

Consists of serpentinite, and clasts of opaque minerals (up to 2 mm) set in a fine-grained carbonate matrix. Both calcite and dolomite are present. Carbonate material also occurs as tiny (± 0.15 mm) globular aggregates (organic ?); opaque dust fills in the inter-globule space and enhances their appearance. The opaque material is mostly hematite and magnetite; however, some chromite grains were suspected. Calcite and serpentinite veinlets are also present in the rock; it consists of about 60% carbonate and 40% serpentinite and opaque material.

Serpentinite Pebble Bed

Sample No.: SR-40-79

Occurrence: Part of a block of serpentinite boulder bed in Kanar Melange (Fig. 14).

Location: 39, Figure 4B.

Consists of clasts of serpentinite (up to 8 mm long) and other material set in a sand-size calcite matrix.

Clasts: Serpentinite - angular-rounded clasts and shards; clasts consist mostly of mesh structured antigorite and some almost isotropic dense serpophite; relict pyroxene is occasionally present; also some bastite(?) is present. Some clasts include calcite pseudomorphs of some mafic minerals which are dusted with opaque material; chrysotile veinlets are present in some clasts. Clasts may be replaced and veined by calcite along edges.

Pyroxene - a few serpentinite pseudomorphs (bastite) occur as tabular clasts; also a single fresh clinopyroxene clast was noted.

Opaque minerals - hematite-magnetite occur as irregularly shaped clasts; also as dust, trains and patches in serpentinite clasts.

Matrix - consists mainly of grayish nonferroan calcite, with some ferroan calcite; both micrite and sparite are present.

APPENDIX 9

Petrographic Description of Some Exotic Rocks Found with Inter-ophiolite Melange Horizons

Pegmatitic Gabbro

Sample No.: SR-26-79

Occurrence: Block

Location: 32, Figure 4B.

Color: Green

Minerals: Plagioclase (Labradorite) - subhedral-euhedral; twinned (albite type); largely sausuritized.

Clinopyroxene -

Apatite -

Sphene -

Opaque minerals and sphene -

Marble

Sample No.: SR-32-79

Occurrence: Boulder

Location: 34, Figure 4B.

Subfoliated rock with deformed recrystallized calcite, some green pleochroic mica (biotite ?) and opaque material.

Schistose Clastic Rock

Sample No.: SR-54-79

Occurrence: Block

Location: 44, Figure 4B.

Consists of clasts of biotite, apatite, tremolite, plagioclase, carbonate, serpentinite, opaque material and (pyroxene + serpentinite) set in a greenish clayey (chlorite ?) calcareous matrix. Calcite veinlets are present. A few clasts of reworked host rock(?) are present.

Meta-gabbro

Sample No.: SR-60-79

Occurrence: Boulder

Location: 47, Figure 4B.

Subfoliated rock consisting of crusted and poorly segregated minerals.

Minerals: Plagioclase (andesine-labradorite) - anhedral-eudral, twinned; partly sericitized.

Clinopyroxene (diopside ?) - anhedral, partly uralitized grain.

Hornblende - uralitic; replaces pyroxene.

Chlorite -

Sericite/Muscovite(?) - occurs in crused material and in feldspar.

Amphibolite

Sample No.: SR-62-79

Occurrence: Boulder

Location: Near 47, Figure 4B.

Foliated rock with segregated arrangement of minerals (Fig. 61).

Minerals: Hornblende - green to brown; pleochroic, prismatic crystals; most abundant.

Plagioclase -

Opaque minerals - magnetite; some sphene.

Apatite -

Chlorite -

Epidote(?) -

APPENDIX 10

Chemical Analyses

A. Atomic Absorption and Neutron Activation Analysis

1. Atomic Absorption Analysis

A total of thirty-nine samples were analyzed for SiO_2, Al_2O_3, total Fe (as Fe_2O_3), MgO, CaO, Na_2O, K_2O, MnO, and TiO_2, using a Perkin Elmer 403 atomic absorption spectrophotometer. These samples plus five standards and three blanks were prepared for analysis using the method of Medlin, Suhr, and Bodkin (1969). The standards used were: USGS igneous rock standards W-1, G-2, AGV-1, BCR-1 and PCC-1. For all standards except W-1, analyses given by Abbey (1973) were followed. For W-1, the following data, as communicated by Professor Attila I. Kilinc of the Department of Geology, University of Cincinnati, were used: SiO_2 (52.6%), Al_2O_3 (14.94%), Fe_2O_3 (11.06%; total iron), MgO (6.52%), CaO (10.92%), Na_2O (2.15%), K_2O (0.6%), TiO_2 (1.08%), MnO (0.17%).

Samples were crused with a jaw crusher and then ground to -200 mesh using a shatterbox with tungsten carbide grinding plates. The samples next were thoroughly homogenized and then heated to 110°C in a furnace and stored in a desiccator so that they were thoroughly dry. A 100 mg portion of these samples was mixed with 500 mg of Lithium metaborate and then placed into preignited graphite crucibles and fused for 15 minutes at 1000°C in a muffle furnace. The crucibles were removed from the furnace,

swirled to collect uncoalesced beads and the molten material was poured into a 200 ml polypropyene beaker containing 40 ml of a 4 percent nitric acid solution. This solution was covered to reduce evaporation and stirred with a teflon coated magnetic stirrer until all solids were dissolved. This final solution was then transferred to clean 50 ml soda-lime glass bottles with plastic stoppers. Each 5 ml of this sample solution was mixed with 35 ml of a one percent lanthanum nitrate solution and this mixture was used for analysis of all oxides except Na_2O and K_2O. Na_2O and K_2O were analyzed using a solution prepared by diluting the sample solution 1:20 with distilled deionized water.

Five standards and three blanks were used to calibrate the instrument. The standards were regularly checked for variation due to electronic drift of the instrument during the analyses.

2. Neutron Activation Analysis

Twenty rock samples were analyzed for 19 trace elements: Ba, Cu, Cr, Cs, Hf, Ni, Rb, Sc, Ta, Th, U and REE (La, Ce, Nd, Sm, Eu, Tb, Yb, Lu). The samples were sent to the Phoneix Memorial Laboratory of the University of Michigan at Ann Arbor and were analyzed by neutron activation techniques.

B. Table Presenting Analytical Data

[All data are in weight percent unless otherwise stated. Numbers following sign '<' mark the neutron activation lower detection limit.]

1. Mor Intrusives

	SR-5-79	SR-9-79	SR-11-79	SR-82-79	SR-95-79	77-SA-4	77-SA-6
SiO_2	37.5	45.6	42.9	47.3	42.2	38.6	37.9
Al_2O_3	11.6	14.4	12.6	15.8	13.7	14.5	9.8
Fe_2O_3*	12.6	6.6	11.1	11.1	12.3	14.3	12.0
MgO	8.4	3.31	7.4	5.9	7.0	8.75	9.4
CaO	18.6	12.3	15.1	9.2	13.7	8.4	14.3
Na_2O	1.6	6.2	2.9	4.8	2.6	1.4	1.0
K_2O	1.1	0.1	0.1	0.3	0.2	0.1	1.0
MnO	0.21	0.15	0.12	0.24	0.16	0.08	0.16
TiO_2	3.5	2.5	3.0	2.7	3.0	3.5	3.1
Total	95.11	91.16	95.22	97.22	94.86	89.63	88.66
$Na_2O + K_2O$	2.7	6.3	3.0	5.1	2.8	1.5	2.0
FeO*	11.34	5.94	9.99	9.99	11.07	12.87	10.8
FeO*/MgO	1.35	1.8	1.35	1.7	1.58	1.47	1.15

* = Total iron

Mor Intrusives (continued)

	SR-5-79	SR-11-79	SR-82-79	SR-95-79
Ba (ppm)	892.63	<124.34	244.9	174.67
Co (ppm)	48.53	42.727	42.226	49.44
Cr (ppm)	524.52	327.3	245.89	282.45
Cs (ppm)	3.98	<0.42	<0.4	<0.45
Hf (ppm)	8.12	5.74	7.445	6.658
Ni (ppm)	173.04	89.803	83.824	114.65
Rb (ppm)	43.784	<30.5	<30.4	<32.99
SC (ppm)	27.845	33.994	23.984	35.313
Ta (ppm)	4.822	2.679	4.228	3.803
Th (ppm)	9.745	6.738	12.51	9.178
U (ppm)	3.007	1.718	3.03	1.183
REE (ppm)				
La	88.751	41.445	69.185	66.642
Ce	177.4	60.77	137.52	133.5
Nd	100.84	51.727	76.966	64.574
Sm	14.166	8.273	10.228	9.623
Eu	4.584	2.674	3.411	3.053
Tb	<0.3	2.107	<0.276	1.912
Yb	2.328	1.637	2.705	1.9
Lu	0.237	0.27	0.319	0.236

2. Porali Conglomerate

	SR-1-79	SR-3-79	SR-7-79	SR-8-79	SR-81-79	SR-90-79	SR-4-79#	SR-92-79#
SiO_2	44.7	46.5	43.2	43.8	46.2	68.1	47.4	47.1
Al_2O_3	15.78	13.68	12.34	14.43	14.39	14.48	16.2	15.3
Fe_2O_3*	11.8	11.6	13.8	10.6	11.4	5.9	11.0	10.9
MgO	4.39	4.7	4.95	4.51	4.64	2.96	5.1	6.4
CaO	12.3	15.4	12.5	14.9	11.5	1.8	7.8	10.9
Na_2O	3.77	3.57	2.54	3.51	2.8	5.1	3.3	1.5
K_2O	2.55	1.28	0.68	1.89	3.38	0.29	5.17	3.9
MnO	0.25	0.13	0.18	0.13	0.21	0.00	0.2	0.19
TiO_2	3.4	3.8	3.8	3.7	3.8	1.2	2.8	3.3
Total	98.94	100.66	93.99	97.47	98.32	99.83	98.97	99.49
$Na_2O + K_2O$	5.95	4.85	3.22	5.4	6.18	5.39	8.47	5.4
FeO*	10.62	10.47	12.42	9.54	10.26	5.3	9.9	9.8
FeO*/MgO	2.42	2.23	2.51	2.12	2.21	1.79	1.94	1.53

* = Total iron

= Dikes in conglomerate; clast samples are unmarked.

Porali Conglomerate (continued)

	SR-1-79	SR-3-79	SR-7-79	SR-81-79	SR-4-79#
Ba (ppm)	856.06	961.13	464.17	1121.7	1097.5
Co (ppm)	34.179	41.571	43.002	32.645	31.47
Cr (ppm)	8.345	8.267	61.342	27.7	7.894
Cs (ppm)	0.914	3.849	0.44	4.842	1.936
Hf (ppm)	7.59	8.121	6.489	7.35	8.289
Ni (ppm)	<51.0	<53.48	75.872	<56.9	<60.5
Rb (ppm)	43.842	32.931	88.665	86.671	99.622
Sc (ppm)	10.631	19.31	21.756	18.878	18.557
Ta (ppm)	7.356	8.249	4.343	6.229	4.551
Th (ppm)	16.935	11.008	9.02	11.851	9.013
U (ppm)	4.423	3.8039	1.803	3.184	2.514
REE (ppm)					
La	110.12	80.4	63.604	80.824	60.902
Ce	219.32	177.8	128.08	164.97	128.92
Nd	119.24	87.917	67.341	67.145	69.79
Sm	13.927	11.775	6.83	11.058	11.64
Eu	4.819	4.42	3.316	3.801	4.082
Tb	1.955	2.196	1.868	1.343	1.907
Yb	3.401	3.075	2.466	2.701	3.062
Lu	0.302	0.246	0.248	0.295	0.356

= Dike in conglomerate; clast samples are unmarked.

3. Bela Volcanics

	SR-2-79	SR-16-79	SR-30-79	SR-37-79	SR-42-79	SR-43-79
SiO_2	44.5	49.8	50.9	51.2	51.4	52.2
Al_2O_3	10.8	14.4	13.8	16.4	13.4	13.6
Fe_2O_3*	10.2	13.5	11.0	11.1	13.4	12.4
MgO	5.6	6.9	6.7	6.6	6.2	5.9
CaO	15.7	9.6	9.5	7.5	11.6	9.2
Na_2O	3.5	2.5	3.6	4.0	2.1	2.8
K_2O	0.4	0.4	0.3	0.2	0.1	0.5
MnO	0.16	0.2	0.8	0.4	0.22	0.21
TiO_2	2.7	2.0	2.4	2.1	2.0	2.2
Total	93.56	99.3	99.0	99.5	100.42	99.01
$Na_2O + K_2O$	3.9	2.9	3.9	4.2	2.2	3.3
FeO*	9.18	12.06	9.9	9.99	12.06	11.16
FeO*/MgO	1.64	1.75	1.48	1.51	1.95	1.89
Fe*	7.13	9.37	7.69	7.76	9.37	8.67
Mg	3.38	4.16	4.04	3.98	3.74	3.56
Fe*/Mg	2.11	2.25	1.9	1.95	2.5	2.43

*Total iron

3. Bela Volcanics (continued)

	SR-68-79	SR-88-79	SR-99-79	SR-104-79	SR-105-79	78-SR-42
SiO_2	46.7	50.3	52.8	49.2	51.5	50.6
Al_2O_3	14.7	15.7	13.0	13.8	14.4	14.9
Fe_2O_3*	13.5	12.7	12.6	13.2	12.1	11.5
MgO	7.5	6.1	5.7	6.64	5.82	6.54
CaO	8.5	9.2	10.5	8.9	10.5	10.1
Na_2O	3.4	2.3	2.9	3.1	2.6	3.2
K_2O	0.4	0.1	0.3	0.2	0.2	0.6
MnO	0.15	0.2	0.18	0.21	0.19	0.18
TiO_2	2.1	2.2	2.2	2.3	1.9	1.8
Total	96.95	98.8	100.18	97.55	99.21	99.42
$Na_2O + K_2O$	3.8	2.4	3.2	3.3	2.8	3.8
FeO*	12.06	11.43	11.34	11.88	10.89	10.35
FeO*/MgO	1.61	1.88	1.99	1.79	1.87	1.58
Fe*	9.37	8.88	8.81	9.23	8.46	8.04
Mg	4.52	3.68	3.44	4.00	3.51	3.94
Fe*/Mg	2.07	2.41	2.56	2.3	2.41	2.04

*Total iron

3. Bela Volcanics (contined)

	SR-16-79	SR-30-79	SR-88-79	SR-99-79	SR-104-79	78-SR-42
Ba (ppm)	<138.28	<141.99	<130.73	<131.14	<137.9	225.89
Co (ppm)	51.106	53.072	44.426	43.08	46.8	42.71
Cr (ppm)	142.27	81.308	114.75	135.1	115.43	116.12
Cs (ppm)	<0.42	<0.49	<0.45	<0.46	<0.48	<0.47
Hf (ppm)	3.147	3.071	3.285	2.747	3.002	2.711
Ni (ppm)	71.94	<80.25	<74.69	98.24	70.99	80.48
Rb (ppm)	<35.01	<35.0	<32.6	<32.9	<34.67	<32.9
Sc (ppm)	42.075	39.818	35.29	35.235	37.86	32.9
Ta (ppm)	0.865	0.533	0.984	0.59	0.774	0.92
Th (ppm)	<0.582	0.648	0.808	0.949	0.795	0.856
U (ppm)	<0.63	<0.65	<0.53	<0.61	<0.57	<0.64
REE (ppm)						
La	10.651	9.61	12.304	10.572	10.922	8.852
Ce	24.684	26.75	31.868	27.826	25.36	18.719
Nd	<36.141	<37.18	<34.168	43.305	<36.28	<36.15
Sm	4.86	5.05	5.322	4.759	4.854	4.06
Eu	1.91	2.021	2.032	1.902	1.885	1.605
Tb	2.433	2.44	2.047	1.258	2.08	1.19
Yb	1.518	1.724	1.857	1.815	1.63	1.72
Lu	0.43	0.435	0.432	0.41	0.349	0.336

4. Bela Intrusives

	SR-10-79	SR-13-79	SR-14-79	SR-21-79	SR-33-79	SR-34-79
SiO_2	46.1	50.5	41.8	50.1	47.9	47.5
Al_2O_3	15.0	14.2	12.1	13.0	14.4	13.7
Fe_2O_3*	15.0	13.9	10.7	15.2	15.5	15.3
MgO	5.3	5.7	7.5	5.7	6.1	5.4
CaO	8.2	8.4	8.6	8.2	7.3	8.0
Na_2O	3.3	2.8	2.8	3.1	3.0	3.8
K_2O	0.2	0.7	0.8	0.9	0.6	1.3
MnO	0.65	0.18	0.18	0.23	0.32	0.25
TiO_2	3.3	2.3	1.5	3.0	3.4	3.3
Total	97.05	98.68	85.98	99.43	98.52	98.55
$Na_2O + K_2O$	3.5	3.5	3.6	4.0	3.6	4.1
FeO*	13.5	12.5	9.63	13.68	13.95	13.77
FeO*/MgO	2.55	2.19	1.29	2.4	2.29	2.55
Fe*	10.49	9.71	7.49	10.63	10.84	10.7
Mg	3.19	3.44	4.52	3.44	3.68	3.25
Fe*/Mg	3.29	2.82	1.66	3.09	2.94	3.29

*Total iron

4. Bela Intrusives (continued)

	SR-45-79	SR-47A-79	SR-52-79	SR-73-79	SR-79-79	78-SR-52
SiO_2	49.3	53.4	46.4	52.0	50.5	49.5
Al_2O_3	13.9	15.9	14.7	13.5	15.3	15.5
Fe_2O_3*	14.9	8.4	14.6	12.8	12.8	12.7
MgO	6.1	6.3	6.41	6.5	6.13	6.8
CaO	10.1	8.3	8.2	7.5	9.6	10.0
Na_2O	3.6	4.0	5.0	3.2	2.8	2.7
K_2O	0.7	0.3	1.2	0.2	0.5	0.3
MnO	0.2	0.18	0.18	0.3	0.17	2.1
TiO_2	2.6	1.1	2.5	2.2	1.7	2.1
Total	101.4	97.88	99.19	98.2	99.5	99.82
$Na_2O + K_2O$	4.3	4.7	6.2	3.4	3.3	3.0
FeO*	13.4	7.56	13.14	11.52	11.52	11.43
FeO*/MgO	2.2	1.2	2.05	1.78	1.88	1.68
Fe*	10.41	5.88	10.21	8.94	8.95	8.89
Mg	3.68	3.8	3.86	3.92	2.7	4.1
Fe*/Mg	2.83	1.55	2.64	2.28	2.42	2.17

*Total iron

Bela Intrusives (continued)

	SR-14-79	SR-21-79	SR-34-79	SR-45-79	SR-73-79
Ba (ppm)	173.28	<108.7	352.89	<141.4	130.28
Co (ppm)	50.874	46.6	43.886	49.53	42.522
Cr (ppm)	432.22	28.134	26.404	8.884	136.12
Cs (ppm)	<0.51	<0.46	1.57	<0.42	<0.44
Hf (ppm)	2.375	6.282	5.078	2.65	4.273
Ni (ppm)	149.71	<61.0	<64.15	<80.8	132.21
Rb (ppm)	<36.23	<34.24	<34.8	<36.0	<31.9
Sc (ppm)	46.611	35.88	30.98	41.752	37.294
Ta (ppm)	0.401	1.204	0.928	0.995	0.849
Th (ppm)	0.962	2.615	2.85	0.908	1.345
U (ppm)	<0.66	0.614	<0.59	<0.68	<0.61
REE (ppm)					
La	10.657	23.99	28.446	12.336	16.48
Ce	30.536	58.13	69.806	33.08	41.124
Nd	42.285	51.671	47.235	<32.54	39.06
Sm	4.784	9.036	9.998	5.907	6.4
Eu	1.623	3.004	3.31	2.02	2.39
Tb	<0.36	2.802	1.593	2.804	1.766
Yb	1.85	3.314	2.686	1.937	2.45
Lu	0.409	0.693	0.475	0.44	0.502

C. Accuracy of Data

Two Measures were Taken to Judge the Accuracy of Data

1. The U.S.G.S. rock standard BCR-1 was prepared in duplicate solutions one of which was treated as an unknown during the atomic absorption analysis for the major elements. A comparison of the obtained results with the standard analyses of BCR-1 (Abbey, 1973) is presented in Table I.

2. The Phoenix Memorial Laboratory also reported total Fe, Na and K contents of twenty sample besides their trace element content. The total Fe, Na and K contents of the same samples, obtained by writer's atomic absorption analyses, are compared with the laboratory results in Table II.

Table I: Analytical comparison for standard BCR-1; (A) after Abbey (1973); (B) writer's atomic absorption analysis.

	A	Number of Observations	Mean(B)	Difference
SiO_2	54.85	10	56.3	1.45
Al_2O_3	13.68	10	13.5	0.18
Fe_2O_3*	13.52	10	13.6	0.08
MgO	3.49	10	3.7	0.21
CaO	6.98	10	7.3	0.32
Na_2O	3.92	10	3.4	0.11
K_2O	1.68	10	1.7	0.02
TiO_2	2.22	10	2.3	0.08
MnO	0.19	10	0.22	0.03

*Total iron

Data in weight percent

Table II. Analytical comparison of Na, K and Fe data (weight percent) for 20 samples; (A) writer's atomic absorption analyses; (B) data reported by Phoenix Memorial Laboratory, University of Michigan (Neutron Activation Analyses).

Sample No.	Na			K			Fe		
	A	B	A-B	A	B	A-B	A	B	A-B
Mor Intrusives									
SR-5-79	1.18	1.1	0.08	1.1*	<1.5	--	8.81	8.4	0.41
SR-11-79	2.15	2.07	0.08	0.1*	<1.5	--	7.76	7.44	0.32
SR-82-79	3.56	3.48	0.08	0.3*	<1.9	--	7.76	7.7	0.06
SR-95-79	1.92	1.82	0.1	0.2*	<1.7	--	6.6	7.84	0.76
Porali Conglomerate									
SR-1-79	2.8	3.06	-0.26	2.12	2.18	-0.06	8.25	7.81	0.44
SR-3-79	2.65	2.77	0.12	1.28*	<2.0	--	8.14	8.06	0.08
SR-4-79	2.45	2.34	0.11	4.3	4.29	0.01	7.69	7.67	0.02
SR-7-79	1.88	1.77	0.16	0.68*	<1.74	--	9.65	9.19	0.46
SR-81-79	2.08	2.18	-0.1	2.8	2.55	0.25	7.97	7.4	0.57
Bela Volcanics									
SR-16-79	1.85	1.69	0.16	0.4*	<1.0	--	9.37	9.52	-0.15
SR-30-79	2.67	2.6	0.07	0.3*	<1.2	--	7.69	8.92	-1.23
SR-88-79	1.7	1.56	0.14	0.1*	<1.0	--	8.88	8.52	0.36
SR-99-79	2.15	2.00	0.15	0.3*	<1.1	--	8.81	8.71	0.1
SR-104-79	2.29	2.1	0.19	0.2*	<1.2	--	9.23	9.02	0.21
78-SR-42	2.37	2.26	0.11	0.6*	<1.1	--	8.04	7.82	0.22
Bela Intrusives									
SR-14-79	2.07	1.5	0.57	0.8*	<1.1	--	7.49	8.72	-0.23
SR-21-79	2.29	2.07	0.22	0.9*	<1.3	--	10.63	11.24	-0.61
SR-34-79	2.81	2.73	0.08	1.3*	<1.5	--	10.7	10.73	-0.03
SR-46-79	2.67	2.58	0.09	0.7*	<1.5	--	10.41	10.27	0.14
SR-73-79	2.37	2.25	0.12	0.2*	<1.3	--	8.94	8.9	0.04

*K_2O content; no comparison made because the laboratory reported only the lower detection limit marked by the numbers with sign (<).

GEOLOGICAL M
OF THE
WAYARO QUADRANGLE

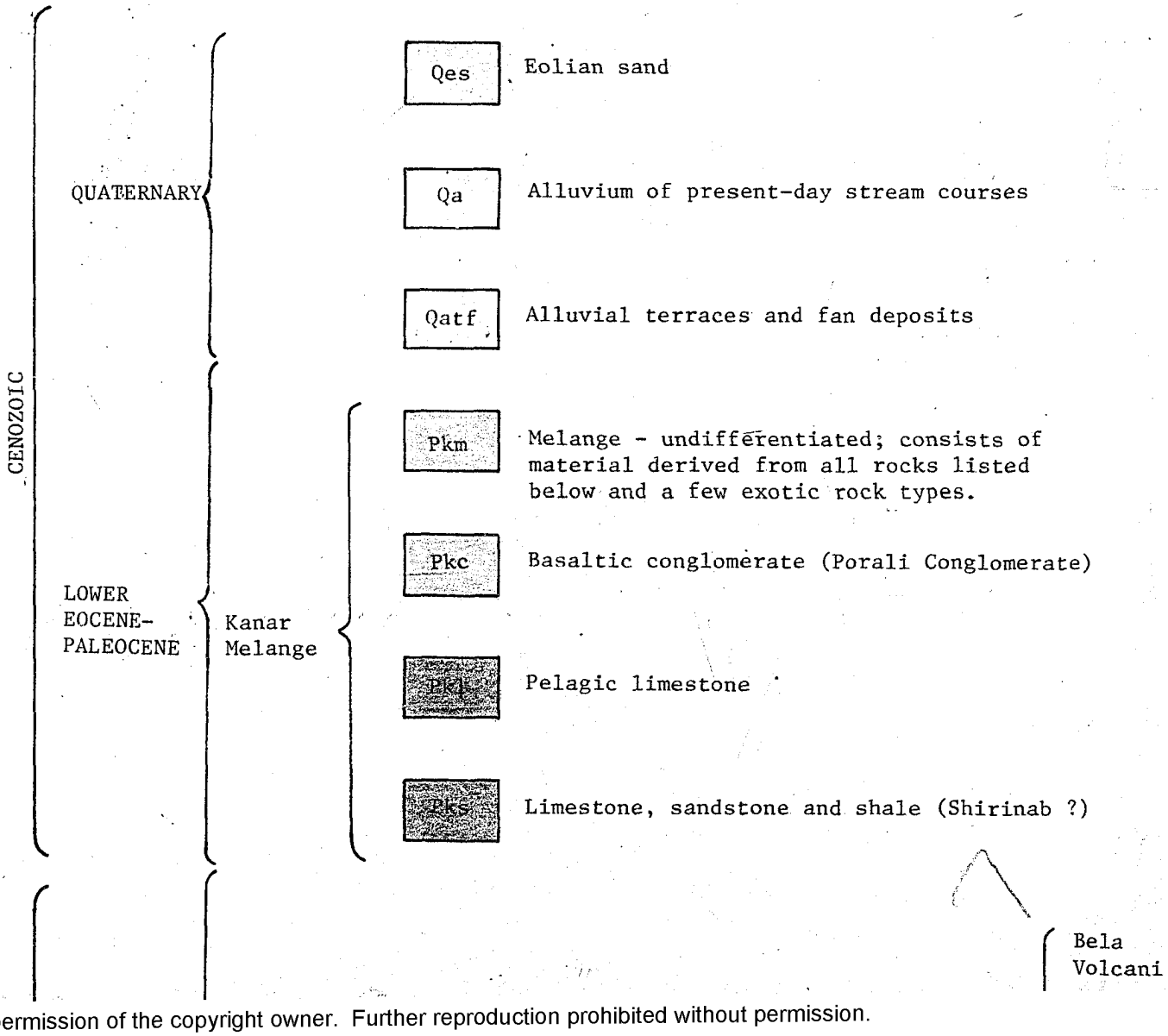

AL MAP
E
NGLE, PAKISTAN

ourses

ts

ists of
listed
s.

nglomerate)

hirinab ?)

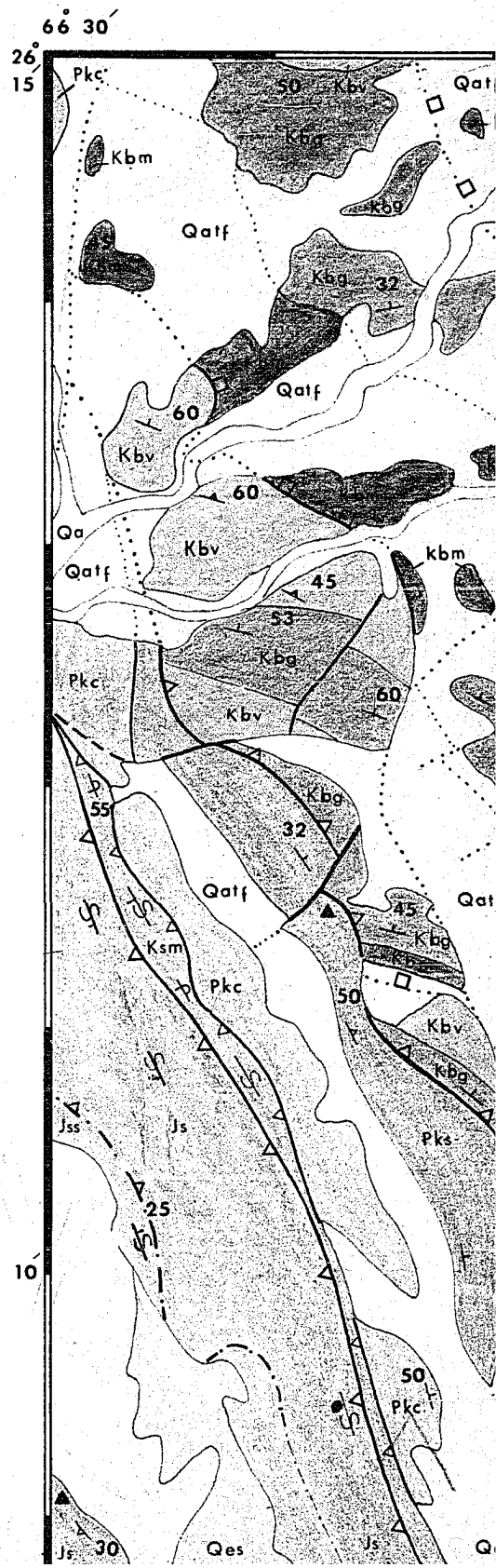

Bela Volcanics

Kbv | Kb vs

a b

a: Basaltic pillow lavas and associated marine limestone, mudstone, shale and chert. b: Similar sedimentary

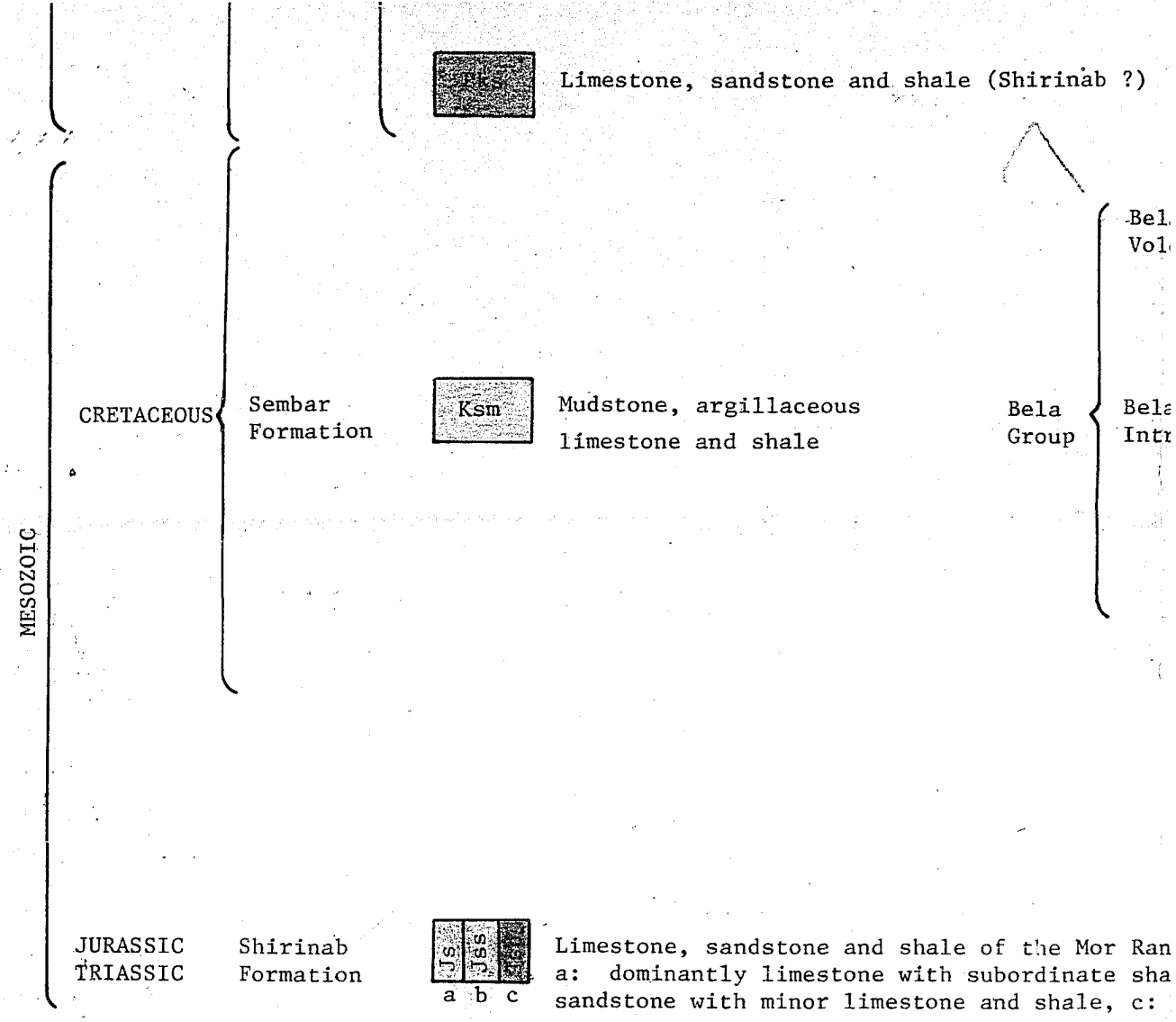

irinab ?)

ela
roup

Bela Volcanics

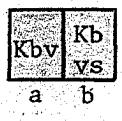

a: Basaltic pillow lavas and associated marine limestone, mudstone, shale and chert. b: Similar sedimentary rocks without lavas.

Bela Intrusives

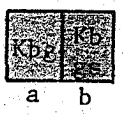

a: Diabase-gabbro sills and associated marine limestone, mudstone, shale and chert. b: Similar sedimentary rocks without sills.

Melange - serpentinized ultramafic rock, serpentinite-carbonate-mud breccia, basaltic lava, gabbro chert, sandstone, shale, limestone, etc. ● : Small exposures of serpentinite-bearing rocks.

he Mor Range and Piaro Ridge
dinate shale, b: dominantly
shale, c: basaltic sill.

d anticline

ce of plunging anticline refolding earlier
s

axial trace

axial trace with plunge

ılt; dashed where interpreted, dotted
ealed

p fault; dashed where interpreted,
re concealed

undetermined sense of movement

tact; dashed where interpreted, dotted
ealed

l contact

ble contact (tectonized)

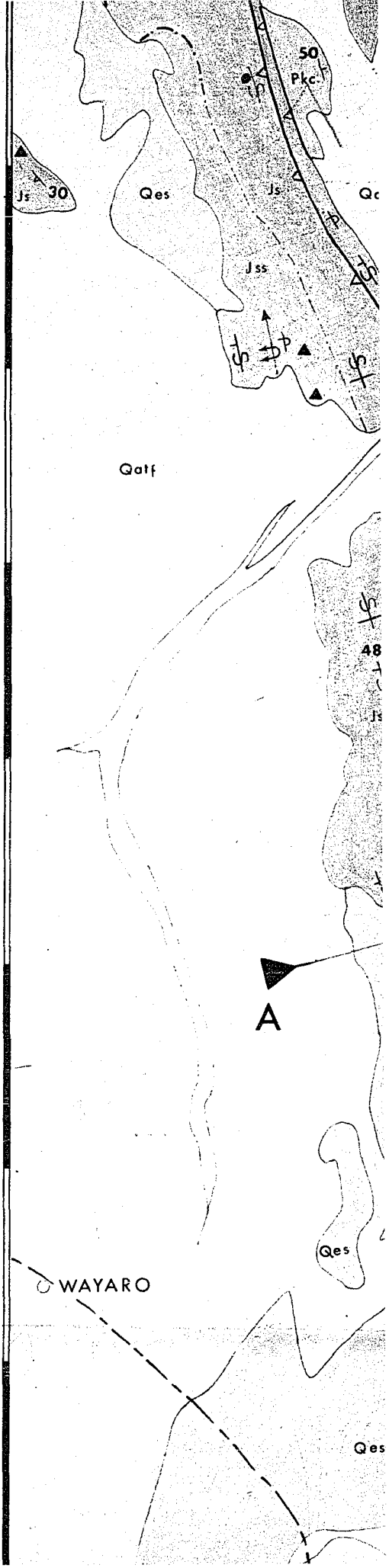

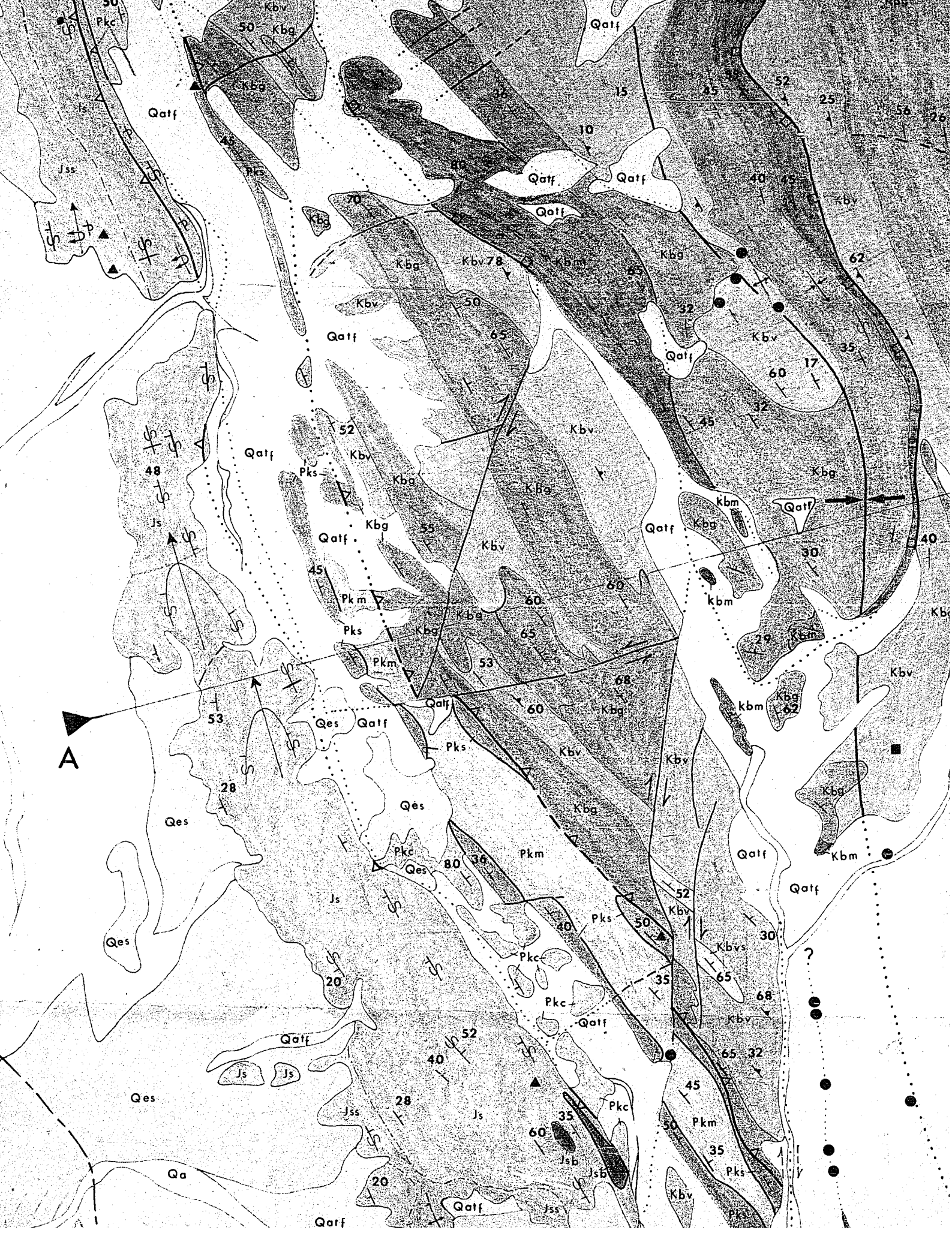

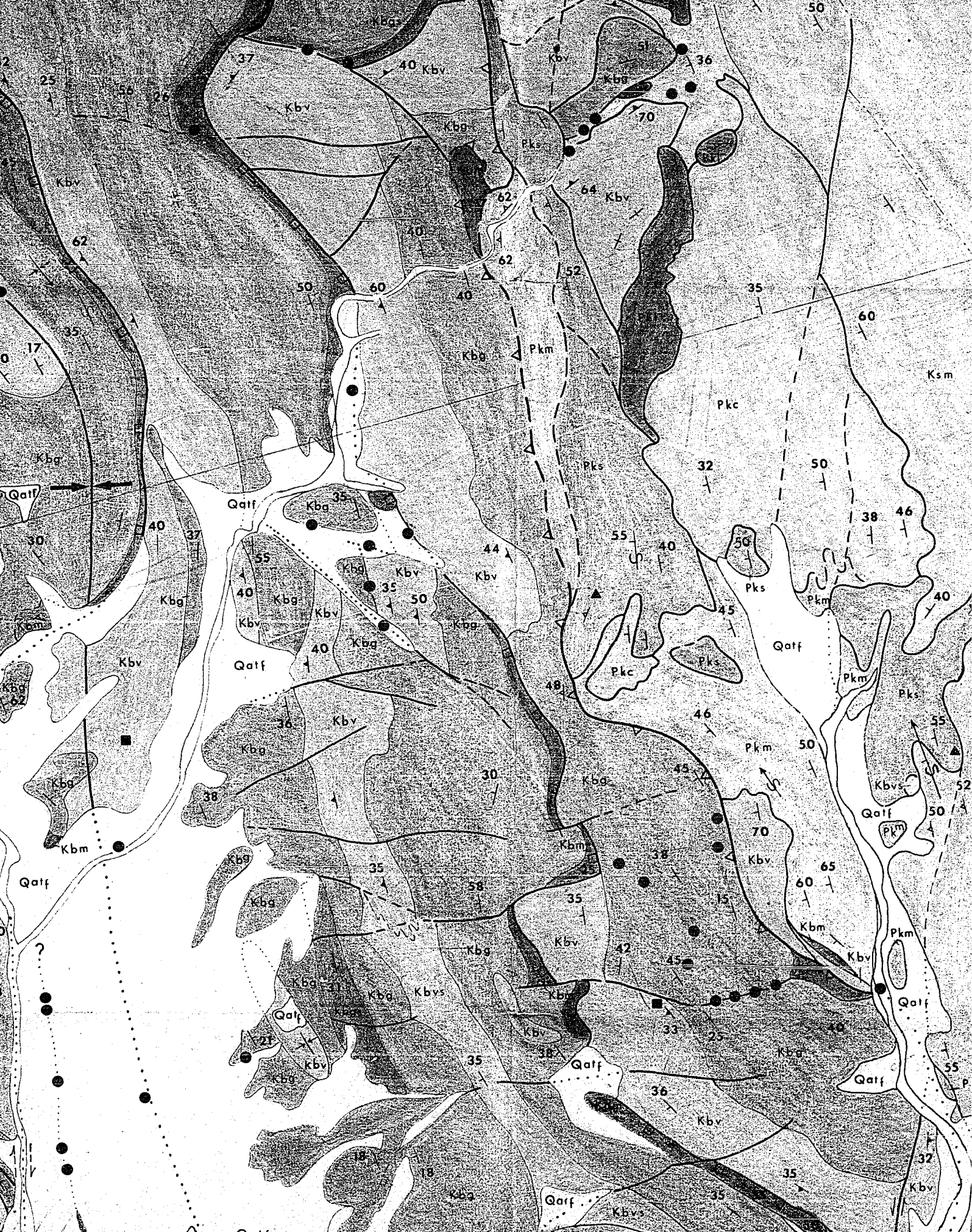
Kbg
Kbv
Kbvs
Kbm
Pks
Pkm
Pkc
Ksm
Qatf
Reproduced with permission of the copyright owner. Further reproduction prohibited without permission.

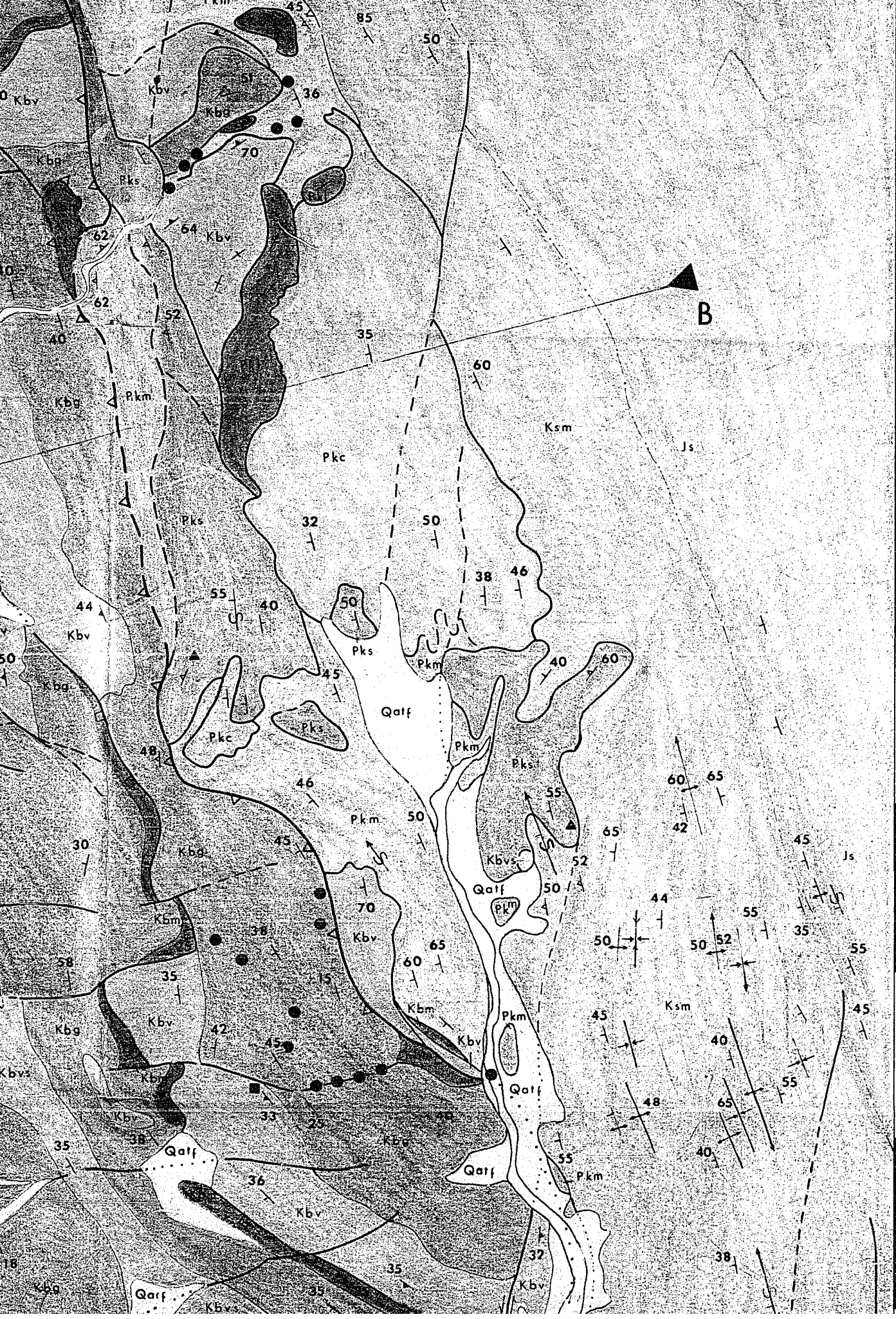

Inverted beds

Horizontal beds

Pillow facings

Foliation or disturbed bedding

Small scale complex folds with:

Inclined axial planes

Horizontal axial planes

Vertical axial planes

Anticlinal axial trace

Anticlinal axial trace with plunge

Synclinal axial trace

Synclinal axial trace with plung

Thrust-fault; dashed where inter
where concealed

Strike-slip fault; dashed where
dotted where concealed

Fault with undetermined sense of

Normal contact; dashed where int
where concealed

Gradational contact

Unconformable contact (tectonize

Barite, galena, pyrite, hematite
showing)

Copper, iron, manganese (prospec

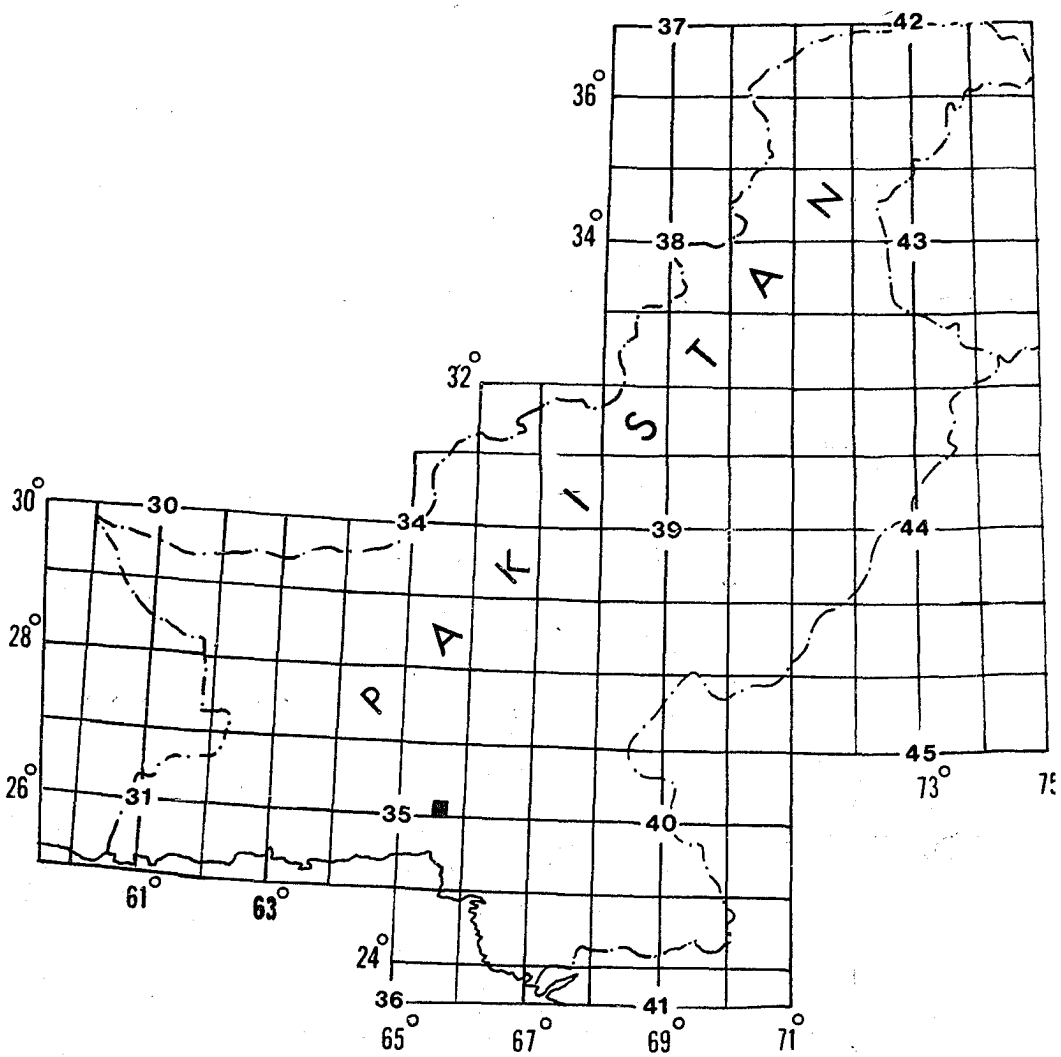

ging anticline refolding earlier

ce

ce with plunge

d where interpreted, dotted

dashed where interpreted,
led

ined sense of movement

hed where interpreted, dotted

act (tectonized)

rite, hematite (prospect or

anese (prospect or showing)

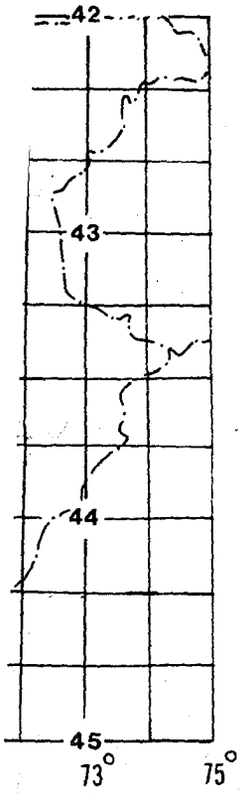

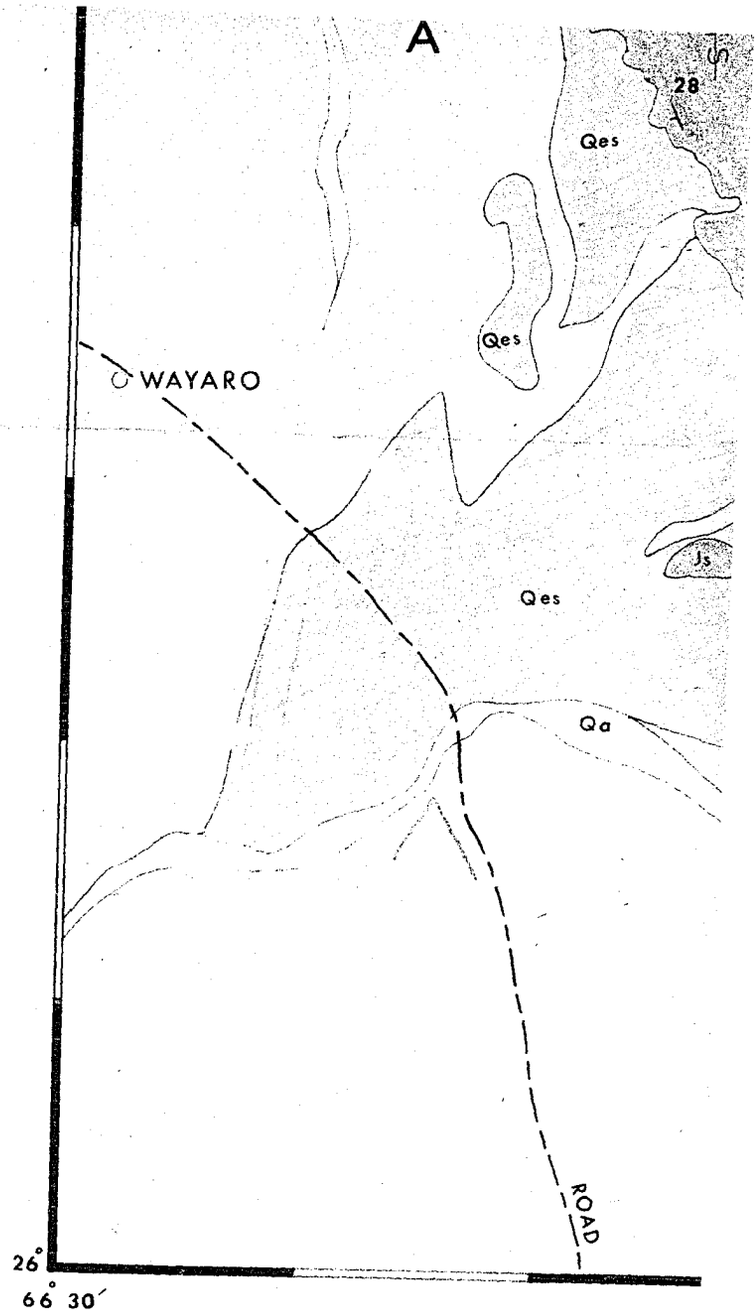

Topographic base taken from Survey of Paki

Sheet 35 J/12, 1973.

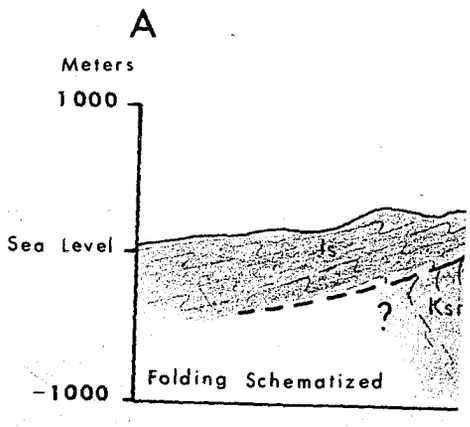

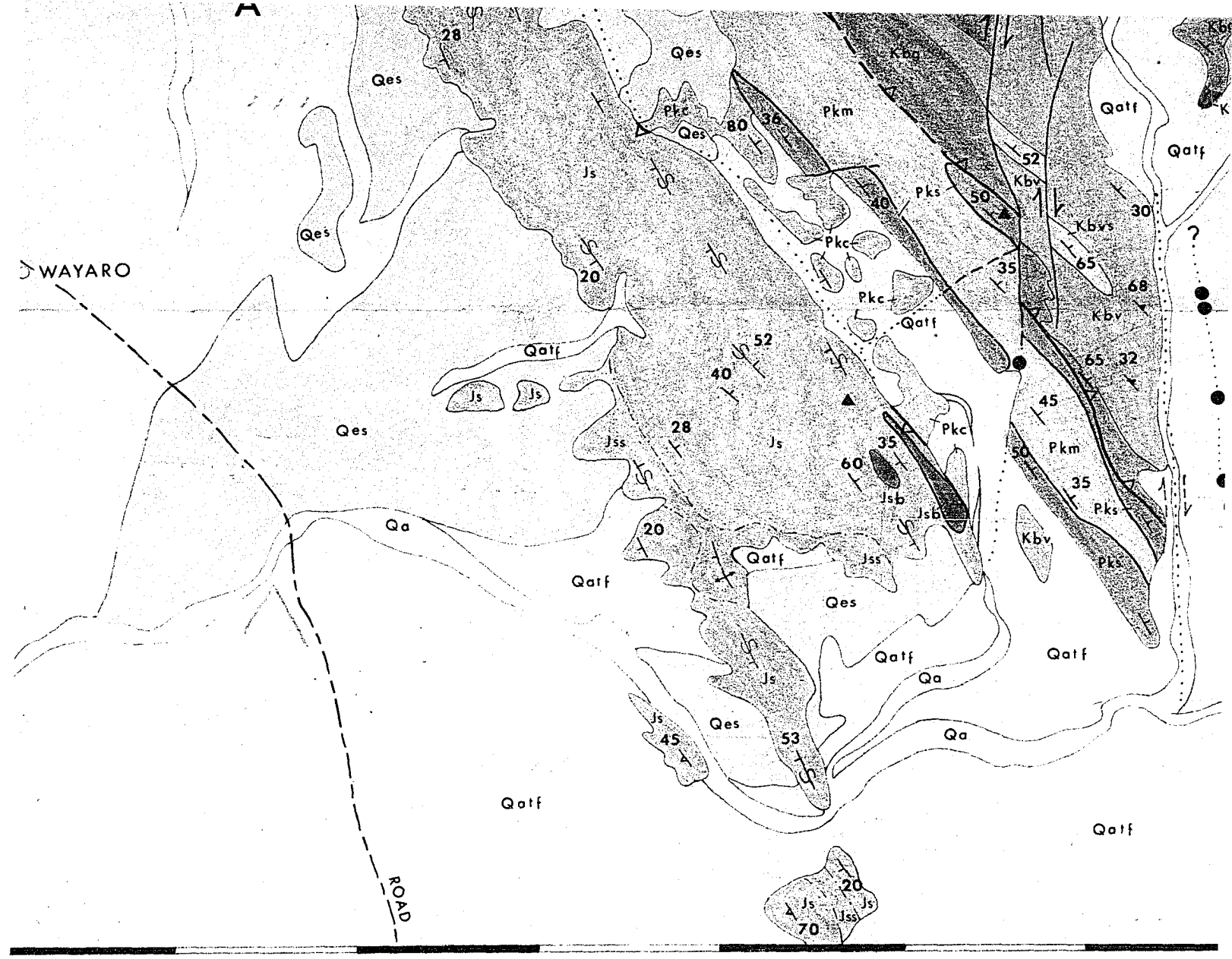

opographic base taken from Survey of Pakistan

heet 35 J/12, 1973.

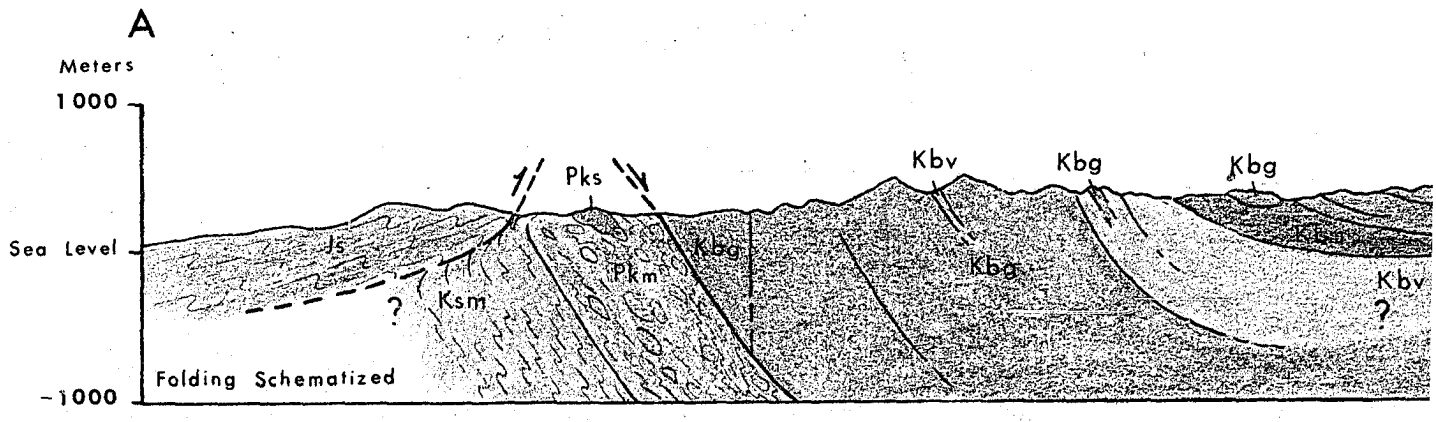

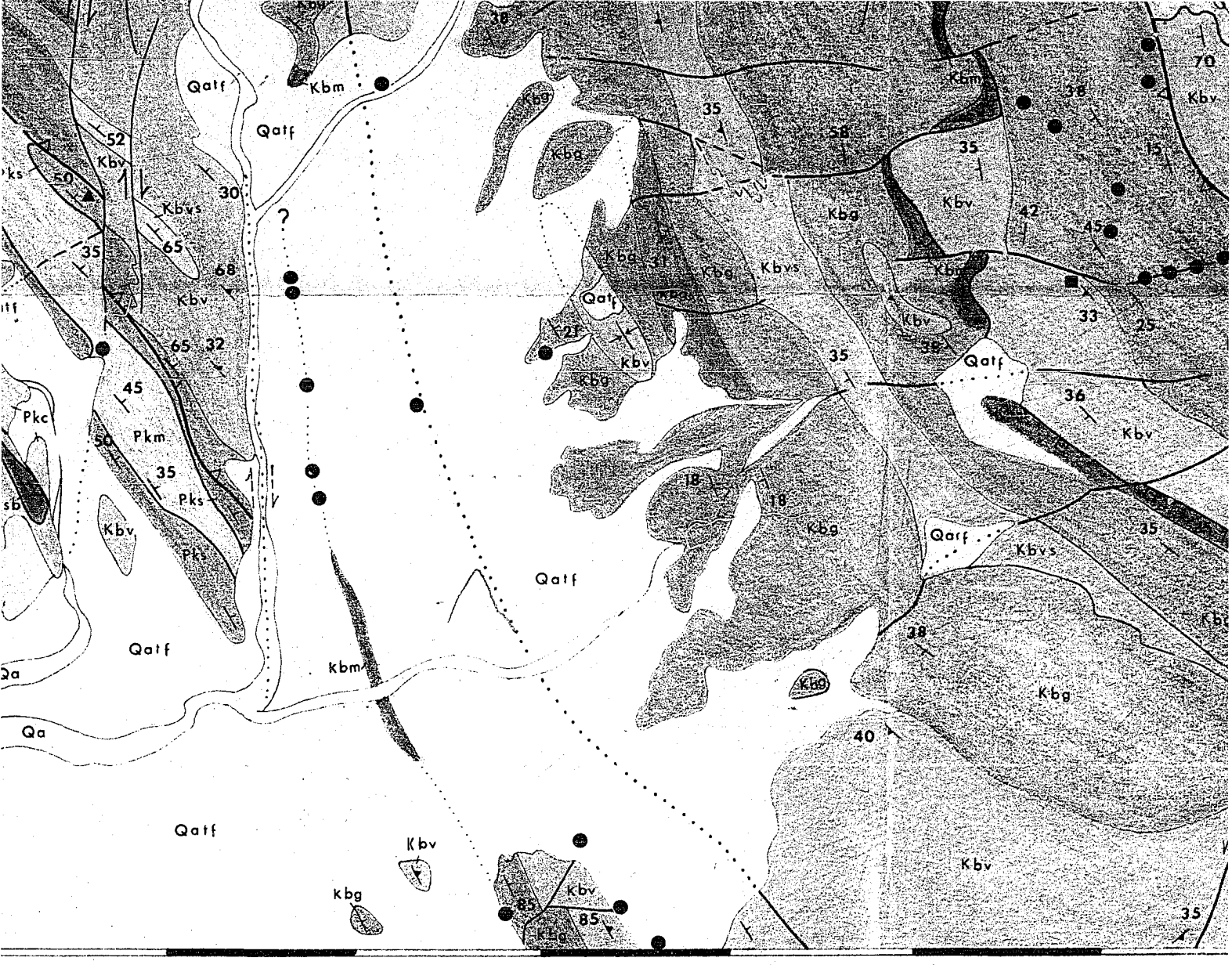

furlongs 8 6 4 2 0 1 2 3 Miles

Meters 1000 500 0 1 2 3 4 5 Kilometers

Scale 1:50,000